CA1
DTC 800
89
D26

Martec Limited

OCEAN SCIENCE &
ENGINEERING

CA1
DTC800-
89
D26

425490

41.D

TP 9850E May 1989

DEVELOPMENT OF A PROCEDURE FOR PREDICTING PROPELLER-ICE INTERACTION FORCES

Prepared for:
Transportation Development Centre
Policy and Coordination Group
Transport Canada

By:

M.W. Chernuka
R.P. Jategaonkar
M.E. Norwood
J.L. Warner

Library and Information Centre / Centre de Documentation
RECEIVED / REÇU
NOV 20 1989
Transport Canada / Transports Canada

MARTEC LIMITED
5670 Spring Garden Road
Halifax, Nova Scotia
B3J 1H6

May 1989

UDL490

DDN 422620

90-01749/

DISCLAIMER

The contents of this report reflect the views of the contractor and not necessarily the official view or opinion of the Transportation Development Centre of Transport Canada.

LANGUAGE NOTICE

Un sommaire en français de ce rapport est inclus avant la Table des matières.

Transport Canada / Transports Canada

PUBLICATION DATA FORM

1. Transport Canada Publication No.	2. Project No.	3. Recipient's Catalogue No.
9850E	6003	

4. Title and Subtitle

Development of a Procedure for Predicting Propeller-Ice Interaction Forces

5. Publication Date

May 1989

6. Performing Organization Document No.

R-87/88-02

7. Author(s)

M.W. Chernuka, R.P. Jategaonkar, M.E. Norwood, J.L. Warner

8. Transport Canada File No.

D1460-156-3

9. Performing Organization Name and Address

Martec Limited
5670 Spring Garden Road
Halifax, Nova Scotia
B3J 1H6

10. DSS File No.

11. DSS or Transport Canada Contract No.

12. Sponsoring Agency Name and Address

Transportation Development Centre (TDC)
200 Rene Levesque Boulevard West
Suite 601, West Tower
Montreal, Quebec H2Z 1X4

13. Type of Publication and Period Covered

Final 1983-89

14. Project Officer

I.M. Bayly

15. Supplementary Notes (Funding programs, titles of related publications, etc.)

16. Abstract

The objective of the study was to investigate propeller-ice interaction pressures using the finite element method.

The finite element method was applied to model the ice block as well as the propeller. A computational procedure has been developed for automatically generating loads for a finite element analysis of a propeller blade subject to ice milling. High rates of loading are involved in propeller-ice interactions and since ice under these conditions is characterized by high densities of microcracking, a smeared-crack damage material model was used.

Several developments in analytical procedures were made to maintain numerical stability in the application of load steps and to account for blade-ice separation.

Detailed propeller-ice interaction pressure profiles were established from finite element investigations of simplified indentation and milling simulations in two dimensions, and the results showed the detailed pressure distribution for various indentor shapes. The numerical procedure was applied to a typical icebreaker propeller blade in its passage through ice, and comparison between measured and predicted peak milling loads (thrust and torque) were in good agreement.

A useful modelling framework has been developed to analyze propeller-ice interaction problems in which both the ice and propeller are modelled.

17. Key Words	18. Distribution Statement
Propeller-ice interaction, ice loads, ice mechanics, ice failure, finite elements	Limited number of copies available from the Transportation Development Centre

19. Security Classification (of this publication)	20. Security Classification (of this page)	21. Declassification (date)	22. No. of Pages	23. Price
unclassified	unclassified		263	-

Transports Canada Transport Canada

FORMULE DE DONNÉES POUR PUBLICATION

1. N° de la publication de Transports Canada	2. N° de l'étude	3. N° de catalogue du destinataire
9850E	6003	

4. Titre et sous-titre	5. Date de la publication
Development of a Procedure for Predicting Propeller-Ice Interaction Forces	Mai 1989
	6. N° du document de l'organisme exécutant: R-87/88-02

7. Auteur(s)	8. N° de dossier — Transports Canada
M.W. Chernuka, R.P. Jategaonkar, M.E. Norwood, J.L. Warner	D 1460-156-3

9. Nom et adresse de l'organisme exécutant	10. N° de dossier — ASC
Martec Limited 5670 Spring Garden Road Halifax, Nova Scotia B3J 1H6	T8200-3-3514
	11. N° de contrat — ASC ou Transports Canada: 12SD-T8200-3-3514

12. Nom et adresse de l'organisme parrain	13. Genre de publication et période visée
Centre de développement des transports (CDT) 200 ouest, boul. René-Lévesque Tour ouest, suite 601 Montréal (Québec) H2Z 1X4	Rapport final 1983-1989
	14. Agent de projet: I.M. Bayly

15. Remarques additionnelles (Programmes de financement, titres de publications connexes, etc.)

16. Résumé La recherche avait pour but d'analyser les pressions interactives entre une hélice et la glace, par la méthode des éléments finis.

Cette méthode a servi à modéliser le comportement d'un bloc de glace et d'une hélice. Un programme informatique a été mis au point pour générer automatiquement des charges servant à l'analyse par la méthode des éléments finis d'une pale d'hélice broyant un bloc de glace. Les interactions hélice-glace sont caractérisées par des régimes de charge élevés entraînant une forte concentration de microfissures dans la glace, d'où la nécessité d'utiliser un modèle d'endommagement par microfissuration.

Plusieurs techniques analytiques ont dû être utilisées afin de parvenir à une stabilité numérique dans les résultats, qu'il s'agisse des incréments de déplacement et donc de tension, ou de la séparation des surfaces de contact pale-glace.

Des répartitions non uniformes des pressions interactives ont été obtenues de la recherche par la méthode des éléments finis, grâce aux simulations bidimensionnelles simplifiées de plusieurs cas de pénétration et de broyage et avec des pénétrateurs de formes géométriques diverses. Cette méthode de prévision numérique a été appliquée à une pale de l'hélice standard d'un brise-glace lorsqu'elle traverse un bloc de glace. Enfin, il y a eu comparaison entre les charges de broyage maximales (poussée et couple), réelles et théoriques, et les résultats ont été trouvés compatibles.

Les résultats montrent l'efficacité du modèle élaboré pour le calcul et l'analyse des forces d'interaction dynamique hélice-glace, et qui a nécessité la modélisation du comportement de la glace et de l'hélice.

17. Mots clés	18. Diffusion
Interaction hélice-glace, charge des glaces, mécanismes glaciels, rupture de la glace, éléments finis.	Le Centre de développement des transports dispose d'un nombre limité d'exemplaires.

19. Classification de sécurité (de cette publication)	20. Classification de sécurité (de cette page)	21. Déclassification (date)	22. Nombre de pages	23. Prix
non classifiée	non classifiée		263	-

ACKNOWLEDGEMENTS

The authors would like to express their thanks to all those who have given advice and assisted in the project. In particular, the authors wish to acknowledge the many useful discussions with Mr. I.M. Bayly of the Transportation Development Centre, Transport Canada.

SUMMARY

Introduction

The propeller of an ice transiting ship must be designed to withstand the dynamic loads imposed by ice and, as well, have an efficient form for open water travel. Thus the compromise in design between strength and form requires that propeller loading be reliably established to assist in more optimum propeller design. This report addresses the problem of establishing, in a more quantitative manner than heretofore, the detailed loading in a propeller-ice interaction process and the resultant stress levels in the propeller.

In establishing the stress levels that a propeller is subject to in cutting through ice, the interaction pressures between the propeller and ice must be specified in detail over the surface of the blade. To do this, analysis procedures must be able to determine material changes occurring in the ice under load and the effect of these changes on the pressure distribution on the blade. To carry out the detailed analysis required, finite element models of both the propeller blade and the ice interacting with the blade would be required. The finite element method allows for a wide range of geometric descriptions of the blade to be considered and it is also very flexible in regard to the material characteristics of ice.

An earlier phase of this work consisted of (i) a parametric finite element study of propellers operating in an ice environment using simplified loading conditions, and (ii) an investigation into the problem of predicting propeller/ice interaction forces. In the current work, numerical modelling of both the propeller and the ice using the finite element method has been carried out. A program is developed to define the propeller-ice interaction pressure and it allows for variations in the loading over the blade surface. The ice model is analyzed in an effort to more realistically determine the loads.

Sea Ice Characteristics

Finite element analysis of the ice block required detailed information on the mechanical properties of sea ice. Accuracy of the finite element analysis of the ice block depends very much on how well these mechanical characteristics can be reproduced. Consequently, an extensive literature search was conducted and a state of the art bibliography compiled on the appropriate mechanical characteristics of ice behaviour.

Under the high rates of strain occurring in propeller ice interactions, ice acts as a brittle material and thus a criterion for the onset of fracture must be defined for the model. This normally takes the form of a three-dimensional failure surface. Stress values on the failure surface represent the limit of elastic material behaviour and thus the onset of fracture. The information acquired in the literature search was used to establish the physical parameters appropriate to sea ice when defining the failure surface. Considerable uncertainty exists in ice

fracture predictions, due to the scarcity of multiaxial ice strength definitions (especially under high rates of strain) used to define the failure surface.

Damage Model for Ice

As the ice is deformed beyond its failure strength, its properties may change due to the inherent material damage sustained as the original crystal structure is disrupted. The damage is in the form of internal micro-fracturing (cracking). Among the most notable changes in material properties arising from this damage is the development of strain softening and the degradation of stiffness. Despite the decrease in ice strength, the material in the failed states cannot, nonetheless, be ignored in the computational investigations. Significant residual material strength exists after micro-fracturing damage is initiated and continuum damage modelling formulations were necessary.

A review was made of several material models of varying sophistication which had potential to describe the damage characteristics associated with the post-failure ice behaviour. A smeared crack damage model, available within the ADINA finite element code, was adopted for this study.

Two-Dimensional Ice Indentation Simulations

Validation of the numerical approach being proposed involved the analysis of two-dimensional indentation problems for several different indentor geometries including rectangular, wedge, circular and elliptical shapes under idealized conditions of plane stress and plane strain. The numerical approach utilized both the smeared-crack damage material model described above and the Drucker-Prager elasto-plastic material model. Perfect contact was assumed. Interface friction was investigated and found to have negligible effect. Associated pressure distributions along the contact surface were determined and resultant indentation forces were computed. From this analysis, it is clear that the pressure distribution is not uniform and its form is very much dependent on the shape of the indentor. A comparison of computed forces to full scale results was performed for the limited cases available. Reasonable results have been obtained considering the uncertainties about the degree of agreement between the material model adopted for numerical simulation purposes and the mechanical properties of the ice employed in full scale tests.

Analyses of two dimensional pseudo-static milling (slicing) simulations were also performed as part of this study with dynamic conditions accounted for by adopting appropriate material properties. In this situation, ice experiences stress conditions which involve much less confinement and thus cracking plays a much more prominent role in the failure of the ice block. Some special numerical procedures had to be invoked to cope with the microcracking of the brittle ice material. The ADINA nonlinear equation solution procedures are not as reliable or economical in simple two-dimensional ice milling simulations as in applications involving other forms of material nonlinearities (particularly metal

plasticity). The abruptness with which stress releases occur in the damage model in conjunction with ice microfracture formation, in fact, do not represent ideal conditions for the application of incremental solution methods based on the equilibrium iterations within ADINA. If equilibrium iterations are used, careful monitoring of solution progress throughout the simulations would be required. As the zone of ice microfracturing progressively developed, the prescribed incremental displacement loading would have to be continuously adjusted in accordance with the amount of material experiencing stress conditions near the microfracturing failure thresholds. Excessive load step incrementation could result in convergence failure for the equilibrium iteration process. Consequently, equilibrium iterations have been deactivated from the ADINA solution procedures employed for ice simulations. As a result numerical instabilities were eliminated and simulation costs were significantly reduced. While engineering accuracy can still be attained with the basic incremental solution procedures, care must nonetheless be exercised in the selection of load steps. Several simulations were thus carried out with decreasing load steps in order to identify a load stepping strategy for which convergence is ensured. The contact force versus applied blade displacement curve converges to its limiting configuration from above as is to be expected for strain softening materials (when loads are in the form of prescribed displacements).

Two-Dimensional Ice Milling Simulations

Several other developments in procedures were also implemented for milling simulations, including provisions for formation of gaps along the blade ice contact surface. Accounting for blade-ice separation properly in ice milling simulations is difficult if it is to be achieved by manual examination of finite element stresses for ice in the contact region and adjustment in the number of nodes with prescribed displacement boundary conditions. Consequently implementation of rods orientated normal to the blade-to-ice contact interface (surface) was proposed. Rod elements orientated normal to the blade-to-ice interface permit prescribed displacement increments to be applied to the ice yet permit frictionless sliding of ice along the interface. Assigning nonlinear material properties to the rod ensured that significant rod forces developed only if strains were compressive. Large stiffnesses (large slopes in the stress-strain curve) are associated with compressive strains and comparatively small stiffnesses with tensile strains, consequently, rod elements automatically define required blade-ice separation without any user iterative modifications to the finite element model. Although some convergence problems were encountered when the nonlinear rod elements were applied for automatic computation of blade-ice separation and the solution procedure involved the use of equilibrium iterations, these problems were eliminated once it was decided to abandon equilibrium iterations in ice milling simulations which involve ice material models that account for tensile microfracturing damage. Provision of rods as gap elements also simplifies the computation of contact forces. Data preparation and result processing procedures have been automated as much as possible.

Numerical results for two-dimensional pseudo-static milling simulations were obtained, as well as associated pressure distributions along the contact surface. Eleven simulations were performed, nine under plane stress conditions and two under plane strain conditions. A number of different cutting angles and widths were considered. Contact pressure was found to be maximum at the tip reducing to zero at some distance from the tip with separation occurring between the ice and indentor beyond that point. Plots of contact force versus cutting angle which were constructed show clearly a rapid increase in milling force with decreasing cutting angle.

Development of Propeller-Ice Interaction Load Generation Module

A computer program PVICE has been developed for automatically generating loads for a finite element analysis of a propeller blade subject to ice milling. It treats the propeller as a series of chordwise strips and permits loaded areas of propeller blade surfaces to be accurately identified on each strip at selected angular positions in its passage through an ice block. In addition to details of the propeller geometry, the user also specifies other variables affecting the propeller-ice interaction process including cutting depth, ship speed and shaft RPM. Various mechanical properties of ice are also input including crushing strength of ice and the coefficient of friction (for the interface between the ice block and the propeller blade). The propeller loading model permits a high degree of flexibility in the mathematical description of the chordwise blade pressure distributions which, when converted into consistent load vectors, are suitable for finite element analyses with the special purpose propeller analysis program, PVAST, based on the finite element method. The restriction that blade pressure loadings adhere to finite element boundaries was also eliminated in this way. Detailed propeller-ice interaction pressure profiles have been supplied from the finite element investigations of simplified indentation and milling simulations in two dimensions.

Comparison to Full Scale Results

The PVICE program, developed for the determination of propeller ice interaction loads, was applied to determine the response of a typical icebreaker propeller blade in its passage through an ice block. Initially, a uniform pressure distribution was applied to that portion of the propeller blade which is submerged within the ice block. Three different cutting radii and 10 different equispaced angular positions of the blade were considered. Under all loading cases, it was found that the maximum stress occurred at the top of the blade root fillet except in a situation where either the area close to the leading edge or the area close to the trailing edge only is loaded. In these latter cases, maximum stress occurred close to the loaded area. To investigate the effects of friction, one of the loading cases was reconsidered with coefficients of friction ranging between 0.1 and 0.4. It was determined that the effect on stresses and deflections is not very significant. To determine the effects of dynamic loading on the blade, the uniform pressure load was applied in the form of a dynamic load at a fixed propeller speed. The

dynamic factor was found to be in the order of 1.20 and the location of maximum stress and the nature of stress variation remained similar to that for the static load cases.

The effect of a detailed (non-uniform) pressure distribution upon dynamic loads, displacements, stress levels and patterns was investigated for the icebreaker propeller blade and compared with the uniform pressure loading. The loads based on the detailed definition of the interaction pressure were significantly less than those based on a uniform pressure distribution over the submerged blade area. The finite element analysis of the displacement variation of the blade surface indicated that under the assumption of a uniform pressure distribution the maximum deflection occurred at the trailing edge of the blade, while under the detailed pressure loading the maximum deflection occurred at the leading edge of the blade. This clearly indicated the effect of concentration of interaction forces at the leading edge. Principal stress levels estimated using the detailed definition of interaction pressures occurred near the blade root area and were very much less than stress levels obtained under uniform pressure loading.

As a validation of the computer procedure developed for the analysis of the propeller-ice interaction process, comparisons were made between predicted ice induced thrust and torque with available data for a range of ship speed and propeller RPM. Variation of ice thrust, torque and bending moment against variation in angle of attack were investigated. It was shown that peak values of dynamic force are critically dependent on angle of attack. This predicted relationship is well supported by experiments. A comparison was made between measured and predicted peak milling loads (thrust and torque). The results were reasonable considering the assumptions made in modelling the ice properties and propeller loading configuration.

Further Work

It is evident from the results that a useful modelling framework has been developed to analyze propeller-ice interaction problems. However, a number of assumptions on values of the critical ice parameters and propeller loading mechanisms were made in the analysis. To establish more clearly the confidence that can be placed on the results, further work is recommended in which the numerical determination of pressure curves and contact forces would be extended to a wider variety of propeller-ice interactions. In addition, recommendations are made that specific data be gathered to better define the inputs required for the ice material modelling and that more attention be given to quantifying ice properties when conducting experiments on structure-ice interaction phenomena.

SOMMAIRE

Introduction

L'hélice d'un navire appelé à naviguer dans les glaces doit pouvoir résister aux efforts exercés par celles-ci, tout en ayant les qualités nécessaires pour propulser le navire avec un bon rendement en eau libre. Il importe donc, dans tout arbitrage entre résistance mécanique et qualités de propulsion, de bien déterminer au préalable les régimes de charge et arriver ainsi à un dimensionnement optimal de l'hélice. Ce rapport rend compte de la recherche visant à déterminer de manière plus quantitative et aussi plus détaillée qu'auparavant les charges dues aux interactions hélice-glace et, par là, les contraintes qui s'exercent sur une hélice lorsqu'elle s'attaque à un bloc de glace.

Pour chiffrer ces contraintes, il faut approfondir les pressions interactives glace-hélice et leur répartition sur la surface de la pale de l'hélice, et ce par des méthodes analytiques permettant de mettre en évidence tant les transformations qui se produisent dans la glace soumise à des efforts tendant à la briser que leur effet sur la répartition des pressions d'interaction sur la pale d'hélice. Pour arriver à une analyse détaillée des forces en jeu, il a fallu modéliser par la méthode des éléments finis à la fois la pale de l'hélice et la glace qu'elle heurte. Cette méthode permet de multiples représentations géométriques de la pale considérée et elle offre une très grande souplesse pour la modélisation des propriétés physiques de la glace.

Une étude antérieure s'était attaquée i) à une paramétrisation par la méthode des éléments finis des hélices fonctionnant dans un milieu glacé, pour laquelle des hypothèses de charge simplifiées avaient été retenues et, ii) à l'analyse du problème de la prévision mathématique des interactions dynamiques hélice-glace. La présente recherche a consisté à produire des modèles numériques de l'hélice ainsi que de la glace heurtée, par la méthode des éléments finis. Un programme informatique a été mis au point permettant de calculer les pressions interactives hélice-glace tout en faisant varier la répartition de la charge sur la surface de la pale. Les résultats ont été analysés dans le but de donner aux calculs des valeurs de charge qui se rapprochent davantage des valeurs réelles.

Propriétés de la glace de mer

L'analyse par la méthode des éléments finis d'un bloc de glace a requis la connaissance détaillée des propriétés mécaniques de la glace d'eau de mer, étant donné que les résultats tirés de cette méthode sont d'autant plus fiables que ces propriétés sont reproduites avec justesse. C'est pourquoi une vaste recherche documentaire a été faite et une bibliographie sur l'état de l'art compilée dans ce domaine précis.

Aux vitesses de déformation élevées qui se produisent au moment où une hélice pénètre dans la glace, celle-ci se comporte comme un matériau fragile, d'où la nécessité d'élaborer pour la modélisation un critère

d'amorce de rupture qui, d'habitude, prend la forme d'une surface tridimensionnelle délimitant le domaine d'élasticité du matériau. En effet, les valeurs de contrainte correspondantes figurent la limite d'élasticité du matériau et, ainsi, l'amorce de la rupture. Les résultats de la recherche documentaire sur les propriétés de la glace d'eau de mer ont servi à dégager les paramètres physico-chimiques appropriés et utiles à la définition du domaine d'élasticité. De fortes incertitudes entourent les prévisions concernant le phénomène de rupture de la glace, en raison du manque de connaissances sur la loi de comportement (notamment aux vitesses de déformation élevées) aux sollicitations multi-axiales, servant à définir le domaine d'élasticité de cette glace.

Modèle d'endommagement par microfissuration

A mesure que la glace se déforme jusqu'à dépasser les limites du domaine d'élasticité, sa structure cristalline cède petit à petit et se disloque au point que l'endommagement qui en résulte peut provoquer des transformations dans les propriétés mécaniques. L'endommagement est dû à la présence de microfissures et ses principales manifestations sont l'amollissement sous contrainte et l'effondrement de la raideur. Malgré l'affaiblissement de la glace, sa résistance, même après qu'elle eut cédé, ne peut pas entrer en ligne de compte dans les calculs. En effet, une résistance résiduelle non négligeable perdure après la microfissuration au point que la modélisation des déformations et contraintes en milieu continu est indispensable.

Les chercheurs ont examiné plusieurs modèles d'endommagement plus ou moins sophistiqués et susceptibles de simuler le comportement d'une glace au-delà du domaine élastique, par la description du phénomène de rupture correspondant. Il a été décidé d'adopter pour les besoins de la recherche un modèle d'endommagement par microfissuration inscrit dans le programme informatique ADINA.

Simulation des essais bidimensionnels de pénétration

La validation de l'approche numérique envisagée a nécessité l'analyse du phénomène en jeu par des essais bidimensionnels de pénétration, utilisant des pénétrateurs de géométries diverses: rectangulaire, en coin, circulaire et elliptique, dans des conditions théoriques de contraintes et de déformations planes. Dans ce but, tant le modèle d'endommagement par microfissuration mentionné plus haut que le modèle Drucker-Prager pour matériaux élastoplastiques ont été utilisés, l'hypothèse d'un contact parfait ayant été retenue. Le frottement interfacial a été approfondi et trouvé négligeable dans ses effets. La répartition des pressions associées le long de la surface de contact a été déterminée et les forces de pénétration correspondants calculées. L'analyse montre clairement que la répartition n'est pas uniforme et qu'elle dépend pour sa forme de celle du pénétrateur. Les valeurs calculées des forces en jeu ont été comparées aux valeurs réelles, dans la limite des cas disponibles. Les résultats obtenus sont considérés comme raisonnables, vu l'incertitude entourant le degré de similitude entre le modèle de simulation numérique adopté et les propriétés

mécaniques de la glace déterminées par des essais de résistance classiques.

Des simulations bidimensionnelles quasi statiques du comportement en broyage ont été menées et analysées, les conditions dynamiques correspondantes dantes ayant été prises en compte par un choix judicieux des propriétés mécaniques. Dans ces conditions, les contraintes exercées sur la glace sont telles que, parce que celle-ci est beaucoup moins confinée, la fissuration vient à jouer un rôle prédominant dans la rupture du bloc de glace. Certains artifices de calcul ont dû être utilisés afin de tenir compte de la microfissuration du matériau fragile qu'est la glace. La résolution des équations non linéaires, utilisant le programme ADINA, n'est ni aussi fiable ni aussi économique dans le cas des simulations bidimentionnelles simples que dans des applications impliquant d'autres formes de non-linéarités (notamment la plasticité des métaux). La brutalité avec laquelle se produit, dans le modèle d'endommagement, la relaxation des contraintes à mesure que se forment les microfissures est loin de favoriser l'application des méthodes de résolution incrémentale par intérations aux conditions d'équilibre du programme ADINA. Mais si cette méthode d'itération devait être utilisée, un suivi attentif et constant sera nécessiare tout au long des simulations. A mesure que s'étend la zone de microfissuration de la glace, les paliers de charge dictés par le déplacement imposé devront être conditionnés par la quantité de matériau qui approche alors le seuil de rupture par microfissuration. Une augmentation excessive de la charge risquerait d'entraîner une divergence des résultats, au lieu de la convergence recherchée. C'est pour cette raison que les itérations du programme ADINA ont dû être court-circuitées, éliminant du même coup les instabilités numériques et réduisant de façon sensible le coût des opération de simulation. Et s'il est possible que cette méthode d'itération satisfasse au degré de précision technique voulu, le choix des incréments de charge reste quand même délicat. Plusieurs essais de simulation ont été faits avec des valeurs décroissants d'augmentation de charge dans le but de déterminer un mode opératoire susceptible de parvenir à une convergence. La courbe des forces de contact en fonction des déplacements imposés finit par atteindre une configuration limite inférieure qui représente la convergence recherchée, et qui, dans le cas des matériaux qui amollissent sous contrainte, décroît à mesure que les incréments de charge vont en s'amenuisant.

Simulations bidimensionnelles en broyage

De nombreux autres développements opératoires ont été adoptés en simulation de broyage, y compris celui de prendre en compte les pertes de contact entre la pale et la glace. Une telle prise en compte s'avère difficile dès qu'il s'agit de vérifier manuellement les contraintes définies par la méthode des éléments finis dans la zone de contact, et de faire les calages nécessaires dans le nombre de noeuds tout en respectant les conditions aux limites à déplacement imposé. C'est pourquoi il a été proposé d'adopter la notion d'éléments de contact orientés perpendiculairement à la surface de contact pale-glace. Grâce à cette notion, il devient possible d'appliquer les incréments de déplacement imposés tout

en permettant à la glace d'effectuer une translation exempte de frottement le long de l'interface. En affectant aux éléments de contact des propriétés physiques non linéaires, on s'assure qu'ils n'exerceront des valeurs élevées de force que si les déformations sont compressives. Étant donné que des valeurs élevées de raideur (forte inclinaison de la courbe contrainte-déformation) sont liées aux déformations compressives et que ces valeurs deviennent relativement faibles en traction, il s'ensuit que les éléments de contact définissent automatiquement la perte de contact requise sans que l'utilisateur n'ait à intervenir pour modifier le modèle d'analyse. Si la convergence a été difficile à obtenir avec la méthode d'analyse qui fait intervenir des éléments de contact non linéaire, surtout s'il fallait procéder à des itérations pour vérifier les conditions d'équilibre, ces difficultés ont été éliminées lorsqu'il a été décidé d'abandonner ce mode opératoire dans le modèle d'endommagement par fissuration dû aux efforts de traction en broyage. Par son adoption, la notion d'éléments de contact permettant la prise en compte des pertes de contact simplifie les calculs y relatifs, surtout avec l'automatisation aussi poussée que possible des étapes de saisie et de traitement des données.

Pour les simulations bidimensionnelles quasi statiques du comportement en broyage, des résultats numériques ainsi que des répartitions des pressions associées le long de la surface de contact ont été obtenus. Onze simulations ont été faites, neuf dans des conditions de contrainte plane et deux en conditions de déformation plane. Des angles et largeurs de coupe différents ont été pris en compte. Les résultats montrent que la pression de contact, maximale à l'extrémité libre du pénétrateur, tombe à zéro à quelque distance de là et que, au-delà de ce point, la séparation se produit entre la glace et la pénétrateur. La courbe des forces de contact en fonction de l'angle montre clairement la montée rapide des forces de broyage à mesure que décroît l'angle.

Générateur de pression interactives

Un programme informatique appelé PVICE a été élaboré permettant de générer automatiquement des pressions interactives pour les besoins de l'analyse par la méthode des éléments finis d'une pale d'hélice broyant un bloc de glace. Dans ce programme, l'hélice est envisagée comme une succession de lamelles horizontales permettant de connaître avec précision les zones chargées dans chaque lamelle, à des moments précis de leur déplacement angulaire à travers le block de glace. L'utilisateur doit, en plus des caractéristiques géométriques de l'hélice, spécifier d'autres variables ayant une influence sur les interactions hélice-glace: rayons de coupe, vitesse du navire, vitesse de rotation de l'hélice, etc. Sont également entrées dans le programme diverses autre données, concernant les propriétés de la glace résistance à l'écrasement et coefficient de frottement (à l'interface block de glace-pale). Ce programme informatique permet, avec un degré élevé de souplesse, de décrire mathématiquement la répartition des pressions dans les lamelles figurant la pale de l'hélice et qui, après conversion en vecteurs de charge cohérents, permettent des analyses par la méthode des éléments finis utilisant pour cela un programme d'analyse particulier appelé

PVAST. De cette manière, la condition que les pressions interactives coincident avec les frontières des éléments finis est également abandonnée. Des répartitions non uniformes des pressions interactives ont été obtenues de cette recherche par la méthode des éléments finis grâce aux simulations bidimensionnelles simplifiées de plusieurs cas de pénétration et de broyage.

Comparaison avec les essais en vraie grandeur

Le programme informatique PVICE a servi également à déterminer la réponse dynamique de la pale d'une hélice standard de brise-glace lorsqu'elle traverse un bloc de glace. On a d'abord appliqué une répartition uniforme des pressions le long de la surface de contact pale-glace. Pour les simulations, trois rayons de coupe et dix positions angulaires équidistantes de pale ont été pris en compte. Quel que soit le régime de charge, la valeur maximale de contrainte se trouve toujours localisée au sommet de la courbe figurant le pied de la pale d'hélice, sauf lorsque la zone proche du bord d'attaque ou du bord de fuit seulement est chargée. Dans ces deux cas, la valeur maximale de contrainte a été localisée à proximité de la zone chargée. Pour approfondir l'influence du frottement, un des cas de charge a été repris avec des coefficients de frottement entre 0,1 et 0,4. Il a été constaté que le frottement a peu d'influence sur les contraintes et les déformations. Pour approfondir l'effet des charges dynamiques sur la pale, une pression uniforme a été appliquée sous la forme d'une charge dynamique à régime de rotation constant. Ainsi, il a été déterminé que le facteur de charge dynamique est de l'ordre de 1,20 mais que ni la localisation de la contrainte maximale ni la répartition des pressions n'a changé par rapport aux cas de charge statique.

Ensuite, on a vérifié l'effet d'une répartition non uniforme des pressions sur les charges dynamiques, les déplacements et le niveau et la distribution des contraintes; effet que l'on a comparé au cas de réparation uniforme de pressions sur la pale d'une hélice de brise-glace. Il a été observé que, dans le cas d'une répartition non uniforme, les charges sont bien inférieures à celles ressortant d'une répartition uniforme, et ce à l'égard de la partie immergée de la glace. L'analyse par la méthode des éléments finis des variations de déplacement de la surface de pale montre que la déformation maximale est localisée respectivement au bord de fuite et au bord d'attaque de la pale, selon que la répartition des pressions est uniforme ou non uniforme, mettant ainsi en évidence l'effet de la localisation concentrée des pressions interactives sur le bord d'attaque. Les niveaux de contraintes principales estimés via une définition détaillée des pressions interactives, beaucoup plus faibles que dans le cas d'une répartition uniforme étaient localisés à proximité du pied de pale.

Pour valider la méthode de prévision devant permettre d'analyser les forces d'interaction hélice-glace, les résultats théoriques de poussée et de couple ont été comparés aux résultats des expérimentations faites à des vitesses et à des régimes variés. Les chercheurs ont également déterminé les variations de poussée, de couple et de moment de flexion en

fonction de l'angle d'attaque. Les résultats indiquent que ce dernier a une très grande influence sur les valeurs maximales des forces dynamiques engendrées, résultat d'ailleurs prévu et bien étayé par les expérimentations faites. Enfin, ils ont comparé les charges de broyage maximales (poussée et couple), réelles et théoriques. Les résultats peuvent être considérés comme raisonnables, vu les hypothèses retenues au départ pour la modélisation concernant les propriétés de la glace et les plans de charge de l'hélice.

Poursuite des travaux

Les résultats montrent clairement l'efficacité du modèle élaboré pour le calcul et l'analyse des forces d'interaction dynamique hélice-glace. Cependant, il faut dire que les chercheurs ont utilisé des valeurs hypothétiques dans le cas de certains paramètres critiques relatifs à la glace et aux mécanismes de charge. Pour accroître la confiance que l'on peut placer dans les résultats fournis par ce modèle, il faudrait pousser la recherche plus loin et procéder à des déterminations numériques des pressions et forces de contact dans une gamme plus étendue de cas d'interactions hélice-glace. En outre, il est recommandé de recueillir des données spécifiques permettant de mieux définir les valeurs à utiliser pour modéliser les propriétés de la glace, et de mieux caractériser celles-ci lors des expériences visant à élucider les phénomènes d'interaction glace-hélice.

TABLE OF CONTENTS

1.0 INTRODUCTION 1
1.1 Background 1
1.2 Earlier Modelling of Propeller-Ice Interaction Processes 1
1.3 Proposed Improvements in Propeller-Ice Interaction Analysis 3
1.4 Mechanical Properties of Ice 4
1.5 Two-Dimensional Ice Block Simulations 6
1.6 Basic Concepts in the Propeller-Ice Interaction Load Generation 7
1.7 Comparison of Full Scale Results 7
1.8 Organization of the Report 8

2.0 LITERATURE SURVEY AND STATE OF THE ART BIBLIOGRAPHY 9

3.0 PROCEDURE FOR GENERATING LOADS FOR A FINITE ELEMENT ANALYSIS OF A PROPELLER BLADE SUBJECTED TO ICE MILLING . . . 11
3.1 Introduction 11
3.2 Equations of Motion 11
3.3 Mechanics of the Blade Milling Process 13
3.4 Computer Program PVICE 18

4.0 MECHANICAL PROPERTIES OF ICE AND MATERIAL MODELLING 35
4.1 Stress-Strain Relationships 35
4.2 Yield Criteria and Failure Envelopes 40
4.3 Damage Models 47
4.4 Typical Values for the Mechanical Properties of Ice . . 59

5.0 DETERMINATION OF PROPELLER-ICE INTERACTION FORCES USING A FINITE ELEMENT MODEL OF THE ICE BLOCK 63
5.1 Selection of Analysis Program 63
5.2 Types of Models Considered 64
5.3 ADINA Analysis 75
5.3.1 Data Generation 75
5.3.2 Use of Rod Elements to Simulate Contact 77
5.3.3 Material Modelling 79
5.3.4 Solution Strategy 84
5.3.5 Termination of Simulations 85
5.4 Results of Analysis 88
5.4.1 Indentation 88
5.4.2 Slicing 104
5.4.3 Three-Dimensional Effects 113
5.5 Incorporation of Results into Computer Program PVICE 113

6.0 ANALYSIS OF TYPICAL ICEBREAKER PROPELLER 123
6.1 Analysis of Blade Passage Through Ice Using Uniform Pressure Loading on Blade 123

TABLE OF CONTENTS (Continued)

6.2 Analysis of Blade Passage Through Ice Using Detailed Definition of Propeller-Ice Interaction Forces 139
6.3 Comparison with Full Scale Measurements 154

7.0 CONCLUSIONS AND RECOMMENDATIONS FOR FUTURE WORK 163

References 167

Appendix A - Evaluations of Analysis Programs A.1

Appendix B - Bibliography
B1 - Brittle Fracture (General References) B1.1
B2 - Propeller-Ice Interaction/Milling B2.1
B3 - Metal Milling/Machining B3.1
B4 - Ice Mechanics/Mechanical Properties of Ice/Testing Methods B4.1
B5 - Ice Indentation and Penetration B5.1

LIST OF FIGURES

FIGURE 3.1 Passage of Blade Through Ice Block 12

FIGURE 3.2 Finite Element Model of Blade 14

FIGURE 3.3 Cutting Views of Blade Section 15

FIGURE 3.4 Ice Milling Conditions in Relation to Angle of Advance 16

FIGURE 3.5 Different Forms of Shadowing 17

FIGURE 3.6 Segmented Blade Embedded in Ice 20

FIGURE 3.7 Blade Section Unwrapped Onto X'Z' Plane 21

FIGURE 3.8 Relationship Between W_1 and W_2 22

FIGURE 3.9 Calculation of W_2 23

FIGURE 3.10 Ice Loading on Face of Blade Section - Crushing Mode 24

FIGURE 3.11 Ice Loading on Face of Blade Section - Shearing Mode 25

FIGURE 3.12 Ice Loading on Back of Blade Section - $W_2 > b$ . . . 26

FIGURE 3.13 Ice Loading on Back of Blade Section - $W_2 = b$ . . . 27

FIGURE 3.14 Representation of Ice Crushing Pressure as a Function of Geometric Parameters 28

FIGURE 3.15 Representation of Ice Shearing Force as a Function of Geometric Parameters 29

FIGURE 3.16 Meshing of Finite Element for Consistent Load Vector Formulation 31

FIGURE 3.17 Definition of $Y_C, \theta_1, \theta_{11}$ and Reference Coordinate System $X_o\ Y_o\ Z_o$ 32

FIGURE 4.1 Effect of Strain Rate on Stress-Strain Relationship 36

FIGURE 4.2 Stress-Strain Curves for Various Types of Ice . . . 37

FIGURE 4.3 Effect of Confining Pressure on Stress-Strain Relationship 38

LIST OF FIGURES (Continued)

FIGURE 4.4	Effect of Confining Pressure on Yield Stress	39
FIGURE 4.5	Comparison Between Confinement on Vertical Sides (A-Type) and Confinement on Top and Bottom (B-Type)	41
FIGURE 4.6	Isotropic Yield Surfaces in Principal Stress Space .	44
FIGURE 4.7	Two-Dimensional Representation of a Yield Criteria for Ice	46
FIGURE 4.8	Failure Envelope Proposed by Jones for Fine Grained Ice of Glacier	48
FIGURE 4.9	Sensitivity of Failure Envelope to Errors in Unconfined Uniaxial Tensile and Compressive Strength Data	49
FIGURE 4.10	Characteristic Uniaxial Response of Elasto-Plastic Material (No Degradation of Elastic Moduli)	51
FIGURE 4.11	Characteristic Uniaxial Response of Material with Strain Hardening	52
FIGURE 4.12	Characteristic Uniaxial Response of Material with Progressive Fracture Type Damage	55
FIGURE 4.13	Characteristic Uniaxial Response of Material with Progressive Plastic-Fracture Type Damage	57
FIGURE 5.1	Types of Models Considered in Ice Block Analysis . .	65
FIGURE 5.2	Rectangular Indentor - Finite Element Model	66
FIGURE 5.3	Circular Indentor - Finite Element Model	67
FIGURE 5.4	Elliptical Indentor - Finite Element Model	68
FIGURE 5.5	Wedge Shaped Indentor - Finite Element Model	69
FIGURE 5.6	Flat Cutter - Finite Element Model #1	70
FIGURE 5.7	Flat Cutter - Finite Element Model #2	71
FIGURE 5.8	Inclined Cutter - Finite Element Model	72
FIGURE 5.9	Refined Finite Element Model	73
FIGURE 5.10	Built Up Meshes for Inclined Cutter - Refined Finite Element Model	74

LIST OF FIGURES (Continued)

FIGURE 5.11 Finite Element Model Group Numbers 78

FIGURE 5.12 Idealized Stress-Strain Curves for Ice Under Multiaxial Conditions 80

FIGURE 5.13 Drucker-Prager Yield Criterion Compared to Concrete Yield Criterion 82

FIGURE 5.14 Contact Force vs. Prescribed Displacement Curves . . 86

FIGURE 5.15 Contact Pressure Distribution for Rectangular . . . Indentor 89

FIGURE 5.16 Indentation Coefficient Versus Prescribed Displacement - Rectangular Indentor 90

FIGURE 5.17 Failure Zone for Rectangular Indentor 92

FIGURE 5.18 Indentation Coefficient C as Function of d/h for Rectangular Indentor 93

FIGURE 5.19 Contact Pressure Distribution for Circular Indentor 95

FIGURE 5.20 Indentation Coefficient Versus Prescribed Displacement - Circular Indentor 96

FIGURE 5.21 Crack Pattern at Failure - Circular Indentor 97

FIGURE 5.22 Indentation Coefficient C as Function of d/h for Circular Indentor 98

FIGURE 5.23 Contact Pressure Distribution for Elliptical Indentor 100

FIGURE 5.24 Indentation Coefficient Versus Prescribed Displacement - Elliptical Indentor 101

FIGURE 5.25 Crack Pattern at Failure - Elliptical Indentor . . . 102

FIGURE 5.26 Contact Forces Versus Prescribed Displacement for Wedge Indentor 105

FIGURE 5.27 Progression of Cracking for Wedge Indentor 106

FIGURE 5.28 Stresses in Ice-Block at Indentor - Ice Interface 107

FIGURE 5.29 Cases for Slicing Analysis 109

LIST OF FIGURES (Continued)

FIGURE 5.30 Stresses in Ice-Block at Cutter-Ice Interface . . . 110

FIGURE 5.31 Contact Force Versus Prescribed Displacement for Cutting Angle of 75° 111

FIGURE 5.32 Contact Force Versus Cutting Angle 112

FIGURE 5.33 Finite Element Model for Negative Cutting Angles . . 114

FIGURE 5.34 Stresses in Ice-Block at Cutter-Ice Interface for Cutting Angle of -45° 115

FIGURE 5.35 Stresses in Ice-Block at Cutter-Ice Interface for Cutting Angle of -75° 116

FIGURE 5.36 Use of Curved Indentor Model to Approximate P_1 . . . 117

FIGURE 5.37 Use of Slicing Model to Approximate P_2 118

FIGURE 5.38 Use of Slicing Model to Approximate F 119

FIGURE 5.39 Blade-Ice Interaction Pressure Distribution Curves Incorporated into PVICE 120

FIGURE 5.40 F Curves Incorporated into PVICE 121

FIGURE 6.1 Finite Element Model of CCGS Pierre Radisson/ Franklin Propeller 124

FIGURE 6.2 Angular Position θ of Blade in Ice 125

FIGURE 6.3 Load Case L3-01 129

FIGURE 6.4 Load Case L3-02 130

FIGURE 6.5 Load Case L3-03 131

FIGURE 6.6 Load Case L3-04 132

FIGURE 6.7 Load Case L3-05 133

FIGURE 6.8 Load Case L3-06 134

FIGURE 6.9 Load Case L3-07 135

FIGURE 6.10 Load Case L3-08 136

FIGURE 6.11 Load Case L3-09 137

FIGURE 6.12 Load Case L3-10 138

LIST OF FIGURES (Continued)

FIGURE 6.13 Load Case L3-01 with Coefficient of Friction = 0.40 141

FIGURE 6.14 Load Case L3-05 with Coefficient of Friction = 0.40 142

FIGURE 6.15 Load Case L3-10 with Coefficient of Friction = 0.40 143

FIGURE 6.16 Dynamic Load Case - L3 145

FIGURE 6.17 Blade Trust Versus Ship Speed 147

FIGURE 6.18 Dynamic Ice Trust Time History 148

FIGURE 6.19 Dynamic Displacement (Z-Component) at Node 71 . . . 149

FIGURE 6.20 Dynamic Displacement (Z-Component) at Node 79 . . . 150

FIGURE 6.21 Dynamic Displacement (X-Component) at Node 71 . . . 151

FIGURE 6.22 Dynamic Stresses - Detailed Definition of Pressure . 152

FIGURE 6.23 Dynamic Stresses - Detailed Definition of Pressure . 153

FIGURE 6.24 Peak Thrust Versus Angle of Attack - 130 RPM 156

FIGURE 6.25 Peak Torque Versus Angle of Attack - 130 RPM 157

FIGURE 6.26 Peak Bending Moment Versus Angle of Attack - 130 RPM 158

FIGURE 6.27 Predicted Versus Measured Thrust for CCGS Pierre Radisson Propeller 160

FIGURE 6.28 Predicted Versus Measured Torque for CCGS Pierre Radisson Propeller 161

LIST OF SYMBOLS

$[\ ]$	Square or rectangular matrix.
$\{\ \}$	Vector.
a	Projection of s on x' axis.
b	Projection of s on z' axis.
C	Coefficient of indentation.
[C]	Damping matrix for finite element solution of equations of motion.
c	Cohesion coefficient for yield surface definition.
D	Size of microfracture.
$\dot{D}$	Microfracture growth rate.
d	Width (diameter) of indentor.
$\{F_h\}$	Force vector for finite element solution of equations of motion thickness of ice layer (sheet).
J_2, J_3	Second and third invariants of the stress deviator.
J_R, J_A	Jaccbian operators for consistent load computations for line loads and pressure loads, respectively.
[K]	Stiffness matrix.
[M]	Mass matrix.
$[M_A]$	Hydrodynamic added mass matrix.
$\dot{N}$	Microfracture nucleation rate.
N_{BLADE}	Number of blades on propeller.
N_o, σ_{no}, σ_1, σ_{go}, η	Material parameters required by the microfracture nucleation and growth laws.
P_1, P_2	Ice pressure distributions on blade sections derived from ADINA simulations.
R	Maximum propeller blade radius.

R_i	Radius for blade section i.
S	Total chord length in unwrapped blade section.
S_{ij}	Stress deviator.
s	Length from leading edge along either front or back of blade section in contact with ice.
t	Time variable.
V_p	Velocity component of a point on the propeller blade arising from propeller rotation.
V_s	Velocity component of a point on the propeller blade arising from ship velocity.
V_R	Resultant velocity of a point on the propeller blade.
W	Width of ice in blade path (for milling simulations).
W_1	Projected width of blade sections in direction of advance.
W_2	Width of ice in the blade path (accounting for shadowing effects).
X_o, Y_o, Z_o	Reference coordinate system for propeller-ice interaction process (last component is aft; second component is normal to ice surface).
X', Z'	Local axes fixed to the blade section (the first component is orientated along direction of advance and passes through the leading edge of the blade).
α, κ	Yield surface parameters for the Drucker-Prager material model.
β	Angle of advance for a point on a blade milling a stationary ice block.
β_i	Angle of advnace for points on blade section i.
γ	Cutting angle for blade section in milling simulations.
ΔA	Increment of area for computation of element consistent load vector for pressures on element surfaces.
ΔR	Increment of radius for computation of element consistent load vector for a line load along the element edge.

δ_p	Prescribed boundary conditions for indentation and milling simulations.
$\{\delta\}$, $\{\dot{\delta}\}$, $\{\ddot{\delta}\}$	Structural displacement, velocity and acceleration vectors.
$\dot{\varepsilon}$	Strain rate.
ε_c	Unconfined uniaxial compressive strain.
ε_u	Unconfined uniaxial ultimate compressive strain.
θ_1	Angle about the Z_o axis from the Y_o axis to the blade spindle axis when the blade first comes in contact with the ice block.
θ_{11}	Angle about the Z_o axis from the Y_o axis to the blade spindle axis when the blade is last in contact with the ice block.
ξ, η	Element parametric (local) coordinates corresponding with constant radius and constant chord directions, respectively.
σ_o	Yield stress in simple tension (for plasticity theory).
σ_1, σ_2, σ_3	Three principal stresses.
σ_c	Unconfined uniaxial compression stress (crushing strength).
σ_m	Mean stress (pressure).
σ_t	Uniaxial tensile strength.
σ_u	Unconfined uniaxial ultimate compressive stress.
ϕ	Angle of friction for yield surface definition.

1.0 INTRODUCTION

1.1 Background

Canadian Arctic sovereignty issues as well as recent hydrocarbon and mineral exploration in the Arctic have increased the importance of ice load design considerations in modern shipbuilding technology and offshore structural engineering. As a result, there is greater interest on the part of regulatory bodies to foster the development of an improved understanding of the full range of structure-ice interaction problems, including the propeller-ice interaction problem, so that design codes and regulations can be suitably amended.

The work presented in this report is the second phase in a program of study for the Transportation Development Center to investigate propeller responses to ice interaction pressures using the finite element method. The initial phase of the work involved two parts. The first part consisted of a parametric study for the purpose of assessing the effect of various geometric changes and loading configurations on propeller stresses using assumed simplified loading conditions [1]. It demonstrated that the description of propeller-ice interaction forces is an important consideration in the stress analysis of propellers. Simplified nominal loadings of uniformly distributed pressure over a depth of the propeller blade immersed in ice were shown to be inadequate for determining accurate stress distribution patterns and critical points of failure. The second part consisted of an investigation of the feasibility of predicting propeller-ice interaction forces more accurately [2]. This component of the study indicated the need for mathematically modelling the ice block, probably with finite elements.

In the current work, the finite element method has been applied to model the ice block as well as the propeller to obtain improved estimates of operational ice loads. The finite element method permits a high degree of geometric generality to be attained. The propeller geometry description can accommodate variations in pitch and skew along its length and permits curvatures on the front face as well as the back face. The finite element method is also very flexible with regard to the detail which can be implemented within the material model and although some important data on the physical characteristics of ice is lacking at present, the material model can be upgraded on an ongoing basis as further reliable basic mechanical data becomes available in the future. Numerical modelling based on the finite element method allows parametric studies to be carried out to assess the sensitivity of various ice-structure interaction processes to variations in mechanical properties and to identify the critical ones for which additional physical experiments are appropriate.

1.2 Earlier Modelling of Propeller-Ice Interaction Processes

A literature search was conducted to ascertain the extent to which analytical and numerical methods have been employed to investigate the

propeller-ice interaction problem. The earliest work identified was that undertaken by a number of Russian investigators in the mid 1960's. Among these, the work of Jagodkin [3] and Ignatyev [4-9] is especially significant since it resulted in the development of a so-called Jagodkin model for propeller-ice interaction.

The original Jagodkin model is based on field observations, which suggest that the fracturing of ice by a propeller blade may be represented as a wedge action. Jagodkin used two modes of failure to describe this action: (i) one of pure crushing where the force for crushing the ice is simply the specific pressure for fracturing the ice by crushing times projected blade area; and (ii) one of crushing and cleaving (shearing), where the force necessary to fracture the ice consists of two terms, a crushing force by the leading edge over a width equal to the average blade thickness, and a cleaving force which represents the force necessary to shear the ice which occurs when the region of ice cut away by the blade becomes thin. If the angle of advance (i.e. the relative values of ship speed and propeller rotation rate) is large, the propeller approaches the ice at an angle larger than its geometric pitch angle, and the back of the blade crushes the ice. At a somewhat smaller angle of advance, the propeller approaches the ice at an angle less than its geometric pitch angle and the face of the blade does the crushing. Finally, at low angles of advance, ice is sheared back into the previous blade path.

Several approximations were adopted in the Jagodkin model, notably with regard to propeller geometry and ice properties. In particular, the ratio between the crushing strength and the shearing strength of ice is assumed to be 4, which agreed reasonably well with results from numerous studies on the strength of ice. Also, the pitch angle is assumed to be constant along its length. The Jagodkin model is nonetheless capable of representing the dominant mechanisms involved in the propeller-ice interaction process, particularly milling. Consequently this model came to be regarded as the state of the art methodology for icebreaker propeller design until relatively recently when related investigations were undertaken in North America and the adequacy of the propeller-ice interaction analysis methods was subject to critical reassessment.

Considerable analytical and related experimental work has now been undertaken. It is not surprising that the recent analytical work has been strongly influenced by the original Jagodkin approach and that some improvements on the original Jagodkin model have now been proposed. For instance, a numerical model for the propeller-ice interaction process which has been developed by Kotras et. al. [10] eliminates some of the most serious deficiencies of the Jagodkin model.

To date, the finite element method has not been applied to the problem of estimating propeller-ice interaction loads. It has nonetheless been successfully applied to other forms of milling, such as metal milling, and to a large variety of ice mechanics problems including strength analysis, buckling, elasto-plastic analysis, creep and crack

propagation (fracture mechanics). Recent work by Tomin et al. [11,12] applied the finite element method to problems of ice indentation, complementing a set of laboratory indentation tests performed by the National Research Council of Canada described in the same references. Consequently, there seemed little doubt that increases in sophistication of the propeller-ice interaction model can be attained through use of modern day computerized analysis methods involving finite elements.

1.3 Proposed Improvements in Propeller-Ice Interaction Analysis

The true propeller milling situation involves complex structure-ice-fluid interactions. Ice pressures experienced by the propeller during milling affect propeller speed and deflections which in turn influence cutting parameters and thus ice pressures. Also since the propeller-ice interaction process is dynamic and takes place in a fluid environment, some hydrodynamics is also involved.

The most direct method of investigating the propeller-ice interaction problem involves the finite element modelling of three related components: the propeller, the ice block and the surrounding fluid. However, this method is expected to be computationally costly not only because of the nonlinearities involved but also because of the magnitude of the three constituent components and coupling between them. Within the ice block extremely complex failure processes must be described. Also, at the interface between the propeller and ice block, sliding-contact conditions must be simulated. Unless some simplifying assumptions are made, the computational costs for analysis could not be justified. Of concern also is that due to the magnitude of these costs, the simulations would be limited to only a few blade configurations and sets of operational circumstances. This would make it difficult to extrapolate to other situations and employ the results for design purposes.

To significantly reduce the costs, the analyses of the propeller blade and the ice block must be uncoupled. Consequently, the first major simplifying assumption to be adopted is that the propeller is to be treated as a series of chordwise strips and the propeller ice interaction process on each strip is to be independent of adjacent strips. This has the advantage of reducing the ice block problem to two-dimensions which is much less expensive and hence permits many different milling configurations to be investigated. When considering the ice block processes, the propeller blade is assumed to be rigid and the influence of propeller deformation on the ice milling process is ignored. In addition, it is assumed that the propeller rotates at constant speed. Variations in propeller speed can be determined from a detailed investigation of the dynamics of the ship propulsion system, but this consideration is ignored within the present investigations. In spite of these assumptions, a rather complicated three-dimensional milling problem nonetheless remains for investigation. Consequently, a number of additional approximations particularly related to the behaviour (failure) of the ice block are adopted.

Three programs are involved in the solution process to determine displacements and stress levels in a propeller subject to ice loads. The first is the nonlinear program ADINA, employed to analyze the complicated nonlinear response of ice strips under the action of a rigid blade. ADINA is a commercial program available for use at computer bureaus.

The second program is PVICE. It identifies loaded areas of propeller blade surfaces on each strip at selected angular positions in its passage through an ice block and determines pressure loads for the propeller-ice interaction process. In general, each propeller blade operates in the shadow of the previous one and experiences pressures on part of the aft facing surface. However, under extreme circumstances the drive engines may stall and the propeller blade will drag through the ice block. PVICE is sufficiently flexible to cope with this range of operational conditions. Using results of two-dimensional simulations, PVICE defines ice pressures on loaded areas of propeller blades. The idealized chordwise pressure distributions, when converted into consistent load vectors, are suitable for direct input to a special purpose propeller analysis program, PVAST [13], based on the finite element method. The program PVICE can be modified quite readily to interface with alternate linear finite element analysis programs. This program has been developed under the current contract.

The third program is PVAST which is used to determine the propeller displacements and stresses under action of the computed propeller-ice interaction pressures. Determining the propeller response to computed ice pressure loads involves the straightforward application of well established procedures of the finite element method [14]. Programs other than PVAST can be utilized. The advantage of PVAST is that, being specially developed for stress and vibration analysis of propellers, it can cope reliably and efficiently with complicated propeller geometry detail. PVAST is one component of the comprehensive suite of vibrations and stress analysis programs for ship structures centered on the finite element program VAST [15] which has been developed by Martec for other clients.

1.4 Mechanical Properties of Ice

Finite element analysis of the ice block requires more detailed information on the mechanical properties of sea ice in addition to the uniaxial tensile strength, uniaxial compressive strength, and shear strength of ice that were required by the original Jagodkin models for propeller ice interaction. Accuracy of the finite element analysis of the ice block depends very much on how well all of the mechanical characteristics of ice can be reproduced numerically in the material models within the finite element programs. Consequently, an exhaustive literature search was conducted and a state of the art bibliography compiled on the mechanical characteristics of ice behaviour.

As is well known, sea ice is an extremely complex material and modelling it represents a very challenging engineering analysis problem.

Sea ice is an anisotropic crystalline solid containing air bubbles, pockets and films of brine, and sometimes solid salts. That mechanical properties are highly variable with observed dependencies on various environmental factors such as temperature and salinity, as well as crystal structure is well documented. Representative values of ice strength were selected for use in ice block simulations.

Experimental data also provides considerable evidence that ice characteristics are very greatly influenced by loading (strain) rate. At high rates of loading representative of propeller-ice interactions, ice displays brittle characteristics in the form of microcracking damage and associated irreversible deterioration of mechanical properties. Because of the possibility of high density microcracking, it is not feasible for numerical simulation purposes to track individual cracks and thus cracks must be accounted for in a continuum sense. Strain softening is one manifestation of microcracking and any material model selected should be able to represent this process. Conventional elasto-plastic material models available in most nonlinear finite element codes are inappropriate for modelling strain softening. The literature search identified several different alternative brittle material models of varying sophistication. One of these alternate material models, a smeared-crack damage material model generally used for the analysis of concrete and available within the ADINA finite element program is adopted for the purposes of this study. Parameters appropriate to sea ice, of course, have to be identified for the material model within the ADINA program. A typical three-dimensional failure surface, nondimensionalized with respect to uniaxial compressive and tensile strength values is therefore used. In addition, confining effects and microcracking damage are accounted for. However, the material model used cannot describe the damage existing in naturally produced sea ice (in the form of air bubbles, brine pockets and films, and cracks). Provisions for extrusion processes was not possible either. These effects will have to be addressed in future work.

For the ADINA damage model, the shape of the failure surface in the compressive octant of principal stress space is defined as a series of piecewise linear contour lines. The failure surface in the remaining octants of stress space is faceted and, being fully defined by only the unconfined uniaxial compressive and tensile strengths of ice, is much less general. The uniaxial compressive and tensile strength values themselves are highly variable and depend strongly on strain rate. Some difficulties were encountered in locating suitable data defining each of the above-mentioned material characteristics for ice with sufficient detail and reliability. Consequently, a number of approximations had to be adopted in the implementation of this damage model to ice problems as shall be described later. The failure surface as defined by experiments of Hausler [16] was employed. It is assumed that variations of the failure surface (arising from strain rate effects for instance) will be limited to the required inputs of uniaxial strength values. If necessary, dynamic conditions would be accounted for by adopting material properties appropriate for the loading rates encountered.

1.5 Two-Dimensional Ice Block Simulations

Because of concerns about the adequacy of the adopted constitutive description of ice, initial simulations involve the analysis of two-dimensional indentation problems for several different geometries including rectangular, wedge, circular and elliptical shapes under the idealized conditions of plane stress and plane strain. Because of the large amount of data preparation, modelling procedures must be automated. A model generation program for two-dimensional ice block indentation simulations is described. It is called IDENTM. The numerical simulations of two-dimensional indentation utilized both the smeared-crack damage material model described above and the Drucker-Prager elasto-plastic material model. For rectangular indentors, conditions of perfect contact are assumed in the sense that neither interface sliding nor interface separation are permitted. For other types of indentors, rod elements are employed to assign prescribed displacement boundary conditions on the interface. As a result, interface sliding is effectively permitted. The effects of interface friction are also investigated using representative values of interface friction identified in the literature search for mechanical properties. In each case, resultant pressure distributions along the contact surface are determined and associated indentation forces are computed. A comparison of the computed forces to experimental results are performed where possible.

Analyses of two dimensional pseudo-static milling (slicing) simulations are also performed as part of this study. Only the damage material model is used. Dynamic conditions were accounted for by adopting appropriate material properties which in essence scale the failure surface. In these milling simulations, ice experiences stress conditions which involve much less confinement and thus cracking plays a much more prominent role in the failure of the ice block.

Several other developments in procedures are required for milling simulations, including provisions for formation of gaps along the blade ice contact surface. Accounting for blade-ice separation properly in ice milling simulations is difficult if it is to be achieved through repeated manual examination of finite element stresses for ice in the contact region, adjustment in the number of nodes with prescribed displacement boundary conditions, and reanalysis. Implementation of rod elements orientated normal to the blade-to-ice contact interface (surface) are proposed since this permits prescribed displacement increments to be applied to the ice block yet permit frictionless sliding of ice along the interface without any reanalysis. Assigning nonlinear material properties to rods ensures that significant rod forces develop only if strains are compressive. Large stiffnesses (large slope in the stress-strain curve) are associated with compressive strains and comparatively small stiffnesses with tensile strains. Consequently, rod elements automatically define required blade-ice separation without any user iterative modifications to the finite element model. Provision of rods as gap elements also simplifies the computation of contact forces. A special modelling program called MILLM is developed. It should be noted that

since the thickness of the cutter is ignored, details on leading edge geometry need not be supplied.

The dependence of contact force and associated pressure distributions along the contact surface are investigated. A number of simulations have to be performed, several under both plane stress conditions and under plane strain conditions. A number of different cutting angles and widths must also be considered.

1.6 Basic Concepts in the Propeller-Ice Interaction Load Generation

The purpose of the computer program PVICE developed under this contract is to automatically generate loads for a finite element analysis of a propeller blade subject to ice milling with PVAST. As mentioned earlier, it treats the propeller as a series of chordwise strips and determines the loaded areas of each strip at selected angular positions in the passage of the propeller blade through an ice block. It utilizes the results from two-dimensional simulations of the ice block in the determination of loads on each strip. Time variation of loads in two-dimensional milling simulations are ignored. Because a limited number of simulations are undertaken, interpolation functions are defined to express the functional variation of forces on cutting parameters and material properties. For instance, a biquadratic function for the dependence of contact force on cutting angle and width is defined from the nine plane strain simulations. Standard interpolation (extrapolation) procedures can then be employed to determine contact force for cutting angles and widths not considered in the ADINA simulations.

Propeller geometry details obviously influence the determination of loaded areas of the propeller blade and hence must be supplied. In addition, the user must specify other variables affecting the propeller-ice interaction process including cutting depth, ship speed and shaft RPM which influence loaded areas of the blade surfaces. Various mechanical properties of ice are also input including crushing strength of ice (for purposes of scaling the yield surface) and the coefficient of friction (for the interface between the ice block and the propeller blade). The propeller loading model, PVICE, permits a high degree of flexibility in the mathematical description of the chordwise blade pressure distributions. Nonetheless some idealizations are implemented. Despite idealizations made on the pressure distributions, total force on each strip is adjusted to be equal to the predictions of simplified indentation and milling simulations in two dimensions. The idealized chordwise pressure distributions, when converted into consistent load vectors, are suitable for direct input to PVAST. The restriction that blade pressure loadings adhere to finite element boundaries was also eliminated in this way.

1.7 Comparison to Full Scale Results

The PVICE program, developed for the determination of propeller ice interaction loads, was applied in combination with PVAST to determine the response of a typical icebreaker propeller blade in its passage through

an ice block. Two different propeller loading options available in PVICE are investigated. Firstly, a uniform pressure distribution is applied on only that portion of the propeller blade which is actually submerged within the ice block. This differs from the analyses conducted in Phase 1 investigations where uniform loads were applied over portions of the propeller blade under the restriction that blade pressure loadings adhere to finite element boundaries which generally approximates rather crudely the actual ice loaded regions. The second loading option involves non-uniform pressure distributions in contact with ice (accounting for blade shadowing effects). Three different cutting radii and 10 different equi-spaced angular positions of the blade are considered. To investigate the effects of friction, one of the loading cases is studied with coefficients of friction ranging between 0.1 and 0.4. To determine the effects of dynamic loading on the blade, the uniform pressure load is also applied in the form of a dynamic load at a fixed propeller speed. Emphasis is on identifying the location of maximum stress and the nature of stress variation.

As a validation of the computer procedure developed for the analysis of the propeller-ice interaction process, comparisons are made between predicted ice induced thrust and torque with available experimental data for a range of ship speed and propeller RPM. Variation of ice thrust, torque and bending moment against variation in angle of attack are investigated. A comparison is also made between measured and predicted peak milling loads (thrust and torque).

1.8 Organization of Report

The work was carried out in the following phases:

(i) State of the art bibliography and literature survey.
(ii) Development of a computer program to generate the loading for a finite element analysis of a propeller blade subjected to ice milling.
(iii) Definition of the mechanical properties of ice.
(iv) Determination of the distribution and limiting values of propeller-ice interation pressure using the finite element model of the ice block.
(v) Application of the procedures developed to the analysis of a typical icebreaker propeller blade.
(vi) Identification of possible future experimental work necessary or desireable in order to verify results.

Phases (i) to (v) of the work are discussed in detail in Sections 2.0 to 6.0 of the report. Conclusions and recommendations for future work are given in section 7.0.

2.0 LITERATURE SURVEY AND STATE OF THE ART BIBLIOGRAPHY

Early in this study, a literature search was conducted to identify relevant references. The search concentrated on the following subject categories:

(i) Propeller/ice interaction/milling;
(ii) Ice mechanics/mechanical properties of ice/testing methods;
(iii) Indentation;
(iv) Brittle fracture; and
(v) Metal milling/machining;

and a bibliography was compiled for each of them. Initially the search involved the examination of various subject indexed reference sources including Applied Mechanics Reviews and computer databases such as EM (Engineering Mechanics) and NTIS (National Technical Information Service of U.S. Department of Commerce) available on the Canadian online literature search system called CANOLE. All previous issues of Conference proceedings identified as a forum for potential publications on ice mechanics and ice-structure interaction including POAC (Port and Ocean Engineering under Arctic Conditions), IAHR (International Association for Hydraulic Research), OTC (Offshore Technology Conference), OMAE (Offshore Mechanics and Arctic Engineering), SNAME (Society of Naval Architects and Marine Engineers) Transactions, and Ice Tech were checked. A number of speciality conferences and symposia which dealt with ice mechanics and ice-structure interaction problems were also identified and they include two symposia on Applied Glaciology (papers published in Annals of Glaciology), the IUTAM Symposium on "Physics and Mechanics of Ice", as well as the ASCE speciality conference called ARCTIC'85. Although the majority of the research work was published in conference proceedings, a number of technical journals including Journal of Glaciology were also used to a lesser extent. Publication lists from institutions involved strongly in ice research such as NRC (National Research Council of Canada in Ottawa) and CRREL (Cold Regions Research and Engineering Laboratory in Hanover, NH) as well as from various funding agencies which support this work such as Transport Canada and Transportation Development Centre were obtained and examined.

Because of the increased importance of ice design considerations in modern shipbuilding technology and offshore structural engineering which has been prompted by recent hydrocarbon and mineral exploration in the Arctic, the amount of technical information published on experimental and numerical analysis of both basic and applied ice problems has increased dramatically. This is manifested in a new series of international conferences called Ice Technology, initiated with one at the Massachusetts Institute of Technology in June 1986, and three new technical journals including Cold Regions Science and Technology, Journal of Energy Resources Technology (Transactions of ASME), and Journal of Offshore Mechanics and Arctic Engineering (Transactions of ASME) which are increasing in importance in so far as publications in this field. Consequently, each of the above mentioned bibliographies have been updated on

an ongoing basis to include publications identified during the contract. The updated bibliographies of references are given in Appendix B.

3.0 PROCEDURE FOR GENERATING LOADS FOR A FINITE ELEMENT ANALYSIS OF A PROPELLER BLADE SUBJECTED TO ICE MILLING

3.1 Introduction

The ultimate objective of the work described in this report was to develop improved analysis methods for investigation of propeller responses to propeller-ice interaction forces based on the finite element method. As was demonstrated in an earlier contract [1], the finite element method is particularly attractive for stress analysis of propellers. The finite element method permits a high degree of flexibility in the geometric representations of the propeller. It is possible to account for variations in pitch and skew along the propeller length and for curvatures on the front face, or on the back face or on both. This is important since a number of the analysis methods proposed by other investigators for studies of the propeller-ice interaction process embodied some quite serious approximations with respect to propeller geometry.

In current work, the program module called PVICE was developed to accurately define the loads for a finite element analysis of a propeller subjected to ice milling. The PVICE program basically represents a modification of the Jagodkin model for propeller-ice interaction. The above mentioned generalization of propeller geometry are properly accounted for in load determination. Greater flexibility in the definition of mechanical properties of ice has been provided for and as more information is collected on ice properties, the PVICE program can be upgraded accordingly. The fact that the model can continue to develop in the future as more is learned about ice itself and ice-structure processes is considered to be extremely important.

After reviewing dynamic processes from the finite element point of view and examining the fundamental mechanics of the blade milling process in the following sections, some of the more fundamental concepts important to the organization of the PVICE program are outlined.

3.2 Equations of Motion

The milling of a propeller blade through an ice block is depicted in Figure 3.1. The equations of motion which govern the response of the blade as it passes through the ice can be expressed as follows:

$$([M]+[M_A])\{\ddot{\delta}\} + [C]\{\dot{\delta}\} + [K]\{\delta\} = \{F(t)\} \qquad (3.1)$$

where $[M]$ is the structural mass; $[M_A]$ is the added mass (to account for fluid effects); $[C]$ is the damping matrix; $[K]$ is the stiffness matrix; $\{\ddot{\delta}\}$, $\{\dot{\delta}\}$, and $\{\delta\}$ are acceleration, velocity and displacement vectors, respectively; and $\{F(t)\}$ is the vector of applied forces acting on the blade.

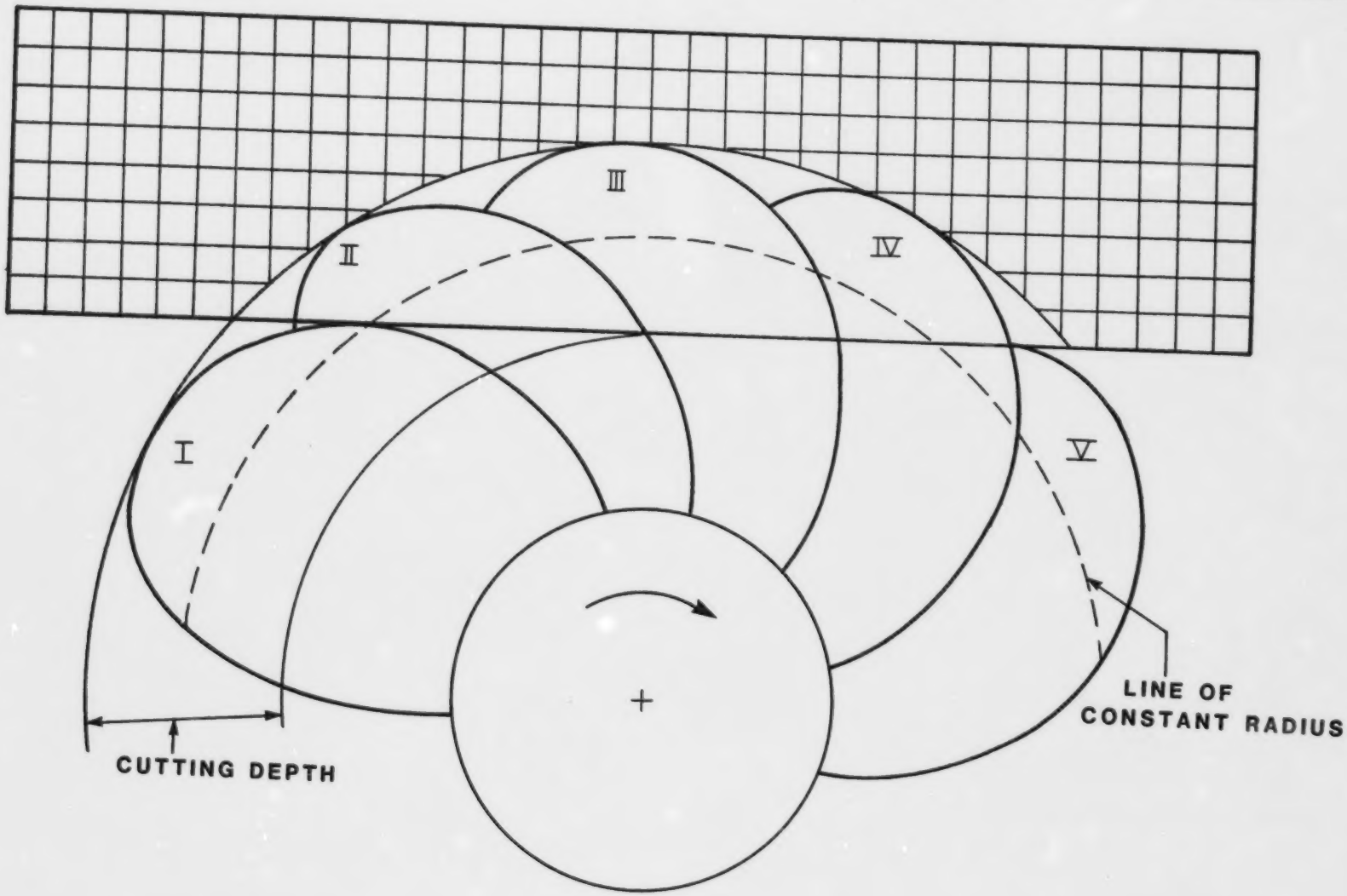

FIGURE 3.1 PASSAGE OF BLADE THROUGH ICE BLOCK

In Equation (3.1), it is assumed that the blade has been discretized by finite elements. A typical FE model of the blade is shown in Figure 3.2. Equation (3.1) is formulated and solved by the finite element program being used (eg. NASTRAN, ANSYS, VAST). The matrices [M], [M_A], [C] and [K] are computed by the FE program. The accelerations, velocities and displacements are obtained in the solution. Once the displacements are known, blade stresses are computed.

The loads required to formulate the force vector {F(t)} must be supplied to the FE program as input. These are the propeller blade-ice interaction forces encountered during the milling process. A procedure for generating these loads has been developed under this contract.

3.3 Mechanics of the Blade Milling Process

Referring to Figure 3.1, five positions of the blade as it passes through the ice block are shown, i.e. position I, where the blade is just entering the ice block, positions II, III, and IV, where the blade is embedded in the ice block, and position V, where the blade is just leaving the ice block. Also, shown in Figure 3.1 is a line of constant radius. Cutting views of the blade section at the line of constant radius for positions II, III, and IV are shown in Figure 3.3.

The condition shown in Figure 3.3 is for the case when the angle of advance (i.e. the relative values of ship speed and propeller rotation rate) is such that the face of the blade is loaded. For a fixed-pitch propeller, this corresponds to situations where the ship is moving forward, the propeller (right-handed) is rotating clockwise, and the angle of advance is less than the geometric pitch angle. As the speed of the ship is increased and/or the propeller RPM is reduced, the angle of advance will become large and will at some point exceed the pitch angle. When this occurs, the back of the blade will become loaded. In each of these conditions, the leading edge is loaded first. However, when the ship is operating in the reverse mode, the opposite situation will occur, i.e. the trailing edge of the blade will be loaded first. Again, depending on the ship speed and propeller RPM, either the face or back of the blade can be loaded. A graphical presentation of milling conditions in relation to angle of advance is shown in Figure 3.4.

The form of milling described above is commonly referred to as the crushing mode. In this mode, the blade effectively cuts a path through the ice which has a width equal to the projected width of the blade in the direction of the resultant velocity (shown in Figure 3.4). The first blade to encounter the ice (under start up conditions) will be subjected to this crushing mode condition. With a high ship speed and a low propeller RPM, the other blades will be subjected to this condition as well. In many cases, however, the ship speed and propeller RPM will be such that 'shadowing' will occur. This refers to the situation when a blade encounters part of the path created by the preceding blade. Two different forms of shadowing can occur, as demonstrated in Figure 3.5. One, as shown in Figure 3.5(a), involves combined shearing and crushing

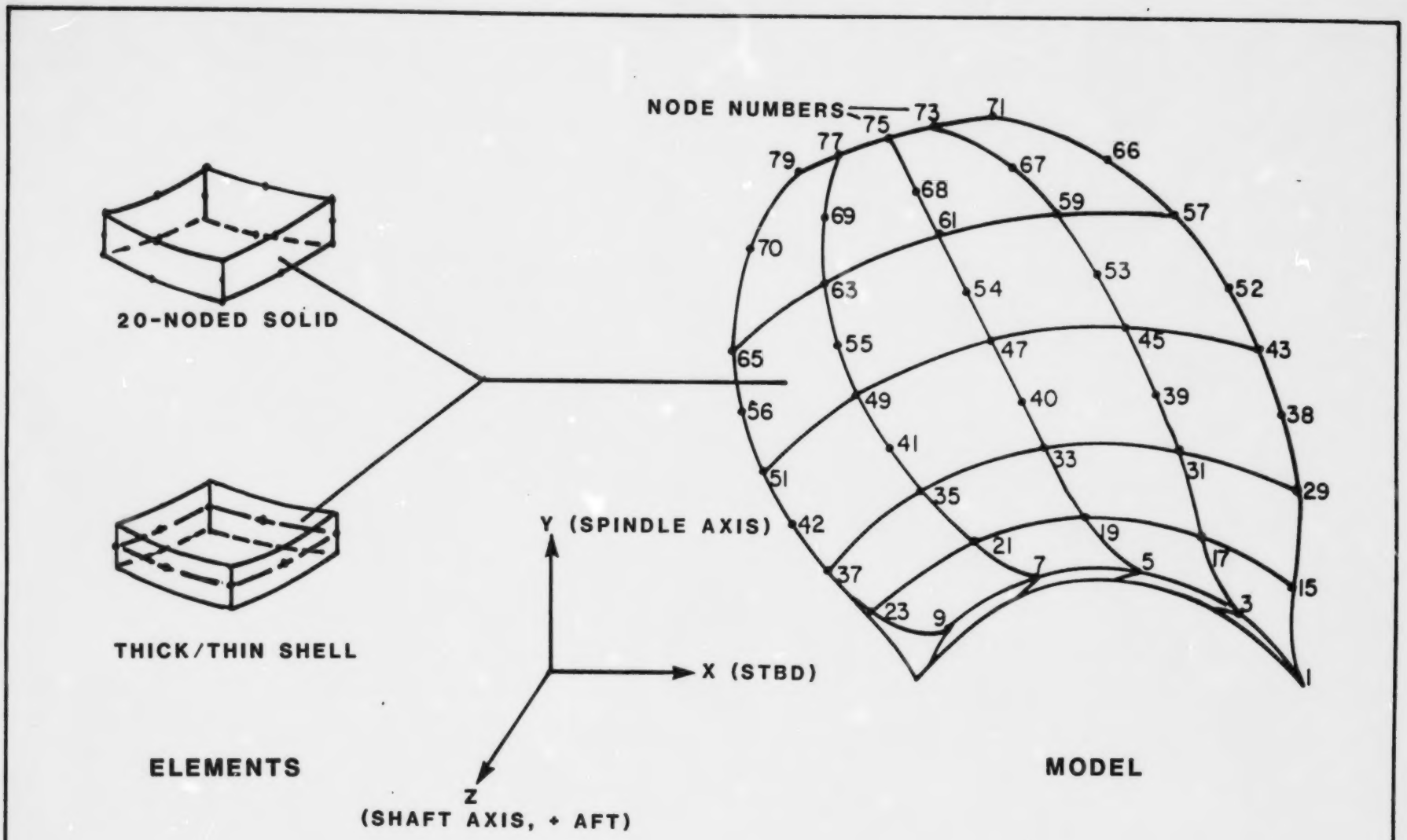

FIGURE 3.2 FINITE ELEMENT MODEL OF BLADE

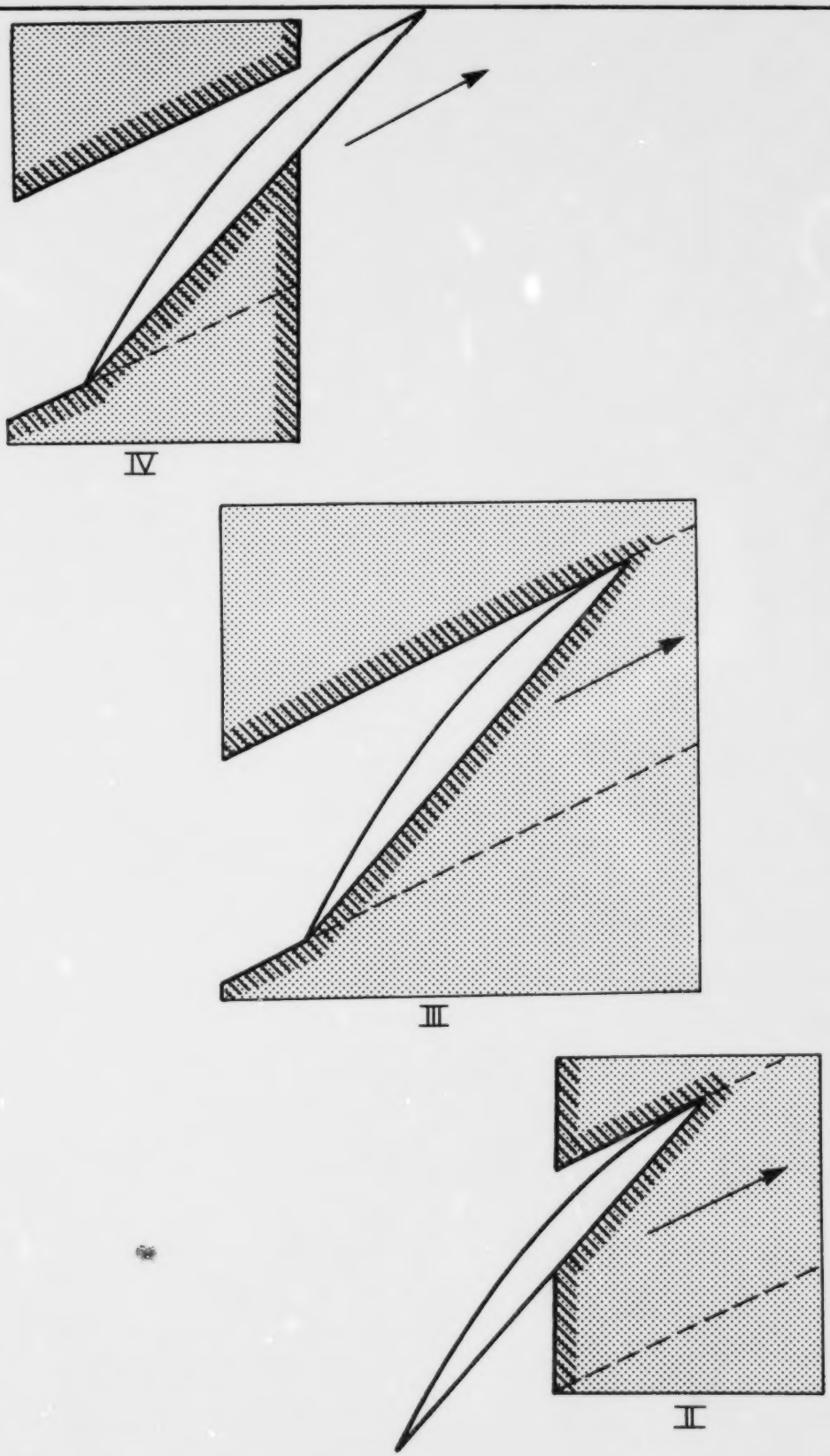

FIGURE 3.3 CUTTING VIEWS OF BLADE SECTION

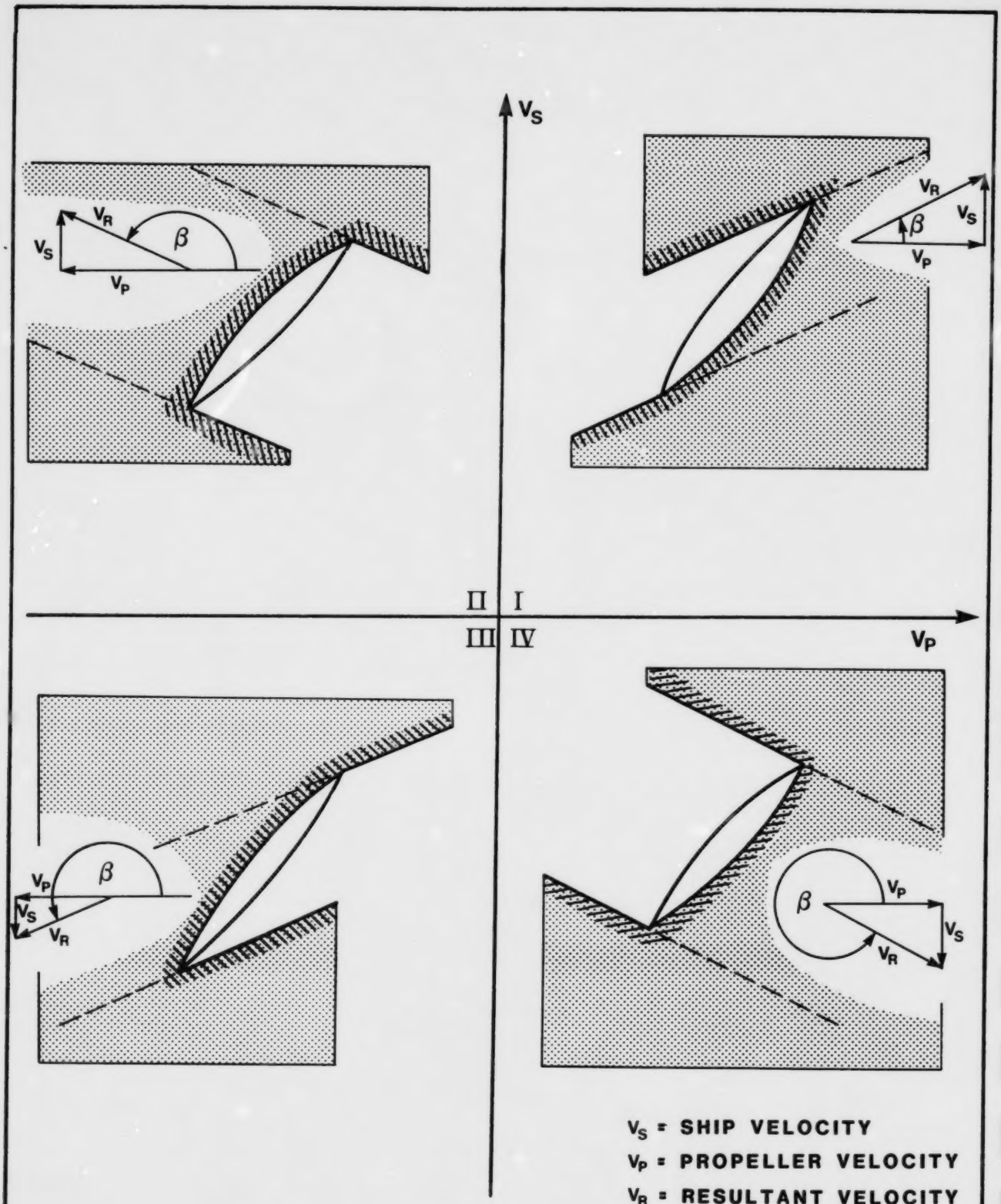

FIGURE 3.4 ICE MILLING CONDITIONS IN RELATION TO ANGLE OF ADVANCE

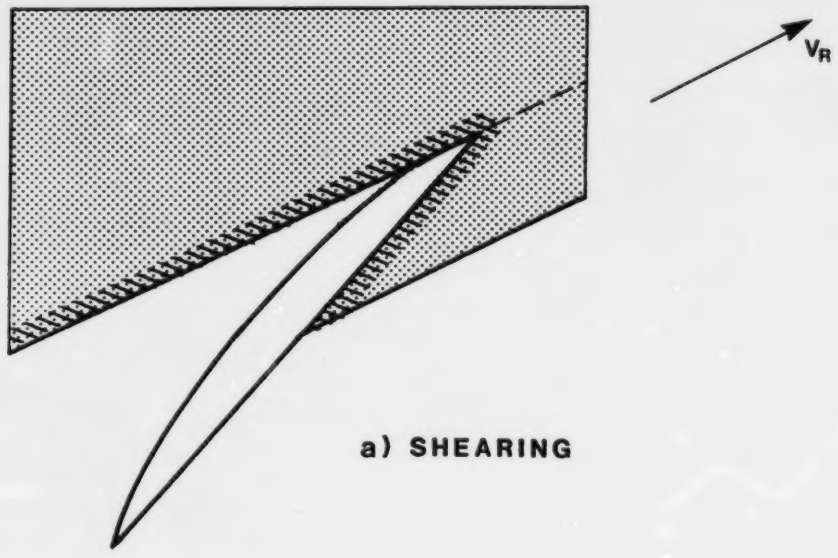

a) SHEARING

b) CRUSHING

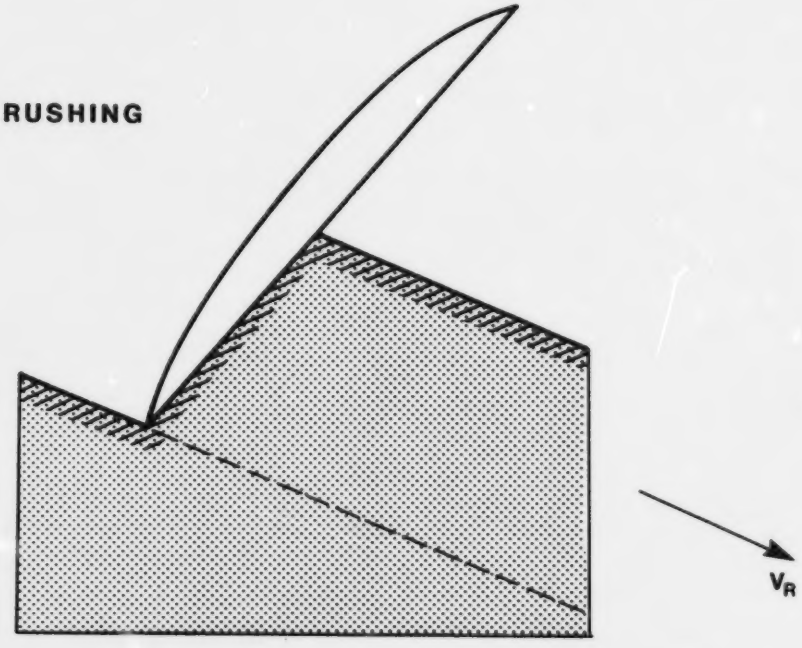

FIGURE 3.5 DIFFERENT FORMS OF SHADOWING

of the ice. This is commonly called the shearing or slicing mode (the term "shearing" will be used in this report), since ice shearing predominates, and is analogous to conventional milling in a lathe [17-21]. The other, as shown in Figure 3.5(b), involves primarily ice crushing. In Figure 3.5, it is assumed that the blade is rotating clockwise. In the shearing mode, the ship is moving ahead, and the leading edge of the blade is loaded. In the crushing mode, the ship is moving in reverse, and the trailing edge is loaded. If, on the other hand, the blade is rotating counter-clockwise, the leading and trailing edges will reverse roles, i.e. the leading edge will be crushing the ice, while the trailing edge will be shearing the ice.

The true propeller milling process involves a complex structure-ice interaction situation. Ice pressure, and thus blade loads, will depend on cutting depth, blade geometry, ship speed, propeller RPM, and the mechanical properties of the ice. This ice pressure will affect propeller speed, ship speed, and cause blade deflection, all of which, in turn, will influence cutting parameters and thus ice pressures. From the discussion of ice mechanics in Section 4.0, it is obvious that a two-dimensional treatment of the ice itself will reduce the complexity of the problem. The problem will be simplified even more if the blade is assumed rigid and the ship speed is assumed constant. These two assumptions are probably justified since the period of loading is small. Furthermore, if the propeller rotational speed remains constant, the angle of advance for a particular radial position on the blade will be constant, and this will reduce the complexity of the problem also. These limitations have been incorporated into the computer program described in Section 3.4.

However, in reality the propeller rotational speed is very much influenced by the ice pressure. As milling begins, torque exerted on the shaft due to ice loads increases as the blades cut into the ice, which also results into greater axial thrust on the shaft. Due to increased torque, the propeller speed is reduced, and the angle of attack of the radial section of the blade is reduced or becomes negative. With this in mind, the program has been structured in such a way that a capability to handle a non-constant blade RPM can be easily incorporated. Obviously, the relationship between torque (which is computed by the program) and blade RPM would have to be defined.

3.4 Computer Program PVICE

A computer program called PVICE has been developed for automatically generating loads for a finite element analysis of a propeller blade subjected to ice milling, as defined and quantified in the following paragraphs. More specifically, it generates the load vector $\{F(t)\}$ defined in Equation (3.1) and produces a table summarizing resultant forces and moments (torque). It is assumed that the program VAST [15] is being used to perform the finite element analysis, and the blade has been modelled using the thick/thin shell element or the 20-noded solid element both of which are available in VAST. It should be noted that PVICE could

be easily modified to accommodate any finite element program offering either one of these elements. In its present form, the load file PREFX.LOD in the VAST format is generated.

Input to PVICE consists of blade detail supplied in the form of a blade finite element model in file PREFX.GOM (again in the VAST format), cutting depth, ship speed, propeller RPM, number of blades, crushing strength of ice and coefficient of friction.

The program divides the blade into a finite number of segments of width ΔR, R being the blade radius. These segments are defined by blade sections of constant radius, as shown in Figure 3.6. The location of segment i is defined by the radius R_i.

The cross-section for each segment is unwrapped onto a x'z' plane as shown in Figure 3.7. The x' axis is in the direction of advance, passing through the leading edge of the blade.

For each section, the parameters W_1 and W_2, as shown in Figure 3.8, are determined. W_1 is defined as the projected width of the section, in the direction of advance. W_2 is the width of ice in the blade's path, taking into account the path created by the preceding blade (i.e. the shadowing effect). As shown in Figure 3.8, three different situations can occur. One relates to either the first blade to encounter the ice, or subsequent blades when the ship speed is large compared to the rotational velocity of the section. In this situation, Figure 3.8(a) W_2 is considered to be very large, and the section must mill (crush) an ice path of width W_1. Another situation occurs when W_2 is less than or equal to W_1, Figure 3.8(c), and dictates milling in the shearing mode. The third situation, shown in Figure 3.8(b), occurs when W_2 exceeds W_1, but is still within the range to dictate milling in the shearing mode. At present the cut off for shearing in PVICE was arbitrarily taken as $W_2 < 2W_1$, but another criteria can be easily incorporated. The method for calculating W_2 is shown in Figure 3.9.

With W_1 and W_2 determined, the form of ice loading on the face and back of a section is identified as described in Section 5 of this report. For the face, two forms of loading are possible: if the face is crushing the ice, the P_1 type pressure distribution, shown in Figure 3.10 is used; if the face is shearing the ice, pressures are concentrated at the leading edge and consequently the concentrated force F shown in Figure 3.11 is used. The angle ϕ has been selected somewhat arbitrarily. The program can be modified to calculate the resultant force directions by integrating the pressures over the variable surface normal. If the back of the section is loaded, either the P_1 type pressure distribution, shown in Figure 3.12, or the P_2 type pressure, shown in Figure 3.13 is used.

The program PVICE has been designed to accommodate P_1, P_2 and F (force per unit width) represented as functions of the geometric parameters a, b, W and r, as shown in Figures 3.14 and 3.15. Curves such as

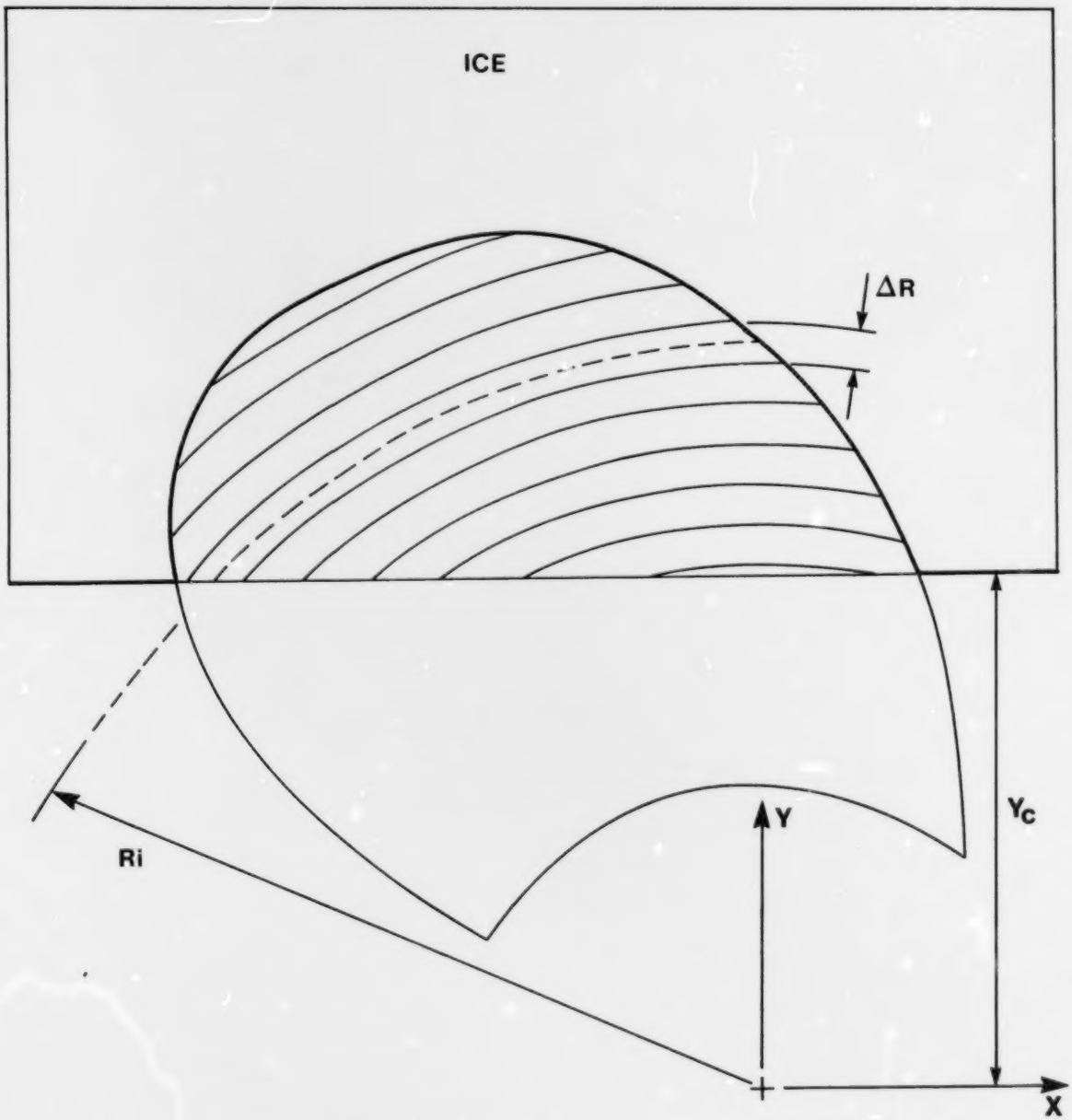

FIGURE 3.6 SEGMENTED BLADE EMBEDDED IN ICE

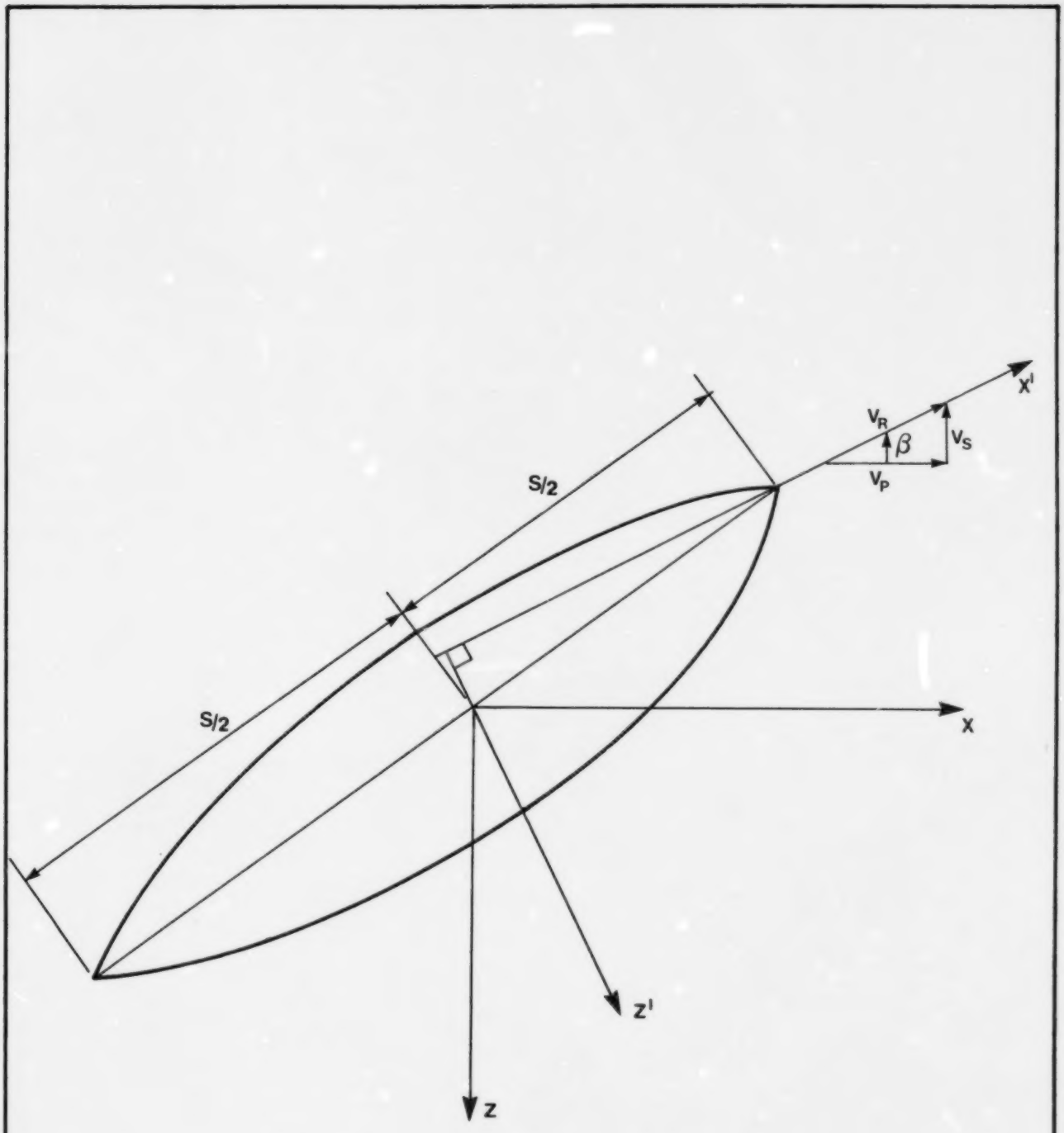

FIGURE 3.7 BLADE SECTION UNWRAPPED ONTO X'Z' PLANE

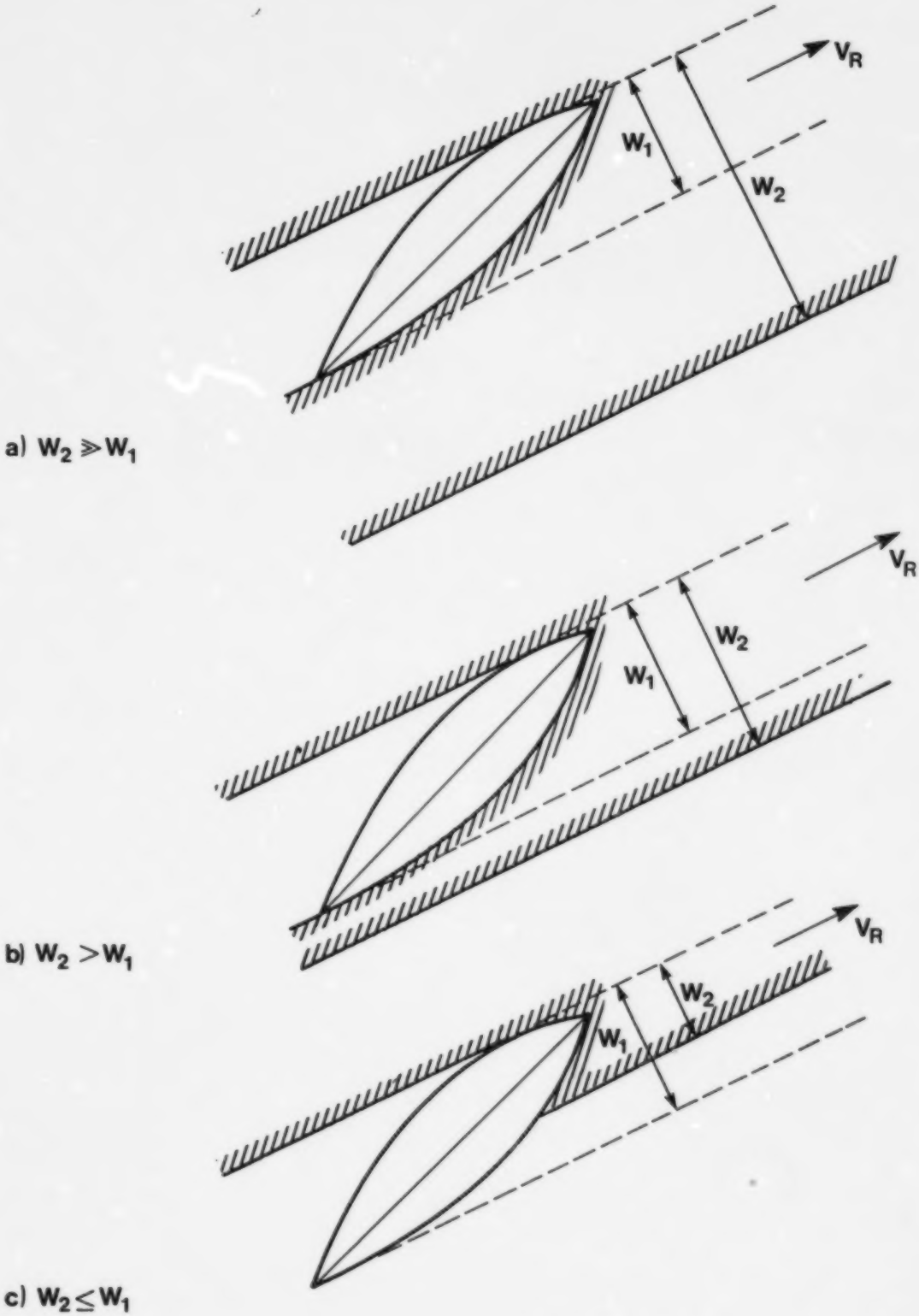

FIGURE 3.8 RELATIONSHIP BETWEEN W_1 AND W_2

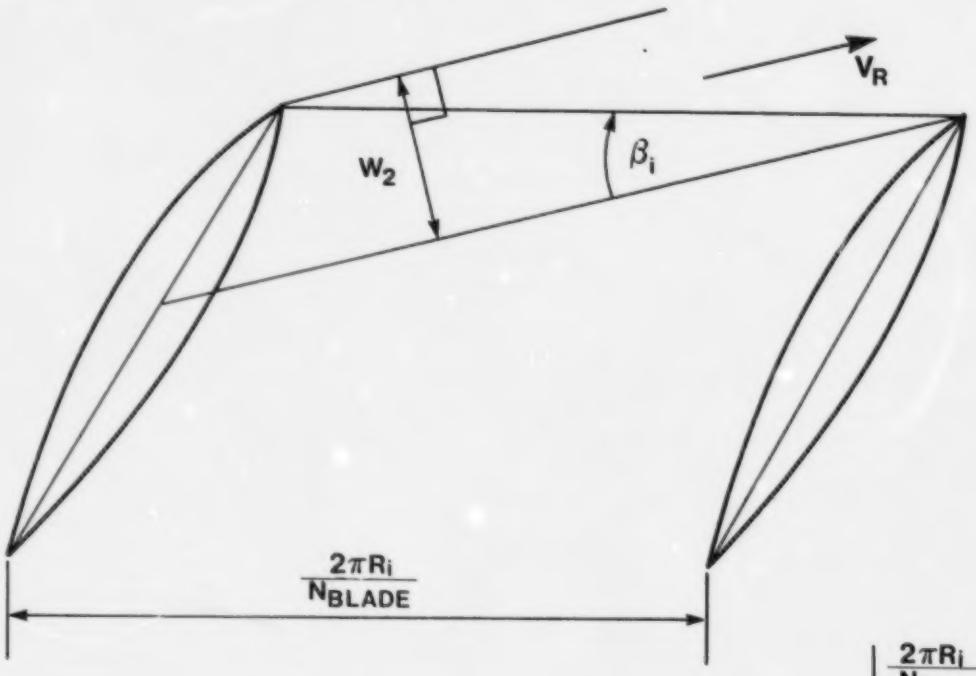

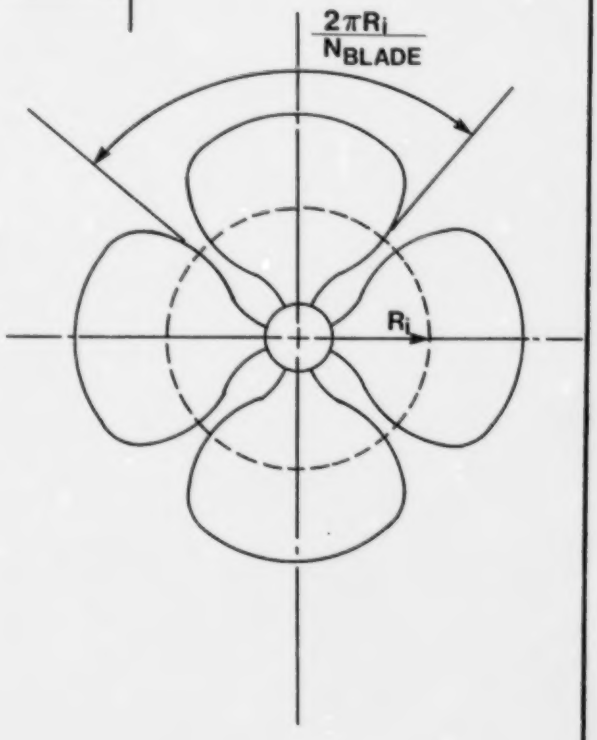

$$W_2 = \frac{2\pi R_i}{N_{BLADE}} \sin \beta_i$$

N_{BLADE} = NUMBER OF BLADES

β_i = ANGLE OF ADVANCE

FIGURE 3.9 CALCULATION OF W_2

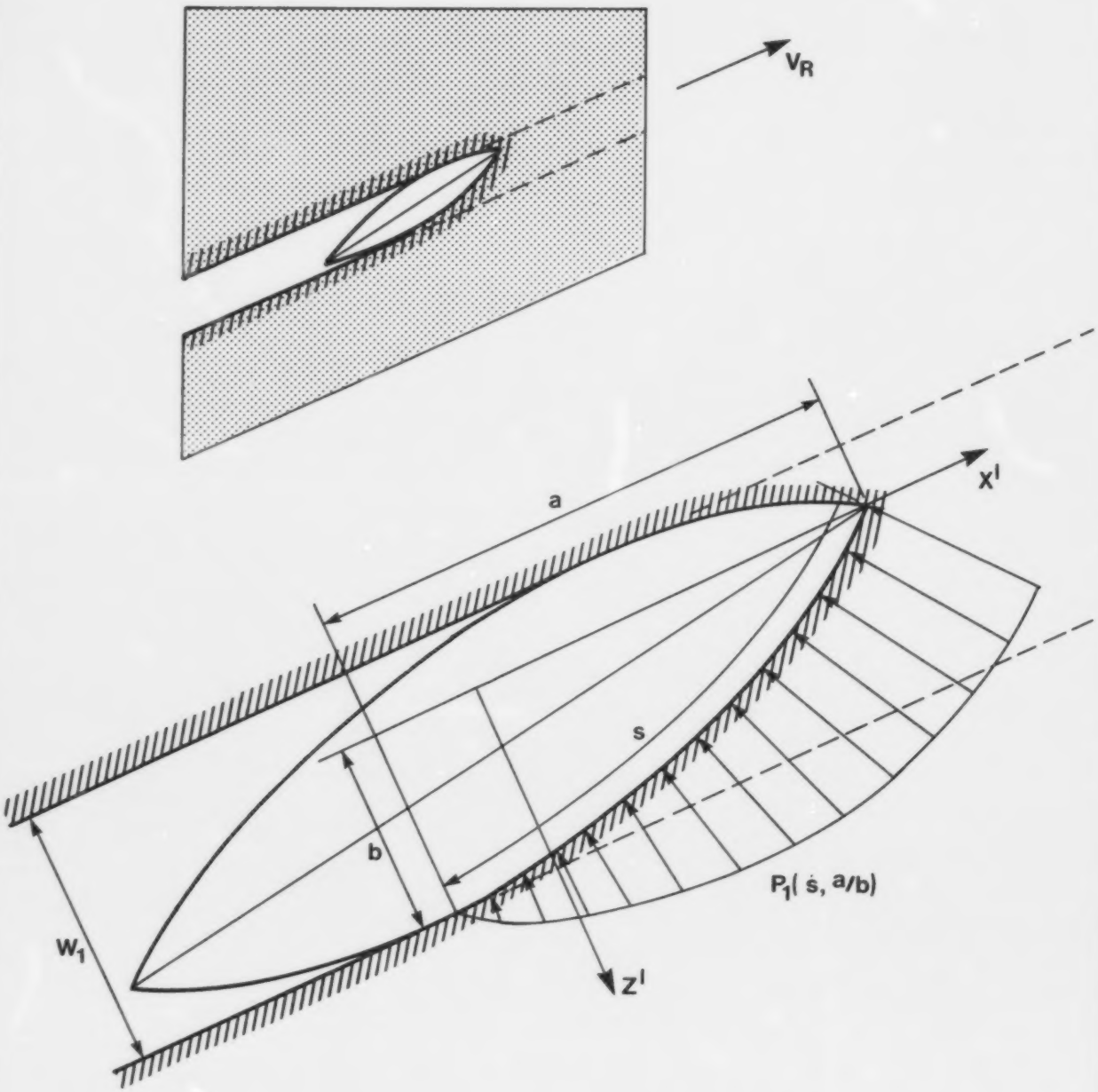

FIGURE 3.10 ICE LOADING ON FACE OF BLADE SECTION - CRUSHING MODE

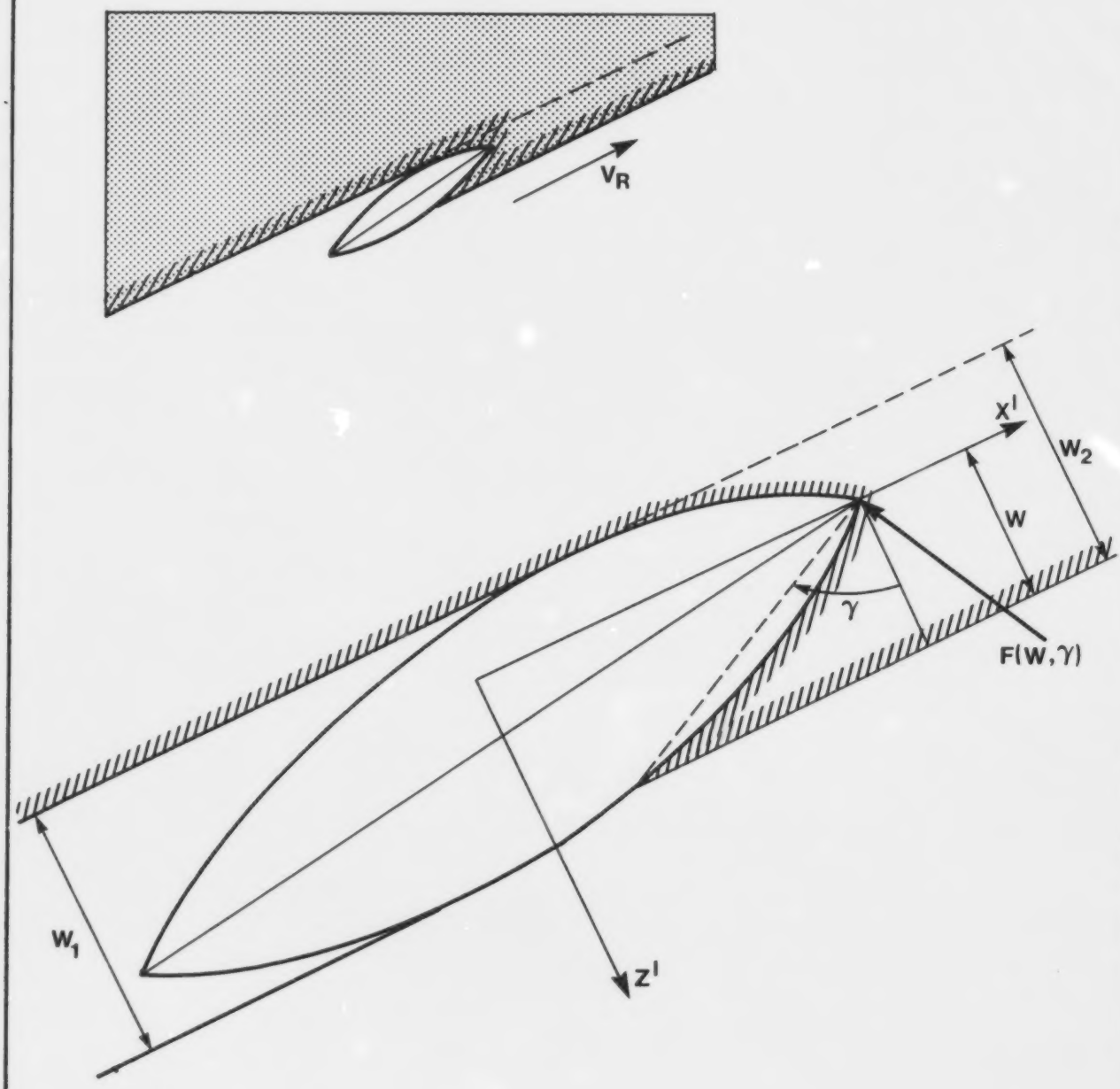

FIGURE 3.11 ICE LOADING ON FACE OF BLADE SECTION - SHEARING MODE

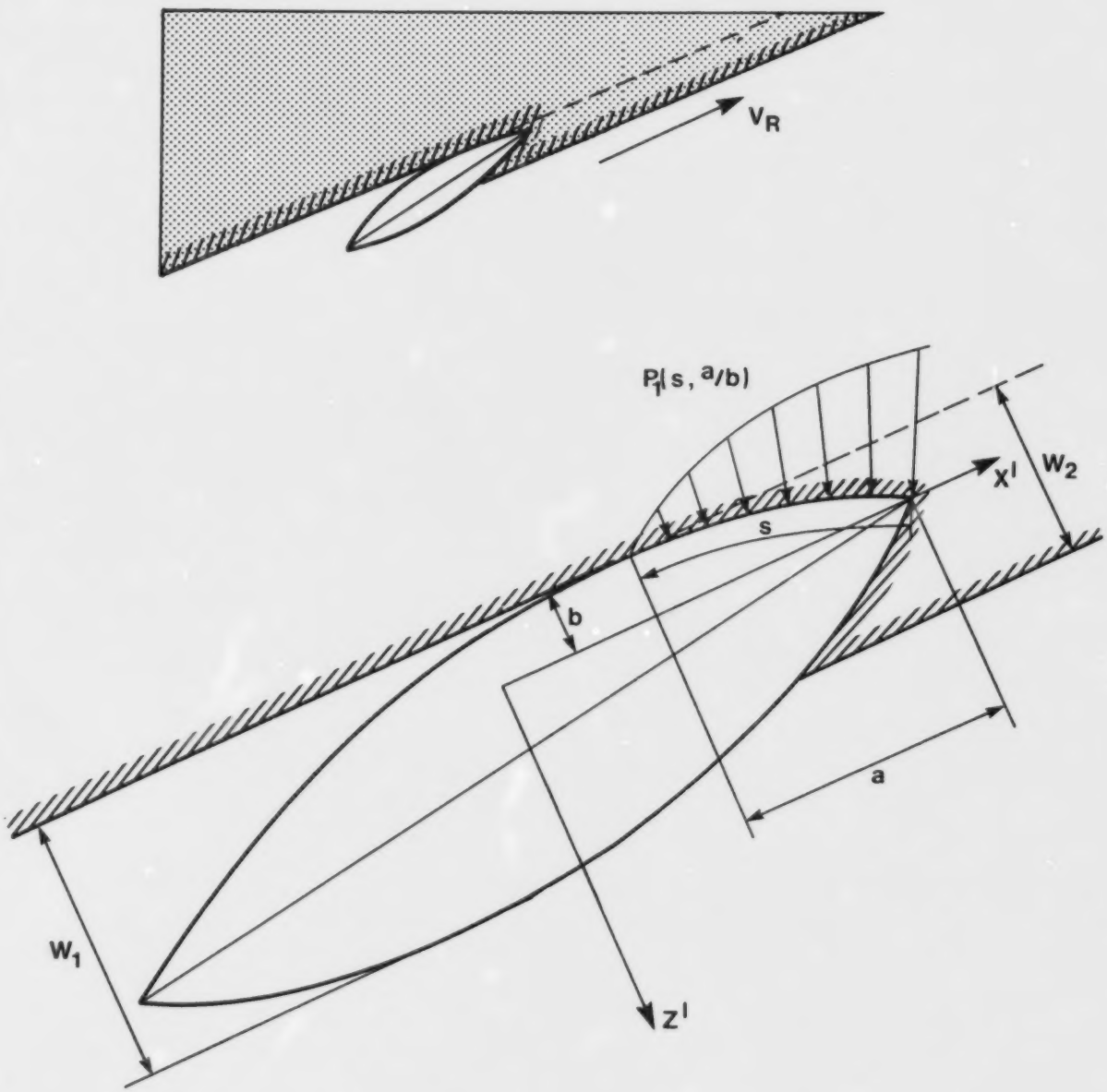

FIGURE 3.12 ICE LOADING ON BACK OF BLADE SECTION - $W_2 > b$

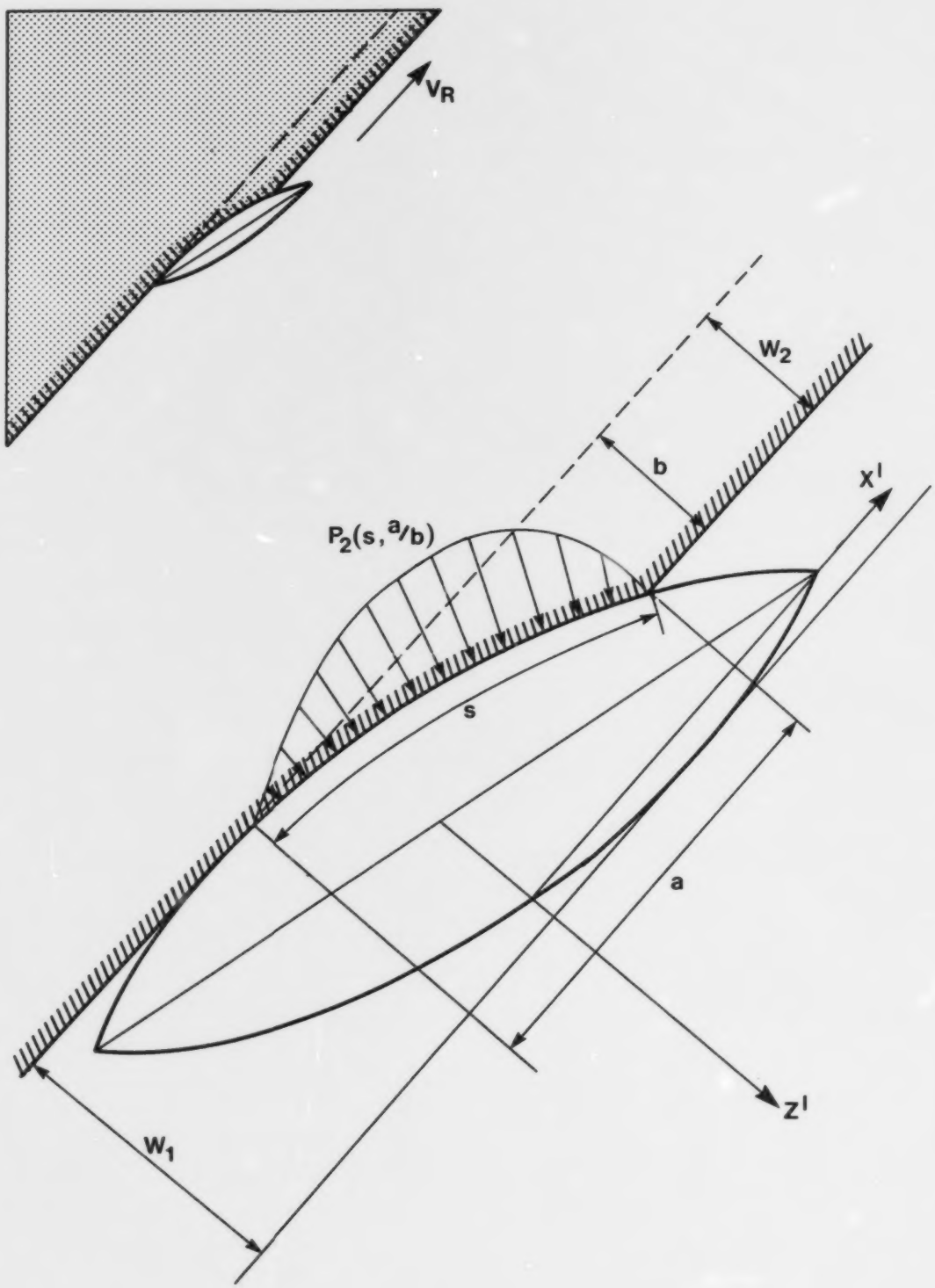

FIGURE 3.13 ICE LOADING ON BACK OF BLADE SECTION - $W_2 = b$

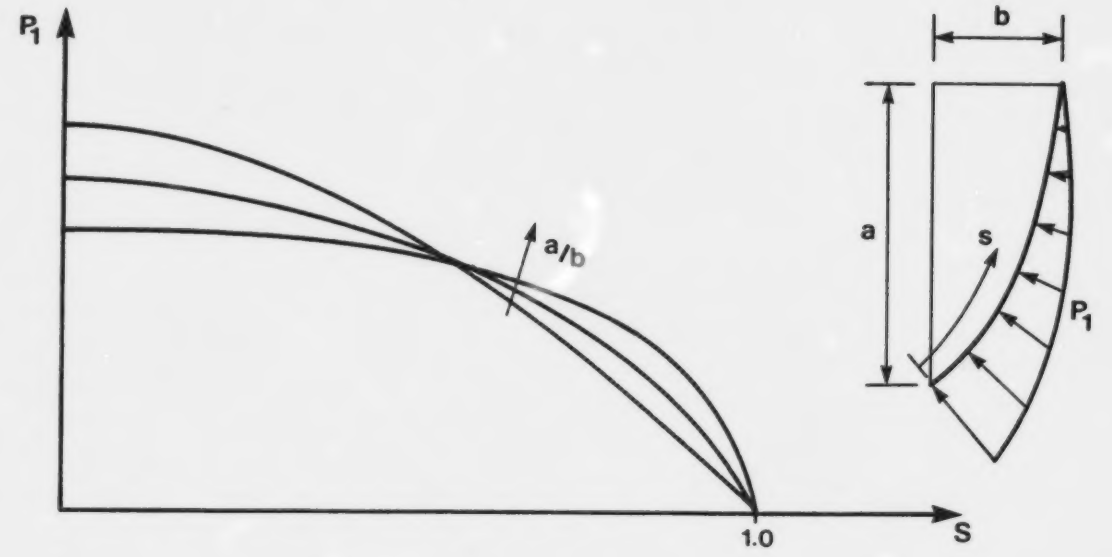

a) P_1 TYPE DISTRIBUTION

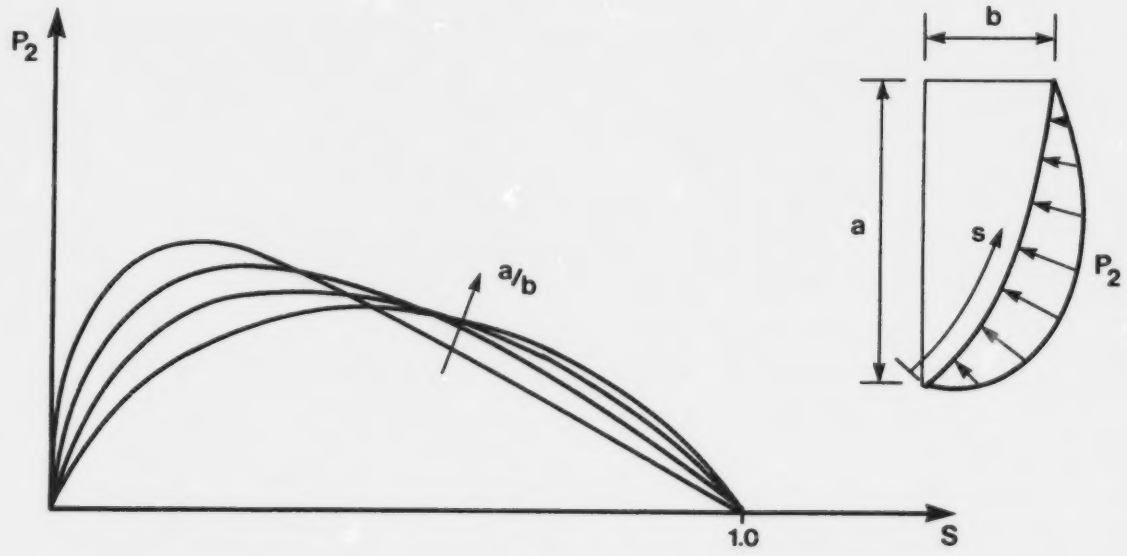

b) P_2 TYPE DISTRIBUTION

FIGURE 3.14 REPRESENTATION OF ICE CRUSHING PRESSURE AS A FUNCTION OF GEOMETRIC PARAMETERS

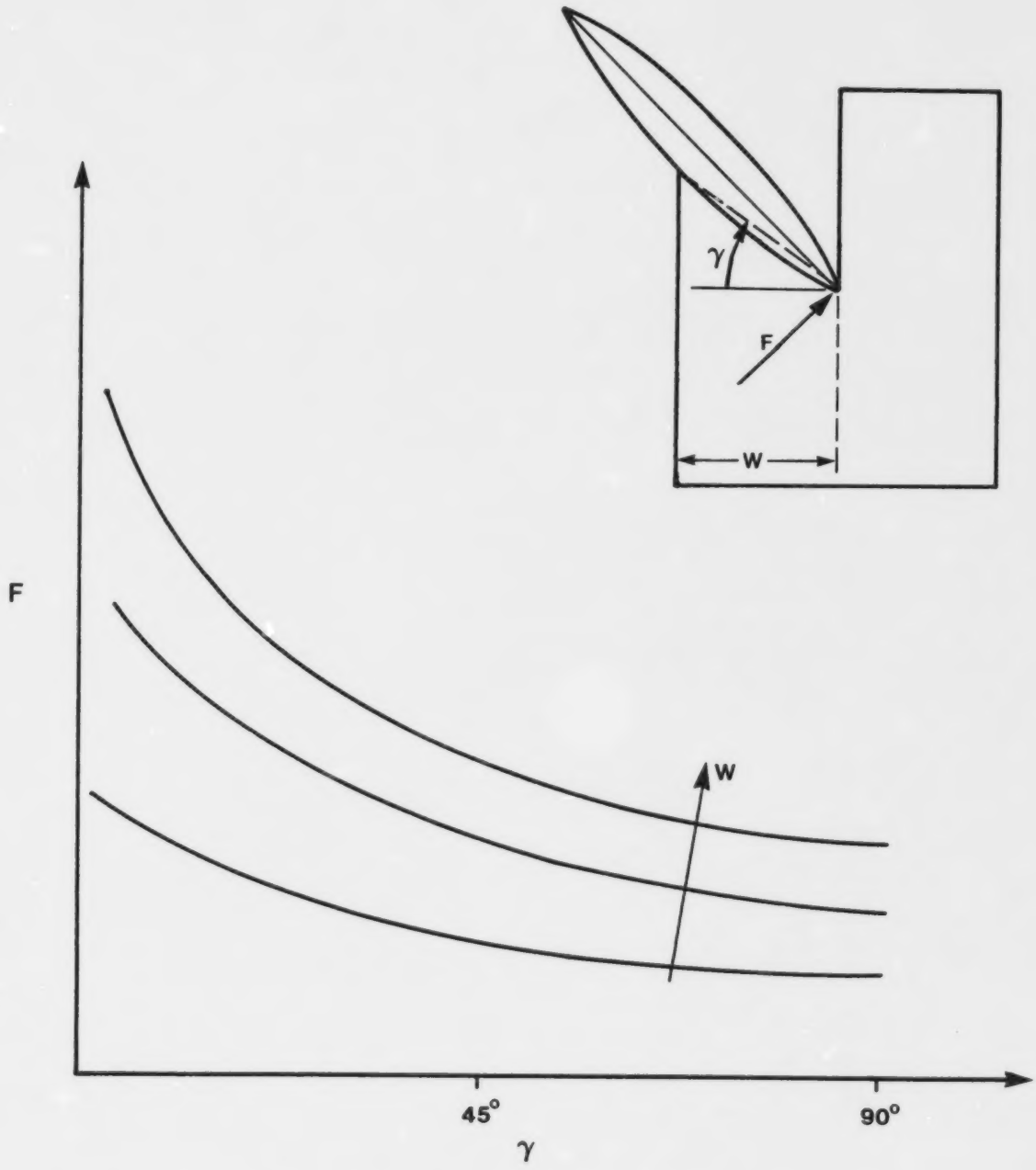

FIGURE 3.15 REPRESENTATION OF ICE SHEARING FORCE AS A FUNCTION OF GEOMETRIC PARAMETERS

the ones shown in Figures 3.14 and 3.15 must be incorporated into PVICE in tabular form. At present, these distribution curves are normalized with respect to the uniaxial crushing strength of the ice. Blade loading is calculated by multiplying the tabulated values by the ice crushing strength provided by the user. Thus different types (strengths) of ice can be represented without entering new tables, provided, of course, the basic shape of the curves remains (or can be assumed) the same. At present, curves obtained from the two dimensional (plane stress) finite element analysis of the ice block have been incorporated in PVICE. These curves are discussed in more detail in Section 5.5. It should be noted that load generation algorithms of PVICE have not yet been generalized to account for three-dimensional ice confinement effects expected on end propeller strips. Different pressure distributions are presumably applicable but not having performed three-dimensional simulations on the ice-block the manner in which pressure curves vary along the length of the blade have not been quantified and until further work is done, it is desireable to treat all strips as operating in plane stress mode.

The ice loading as described is then applied to the finite element model of the blade, Figure 3.2. The elements subjected to ice loading are identified. Each element identified is divided into a 10 x 10 mesh as shown in Figure 3.16. Each point of the mesh is checked to see if it is loaded. If it is, a consistent load vector (see, for example, References 14 and 22) for a concentrated load at the point is computed. If the blade loading is in the form of a pressure distribution, as per Figures 3.10, 3.12 and 3.13, the load on an element of area is obtained by multiplying the pressure by the area ΔA, shown in Figure 3.16. On the other hand, if the blade loading is in the form of a force (per unit width), as per Figure 3.11, the concentrated load is obtained by multiplying the force (per unit length) by the width ΔR. The coordinates of the grid points, the incremental area, ΔA, and the incremental radius, ΔR, are determined using element shape (interpolation) functions expressed in terms of a set of local coordinates ξ and η.

If a coefficient of friction is supplied by the user, friction between the blade surface and ice will be accounted for. A tangential force at each grid point, equal to the coefficient of friction times the corresponding normal force (i.e. simple Coulomb friction) is computed.

At present the program is limited to right-handed blades rotating clockwise, (i.e. providing ahead thrust). However, the ship speed can be ahead or astern. Consequently, only the ice milling conditions of quadrants I and IV of Figure 3.4 can be represented. For a given Y_c (see Figure 3.17), the program computes the angles θ_1 and θ_{11}. Angles for nine other equally spaced positions between θ_1 and θ_{11} are also computed. A load-time history for these eleven blade positions is then determined, unless a static load is requested by the user, in which case loads for a specified blade position are then determined. The $X_0Y_0Z_0$ coordinate system shown in Figure 3.17 is defined as the reference system, and pertains to the condition when the blades spindle axis is normal to the ice surface. Resultant forces and moments with respect to

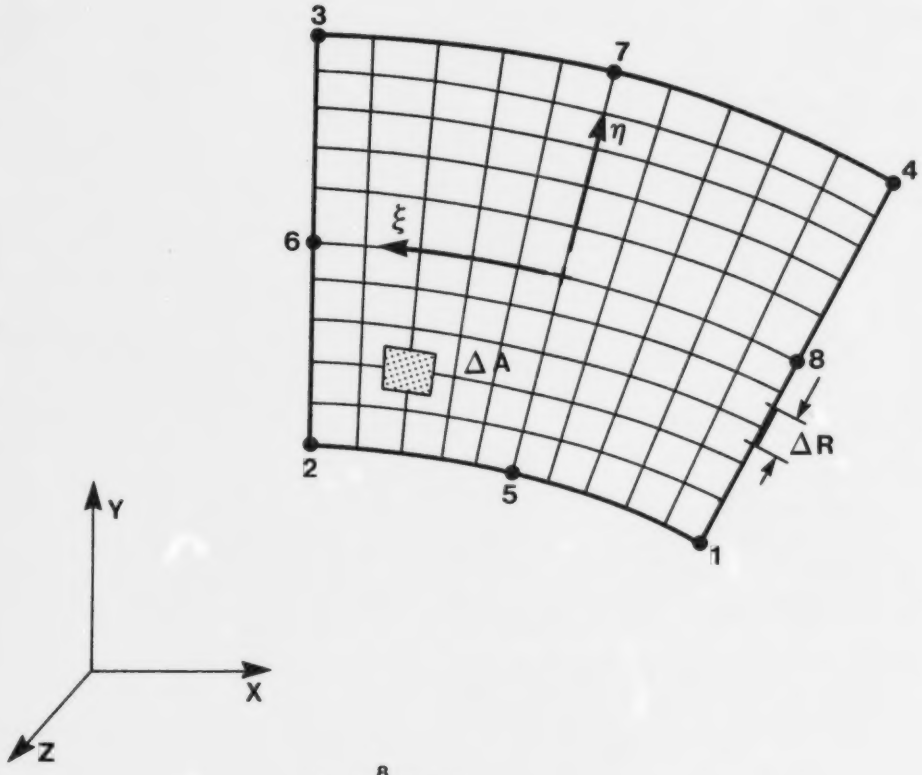

$$X = \sum_{i=1}^{8} N_i X_i$$

$$Y = \sum_{i=1}^{8} N_i Y_i$$

$$Z = \sum_{i=1}^{8} N_i Z_i$$

$$\Delta R = \det J_R \, d\eta$$

$$\Delta A = \det J_A \, d\xi d\eta$$

N_i = **ELEMENT SHAPE FUNCTION** (Reference 95)

ξ, η = **ELEMENT LOCAL COORDINATES**

J_R, J_A = **JACOBIAN OPERATORS**

FIGURE 3.16 MESHING OF FINITE ELEMENT FOR CONSISTENT LOAD VECTOR FORMULATION

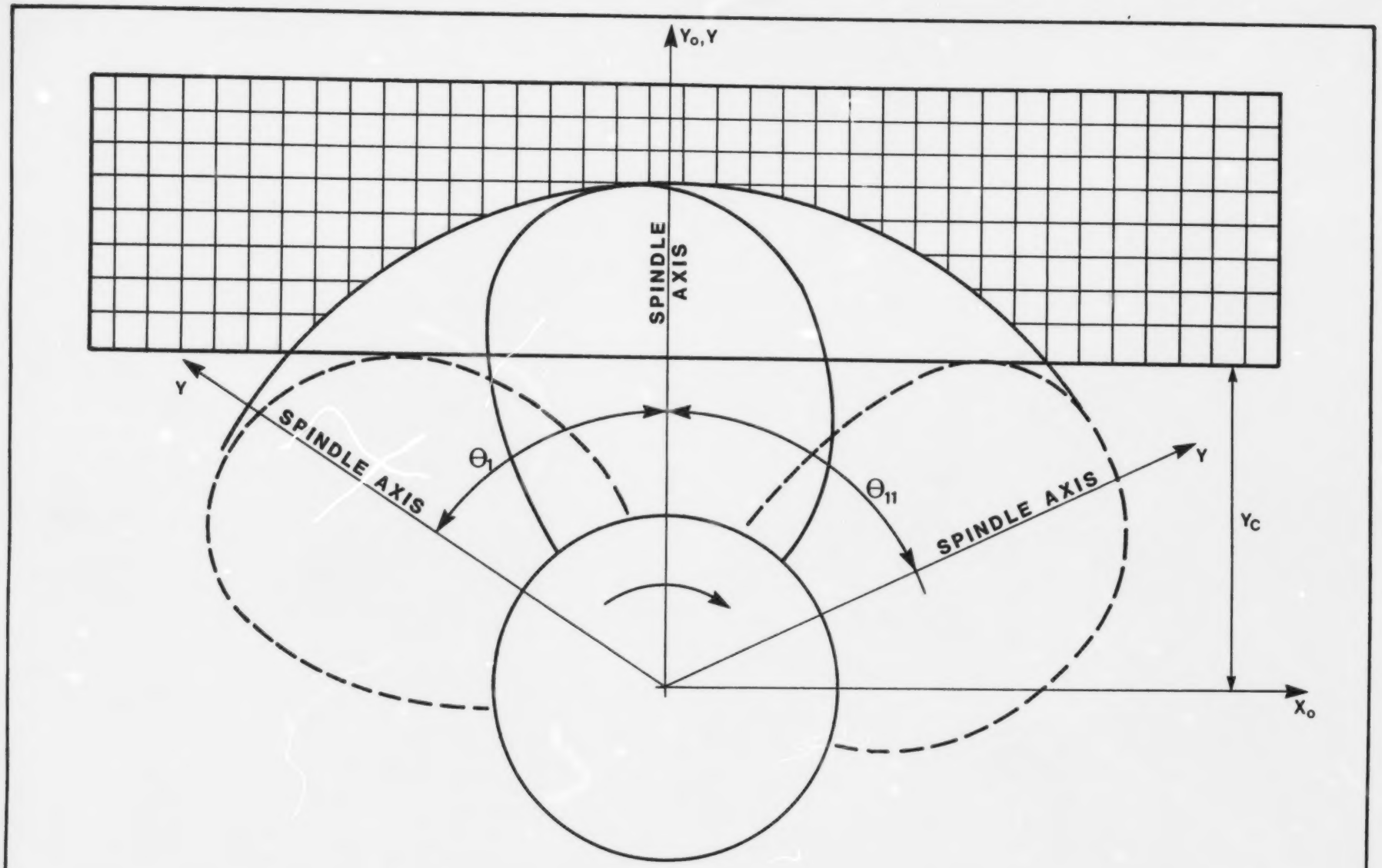

FIGURE 3.17 DEFINITION OF Y_c, Θ_1, Θ_{11} AND REFERENCE COORDINATE SYSTEM X_0 Y_0 Z_0

the reference coordinate system are computed and printed. The components of the load vector $\{F(t)\}$ are computed with respect to the XYZ coordinate system defined in Figure 3.2.

If blade 'shadowing' occurs, a message indicating this is printed, and the results pertain to the 2nd (and third, etc.) blade pass. The loading for the first blade pass should then be determined by another run with one blade only. The resultant forces and moments with respect to the reference coordinate system for the entire propeller can be determined by superposition, taking the phase difference (computed and printed by the program) into account.

The data input and format for PVICE are given in Table 3.1.

TABLE 3.1

DATA INPUT FOR PROGRAM PVICE

Card	Items	Format
1.	YC	(F10.3)
	YC = distance from shaft axis of rotation to ice (see Figure 3.17)	
2.	VS, RPM, NBLADE	(2F10.3, I5)
	VS = ship speed (positive for ship moving ahead) RPM = propeller rotation speed NBLADE = number of blades	
3.	SIGMAC, CF	(2F10.3)
	SIGMAC = uniaxial unconfined compressive crushing strength of ice CF = coefficient of friction	
4.	ILOAD	(I5)
	ILOAD = 1 for static analysis = 2 for dynamic analysis	
5.	NPSTAT (omit if ILOAD=2)	(I5)
	NPSTAT = the position (2 to 10) for which the static loads are to be computed.	

Notes:

1. Details about propeller geometry, including radius, variations of pitch, chord, rake and skew with radius and leading edge shape are inherently included in the finite element model to be input in file PREFX.GOM. For information on data format see independent documentation on the finite element program VAST [15].

2. Tables describing dependencies of P_1, P_2 and F on geometric parameters have been incorporated into the PVICE program.

4.0 MECHANICAL PROPERTIES OF ICE AND MATERIAL MODELLING

4.1 Stress-Strain Relationships

Ice is a complex material and since systematic investigation of its mechanical properties commenced relatively recently, there is still considerable disagreement on how to model it. Based on a review of recent literature and discussions with authorities on the subject, the following represent some ideas on ice modelling for the purposes of estimating propeller-ice interaction forces.

Generally sea ice behaves as a viscoelastic material [23] with highly nonlinear response but if rates of straining are increased sufficiently, its deformations can be considered linear elastic up to a point of brittle failure [24-27]. Although it is difficult to accurately predict the strain rate in the ice block when milled by propellers without carrying out a detailed modelling of the milling process, some simple preliminary computations suggest that the strain rate is at least 10^{-2} sec^{-1} which on the basis of published ice test data is sufficient to produce brittle material behaviour [p. 289, 28].

The perfect elastic-plastic material model is probably the simplest material model which depicts the main performance characteristics of ice at low loading rates. Unlike metals, however, ice generally has different limiting tensile and compressive strengths. In this sense, ice resembles concrete or rock. Any analysis program to be used to analyze ice milling should therefore be capable of assuming distinct properties for tension and compression. As demonstrated by Figure 4.1, due to Michel [29], while loading rates with strain rate, $\dot{\varepsilon}$, $\leq 10^{-5}$ sec^{-1} produce plastic deformations, with increased loading rates, such that $10^{-5} \leq \dot{\varepsilon} < 10^{-1}$ sec^{-1}, ice behaves increasingly like a perfect elastic material with brittle failure by crack propagation under tensile or compressive conditions. For strain rates $\dot{\varepsilon} > 10^{-1}$, ice behaves as a brittle material.

While the above simple model is probably acceptable for most engineering computational analyses involving ice, its adequacy for the propeller milling of ice must be reexamined. Recent literature consistently demonstrates a nonlinear response [30-32], as illustrated in Figure 4.2 in stress-strain curves from uniaxial tests conducted by Sinha [32] on various types of ice. Admittedly quite low rates of material loading were considered by Sinha, but tests conducted by Jones [31] on polycrystalline ice showed that similar behaviour is displayed at higher loading rates with the addition of confining pressure. It is also clear from Figure 4.3 that increasingly higher failure stresses develop under the action of confining pressures. Apparently confining pressure has the effect of suppressing the cracking responsible for the brittle failures associated with unconfined uniaxial tests and thereby permitting plastic yielding and flow to occur. Further evidence of this is given in Figure 4.4 where yield or maximum stresses are plotted against confining

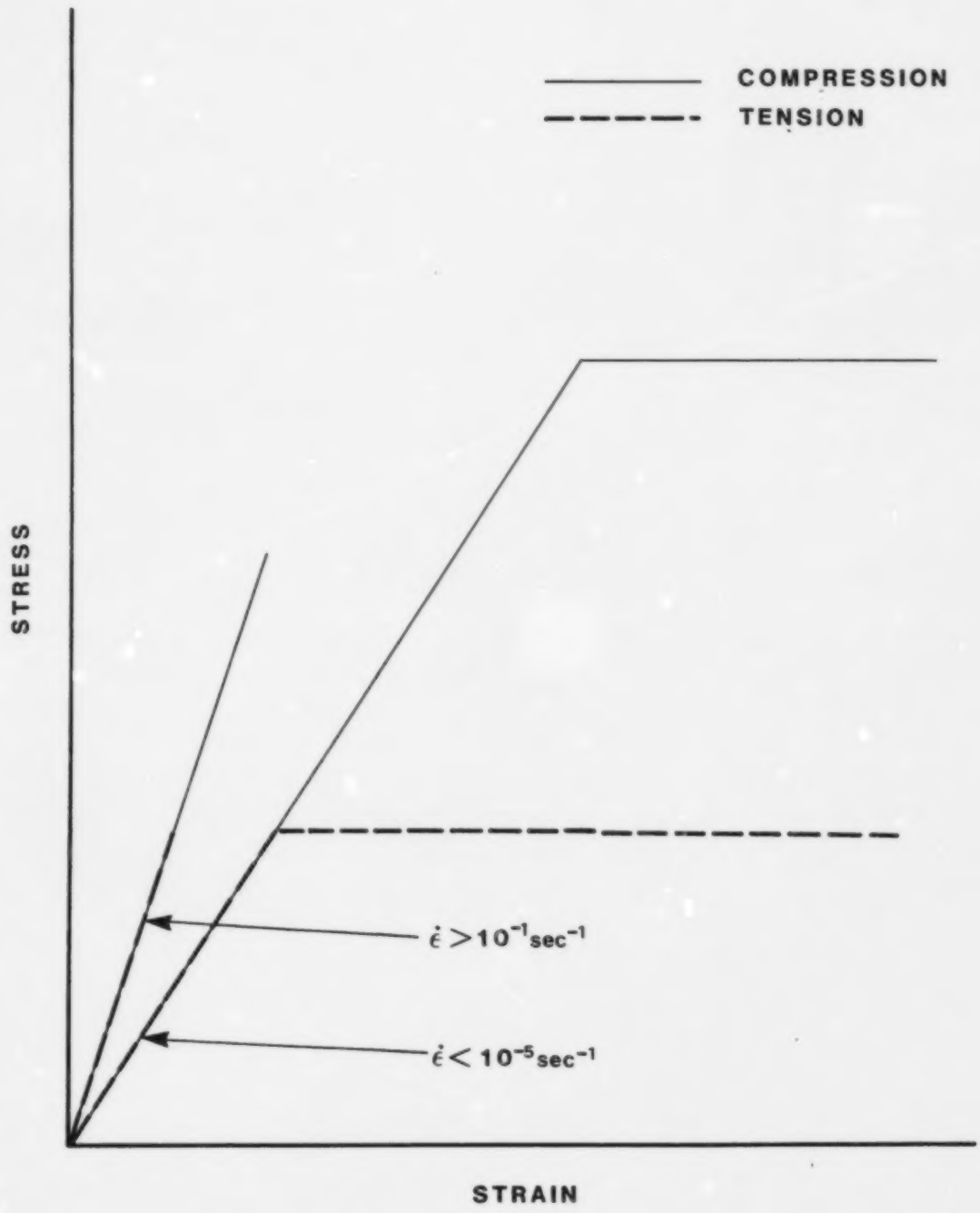

FIGURE 4.1 EFFECT OF STRAIN RATE ON STRESS-STRAIN RELATIONSHIP [29]

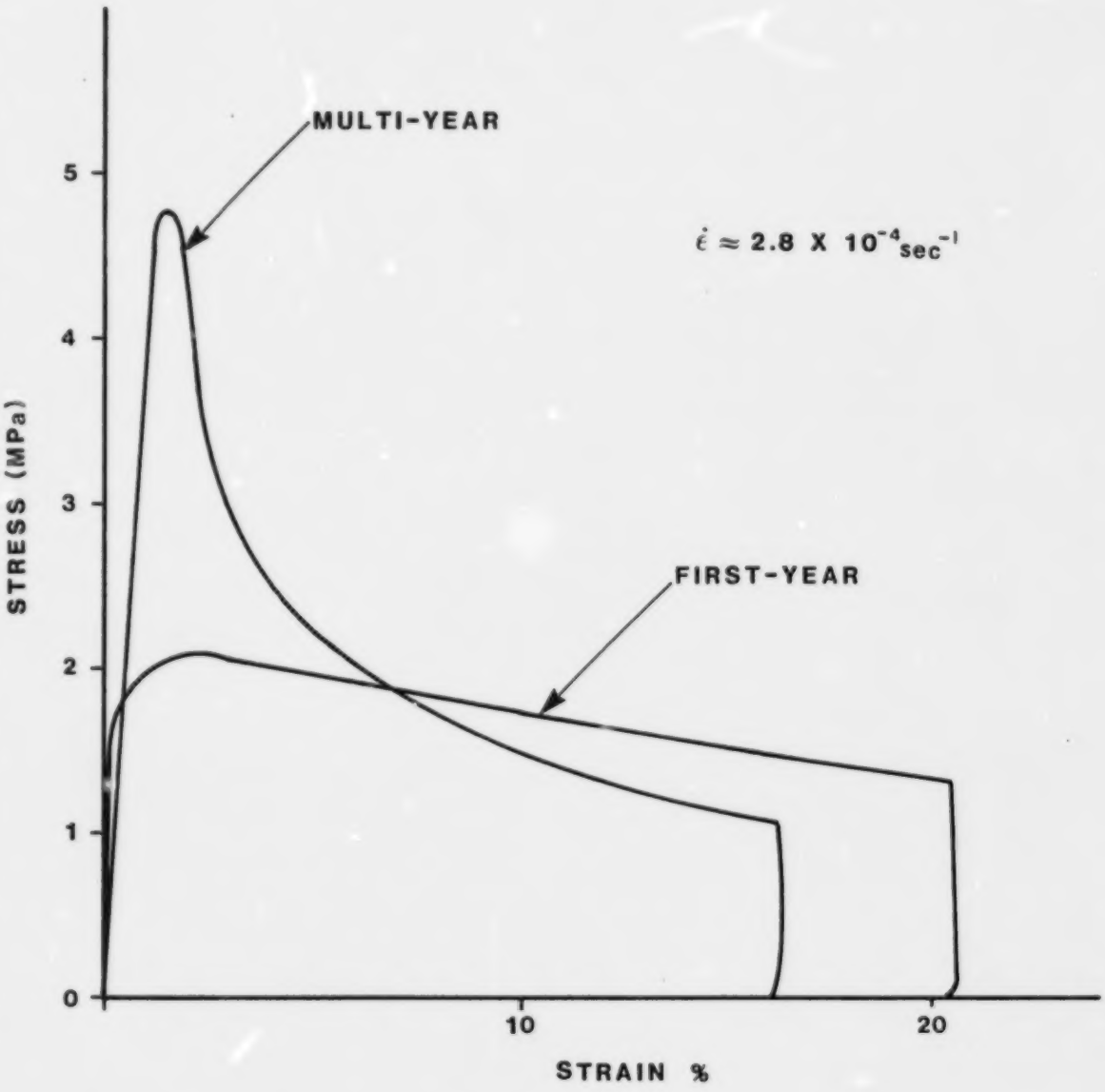

FIGURE 4.2 STRESS-STRAIN CURVES FOR VARIOUS TYPES OF ICE [32]

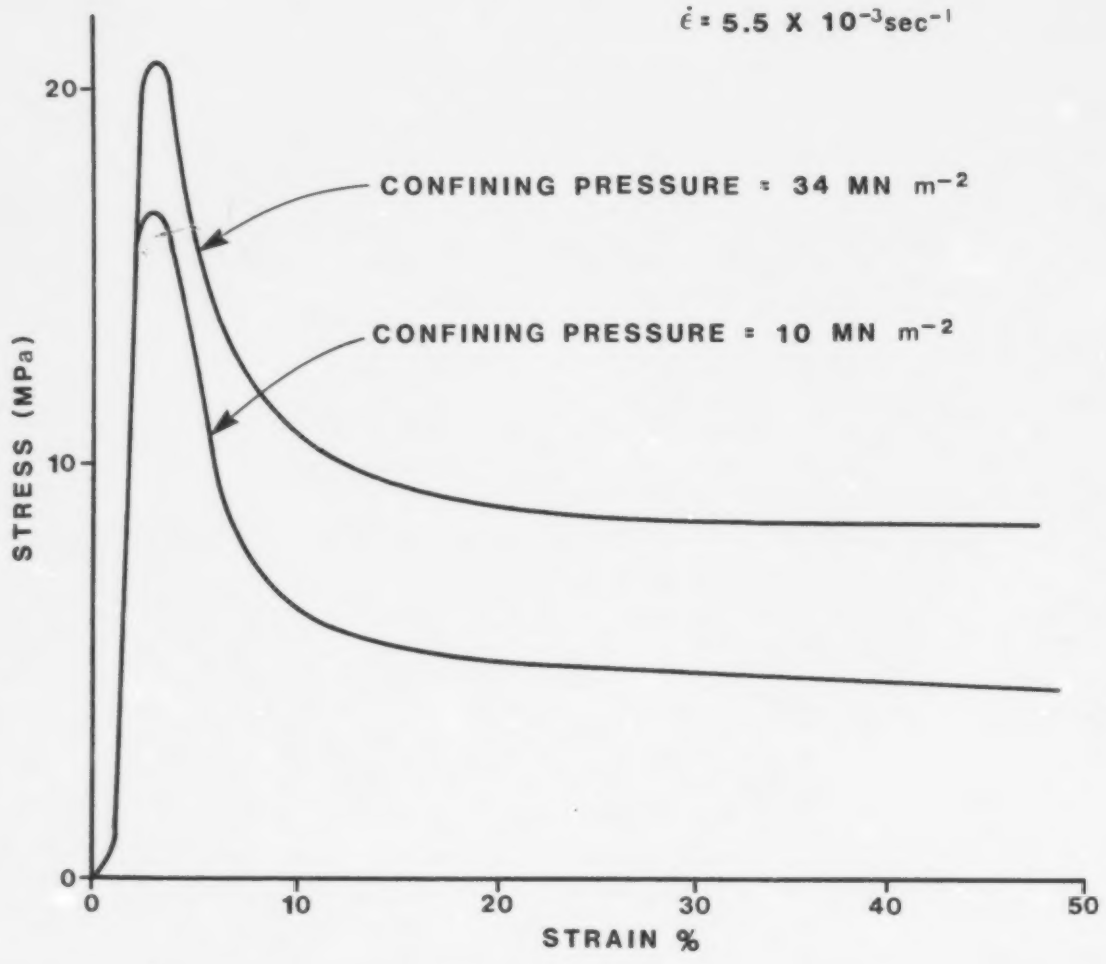

FIGURE 4.3 EFFECT OF CONFINING PRESSURE ON STRESS-STRAIN RELATIONSHIP [31]

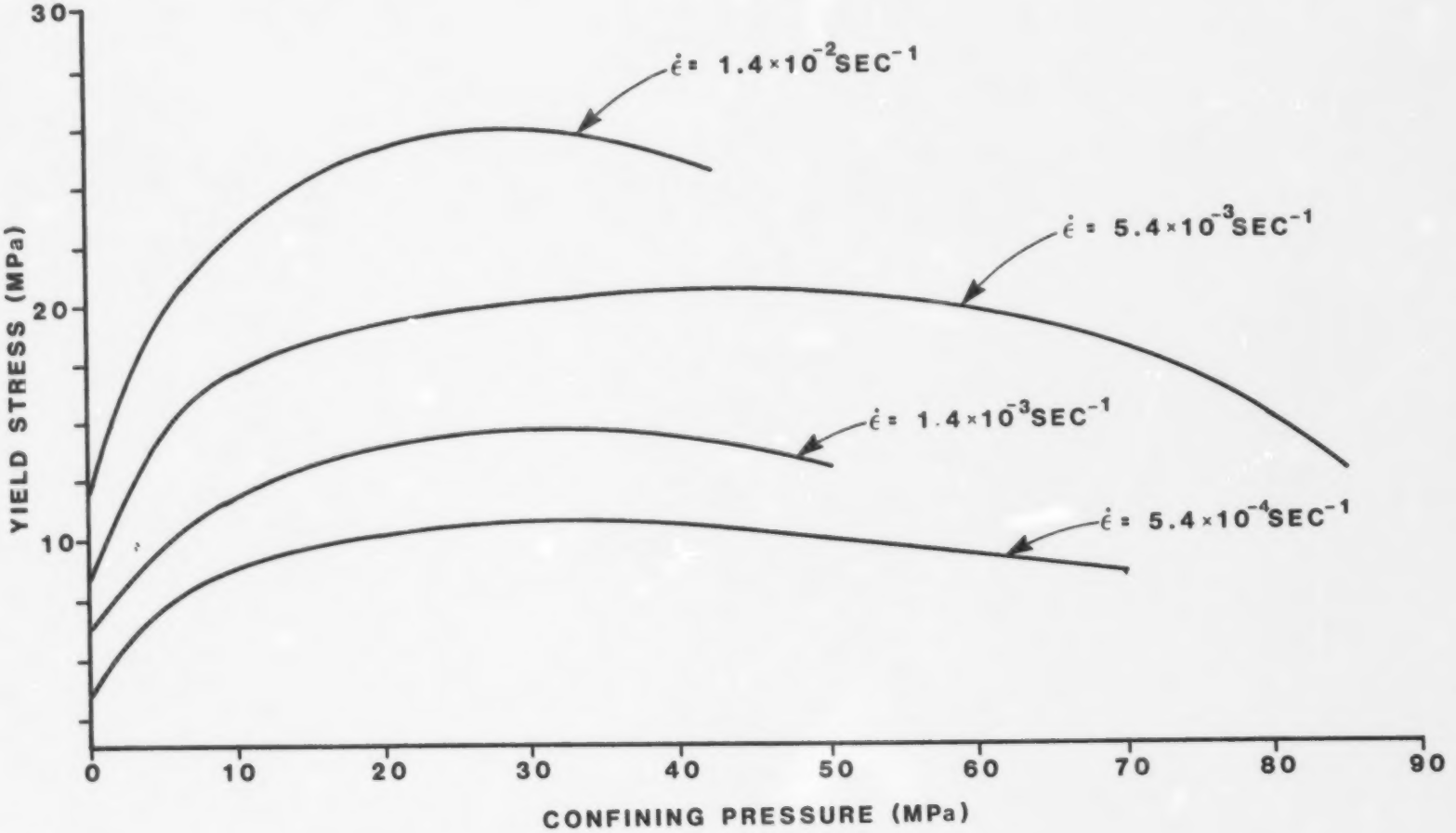

FIGURE 4.4 EFFECT OF CONFINING PRESSURE ON YIELD STRESS [31]

pressure for various strain-rates. The effect of confining pressure appears to decrease for low strain rates since ice deforms plastically even in unconfined tests at low strain rates. (These observations are consistent with the tendency for brittle rock to display ductile characteristics under large hydrostatic pressure [p. 135, 33]).

Similar strengthening of ice has also been observed by Timco and Frederking when confinement plates were used in uniaxial strength tests [30]. Their tests differ from those of Jones in that orthogonal confining pressures on faces parallel to the direction of the test load may be unequal. Significant anisotropy may develop in failure strengths especially when ice samples have a columnar structure. As illustrated in Figure 4.5, greater strength is associated with confinement on vertical sides of the sample (type A) than with confinement on top and bottom of the sample (type B).

Initially, it was not clear how relevant the experimental data demonstrating a nonlinear stress-strain material behaviour really will be to our ice block modelling exercise. The stress-strain curves are altered by confining pressure and loading rate. They are influenced by structural anisotropy of the ice material (grain orientation) as well. Considerable data is therefore required to fully describe all these influences on stress-strain curves. Moreover, further thought had to be given to the programming implications as it was considered unlikely that any commercial program permits the required degree of flexibility in the definition of the stress-strain curves. Consequently, a number of questions were raised. How would an algorithm to achieve this flexibility in material performance be organized? Is it worthwhile? Is the performance of the ice material significantly (sufficiently) altered to justify the program development? Are there any numerical problems such as instability foreseen particularly when stress-strain curve decreases sharply from points of maximum stress as in the multi-year ice data curve on Figure 4.2.

It is very difficult to answer these questions without actually implementing many of the proposed enhancements in program capabilities. Nevertheless on the basis of the above review of evidence on the nonlinear stress-strain ice characteristics, it is obvious that flexibility in the stress-strain curve is required to attain an acceptable description of the response of the ice material in the milling application. Therefore, any analysis program selected for analysis of simplified ice milling problems in two- and three-dimensions must possess the ability to model materials with highly nonlinear stress-strain curves up to failure. If this capability is not precoded, the facility to provide suitable user subroutines must exist.

4.2 Yield Criteria and Failure Envelopes

The failure envelope, or alternately, yield surface according to structural mechanics terminology, defines the limits of elastic material behaviour. Stresses outside the failure envelope cannot exist. Those on

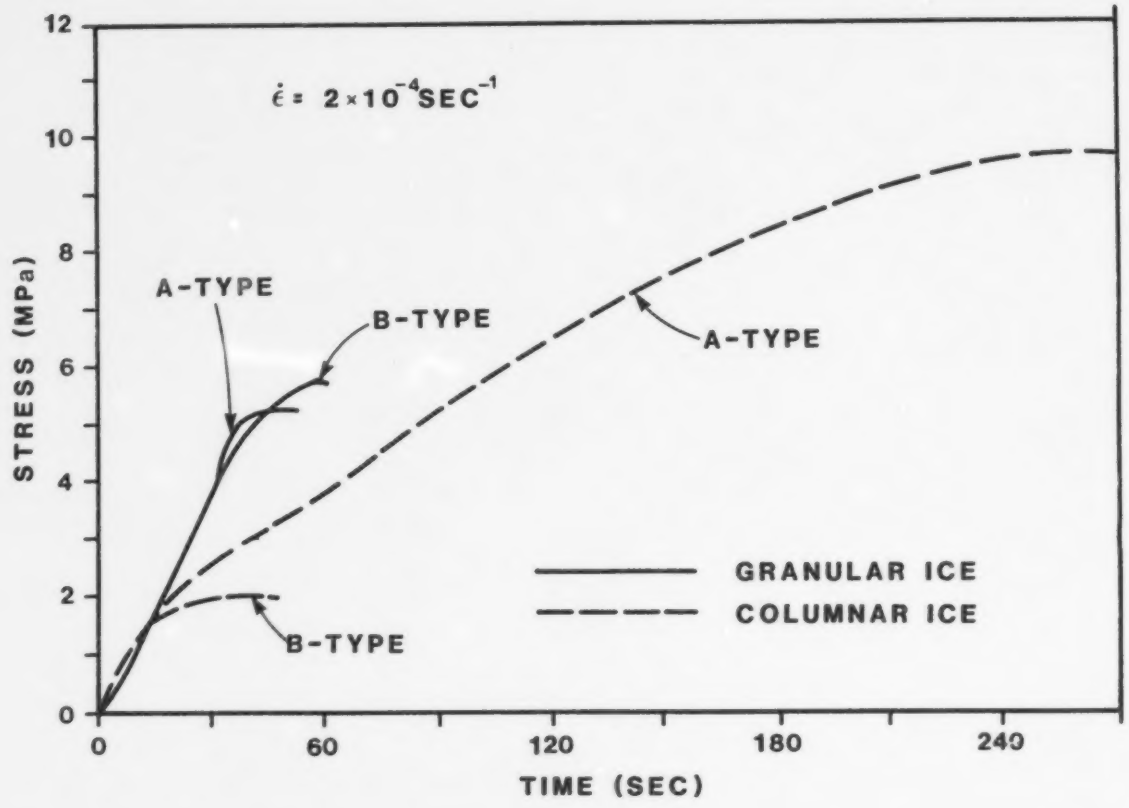

FIGURE 4.5 COMPARISON BETWEEN CONFINEMENT ON VERTICAL SIDES (A-TYPE) AND CONFINEMENT ON TOP AND BOTTOM (B-TYPE)

the envelope represent the onset of fracture or, alternately, plastic yielding, depending upon whether the material behaviour is brittle or ductile. Plastic strain increments are related to current stresses and stress increments subsequent to yielding by what is termed a flow rule. When the flow rule defines strain increments normal to the yield function, (in the multi-dimensional principle stress space), associated plasticity is said to occur. Plastic strain increments defined relative to a plastic potential other than the yield function gives nonassociated plasticity. The yield criteria in general changes during plastic flow and the hardening rule identifies those changes.

Several of the classical yield surfaces definitions [34-36] for isotropic materials, (including Tresca, Huber-von Mises, Mohr-Coulumb and Drucker-Prager which generally are applicable to metals, concrete and other common engineering materials), are precoded in general purpose nonlinear finite element programs. As hydrostatic pressure frequently plays a relatively minor role in defining plastic deformations, it is convenient to express yield surfaces in terms of invariants of the stress deviators (deviations of stresses from the mean pressure),

$$S_{ij} = \sigma_{ij} - \frac{1}{3}\sigma_m \delta_{ij}$$

where, σ_m is the mean pressure, defined as

$$\sigma_m = \frac{(\sigma_x + \sigma_y + \sigma_z)}{3}$$

In particular, with the invariants

$$J_2 = \frac{1}{2} S_{ij} S_{ij} = \frac{1}{6}[(\sigma_1-\sigma_2)^2 + (\sigma_2-\sigma_3)^2 + (\sigma_3-\sigma_1)^2]$$

$$J_3 = \frac{1}{2} S_{ij} S_{jk} S_{ki}$$

$$= \sigma_1\sigma_2\sigma_3 + \frac{1}{27}(\sigma_1+\sigma_2+\sigma_3)[2(\sigma_1+\sigma_2+\sigma_3)^2 - 9(\sigma_1\sigma_2+\sigma_2\sigma_3+\sigma_3\sigma_1)]$$

the yield criterion then reduces to

$$F = F(J_2, J_3) = \text{const}$$

Tresca and Huber-von Mises yield criteria are both of this form. The von Mises criteria stipulates that plastic flow occurs when the second stress invariant is constant and can be simply expressed as

$$F = J_2 - \frac{\sigma_o^2}{3} = 0$$

where σ_o is the yield stress in simple tension. By the Tresca yield

condition, the condition for plastic flow is that the largest principal shearing stress equals the yield stress in simple shear, $k = \frac{\sigma_o}{\sqrt{3}}$, or

$$F = 4J_2^3 - 27J_3^2 - 36k^2J_2^2 + 96\,k^4J_2 - 64k^6 = 0$$

Geometrically the von Mises criteria is an infinitely long cylindrical surface with axes corresponding to the hydrostatic stress line $\sigma_1=\sigma_2=\sigma_3$ in principal stress space whereas the Tresca criteria is an inscribed hexagonal cylinder as shown in Figure 4.6.

For materials with reduced strength in tension, other more complex yield criteria are more appropriate. Two criteria characterized by a linear increase in shear failure strength with increasing bulk stress are possible. One of them is the Mohr-Coulomb criteria defined by

$$F = \underset{m}{\sigma} \sin\phi + \sqrt{J_2}\cos\theta - \frac{\sqrt{J_2}}{\sqrt{3}^3}\sin\phi\sin\theta - c\cos\phi = 0$$

where

$$\theta = \frac{1}{3}\sin^{-1}\left[-\frac{\sqrt{3}^3}{2}\frac{J_3}{\sqrt{J_2}}\right] \qquad -\frac{\pi}{6} < \theta < \frac{\pi}{6}$$

and where ϕ is the angle of friction and c is the cohesion of the material measured in a triaxial compression test. Generally both ϕ and c depend on some strain hardening parameter K. Another useful yield criterion for this type of material is the Drucker-Prager criterion given by

$$F = 3\,\alpha\sigma_m + \sqrt{J_2} - K$$

where

$$\alpha = \frac{2\sin\phi}{\sqrt{3}\ (3-\sin\phi)}$$

and

$$K = \frac{6c\cos\phi}{\sqrt{3}\,(3-\sin\phi)}$$

Typical yield surface geometries in principle stress space for these so called frictional materials are also demonstrated in Figure 4.6.

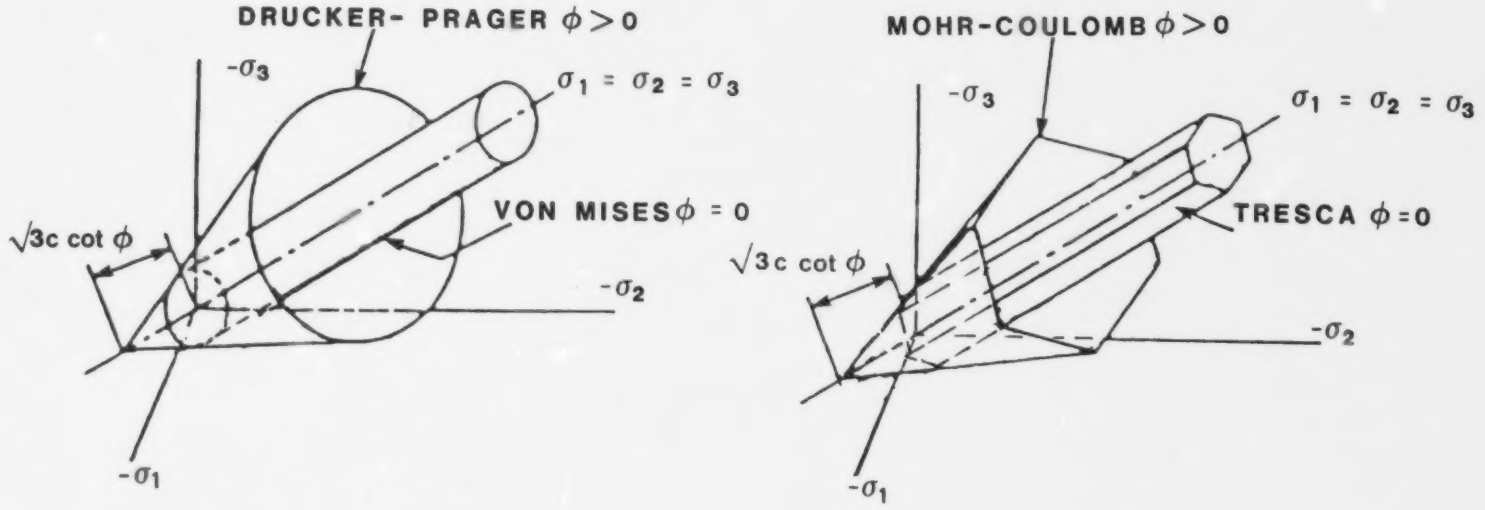

a) DRUCKER-PRAGER AND VON MISES

b) MOHR-COULOMB AND TRESCA

FIGURE 4.6 ISOTROPIC YIELD SURFACES IN PRINCIPAL STRESS SPACE

Failure of brittle materials are better described by criteria permitting quadratic variations of shear strength with bulk stresses. The parabolic Mohr-Coulomb yield criteria is one example. Its yield surface is given by

$$F = \sqrt{3J_2} + \sqrt{3}\beta\sigma_m) - \bar{\sigma}$$

where

$$\bar{\sigma}^2 = 3(c^2(K) - \frac{\alpha^2}{3})$$

and

$$\beta = \frac{\alpha}{\sqrt{3(3c^2(K) - \alpha^2)}}$$

The constant α is determined from the angle of friction using the relation

$$\frac{3\alpha}{\sqrt{1 - 3\alpha^2}} = \sin\emptyset$$

An empirical generalization of the classical parabolic Griffith fracture criterion [37] in σ-τ space by Fairhurst [38] which permits arbitrary ratios of uniaxial compressive and tensile strengths has been found to be very convenient for approximating the phenomenological or macroscopic fracture strength of rock under special multiaxial states of stress associated with cavity formation [39] since strength ratios observed experimentally typically range from 5 to 22 [40]. However, the derivation of a corresponding failure surface in three-dimensional principal stress space is not known to be available at the present.

Under ductile conditions associated with low strain rates in ice, the Tresca or von Mises yield criterion are considered acceptable. On the other hand when loading is rapid and quasi-brittle fracture occurs, the Mohr-Coulomb criterion which permits increasing shear strength with increasing bulk stress is more appropriate. The parabolic failure envelope similar to that of the Griffith criterion might also be considered providing the condition that the ratio of compressive strength to tensile strength equal to 8 is relaxed. However, as noted by Mellor [41] none of the above account fully for known failure characteristics of ice. He suggests that since the shear resistance of ice can be destroyed solely by hydrostatic pressure at typical temperatures, the failure envelope must eventually converge to the hydrostat line in the manner illustrated in Figure 4.7.

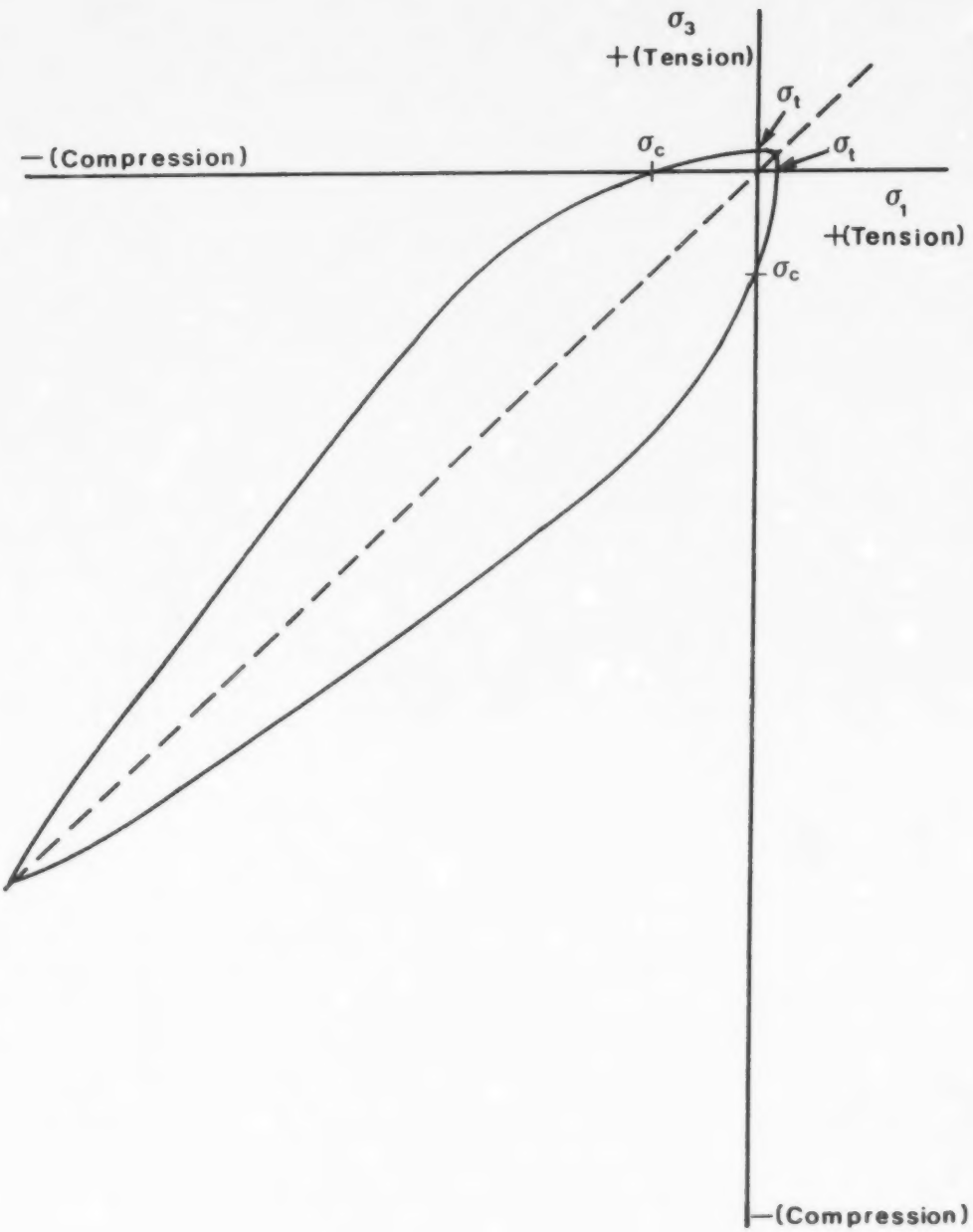

FIGURE 4.7 TWO-DIMENSIONAL REPRESENTATION OF A YIELD CRITERIA FOR ICE [41]

Considerable uncertainty in ice fracture predictions for multiaxial stress situations is due to the unreliability of the failure envelope definitions which arises from the scarcity of multiaxial ice strength measurements. In biaxial situations, testing has been limited to the plane strain tests of Frederking [24, 42].

Experimental determination of triaxial yield envelopes poses even greater difficulties. Until very recently little triaxial strength testing was conducted and since those tests were performed on a standard triaxial cell, applied stress ratios were subject to the conditions $\sigma_1 \neq \sigma_2 = \sigma_3$ [43-44, 31]. Jones used this procedure to define the failure envelope of Figure 4.8 for fine grained ice of glaciers. Hydrostatic pressures of order 15 to 20 atmospheres encountered at glacier beds were considered. A new multi-axial testing machine with a closed loop control system and brush type loading platens was recently used by F.J. Hausler [16] to perform more extensive triaxial ice strength tests. An increased number of stress ratios available through the above mentioned improvements in test equipment permitted a facetted failure surface to be defined. Although brush type platens were adopted with the aim of minimizing lateral strain constraints on the loaded ice faces, some concern has been expressed by Dr. N.K. Sinha that stress concentrations at the bristles induce premature cracking activity which reduces strength data obtained.

Various investigators have nonetheless proposed failure envelopes for ice from uniaxial data and sometimes a limited amount of biaxial data. For instance by interporating suitable curves to three or four uniaxial strength data points it was possible to define two-dimensional failure envelopes [45-47, 30]. However, two factors limit the accuracy of the envelopes thus generated. Typical uniaxial fracture strengths in compression, σ_c^*, are at least two to three times the corresponding uniaxial fracture strength in tension σ_t^*. Also a high degree of uncertainty generally exists in the σ_c^* and σ_t^* data points due to significant scatter in experimental data. Frederking and Sinha demonstrate the importance of testing machine compliance and end smoothness on reliability of uniaxial test data [48-50]. The strong dependence of the ellipticity of the failure envelope on the data points used thus implies an even larger uncertainty in the shape of the interpolated failure envelope, particularly along the major axis defined by $\sigma_1 = \sigma_3$, as demonstrated in Figure 4.9. Greater reliability should follow from the use of some biaxial data in envelope definition [42, 45-47].

4.3 Damage Models

As ice is deformed beyond its failure (or yield) strength, its strength properties may change due to the inherent structural damage sustained as the original crystal material is disrupted. Among the most notable changes in material properties is the development of strain softening and the associated degradation of stiffness caused by internal micro-fracturing (cracking). Despite the decrease in ice strength associated with damage occurring, the material in the failed (or yielded)

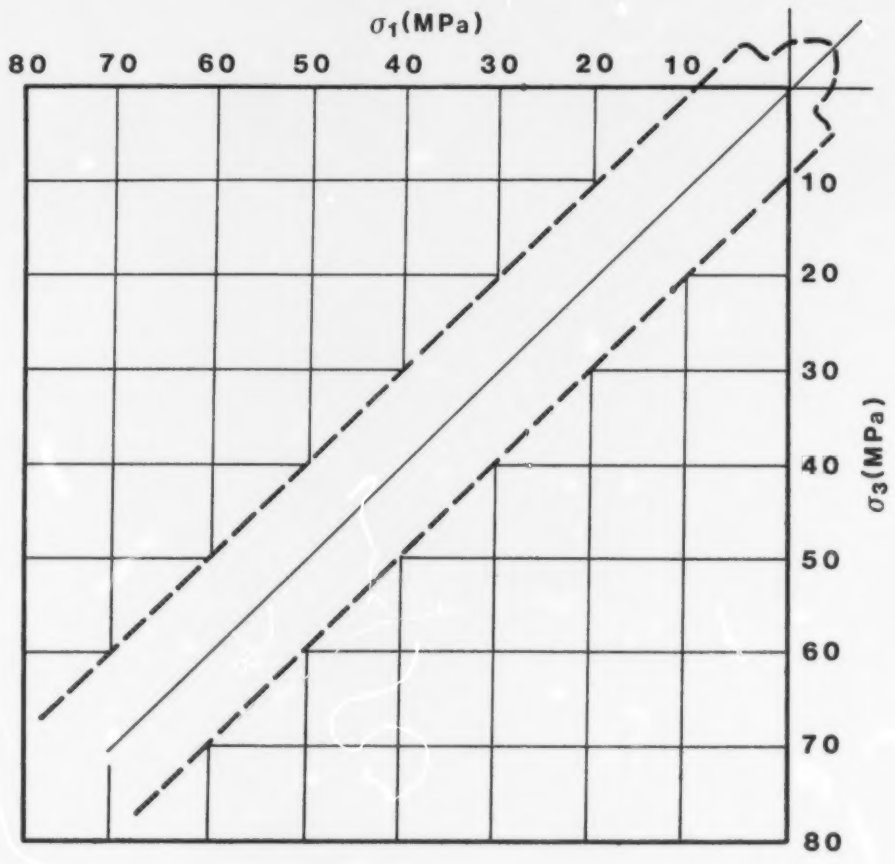

FIGURE 4.8 FAILURE ENVELOPE PROPOSED BY JONES [24] FOR FINE GRAINED ICE OF GLACIER

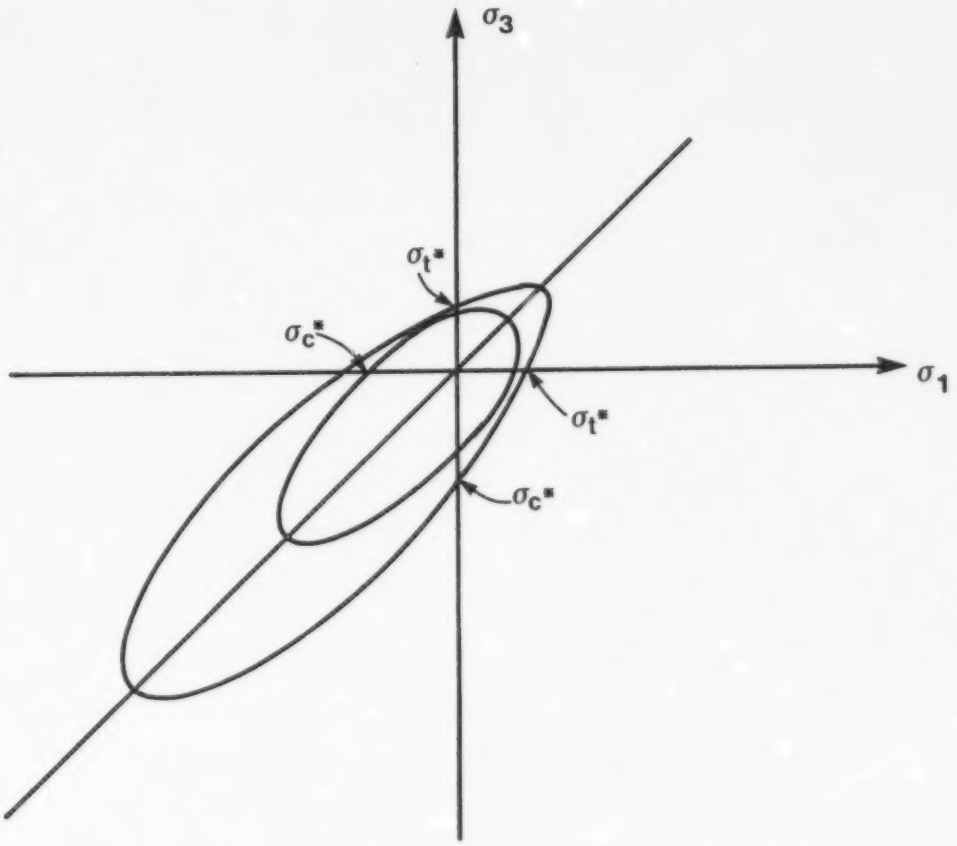

FIGURE 4.9 SENSITIVITY OF FAILURE ENVELOPE TO ERRORS IN UNCONFINED UNIAXIAL TENSILE AND COMPRESSIVE STRENGTH DATA

states cannot, nonetheless, be ignored in computational investigations. Significant residual material strength exists after micro-fracturing damage is initiated and relatively new and perhaps unconventional constitutive modelling formulations appear necessary. There appears to be several material models of varying sophistication which could be used to describe the damage characteristics associated with the post-failure (yield) ice behaviour: (i) perfectly elasto-plastic; (ii) strain hardening and softening; (iii) two-phase material description; (iv) progressive damage models from geomechanics; (v) endochronic constitutive modelling of ice; (vi) impact damage models of Stanford Research Institute. Each of these models are discussed in detail below.

Perfectly elastic-plastic:

This is perhaps the simplest material idealization which can be contemplated for modelling the simplified two-dimensional milling situation. Most general purpose finite element and finite difference program codes for nonlinear applied mechanics applications offer this material modelling capability because of its suitability for modelling metals. However, no change in stresses is associated with increases in strain (load) after the yield stress is reached (see Figure 4.10). This implies that unlimited dislocation movement, developing from yield on crystal slip planes, occurs within the material. There is no degradation of elastic moduli as demonstrated by the parallel unloading curves in Figure 4.10. Since the above mentioned performance characteristics are inconsistent with experimental observations for brittle materials and for ice in particular, the potential of the perfectly elasto-plastic model is not considered to be good.

Strain hardening and softening:

Strain hardening represents the progressive material strengthening associated with increases in strain as illustrated in the typical uniaxial response curve of Figure 4.11. Implied here is a dislocations pileup which gradually impedes further material deformation. Unloading curves are parallel and no material degradation is thus again indicated. Plastic deformations are irreversible (permanent). Insufficient testing has been conducted with ice specimens which are repeatedly loaded and then unloaded to ascertain at what strains, permanent plastic deformations are produced. It is conceivable, though, that at some strain before maximum stresses are attained, permanent plastic deformations do develop with the possibility of some limited hardening.

Nonetheless, available experimental data consistently shows strain softening as the dominant phenomenon associated with large strains of ice. As stated earlier, this loss of strength develops from damage occurring in the form of microcracking or fracturing within the ice block. The simplest way to account for strain softening in material models is to implement decreasing failure surfaces in a manner consistent with the notion of the strain hardening parameter in plasticity theory. However, deformations associated with idealized strain softening materi-

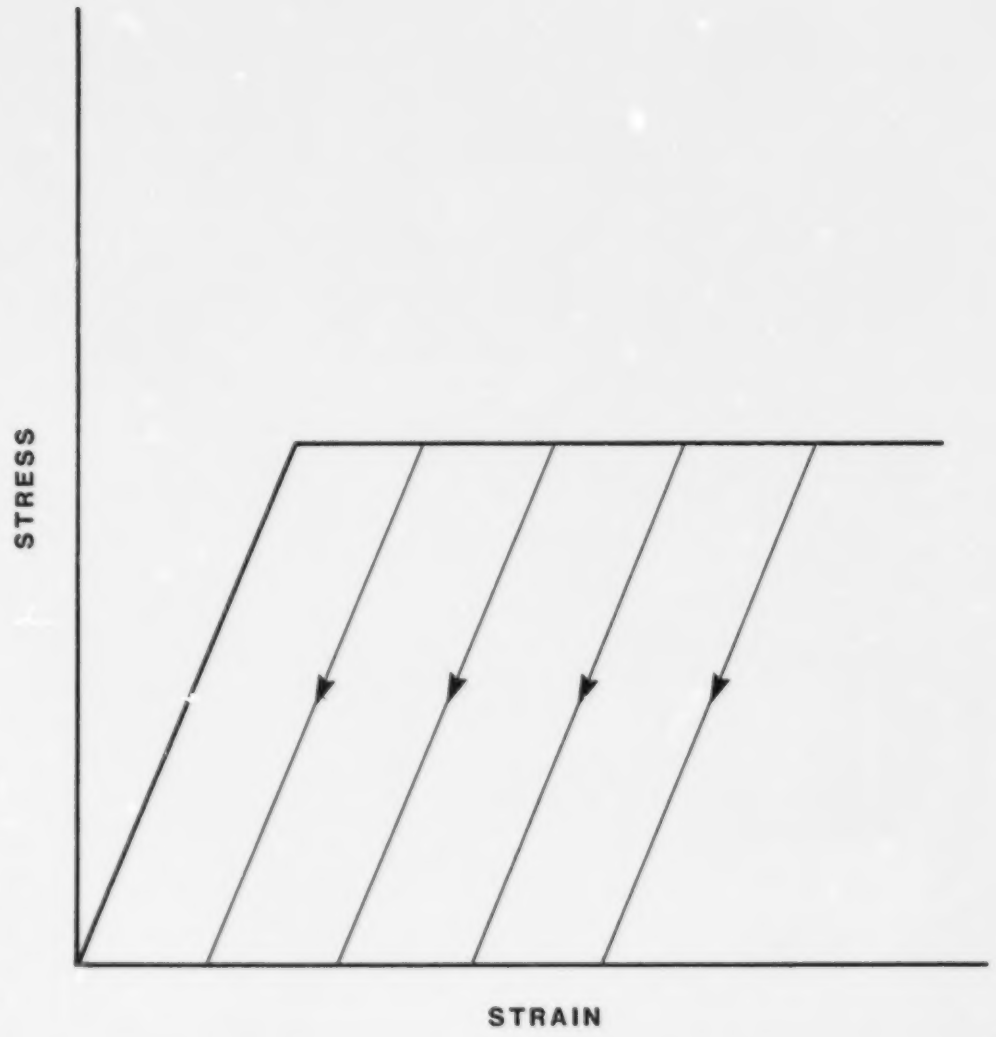

FIGURE 4.10 CHARACTERISTIC UNIAXIAL RESPONSE OF ELASTO-PLASTIC MATERIAL (NO DEGRADATION OF ELASTIC MODULI)

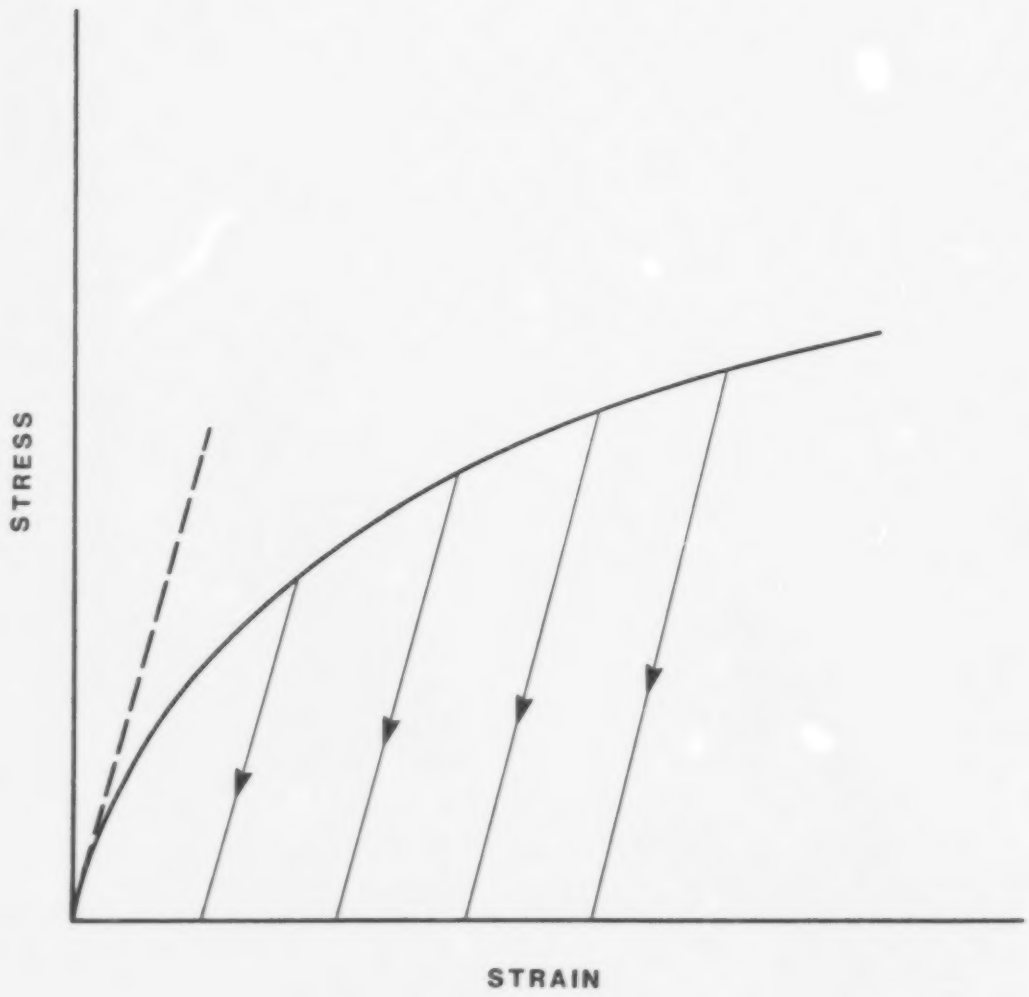

FIGURE 4.11 CHARACTERISTIC UNIAXIAL RESPONSE OF MATERIAL WITH STRAIN HARDENING

also are unstable beyond a certain stage in straining and deformations are localized along a planar band [51-55]. In numerical implementations of progressive deformations for softening materials, this localization of instability has been observed to be sensitive to mesh size [56-60]. St. Pietruszczak and Mroz [60] have demonstrated how adoption of a smeared shear band concept decreases the sensitivity of the analysis to such discretization details. A characteristic dimension of the shear band, identifiable from simple compression tests is required as input to their numerical model. But acceptable descriptions of softening materials requires more than a simple adjustment to the size or shape of the failure surface. For added sophistication, material dilatancy which generally accompanies microfracture must also be accounted for. Considerable progress has been made in the application of dilatant softening material models to rock [61-64] and concrete [65-69].

Two-phase material description:

The material models examined above are all developed on the basis of yield criteria and flow rules from plasticity. An alternative material idealization involves considering two distinct material phases, a pre-failure phase and a post-failure phase. This idealization appears to describe the main characterisics of brittle material behaviour better than the conventional plasticity models. According to theories of classical brittle failure, an idealized brittle material is one which is linear elastic until failure conditions are reached when it suddenly transforms into a crushed material with some associated change of strength (stiffness) characteristics [70]. Failure of the basic (intact) material is reliably defined by some appropriate failure envelope as described earlier. Deformations of the crushed material on the other hand are governed by a linear Mohr-Coulomb failure criterion which as explained earlier requires only a material cohesion coefficient and angle of friction (envelope slope) for its definition. To complete the description of the crushed material, a nonzero volumetric strain (dilation) arising from the increased material porosity associated with the transition to the crushed state must be suitably accounted for. Unfortunately, the volumetric straining associated with the crushing of even common brittle materials such as rock, of interest to construction and mining industries, are largely unknown. Needless to say, insufficient data prevents the reliable description of this phenomenon for ice. The abruptness of the change in material properties, especially the dilation, is also expected to represent a serious computational (numerical) problem and may conceivably therefore limit the degree of success attainable if this material model were to be incorporated into a finite element analysis program. This is tantamount to introducing shocks to the equilibrium system being modelled especially if numerical procedure involves sizeable volumes reaching failure conditions simultaneously. Use of constant stress elements in the structural model, for instance, constitutes one potential difficulty since whole elements must undergo this change of state when appropriate conditions are reached. Excitation of large dynamic stress transients seem to be unavoidable in these circumstances.

Progressive damage models from geomechanics:

Another material idealization termed the 'progressive damage model' that has been recently developed by Dougill [65-67] is very promising in its potential for describing the behaviour of brittle materials better than the two-phase material models. The development of this model was also stimulated by the realization that strain softening can be physically attributed only to microcracking or fracturing. Attempts to explain experimentally observed softening behaviour in terms of defect slide as in plasticity are unconvincing.

As is implied by its name, a progressive damage model is characterized by progressive fracturing of a continuum as opposed to abrupt failure as in two-phase material models. Elastic properties of a continuum are thus gradually (and irreversibly) degraded as fracturing develops. Figure 4.12 demonstrates graphically the implications of the progressive damage model on stress-strain curves. Notice that unloading curves have decreasing slopes for increasing strains. Another significant difference from the plasticity models is that strains return to zero when stresses are removed. Recall that in plasticity models, strains or deformations were irreversible.

Progress of fracturing is expressed in terms of an internal state variable termed a damage parameter. In its simplest form, the state variable is a distributed scalar quantity [71-73]. However, scalar representations of damage yields an isotropic constitutive model and consideration of higher order tensorial representations appears unavoidable for prediction of the crack-induced anisotropies generally observed in brittle materials. Dragon and Mroz [74] defined damage as the product of crack face normal with the displacement discontinuity on the crack surface to achieve a formulation capable of describing crack growth in either cleavage or slip modes. Observing that microcrack growth results only from tensile strains, on the other hand, suggests microcrack definition by vectors orientated normal to the crack plane and equal in length to the crack area. Vector representations of microcracking damage have been adopted by several investigators [75-77].

The actual implementation of the progressive damage model can be achieved in a number of different ways. A loading surface is defined which encloses all stress states that can be reached without further fracturing or damage. The surface, of course, depends on certain material dependent fracturing parameters (constants) to be determined by curve fitting to experimental data. Strain increments can be defined relative to the surface as by the flow rule in plasticity. Provisions for hardening are also possible. For monotonic loading, it is reasonable to assume that hardening, if any, be isotropic. Under conditions of unloading and reloading, kinematic hardening appears more appropriate. This approach to the implementation of progressive fracture was in fact described by Bazant and Kim [69]. When the capabilities of a damage model are complemented with those of the strain-hardening plasticity model, realistic constitutive modellings of geomaterials can be achieved

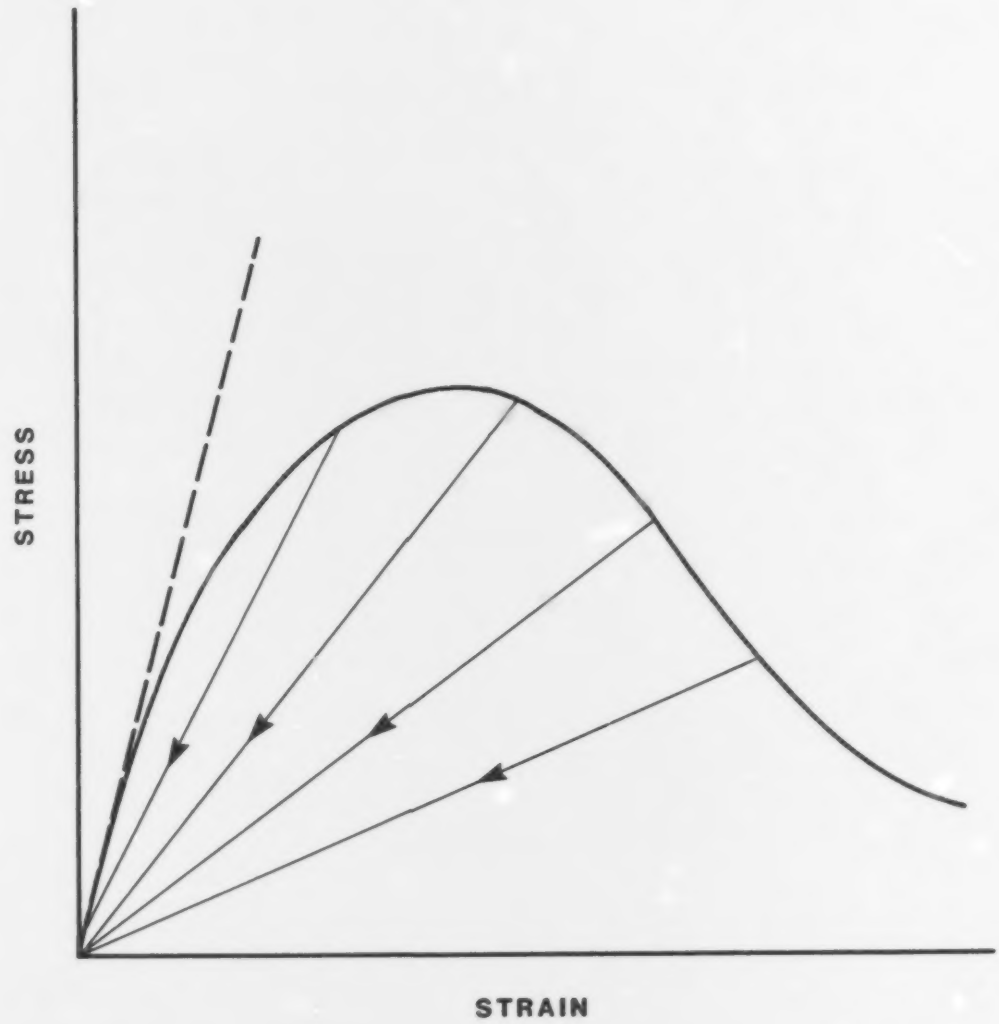

FIGURE 4.12 CHARACTERISTIC UNIAXIAL RESPONSE OF MATERIAL WITH PROGRESSIVE FRACTURE TYPE DAMAGE

[69, 78]. The uniaxial stress-strain curves for the so-called plastic-fracturing material are shown in Figure 4.13.

Another constitutive model for the mechanical behaviour of brittle materials based on progressive fracturing theory has been presented by Resende and Martin [79]. This material model appears to be mathematically well developed and is probably suitable for application to rock and concrete. A degradation of stiffness again gradually develops from the progressive fracturing of the material. This progressive damage model does not use any specific yield criterion but instead makes use of an internal variable defined as a damage parameter and relates the rate of damage to the stress and strain history. This damage relationship termed an 'evolution law' is postulated in an equation form, the coefficients for which are determined either experimentally or empirically. These progressive damage models therefore resemble the endochronic models of the next section.

There appears to be no evidence as yet in the open literature that either of these models has been applied to problems involving ice. Due to the brittle nature of ice behaviour at high strain rates, the application of progressive fracture theory to ice seems to be a simple logical extension of the formulations as described for rock or concrete and certainly it is worth considering at some stage of this project. The definition of an evolution law for ice may have to be somewhat arbitrary due to the absence of adequate relevant experimental data in the literature and perhaps a number of trials would be required just to assess its suitability.

Endochronic constitutive models

The endochronic theory of inelasticity and failure has been developed and proven effective for geomechanical materials including concrete, rock, sand, and soils [80-99]. The motivation for this development was deficiencies with plasticity theories. In particular, satisfactory hardening rules had not been identified. Also, formulations of inelastic dilatancy, hydrostatic pressure sensitivity, and strain-softening tendency in plasticity theories were not adequate.

The central concept in endochronic modelling is the intrinsic material 'time-scale'. This is a scalar parameter which depends on the length of the path traced by the states of the material in the strain space. Several material constants are defined by appropriate curve fitting to stress-strain relationships derived from uniaxial compression experiments. These constants enable the material deformation history for biaxial and triaxial loads to be described. The hardening or softening of the material during the evolution of inelastic strain can be modelled. Also, an additional term can be introduced to model inelastic dilatancy due to shear. An important advantage of this approach is its ability to describe plastic material behaviour without the need for the identification of material yield surfaces. Another is that it can represent unloading irreversibility without the use of inequalities

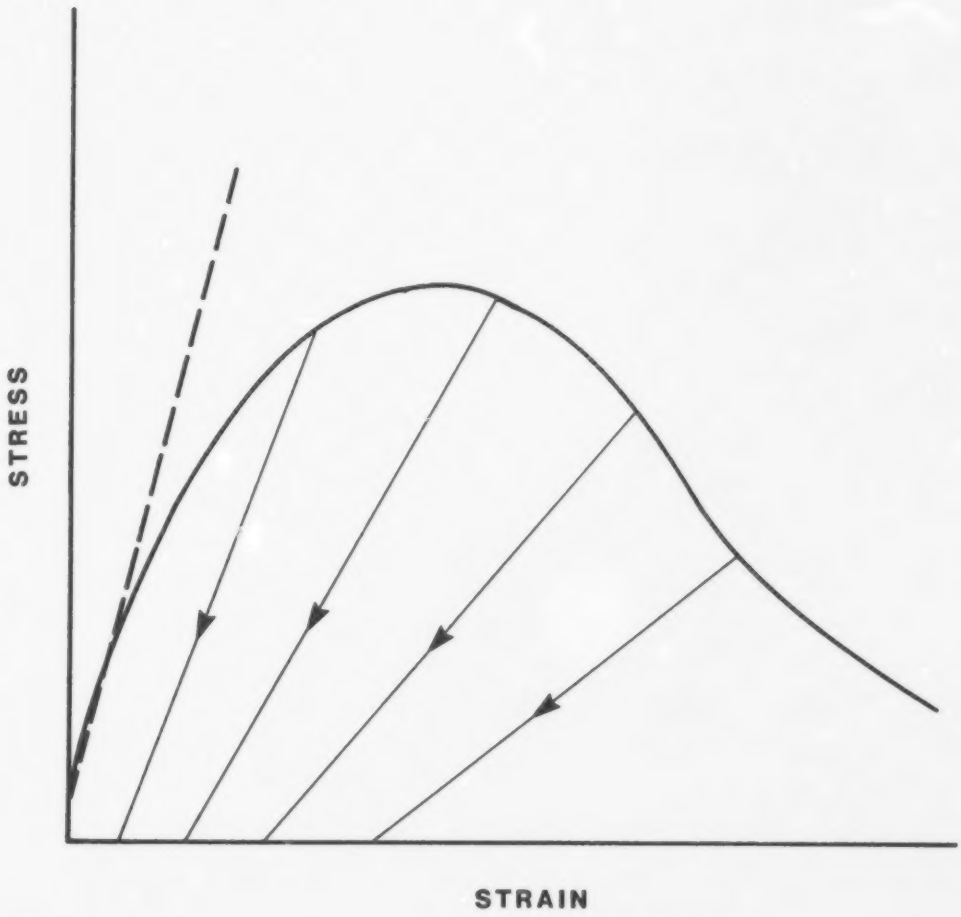

FIGURE 4.13 CHARACTERISTIC UNIAXIAL RESPONSE OF MATERIAL WITH PROGRESSIVE PLASTIC-FRACTURE TYPE DAMAGE

(unloading criteria) which makes endochronic theory extremely effective for cylic loading.

The most significant difference between endochronic theory and classical plasticity or plastic-fracturing theory is that it cannot be reduced to an incrementally linear form. This suggests convergence difficulties in numerical computations but endochronic theory has been successfully adopted in finite element programs.

Endochronic constitutive modelling has only recently been applied to ice [100]. It appears to be capable of providing a realistic model of ice including strain hardening, strain softening, and dilatancy functions.

Impact damage models of Stanford Research Institute

For brittle materials such as concrete or rock where microcrack development is an important consideration in describing material failure, the adoption of a material damage approach to finite element fracture analysis is attractive [101-103]. Above the use of damage models for ice has been proposed. Due to the high loading rates associated with ice milling, dynamic fracture considerations should also be suitably accounted for within the damage model. Stanford Research Institute has developed a powerful damage modelling computer program called NAG/FRAG which describes either ductile or brittle fracture associated with impact loadings [104-107]. The NAG/FRAG program accounts for nucleation and subsequent growth of cracks or voids as a function of stress level and stress duration, coalescence of cracks to form fragments, and the possible eventual separation of fragments. Numerous crack orientations are permitted within each element and the effects of inherent material flaws and faults can also be accounted for. The program has been refined to the point that even size of fragments can be reliably predicted.

While the Stanford Research Institute damage model appears to hold considerable potential as the basis of an ice damage model for propeller-ice interaction studies, the requirement for further development work is nonetheless indicated. The microfracture nucleation and growth (NAG) laws employed are empirical in the sense that observational assessments of microfracture impact damage for several different types of material when correlated with loading history yielded the following expressions:

$$\dot{N} = \dot{N}_0 \exp \frac{\sigma - \sigma_{no}}{\sigma_1} \qquad \dot{D} = \frac{\sigma - \sigma_{go}}{4\eta} D$$

where the nucleation rate $\dot{N}$ varies exponentially on the tensile stress σ, and the growth rate $\dot{D}$ is a linear function of stress and the size of microfracture D. The remaining parameters including $\dot{N}_0$, σ_{no}, σ_1, σ_{go}, and η, constitute material fracture properties and would have to be established by curve fitting to data obtained for ice. In fact, the

relevance of the above expressions to ice ought to be reassessed considering that the strain rates associated with ice milling are probably lower than in the impact applications for which the programs were developed and the uniqueness of ice properties attributed to its comparatively high homologous temperatures.

Concrete variable modulus model

Ice exhibits many of the same characteristics as concrete and material models proposed for concrete is applicable to ice. One of these material models is the variable modulus model of Bathe and Ramaswamy [108]. The model accounts for various nonlinear effects important in the description of structural response of brittle materials including (a) a nonlinear stress-strain relationship for loading in compression (resulting in isotropy at low compressive stresses and orthotropy at higher stresses), (b) tensile cracking and compression crushing material failures defined by a failure surface, and (c) strain softening to describe material weakening caused by the development of micro-cracking damage. These nonlinearities depend strongly on the triaxial state of stress. Equivalent uniaxial stress-strain curves are introduced in the principal stress space and then the effective uniaxial moduli are adjusted to match triaxial maximum stress data.

The stress-strain relationship is linear in tension. A tensile cracking cutoff is also provided. It is implemented by examining stresses at integration points and if the cutoff tensile stress is exceeded, a failure plane is assumed to form normal to the principal stress direction. The normal stiffness across the plane is decreased to a user-specified factor times the original stiffness. The shear stiffness is similarly reduced. The default stiffness reduction factors are 0.001 for normal stiffness components and 0.5 for shear stiffness components.

The above described material model has been incorporated into ADINA [109]. It has been adopted in our ice block analyses and further details can be found in the next chapter.

4.4 Typical Values for the Mechanical Properties of Ice

The uniaxial compressive strength and the uniaxial tensile strength of ice depend upon physical properties of ice as well as external factors. Physical properties include again structure and grain size of ice, salinity, temperature, porosity and air content. These properties are essentially the results of formation history of ice and the type of water, i.e. seawater or river and lake water. The external factors such as the rate at which the load is applied, i.e. strain rate and the confining pressure affect the strength values significantly. The latter effect can be accounted for by adopting the appropriate parameters in defining the failure (yield) envelope for ice and is discussed in Section 5.3.

The procedure developed under this contract for determination of propeller-ice interaction forces depends upon the specification of unconfined compressive strength of ice; and therefore this section is intended to provide some guidance in adopting the appropriate value for this parameter. The functional relationship between each of the above mentioned factors and the compressive (or tensile) strength of ice is still not well established and some judgement has to be exercised in selecting the right value.

Freshly formed ice, commonly termed as first-year ice, generally exhibits lower compressive strength than the strength of ice which has a history of formation over a long period, usually referred to as multi-year ice. The test results reported in the technical literature indicate that the compressive strength of first-year Beaufort Sea ice varies between 2.0 MPa to 4.0 MPa at a constant nominal strain rate of about 2×10^{-4} sec^{-1} [30, 110]. The strain rate influences the compressive strength significantly; and at a strain rate of around 10^{-4} sec^{-1}, it reaches its peak value of about 8.0 to 9.0 MPa for fresh water ice. For strain rate greater than the rate of 10^{-4} sec^{-1}, the strength drops to a slightly lower value and the failure is characterized by brittle behaviour [111]. The effect of salinity is generally to reduce the compressive strength of ice [43], and therefore sea ice is likely to exhibit lower crushing strength than the freshwater ice.

Whilst there is a lack of sufficient data in the technical literature concerning the compressive strength of ice, any information about the tensile strength of ice is virtually non-existent. The published results are scarce and the effect of various parameters upon the tensile strength of ice is not well documented. The available data indicates that the tensile strength of ice varies between 0.4 MPa to about 1.9 MPa [112-114].

In addition to the compressive and tensile strengths of ice, other mechanical properties such as Young's Modulus and interface friction coefficient also play an important role in the finite element analysis of an ice-block and thus affect the analytical determination of propeller-ice interaction forces. Generally the value of Young's modulus for multi-year ice tends to be higher than the corresponding value of first-year ice [115].

Young's Modulus depends upon strain rate. At a low strain rate of less than 10^{-5} sec^{-1}, the value of Young's Modulus for multi-year ice is about 3,000 to 6,000 MPa, and tends to increase with increase in strain rate so that for a strain rate between 10^{-4} to 10^{-3} sec^{-1}, it is about 10,000 MPa [116-118].

The coefficient of friction between steel surface and ice depends upon various factors such as surface roughness, salinity of ice, temperature, time in contact, and relative velocity between the two surfaces. Under static conditions friction coefficient is usually high, probably in the region of 0.40, but decreases rapidly as the relative velocity

increases and can be as low as 0.05 [119-120]. For practical purposes, the coefficient of friction of about 0.05 to 0.1 appears to be reasonable for propeller-ice interaction problem.

5.0 DETERMINATION OF PROPELLER-ICE INTERACTION FORCES USING A FINITE ELEMENT MODEL OF THE ICE BLOCK

5.1 Selection of Analysis Program

Several criterion were identified for consideration in the selection of an analysis program. These were: (i) the ability of the program to adequately model the mechanical behaviour of ice; (ii) modelling features and types of analysis offered; (iii) user supplied subroutine options; (iv) graphics available for input verification and presentation of results; (v) cost; and (vi) vendor support.

A number of commercially available programs were critically examined. These included NONSAP, ADINA, MARC, ANSYS, ABAQUS and PISCES. Program evaluations are given in Appendix A.

Unfortunately, assessments based on analysis costs can be reliably performed only by considering suitable benchmark problems and undertaking comparative studies of costs in the operational environment in which they would have to be run. Different programs while offering the same modelling capabilities may differ enormously in their cost of execution due to inherent differences in efficiencies of the algorithmic coding. For programs run on different computer bureaux, formulae related to the cost of computer resources as well as royalties on vendor produced software require consideration. Not surprisingly, a definitive conclusion on the most cost effective program could not be reached but from observations based on available literature, a judgement, albeit subjective, was formed.

Of the various programs evaluated, ADINA was selected as the one most appropriate for the problem at hand. The Drucker-Prager and concrete damage material models available in ADINA were considered appropriate for representing the mechanical behaviour of ice (see Section 5.3.3). In order to simplify the analysis, and reduce costs, it was felt that the propeller blade should be assumed rigid. It should be emphasized that the approximation is utilized only for the ice-block analysis in which propeller-ice interaction forces are determined. (For the purpose of determining the propeller response under the influence of the propeller-ice interaction forces, the propeller is assumed to be linear elastic.) The rigid blade condition can be handled using the prescribed displacement feature in ADINA. The program offers an excellent dynamic analysis capability. Although the contract did not call for dynamic analysis to be carried out, it was felt that inertial effects could prove to be important, and might have to be considered at a later date. It was also felt that the ability of the program to accept a user supplied subroutine for material modelling could prove useful. Because suitable model generation programs were to be developed, graphical data verification was considered necessary. Displacement and stress interpretation is also simplified by the use of appropriate graphics programs. Because of previous work, Martec had developed interface programs for its own graphics package and ADINA output. In-house graphics and interface

programs were available for the ADINA output, thus reducing the computer bureau requirements for the project. As already noted, analysis costs could not be truly assessed. However, all nonlinear analysis programs are inherently costly, and the general feeling is that ADINA is as economical to run as other programs in its class.

5.2 Types of Models Considered

The types of ice block models considered are shown in Figure 5.1. For the indentation type (Figure 5.1(a)), flat, curved (circular and elliptical) and wedge shaped indentors were used. For the slicing type (Figure 5.1(b)), both flat and inclined cutters were considered.

It is assumed that the dimensions of the ice block are large compared to the indentor or cutter. However, because the finite element solution is approximate, the full extent of the ice block need not be modelled, and it suffices to take an ice block sufficiently large that boundary conditions will not unduly influence the results. The plan dimensions of the ice block models have therefore been taken to be approximately five to six times the width of the indentor or cutter. Only two-dimensional models have been considered. Consequently, only plane strain or plane stress situations can be represented. Furthermore, the indentors are assumed to be symmetric, and symmetry is exploited in the indentation analysis.

Special computer programs were developed to generate the finite element models of the ice block. Plots of the indentation models are shown in Figures 5.2 to 5.5. Note that only the ice on one side of the line of symmetry has been modelled.

Plots of the various slicing models used are shown in Figures 5.6 to 5.10. The models shown in Figures 5.6 to 5.8 were used in early investigations, whereas the more refined models shown in Figures 5.9 and 5.10 were used later. The refined models are characterized by an increased amount of mesh refinement in the vicinity of the cutter tip. The fact that such a refinement was necessary became obvious during the early investigations.

In the case of the slicing models, it is assumed that the cutter has advanced some distance into the ice. The model shown in Figure 5.6 includes the milled volume of ice. During the analysis of this model, complex patterns of ice failure were encountered, including severe cracking inside the milled edge. This lead to numerical (convergence) problems and prohibitively large computer costs. The model shown in Figure 5.7, which does not include the milled volume of ice, was then tried. A successful analysis was obtained, and consequently, the milled volume of ice was not included in subsequent models.

All models were formulated using the 8-noded two-dimensional solid element available in ADINA. In some models, a gradual coarsening of the mesh from the indentor interface where largest stress gradients are

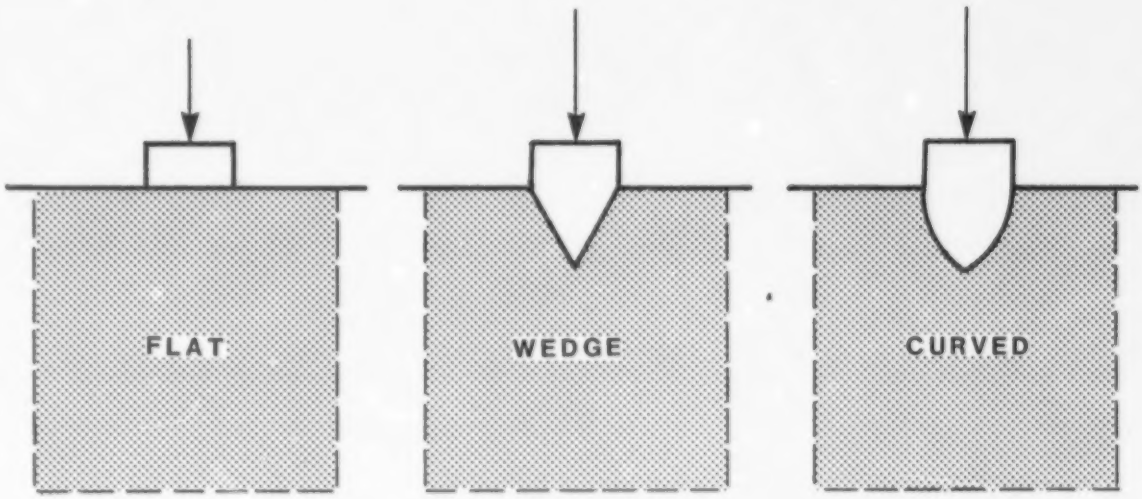

A) INDENTATION

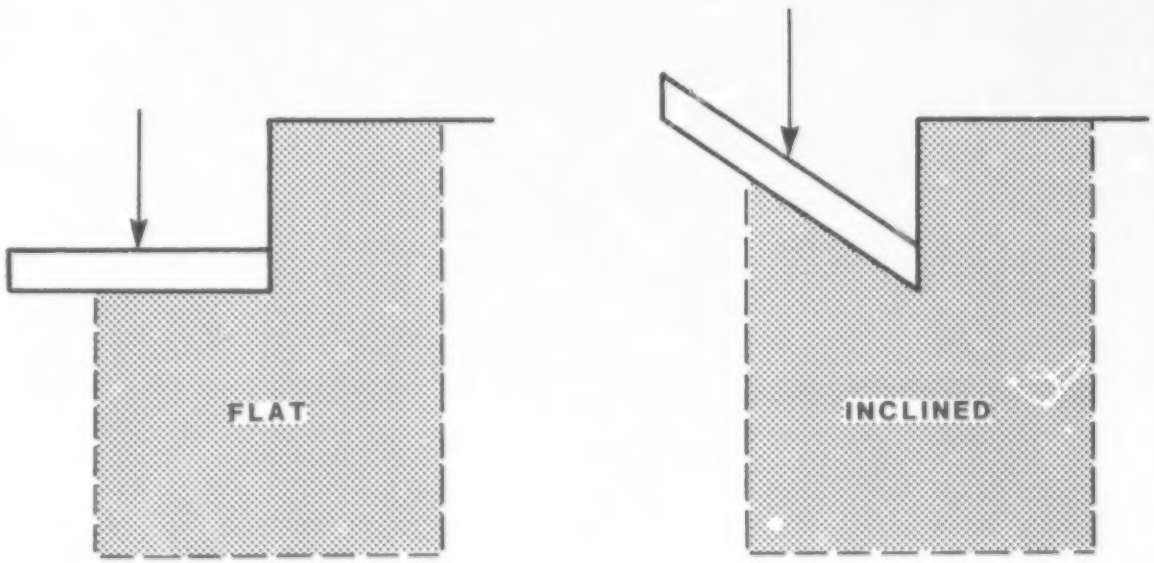

B) SLICING

FIGURE 5.1 TYPES OF MODELS CONSIDERED IN ICE BLOCK ANALYSIS

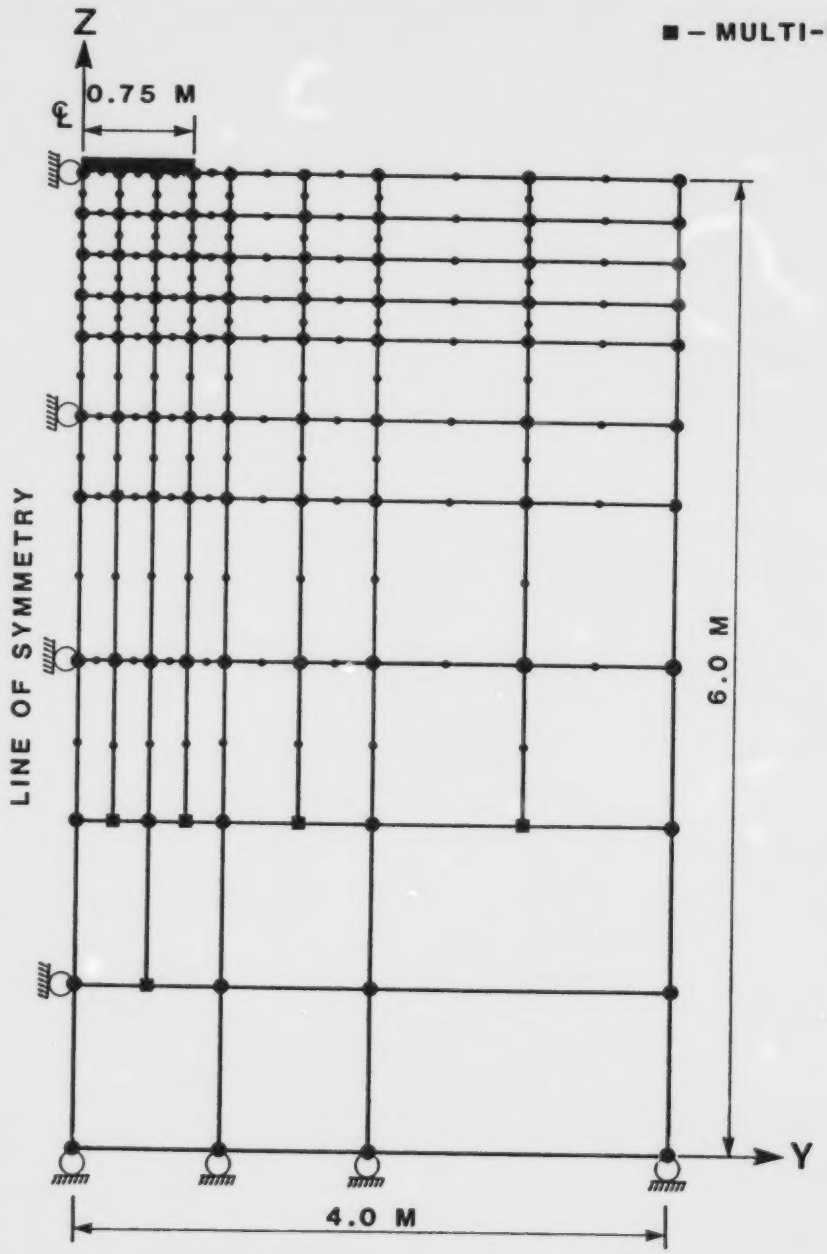

FIGURE 5.2 RECTANGULAR INDENTOR - FINITE ELEMENT MODEL

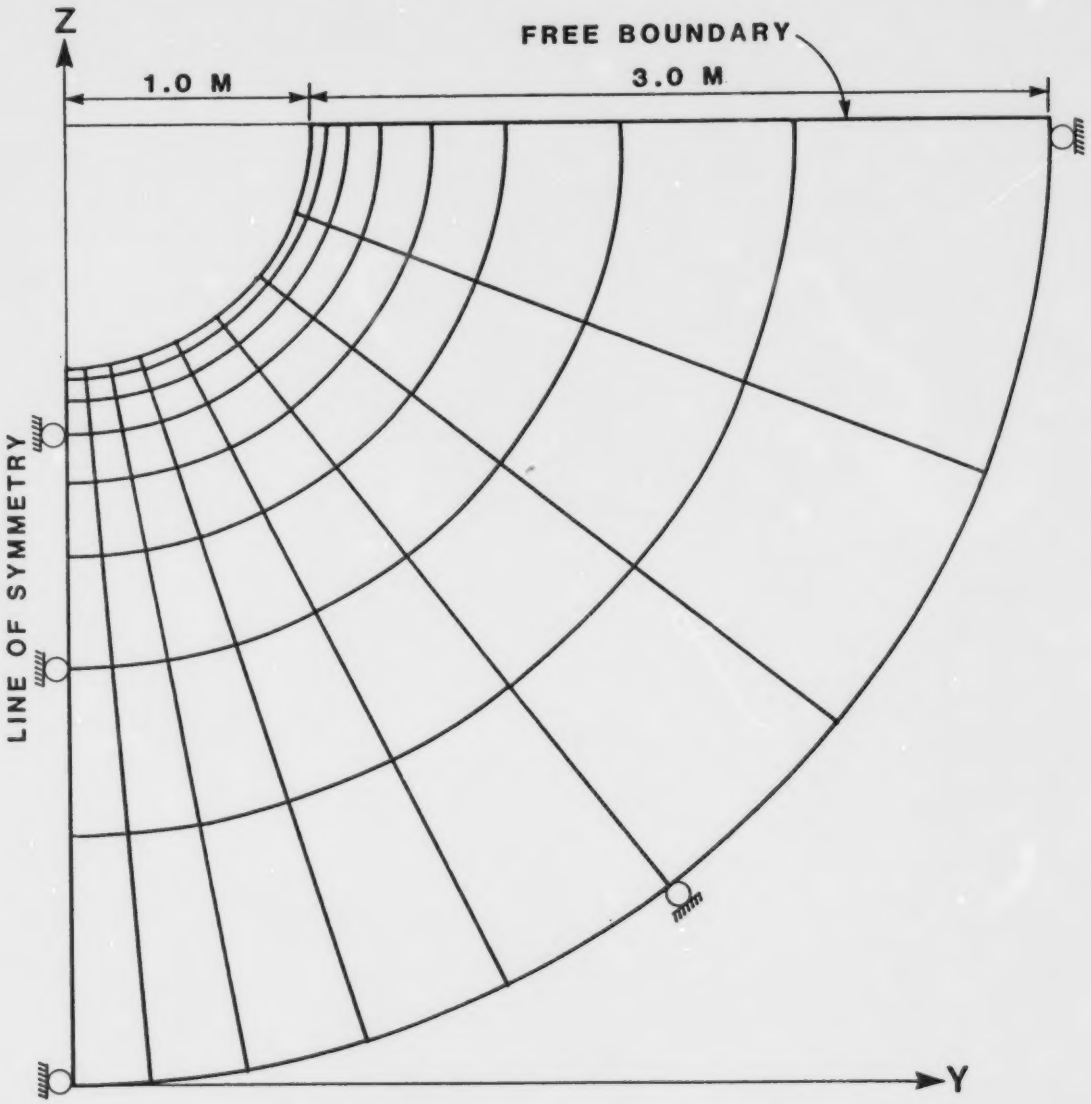

FIGURE 5.3 CIRCULAR INDENTOR - FINITE ELEMENT MODEL

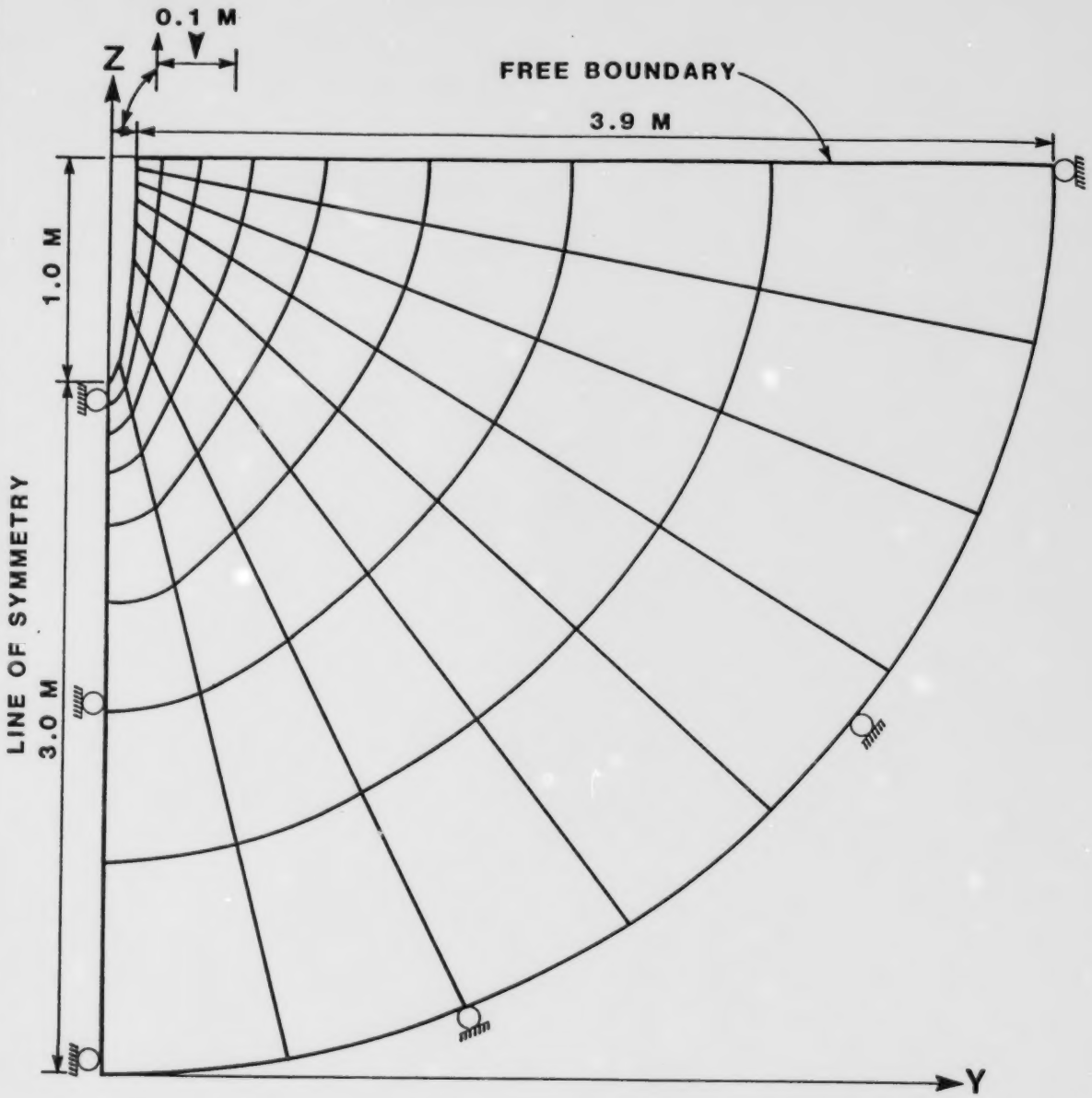

FIGURE 5.4 ELLIPTICAL INDENTOR - FINITE ELEMENT MODEL

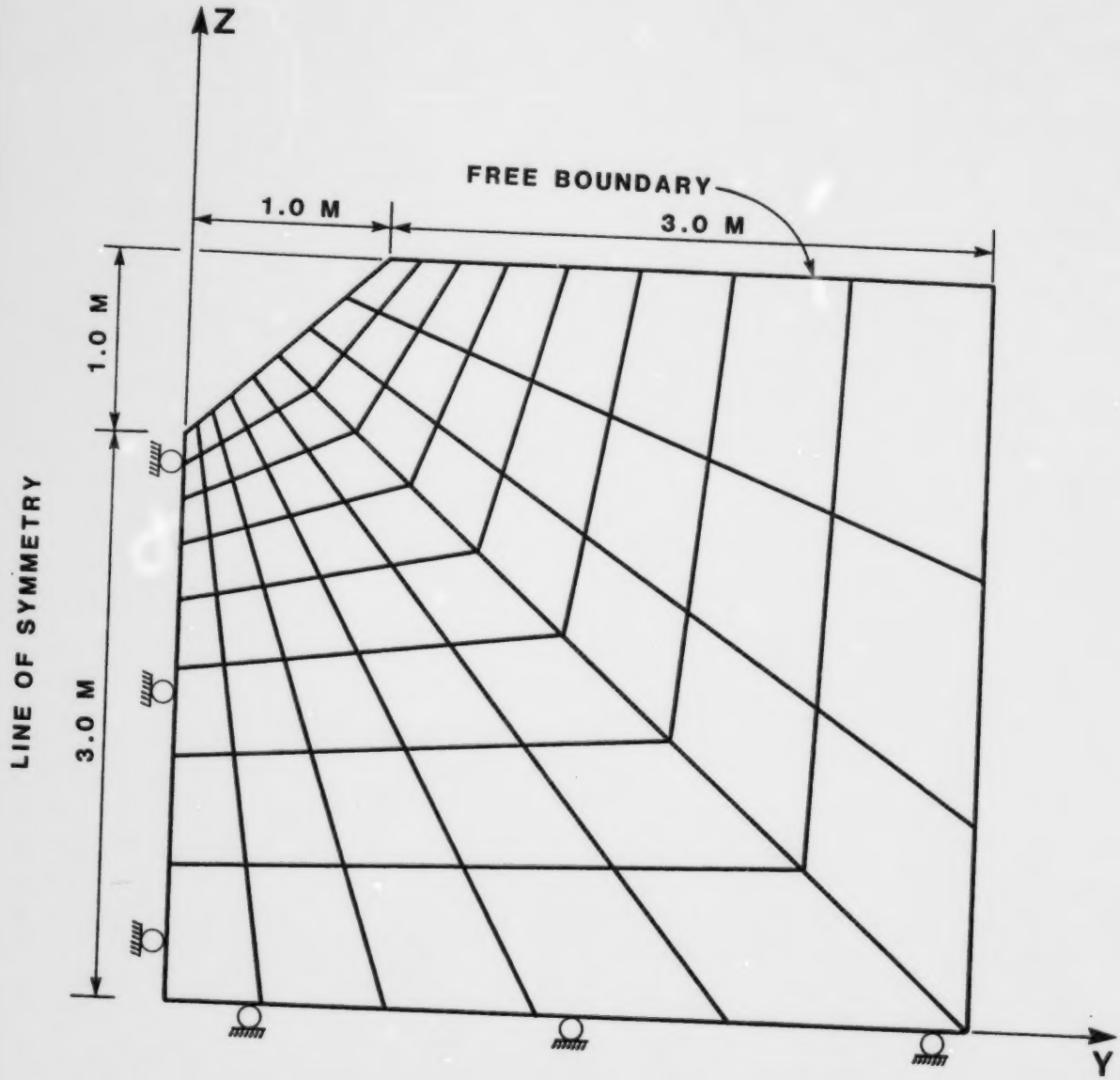

FIGURE 5.5 WEDGE SHAPED INDENTOR - FINITE ELEMENT MODEL

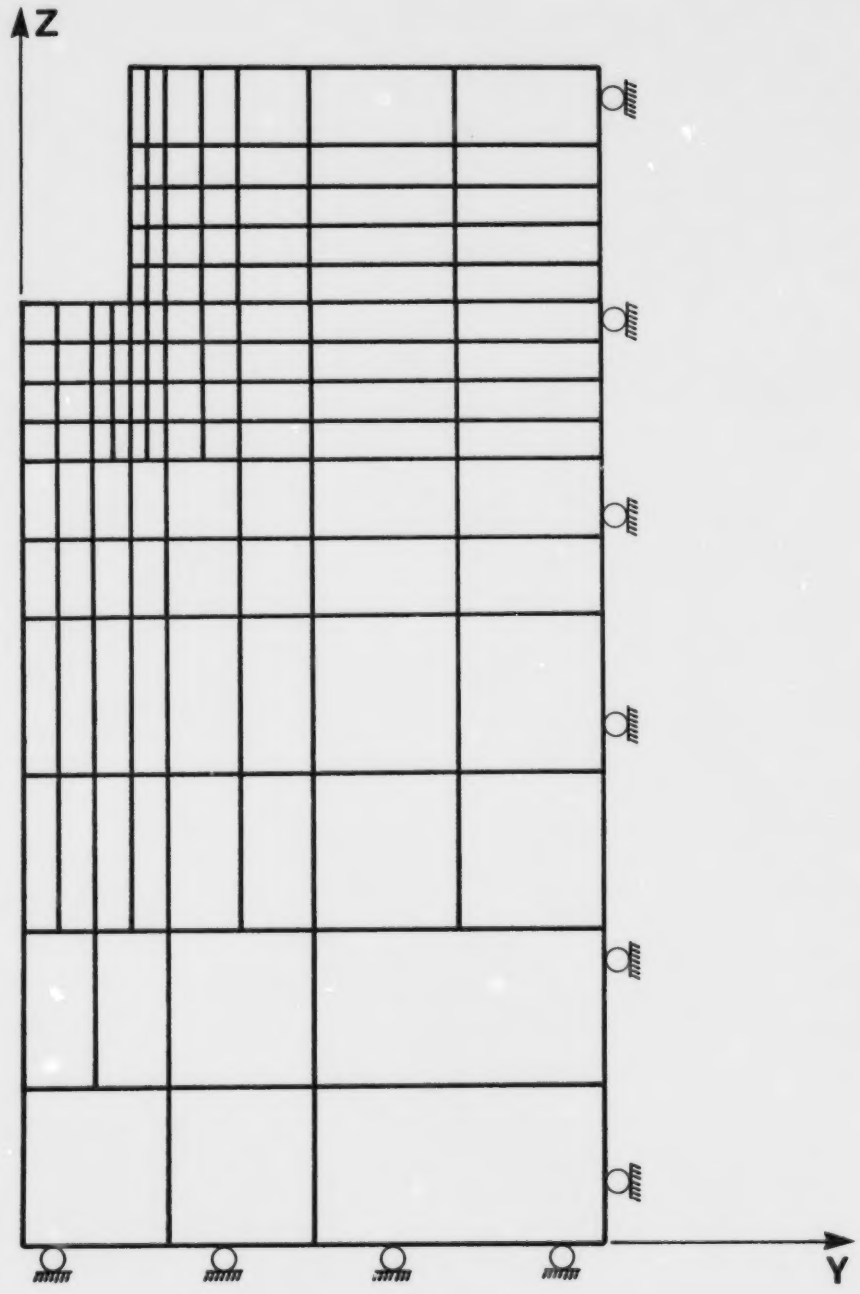

FIGURE 5.6 FLAT CUTTER - FINITE ELEMENT MODEL #1

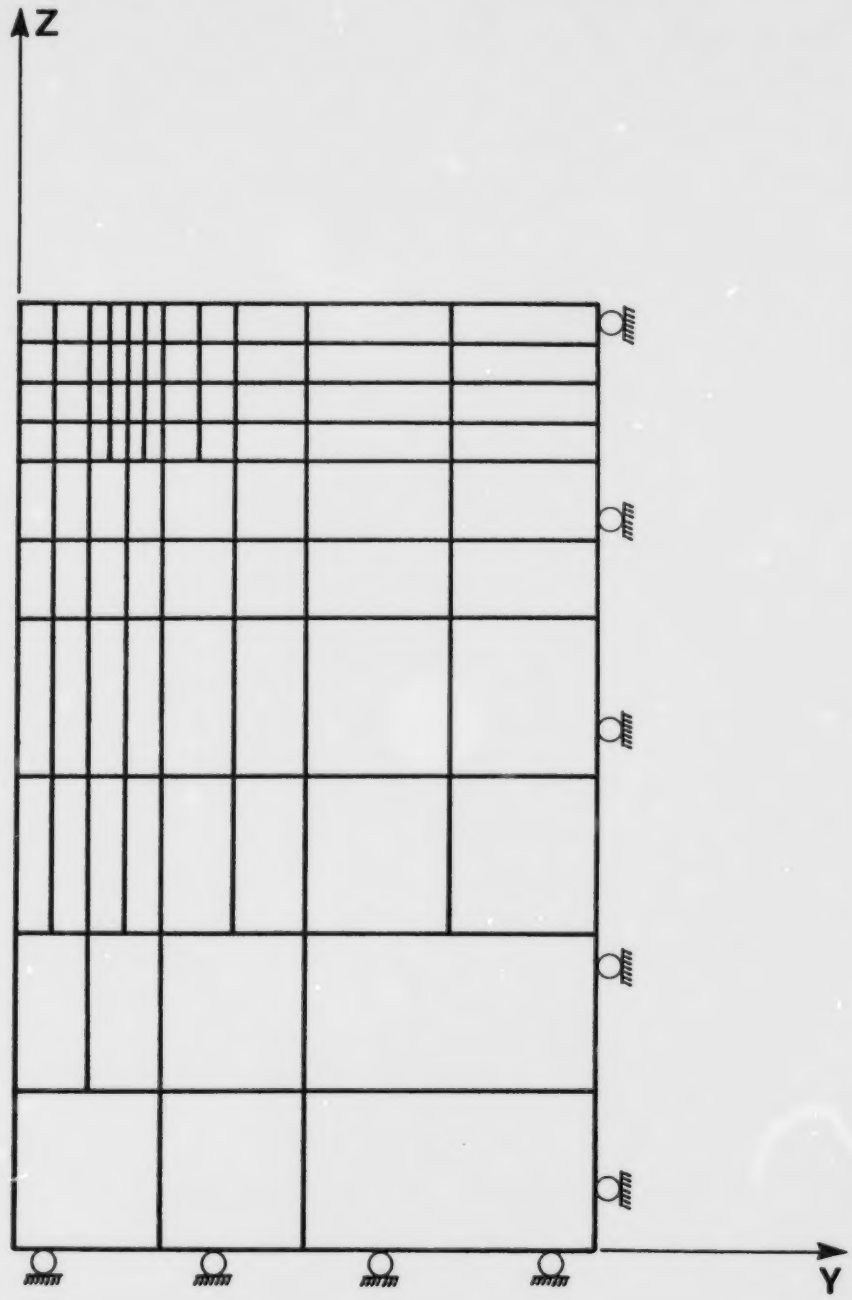

FIGURE 5.7 FLAT CUTTER - FINITE ELEMENT MODEL #2

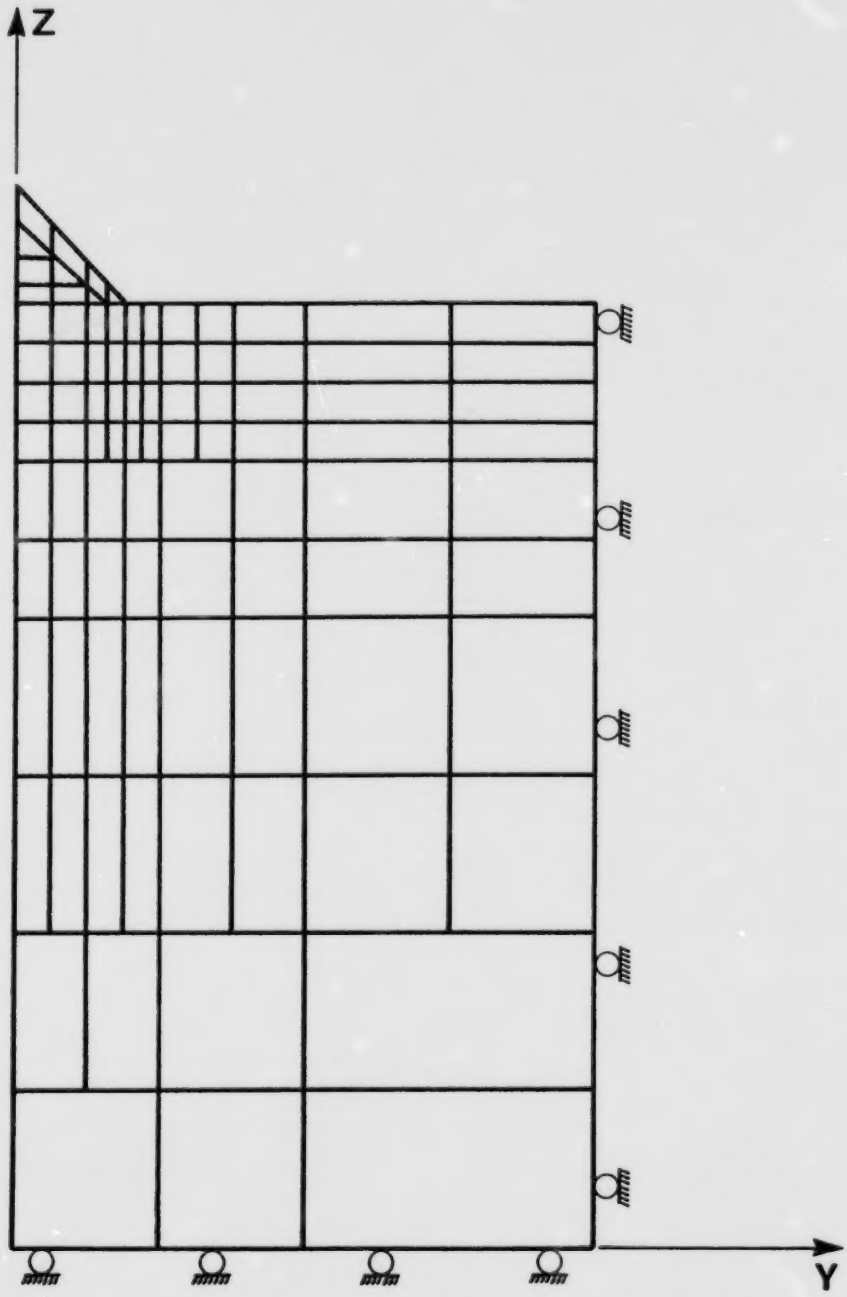

FIGURE 5.8 INCLINED CUTTER - FINITE ELEMENT MODEL

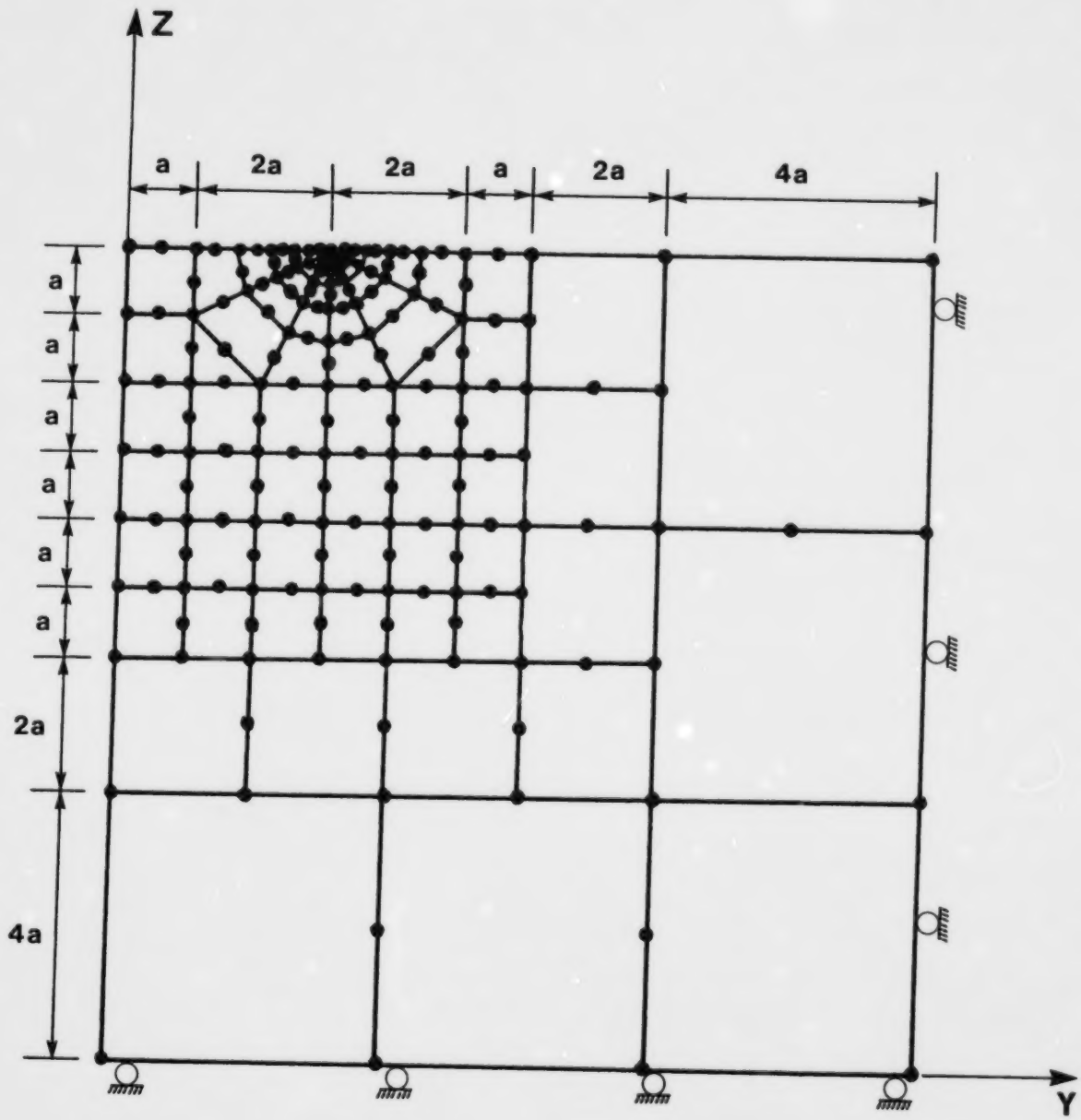

FIGURE 5.9 REFINED FINITE ELEMENT MODEL

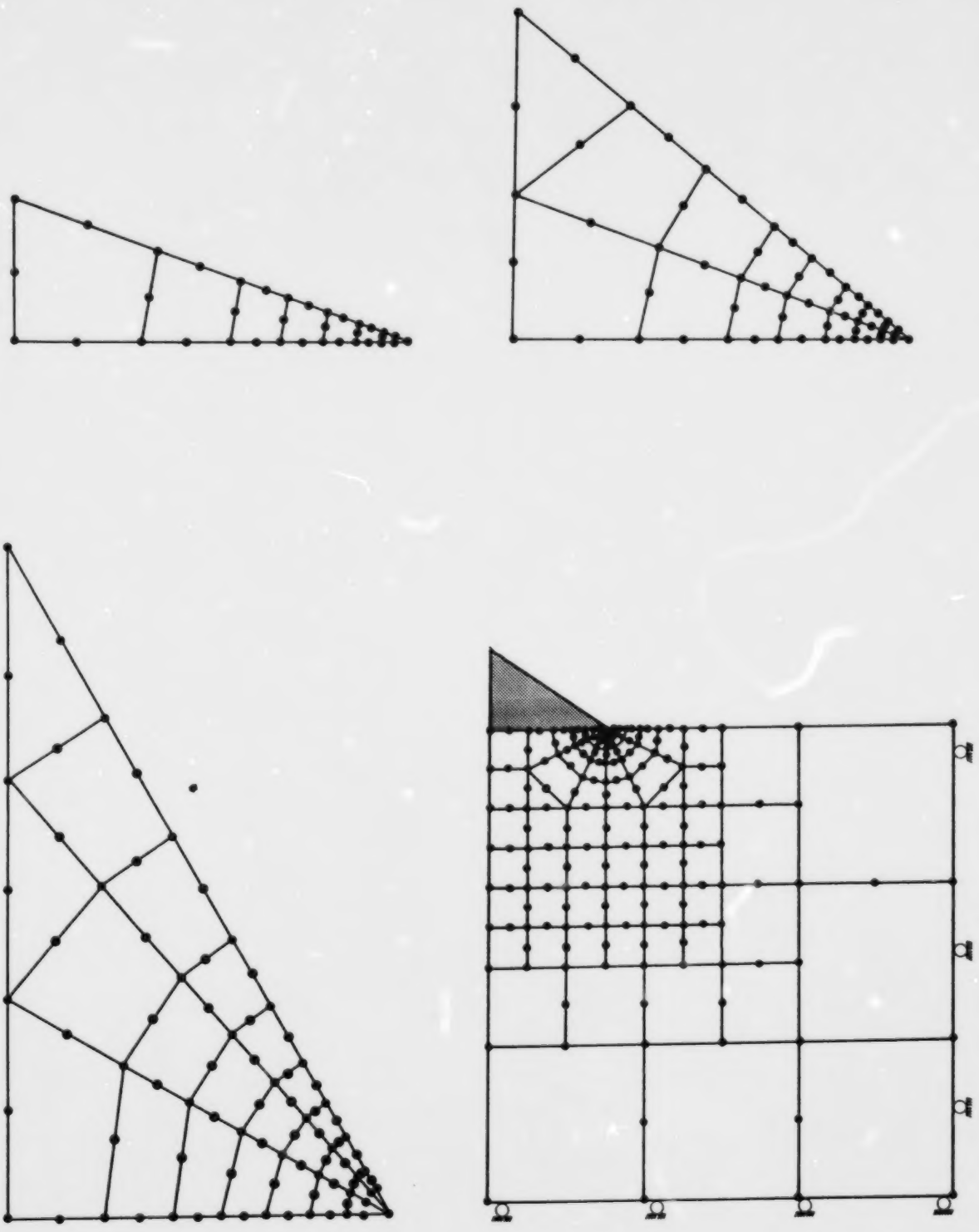

FIGURE 5.10 BUILT UP MESHES FOR INCLINED CUTTER - REFINED FINITE ELEMENT MODEL

expected towards the boundaries where less pronounced variations in stresses should occur was employed to reduce the problem size. On interfaces which are connected to a single element on one side of it and to two elements on the other side, special nodes known as "irregular nodes" are located. These nodes result in displacement incompatibility across the interface unless supplementary equations, commonly referred to in finite element literature as "multi-point constraint equations" are applied to force the displacements at the irregular node to adopt values implied by the linear shape functions of the single connecting element.

5.3 ADINA Analysis

5.3.1 Data Generation

The finite element models shown in Figures 5.2, 5.6, 5.7 and 5.8 were generated manually. The models shown in Figures 5.3, 5.4 and 5.5 were generated by a program called IDENTM, developed specifically for indentation type problems. The models shown in Figures 5.9 and 5.10 were generated by a program called MILLM, developed specifically for milling problems of the slicing type. Brief descriptions of both programs developed under this contract are given below.

Consistent with all data generation activities organized by Martec, data formatting appropriate for input to the VAST finite element analysis program were adopted for the finite element models generated by IDENTM and MILLM. In this way graphpical model verification programs associated with VAST could be used to check models prior to submitting them for analysis.

Because ADINA was employed in the investigation, the data had to be subsequently reformatted by a program called ADIDAT [121]. The program reformats coordinate and element data automatically but defines the nonlinear aspects of the problem as required by ADINA through interactive prompts.

Program IDENTM:

The program IDENTM was developed to facilitate generation of geometry data for finite element models to be used to investigate the effect of tip detail on indentation forces and stress distributions within the ice block. Indentors of various shapes have been allowed including wedge, semicircular and elliptical geometries.

A minimum of input data describing indentor geometry is required. Basically the user must make a selection from a list of available indentor types and then specify appropriate geometric parameters defining that indentor type. Different shapes of ice block are also permitted but generally the two available options involve external dimensions of the ice block as a magnification of the indentor shape or alternately a rectangular shape. A parametric patch meshing method (similar to the Coon's patch) has been employed to define finite element models around

the indentor. The ice block region under analysis is assumed to be mapped into a quadrilateral in parametric space. The geometry of each bounding curve is defined. Options are provided for a single curve definition or multiple piecewise curve definitions (i.e. two straight lines in global coordinate space). Mesh spacing along four quadrilateral edges in parametric space is then defined and through linear interpolation all internal grid points are generated.

Control on finite element solution accuracy is through mesh density. An arbitrary number of elements along indentor face and outwards away from it can be stipulated. Even greater flexibility is provided through use of nonuniform mesh spacing (with respect to patch parametric coordinates). Either uniform or variable meshes (with respect to patch parametric coordinates) may be produced. Variable meshes are desirable when significant stress gradients are expected. Finer meshes would obviously be adopted in portions of the model where stress gradients are largest and stress variations have the most complex functional variation. It is well known that piecewise element stress variations approximate an arbitrary stress function progressively better as number of elements is increased. Two options for variable meshes are provided; element sizes defined as geometric ratios or user-defined proportionality factors.

Rod elements orientated perpendicular to indentor surface, to be used to model indentor-to-ice interface contact and separation, were also included in the finite element model (see Section 5.3.2). Rod elements are also instrumental in the application of the prescribed displacement boundary conditions. Furthermore, rods are important in the determination of forces (and hence pressures) experienced by the blade (when arbitrary finite element meshes are employed). Important to the implementation of rod element is the definition of appropriate skewed coordinate systems.

Program MILLM:

The program MILLM was developed for the automatic finite element model generation for milling simulations shown in Figure 5.1(b). The need for greater refinement in finite element models for such simulations developed from observed sharp interface pressure gradients in the vicinity of the milling blade tip when coarser meshes (Figures 5.2 and 5.8) were employed initially. A gap developed along most of the cutter-to-ice interface and nonzero interface pressure distributions were associated with a single ice element at the cutter tip in the original model. There was some concern that accuracy of interface pressure distributions might be limited by the quadratic variation of element stresses in ice block elements along the interface.

An increased amount of mesh refinement at the cutter tip should indicate how important to solution accuracy the grid around the cutter tip is. This is the approach which would typically be adopted in linear elastic analysis. Because the present ice analysis is nonlinear and

involves continuum damage material behaviour (with softening characteristics for large strains), certain amount of caution was required. The first point to note is that the refined mesh at the cutter tip will have maximum benefit for small structural loads (in the form of prescribed displacements along the cutter-to-ice interface). As material nonlinearities develop in the form of microcracking (stress release at element integration points across the plane of maximum tensile stress) and ultimately in the form of crushing (final material failure leaving no residual strength) within a zone progressing out from the cutter tip, larger elements are encountered (at the damage front). Elements at the cutter tip are stress relieved and fine meshing in that vicinity becomes increasingly less important.

The second point is that because of the softening characteristics of the damage model for large strains, the reliable performance of the material model is dependent on the finite element mesh. An overly refined finite mesh may lead to the phenomenon observed in softening materials called strain localization. Strains concentrate into a progressively narrower band of elements and loads required to propagate the crack band decreases. Because of this, extra care was exercised when assessing finite element results obtained with the refined model to confirm that strain localization was not occurring.

A square finite element model of the form shown in Figure 5.9 can be generated by MILLM, and, optionally, one of the three meshes in Figure 5.10 appended to the upper left hand corner. Which of the three meshes is adopted under the cutter depends on the cutting angle, i.e. the angle made by the horizontal and cutter.

Model group numbers are defined in Figure 5.11. The number of elements and node points are invariant in all element groups except #3 and #4. Depending on cutting angle between one and three element layers could be employed in element group #4 in order to prevent gross element distortions or deterioration in element proportioning. The number of nodal points along the cutter-to-ice interface increases by two for each new element layer and the number of rod elements employed in the first element group increases correspondingly.

Because of the complexity of the mesh and associated difficulty of numbering of nodes in a manner which is optimal for efficiency of the equation solvers in the ADINA analysis program, a bandwidth reduction algorithm had to be inserted into MILLM. The bandwidth reduction algorithm produces significant savings in computational effort and storage requirements during the solution of equilibrium equations.

5.3.2 Use of Rod Elements to Simulate Contact

During the early runs it was observed that small negative stresses near the trailing end of the structure (indentor or cutter) are present. This suggested a possible separation of the structure away from the ice-block. Several commercial finite element programs have capabilities

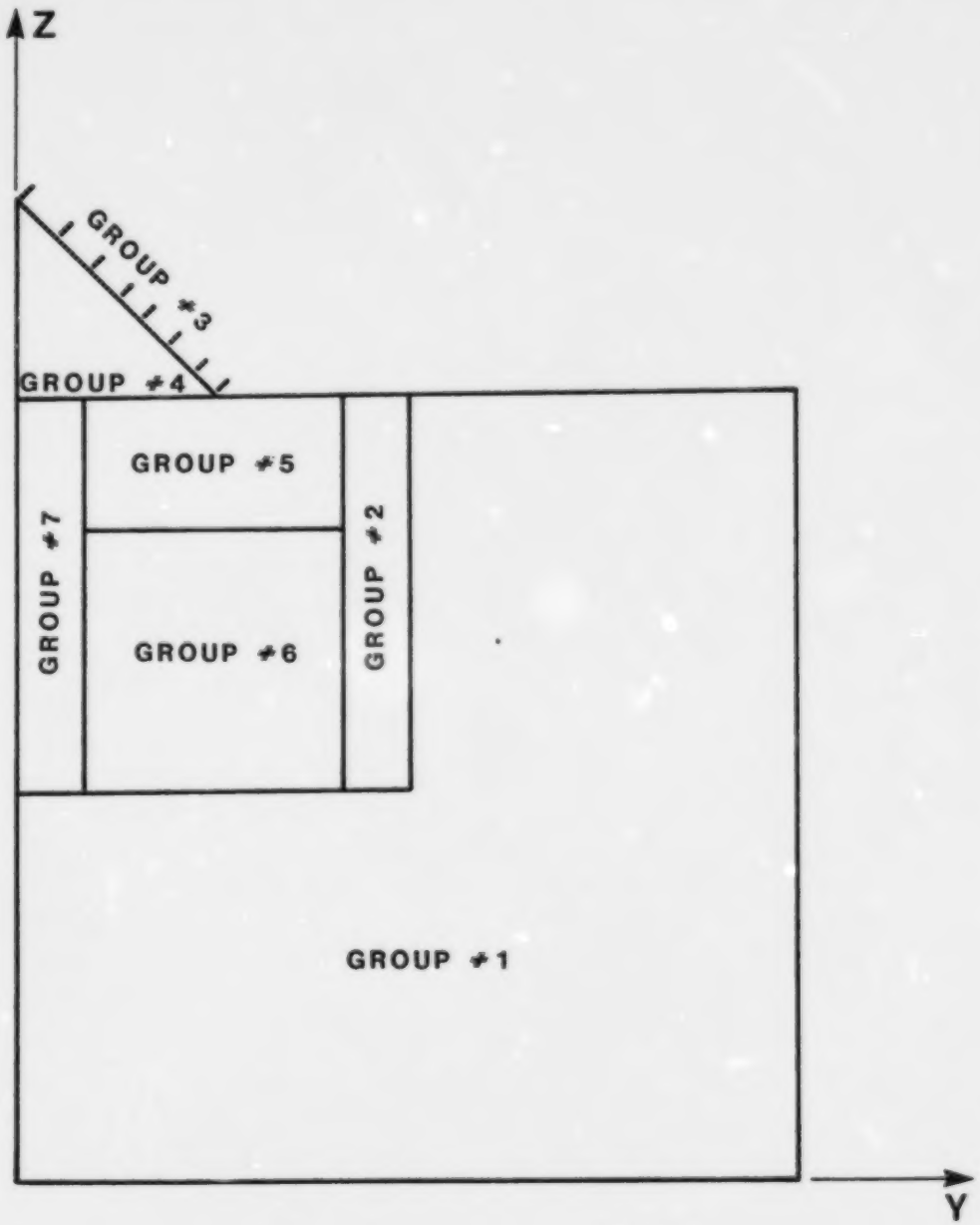

FIGURE 5.11 FINITE ELEMENT MODEL GROUP NUMBERS

which automatically account for the separation of two contacting surfaces but the version of ADINA available for this contract did not. In order to permit the effects of this separation to be studied, fictitious rod elements had to be explicitly introduced between the structure and the ice. The material properties assigned to the rod elements gave them large stiffness values for compressive strains and a very small, almost zero, stiffness value for tensile strains. This resulted in large compressive loads in the rod elements when simulating contact between the structure and the ice, and virtually zero tensile loads when simulating the condition of separation. The reason for nonzero tensile forces instead of exactly zero forces is to avoid computational problems associated with semi-definiteness of the global stiffness matrix once crushing failure begins to develop.

5.3.3 Material Modelling

It has been pointed out (Section 4.0) that the reliable prediction of structure-ice interaction forces depend largely upon the degree of accuracy with which the following two ice characteristics are represented: (i) stress-strain relationship, for both pre- and post-failure behaviours; and (ii) yield criterion, which must deal with the multi-axial stress-state might exist at the time of failure.

Concrete Model Material Model:

The ADINA concrete model embodies a nonlinear stress-strain relationship which permits the essential features of the relationship as it relates to ice including strain-softening to be represented. Available data [111, 24, 16, 122] was scrutinized and a representative uniaxial stress-strain curve shown in Figure 5.12 was adopted for the analyses. The stress-strain curve for the concrete material model is defined by four physical quantities (the uniaxial maximum compressive stress and corresponding strain; the uniaxial ultimate compressive stress and corresponding strain) and consequently it is an approximation to the true experimental stress-strain curve. The general multi-axial stress-strain relationships are derived from the uniaxial stress-strain relation using another two material constants. This extension to the stress-strain relationship for multi-axial conditions, as shown in Figure 5.12 is qualitative only. Available experimental results as presented by Jones [31] and El-Taha et al. [123] tend to be associated with compression tests conducted under pure hydrostatic pressure, i.e. $\sigma_1=\sigma_3$ (see Section 4.2). Relatively high levels of confining pressure are generally involved. The adequacy of the specified multi-axial stress-strain curve of Figure 5.12 should be re-examined as more data become available.

The failure surface represented by the concrete material criterion as defined in ADINA is an approximation of the idealistic shape for the failure surface of ice. The shape of the yield envelope in compression-compression octant of principal stress space can be defined using piecewise continuous contour lines on planes perpendicular to one of the principal stress axes. The failure surface in the remaining octants of

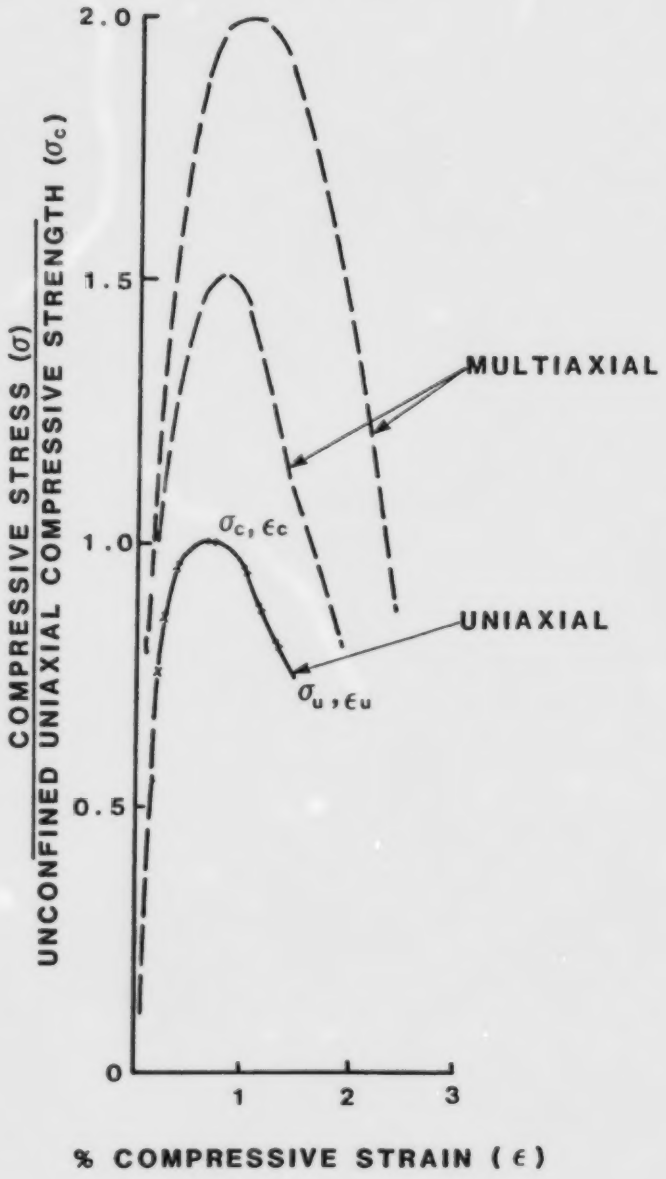

FIGURE 5.12 IDEALIZED STRESS-STRAIN CURVES FOR ICE UNDER MULTIAXIAL CONDITIONS

stress space are faceted and require only input of the unconfined uniaxial tensile strength of ice. The failure envelope used for the concrete model is shown in Figure 5.13 on the plane defined by first principal stress equal to zero. The Drucker-Prager material model also permits stress release mechanisms subsequent to the formation of cracks. When the maximum principal stress exceeds the uniaxial cut-off tensile value, a tensile failure plane is formed perpendicular to this stress. The normal stiffness across this plane is decreased to the original stiffness times the normal stiffness reduction factor (parameter STIFAC in ADINA input). Similarly, the shear stiffness is decreased to the original shear stiffness times the shear stiffness reduction factor (parameter SHEFAC in ADINA input). This represents a significant computational advantage of the concrete model over the Drucker-Prager model. It also has a significant effect on the final results as will be explained in the next section.

The initial value of Young's Modulus was taken as 9,600 MPa. Values of 6.0 MPa and 0.9 MPa were selected for, respectively, the unconfined uniaxial compressive and tensile strengths of ice. Based on the discussion in Section 4.4, these values appear to be fairly representative of the actual properties of sea ice under high strain rate. The values of other parameters necessary to define material model properties for ice are given in Table 5.1.

Drucker-Prager Material Model:

The uniaxial stress-strain relationship utilized for the Drucker-Prager model is associated with elastic-perfectly plastic material. No strain hardening (or softening) was assumed. Young's modulus was adjusted to reflect the amount of microcracking damage ultimately sustained in the ice material as suggested by the results from the concrete model. A different Young's modulus was associated with each of the three element groups utilized in this finite elelment analysis. Values of Young's modulus range from 9600 MPa for the linear element group of 2400 MPa for the element group nearest to the indentor where maximum damage is sustained.

The failure surface represented by the Drucker-Prager criterion is also an approximation. For the purpose of this study, it was idealized as a best fit to the failure envelope for the concrete model by adjustment of the yield surface parameters α and K as defined in Section 4.2. However, the choice of parameters in the Drucker-Prager model is limited and in particular, a good representation in the tension-tension region is particularly difficult to attain.

The Drucker-Prager material model also differs from the concrete model in the manner that the presence of stress release mechanisms subsequent to formation of cracks in the former material model are accounted for. The Drucker-Prager material model has a tension cut off option which limits the magnitude of tensile stresses but does not carry out the redistribution of stresses was tried but was unsuccessful. As a result,

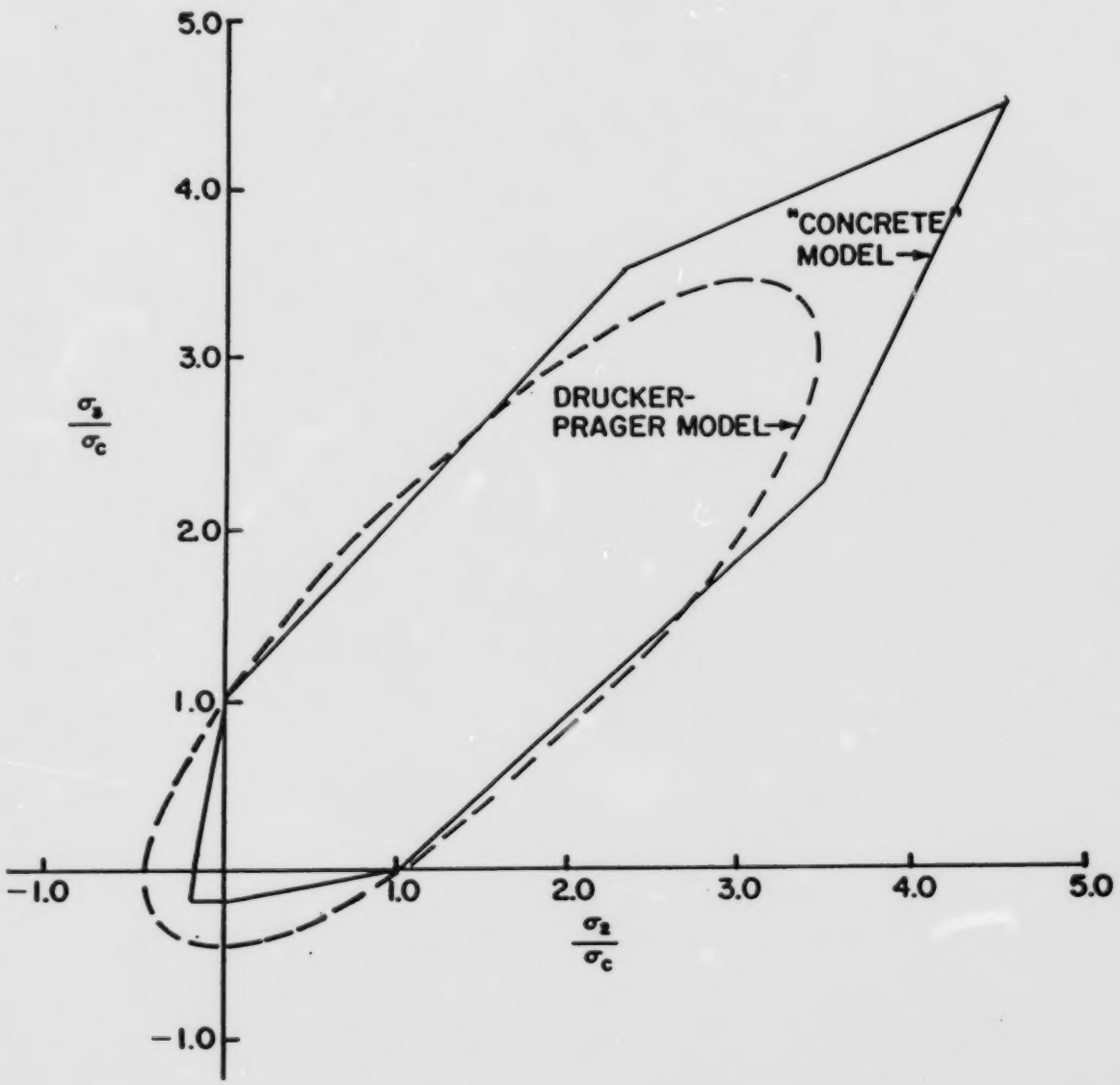

CONCRETE MODEL - FAILURE SURFACE PARAMETERS (SEE TABLE 5.1)

DRUCKER PRAGER MODEL - YIELD FUNCTION PARAMETERS $\alpha = 0.2375$, $K = 2.04$

FIGURE 5.13 DRUCKER-PRAGER YIELD CRITERION COMPARED TO CONCRETE YIELD CRITERION

TABLE 5.1

ADINA CONCRETE MATERIAL MODEL

Uniaxial Parameters	
Initial Tangent Modulus	9600.0 MPa
Poissons Ratio	0.33
Coefficient of Thermal Expansion	0.0
Uniaxial Cut-off Tensile Strength (σ_t)	0.90 MPa
Unconfined Uniaxial Maximum Compressive Stress (σ_c)	-6.00 MPa
Compressive Strain at σ_c (ε_c)	-0.007
Unconfined Uniaxial Ultimate Compressive Stress (σ_u)	-4.50 MPa
Unconfined Uniaxial Ultimate Compressive Strain (ε_u)	-0.015

the alternative of varying Young's modulus with amount of microcracking damage expected was attempted. However it too was not satisfactory. The main shortcoming of this approach is that aprioi knowledge about the pattern is being assumed. In new situations, this information may not be available. The modified value of Young's modulus is also an approximation not only in that it applies to all elements of an element group but also since it applies for the whole load history (rather than for the one state of material damage for the load point of interest). The value of attempting to emulate a damage material model with the elasto-plastic model is further reduced through the development of permanent plastic strains beyond the yield strain (zero strains are not realized when the structure is unloaded). Another questionable aspect of the adjustment of Young's modulus in the manner proposed is that "cracking" in early stages of loading develops normal to the principal compressive indentor loads. Reduction in Young's modulus consequently will be considerably less than that implied by the proportion of integration points which reached conditions where fracture occurs.

5.3.4 Solution Strategy

The development of the two-dimensional ice-block model for analysis by ADINA was not without difficulty. The problems encountered were primarily numerical in nature. ADINA utilizes an incremental solution procedure to solve the nonlinear equilibrium equation systems with loads being applied in a stepwise fashion. However, because the governing equilibrium equation for the continuum described by the concrete model are nonlinear and a tangent stiffness matrix approximation is used to compute incremental displacements for each load step, an imbalance will generally develop between the externally applied nodal loads and the vector of nodal point forces that are equivalent to computed element stresses. In order to reduce this imbalance and thereby diminish the resulting error in the solution to an acceptable level, it is desirable that an equilibrium iteration procedure be activated. Basically the structure is repeatedly loaded by out-of-balance forces until specified iteration termination conditions are realized. Two options are provided with ADINA for performing equilibrium iterations, the modified Newton-Raphson scheme and the BFGS (Broyden-Fletcher-Goldfarb-Shanno) scheme. The modified Newton-Raphson scheme involves use of the latest updated tangent stiffness matrix for the iterations whereas the BFGS scheme involves the generation of secant approximation matrix updates on each iteration. Normally incremental procedures used in combination with equilibrium iterations permit load increments to be increased and overall solution costs to be reduced.

In the early stages of the analysis, the concrete material model with provision for macro-fracturing damage was used, and rod elements were not included to represent the contact between ice and structure. In indentation problems where the boundary conditions imposed were such that a significant degree of material confinement was introduced, such as the flat indentor (Figure 5.2), the execution of ADINA posed no problem and in general two or three equilibrium iterations were found to be adequate

for lowering out-of-balance forces below the specified tolerances. This was not the case in slicing simulations, which provide decreased amounts of material confinement because of the changes in applied boundary conditions. For these problems, increased micro-fracturing damage developed. Maintaining solution stability was also more difficult. The stress releases associated with integration point stresses exceeding the tensile stress limits as defined by the failure surface caused large out-of-balance forces in the model. Therefore it became vital to limit the amount of micro-cracking which developed in each load increment in order to ensure that the convergence of out-of-balance forces could be attained within a reasonable number of equilibrium iterations. The load increments in the form of prescribed displacements had to be continuously adjusted in accordance with the amount of material experiencing stress conditions near the micro-fracturing failure threshold. This involved the time consuming process of manually scrutinizing the results at each load increment prior to specifying the next step in the loading function. Solutions attempted by relaxing the tolerance limits which determine the convergence of the solution proved to be of marginal benefit.

It was discovered that the use of rod elements in the model also leads to numerical problems during the equilibrium iteration stage. It is felt that sudden changes occurring during the separation of two surfaces from compressive forces in the rod elements (associated with very high stiffness value) to very small tensile stresses (and the corresponding very small stiffness value) may be responsible. Even with the alternate material models and very small load increments, a solution could still not be obtained.

In view of the above described computational difficulties, it was finally concluded that this approach with equilibrium iterations was inherently very costly and would not be feasible for production runs. The possibility of abandoning the equilibrium iterations altogether when performing a nonlinear finite element analysis for the numerical simulations with significant micro-cracking damage was investigated. An immediate benefit of dropping the equilibrium iterations is that the computational cost for the analysis was reduced significantly. Because of concern about deteriorations in accuracy, the simulations were performed using several different load stepping strategies with decreasing load step size and the contact force versus prescribed displacement curve was observed to converge to a limiting configuration. As one would expect, for strain softening materials such as represented by the concrete material model, the convergence of the curve was found to be from above as the size of the load steps decreased.

5.3.5 Termination of Simulations

Contact force versus prescribed displacement curves for a milling simulation carried out early in the contract using the two material models, i.e. Drucker-Prager and concrete models, are shown in Figure 5.14. It is seen that the analysis based on the Drucker-Prager material model yielded a substantially larger indentation force than the analysis

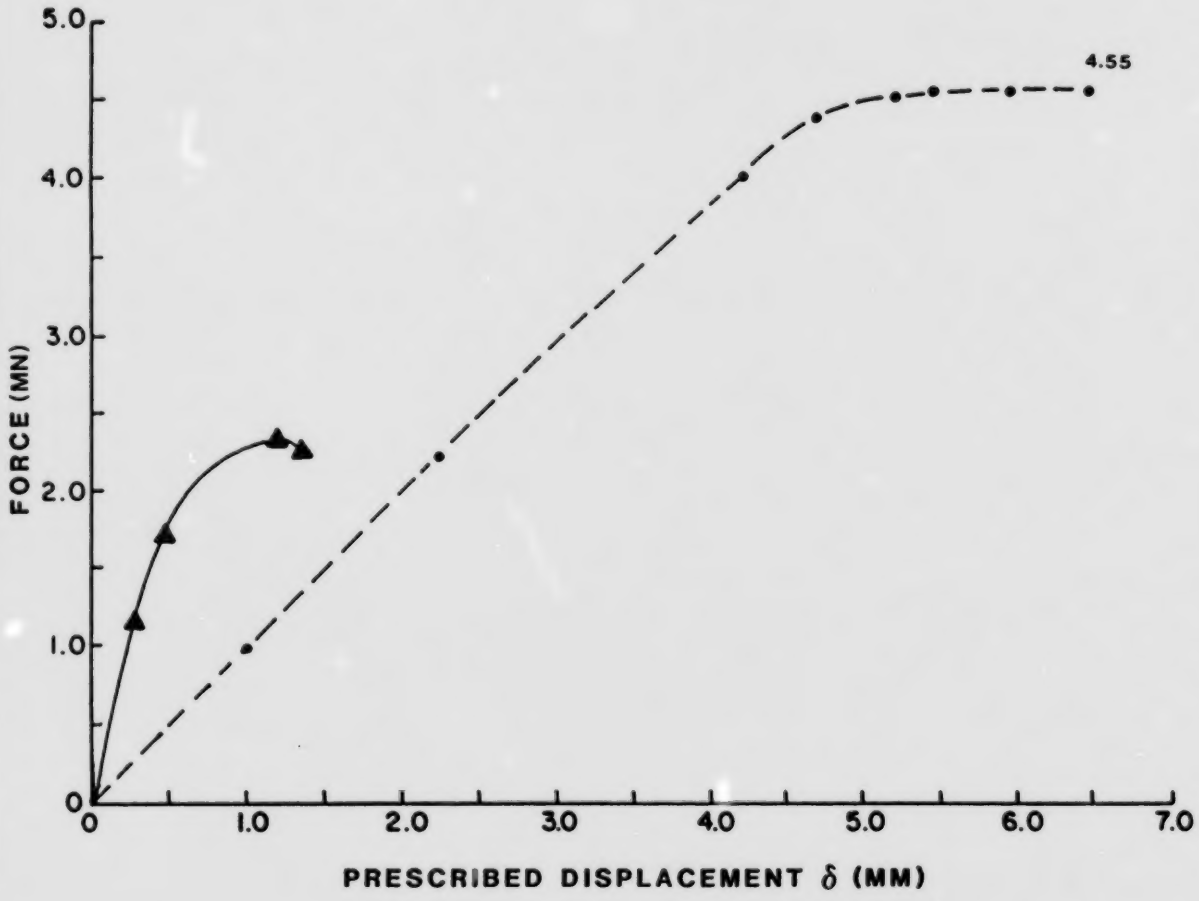

▲–CONCRETE MODEL
•–DRUCKER-PRAGER MODEL

FIGURE 5.14 CONTACT FORCE VS PRESCRIBED DISPLACEMENT CURVES

based on the concrete material model. The observed response characteristics follow directly from the constitutive modelling assumptions (particularly with regard to stress-strain relationships) incorporated in the two material models. Thus, it may also be noted that the contact force versus prescribed displacement curves in the cases corresponding to the concrete material models depicted the drooping type of force-displacement behaviour characteristic of strain-softening materials. The reduction of strength beyond the point of maximum strength is quite sudden. On the other hand, the type of behaviour exhibited by the results based on the Drucker-Prager model is more akin to that for a perfect elastic-plastic material under uniaxial loads.

In both cases, the increases in contact force with load (in the form of prescribed displacements at the contact surface) is linear during the early stages of the simulation as shown in Figure 5.14. However, as the applied load continues to increase, the response curve for the concrete material model deviates increasingly from the straight line. The slope of the response curve eventually becomes zero and then negative. The simulation is able to proceed under these conditions only because loads are applied in the form of prescribed displacements.

The concrete material model, on the other hand, utilizes a nonlinear stress-strain relationship (Figure 5.12) which accounts for the curvilinear nature of the response curve shown in Figure 5.14. Similar behaviour is also exhibited in the results obtained for the indentation problems with the concrete material model (to be discussed in Section 5.4.1). During the interaction process, gradual degradation of the material stiffness takes place. When the magnitude of the contact force reaches its peak value, sufficient material is damaged due to compressive crushing and to a lesser extent due to tensile cracking, that the total resistance offered by the material against any additional relative motion is reduced. From the numerical simulation point of view, it is the maximum indentation force that is of greatest interest. Any further loading was found to result in a very rapid reduction in the contact force indicating severe degradation of the material stiffness in front of the indentor. At some point numerical instabilities develop during the solution process even without the equilibrium iteration. Simulations beyond the point of maximum load are difficult and costly to perform. Consequently, once this maximum force is reached, the material may be regarded to have failed on a macro-level. The simulations are then terminated.

It should be noted that the physical indentation process continues beyond this point at which simulations are terminated. As the indentor advances, failed ice is extruded or deflected out of its path and eventually contact with the ice block is re-established. Contact forces (interface loads) then develop until the ice block fails and the process is repeated.

On the otherhand, the curve corresponding to the Drucker-Prager material model remains straight, almost all the way until the maximum contact force is reached. This can be explained by observing that for

plastic flow of the material in front of the indentor, there is no strain hardening. Consequently, the material in front of the indentor is incapable of providing any significant increases in resistance to the relative movement between the indentor and the ice sheet. In other words, the maximum contact force is reached with little increase in load after material yielding begins. The material at this stage can be considered to have failed at macro-level. Continuation of analysis for subsequent loading steps is practically of little or no significance. Therefore, simulations are terminated at this point.

5.4 Results of Analysis

5.4.1 Indentation

Rectangular Indentor:

The finite element model used for the analysis of the rectangular indentor problem is shown in Figure 5.2. Loads in the form of prescribed displacements were applied in small increments at the nodes defining the interface between the indentor and the ice block. For each load step, the stresses at the element integration points (2x2 Gaussian formula) were extrapolated to nodes by assuming that element stresses varied in a bilinear manner over the element. Stresses on the contact surface were integrated numerically to determine the indentation force. In order to assess the accuracy of the computed force, the total reaction in the z-direction (see Figure 5.2) was obtained by integrating the stresses in the linear elements adjacent to the boundary. In general, the reaction force in the direction of movement was found to be in good agreement with the computed indentation force. Thus, it was concluded that the method of extrapolating stresses at element integration points to nodes is satisfactory. For subsequent models, this uncertainty was eliminated by the introduction of rod elements as explained in the next section.

Two extreme situations occur for indentation problems depending upon the ratio of indentor width to the thickness of the ice-sheet, i.e. aspect ratio. Therefore two separate analyses were performed for this model, one with plane stress material conditions corresponding to high aspect ratios and another with plane strain material conditions for small aspect ratio conditions. The pressure distribution generated during the indentation action close to the point that the maximum contact force was produced is shown in Figure 5.15 for each case. This pressure distribution corresponds to the stresses in elements within the ice block in contact with the indentor. The variation of contact force with the prescribed displacement is plotted in Figure 5.16. At the initiation of the loading, high contact stresses are produced near the edge of the indentor. As the indentor advances into the ice sheet, the integration point stresses for the element near the indentor tip reach the ice crushing strength value. This value is established within the program based on the failure envelope specified for the material. When this happens, the program assumes that the failed material at the integration point strain-softens in all directions until the minimum principal strain reaches the

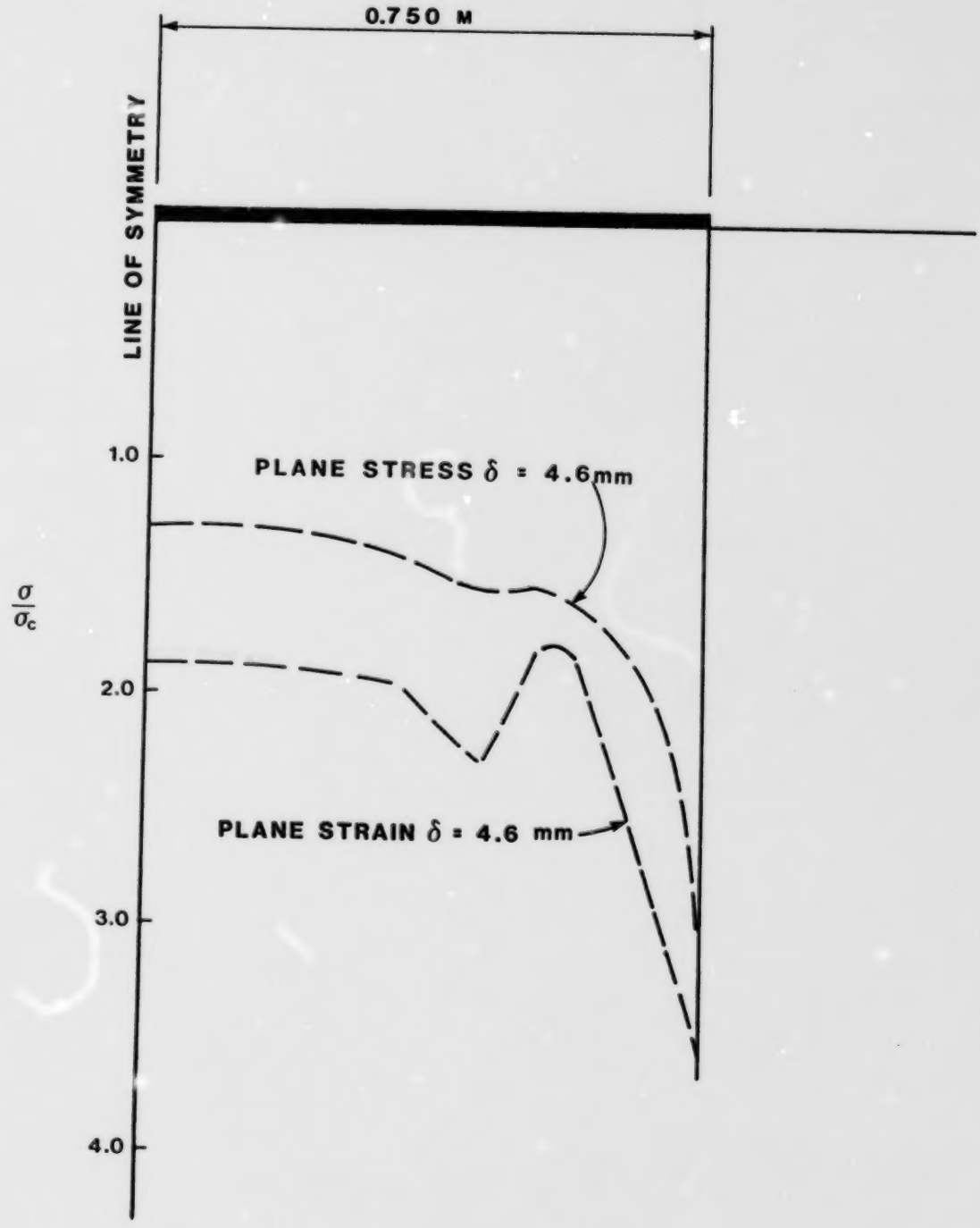

FIGURE 5.15 CONTACT PRESSURE DISTRIBUTION FOR RECTANGULAR INDENTOR

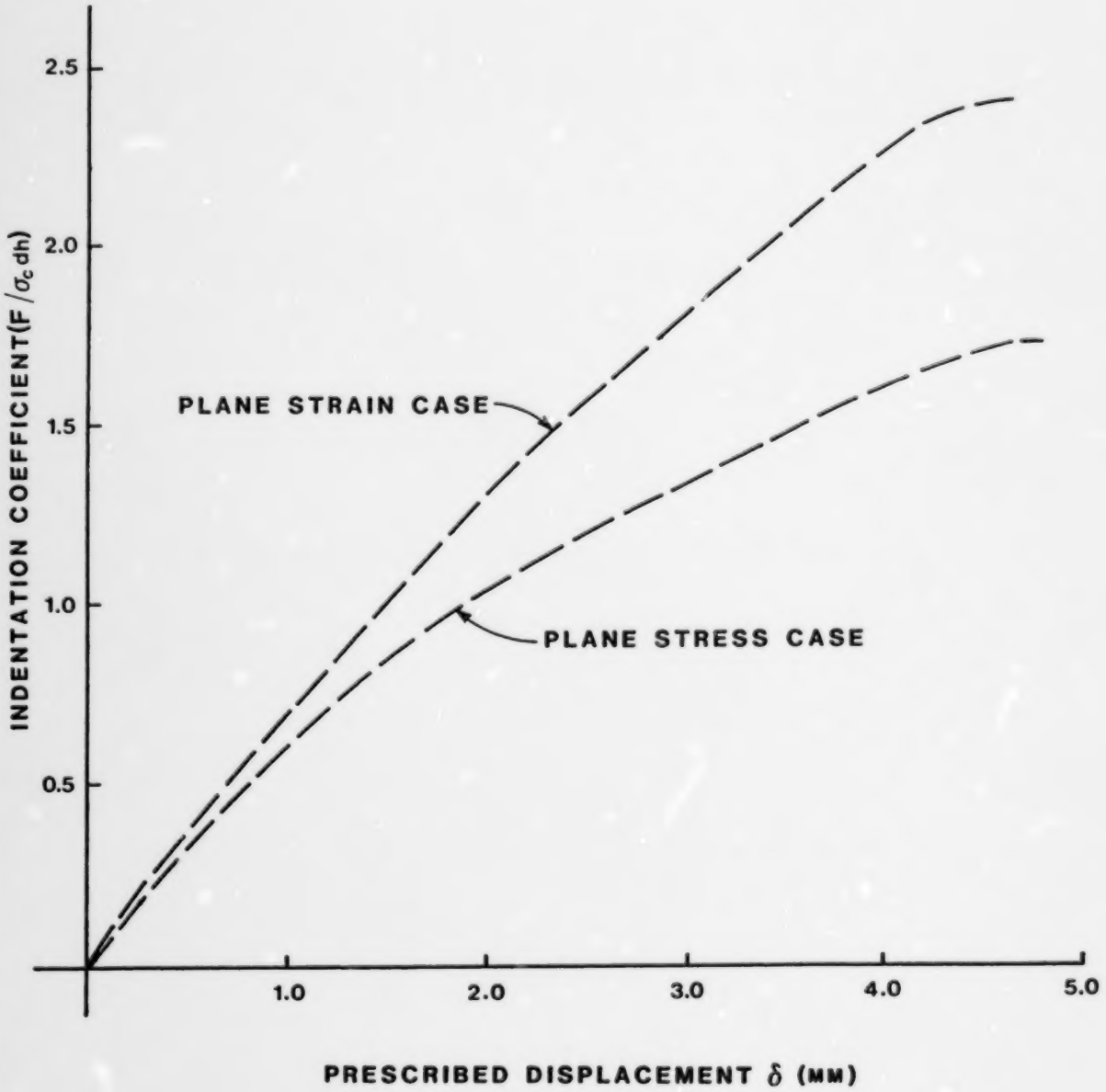

FIGURE 5.16 INDENTATION COEFFICIENT VERSUS PRESCRIBED DISPLACEMENT - RECTANGULAR INDENTOR

ultimate strain value (ε_u). (Principal strains are used because strains not stresses increase monotically with increasing load.) At this stage, all stresses are released and, from then on, the material has no more stiffness [124]. The material can be considered to have failed and offers no more resistance to the load which is then transferred to adjacent material. The development of the advancing failure zone under the indentor with increasing prescribed displacements can be seen in Figure 5.17. During the whole loading procedure, the extent of the cracked zone in the finite element model is limited to elements near the free surface. Note that all this happens with very small displacements.

The average contact pressure, nondimensionalized with respect to unconfined uniaxial crushing strength of ice, σ_c, is calculated as follows:

$$C = \frac{F}{\sigma_c dh}$$

where F is the calculated indentation force, d is the width of indentor and h is the elemental third dimension for the ice block (i.e. dh is the contact area). C is generally termed as the coefficient of indentation. The estimated values of C, based on ADINA results, for the two cases analyzed here are compared with the known experimental results in Figure 5.18. These experimental tests were conducted by Michel and Blanchet for a floating ice sheet [125]. The maximum speed of movement of ice was of the order of 6.8 cm/sec which gave computed indentation rates varying from 0.017 to 0.34 sec^{-1}. In this range, ice can normally be considered to be a brittle material. The estimated value of the indentation coefficients, C, under plane stress condition is plotted at an aspect ratio of 100, which approximates the theoretical value. Generally, in an indentation type ice-structure interaction where the aspect ratio is less than 20, the failure of ice-sheet is mainly due to crushing of the ice and the influence of in-plane stresses is dominant. For the aspect ratio greater than 20, the presence of large compressive stresses in a relatively thin ice sheet lead to instability and the buckling phenomenon governs the failure load. Buckling is supressed in numerical simulations by virtue of the plane stress or plane strain material assumptions.

The plane strain condition theoretically refers to the situation where ice thickness is infinitely large and hence the aspect ratio is zero. In practice, when the thickness of the impinging ice sheet is large, the failure takes place by cleavage across its thickness [125] hence implying a stress state which is not, strictly speaking, two-dimensional.

Circular Indentor:

Finite element models for circular and elliptical indentor geometries were generated using the program, IDENTM. The use of this program facilitated the examination of alternative grid configurations that would provide grid refinement in areas where large stress gradients were antic-

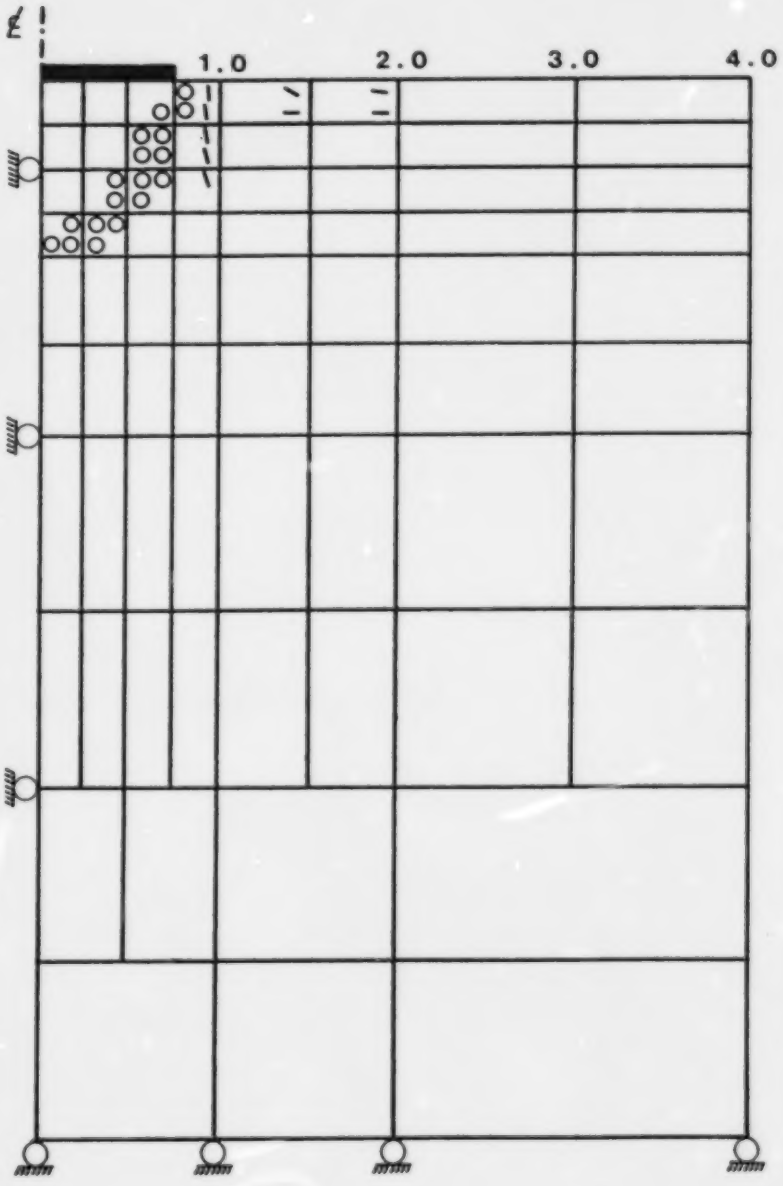

LEGEND

O–COMPRESSIVE CRUSHING

\–TENSILE CRACK

FIGURE 5.17 FAILURE ZONE FOR RECTANGULAR INDENTOR

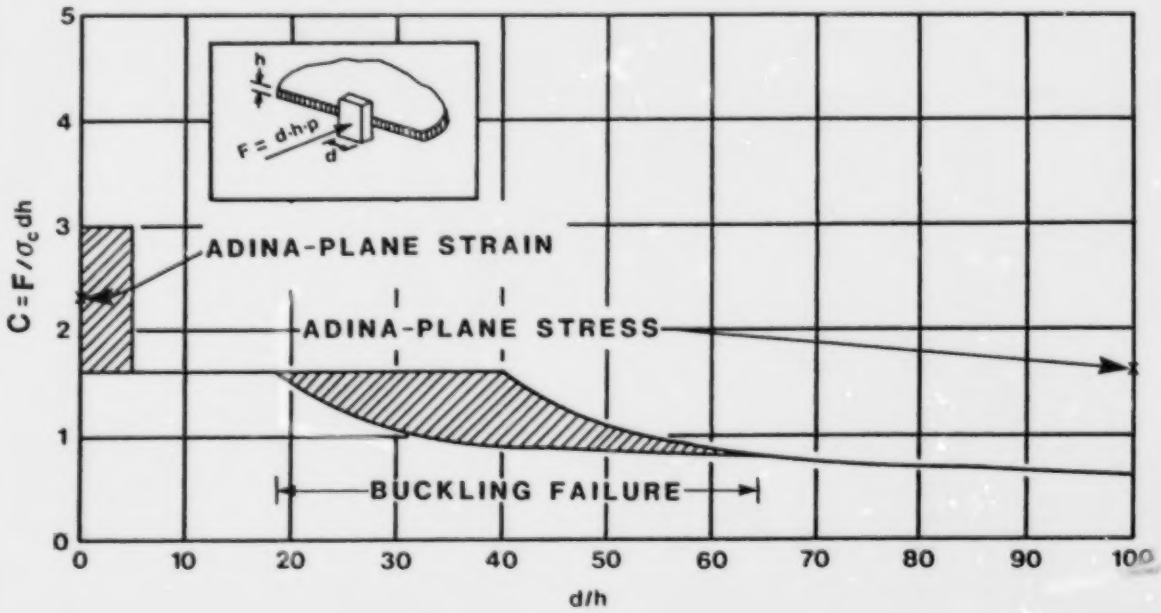

FIGURE 5.18 INDENTATION COEFFICIENT C AS FUNCTION OF d/h FOR RECTANGULAR INDENTOR [125]

ipated. The grid that was eventually adopted for the analysis of circular indentor is shown in Figure 5.3. The greatest refinement of elements is utilized along the contact surface, especially near the line of symmetry, since this area involves strongest stress gradients.

A potential difficulty with this type of indentation problem wherein nonrectangular geometry is involved along the contact surface is the integration of interface pressures (defined by interpolation from nodal stress) to evaluate the contact force. However, the incorporation of rod elements as gap elements simplifies the computation of contact forces. At each load step, the force in each rod element is equal to the integrated force at the corresponding node where the rod is attached. If the line of action of these rod forces is the same, the total contact force along the orientation of rod elements is then determined by simple summation of individual rod forces. Should the direction of rod elements vary along the contact surface, it is necessary to determine the component of the rod forces along the direction of prescribed movement. This component of the rod forces can be summed to evaluate the indentation force in the direction of prescribed movement at each step of the loading. From this, the average contact pressure over the diameter of the circular indentor in nondimensionalized form, i.e. indentation coefficient, can be calculated as follows:

$$C = \frac{F}{\sigma_c dh}$$

where F, σ_c and h are the same as above and d is the diameter of the indentor.

Since the model is symmetrical with respect to the vertical Z axis, constraints in the Y direction were imposed along the line of symmetry. Radial constraints were applied at the nodes along the outer radius of the model.

The analysis was carried out for both the plane stress case and the plane strain case and the results have been presented in Figures 5.19 and 5.20. It may be of interest to note that as the applied load (prescribed displacement in the Z direction) approaches its maximum value, the development of the cracked zone is rapid and at failure conditions, it extends over a significant proportion of the finite element model as illustrated in Figure 5.21. Recall that in the case of rectangular indentor, the cracked zone was limited to a small area even at failure. Another point of interest is that the imposition of constraints for the nodes along the free boundary made very little difference to the cracking pattern in the vicinity of the leading tip of the indentor.

For the purposes of validating the results from numerical simulations, the indentation coefficient, C, was compared with the mean effective pressure obtained experimentally for cylindrical structures by Sodhi and Morris [126]. Figure 5.22 shows the variation of the indentation coefficient with respect to the aspect ratio d/h for a velocity of ice

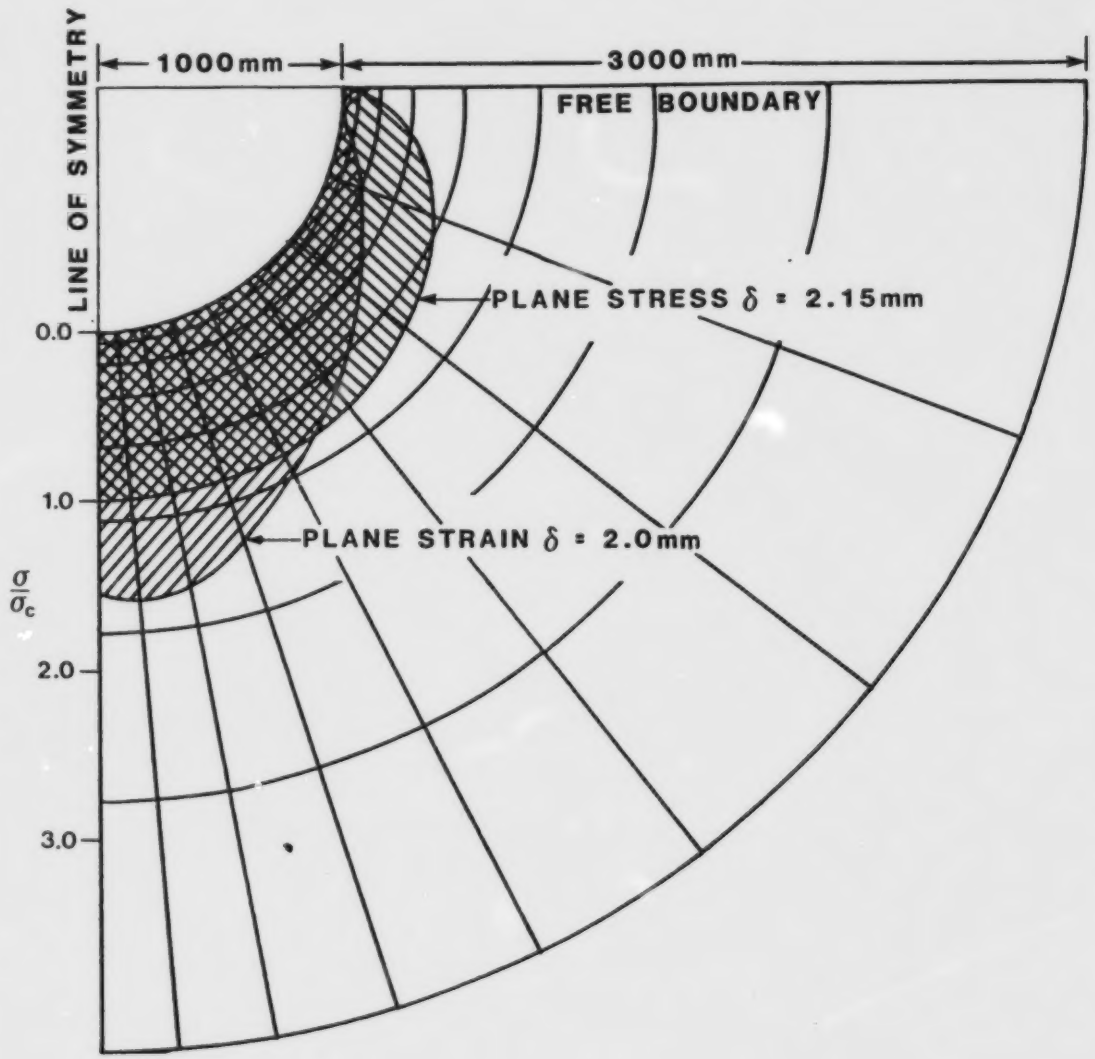

FIGURE 5.19 CONTACT PRESSURE DISTRIBUTION FOR CIRCULAR INDENTOR

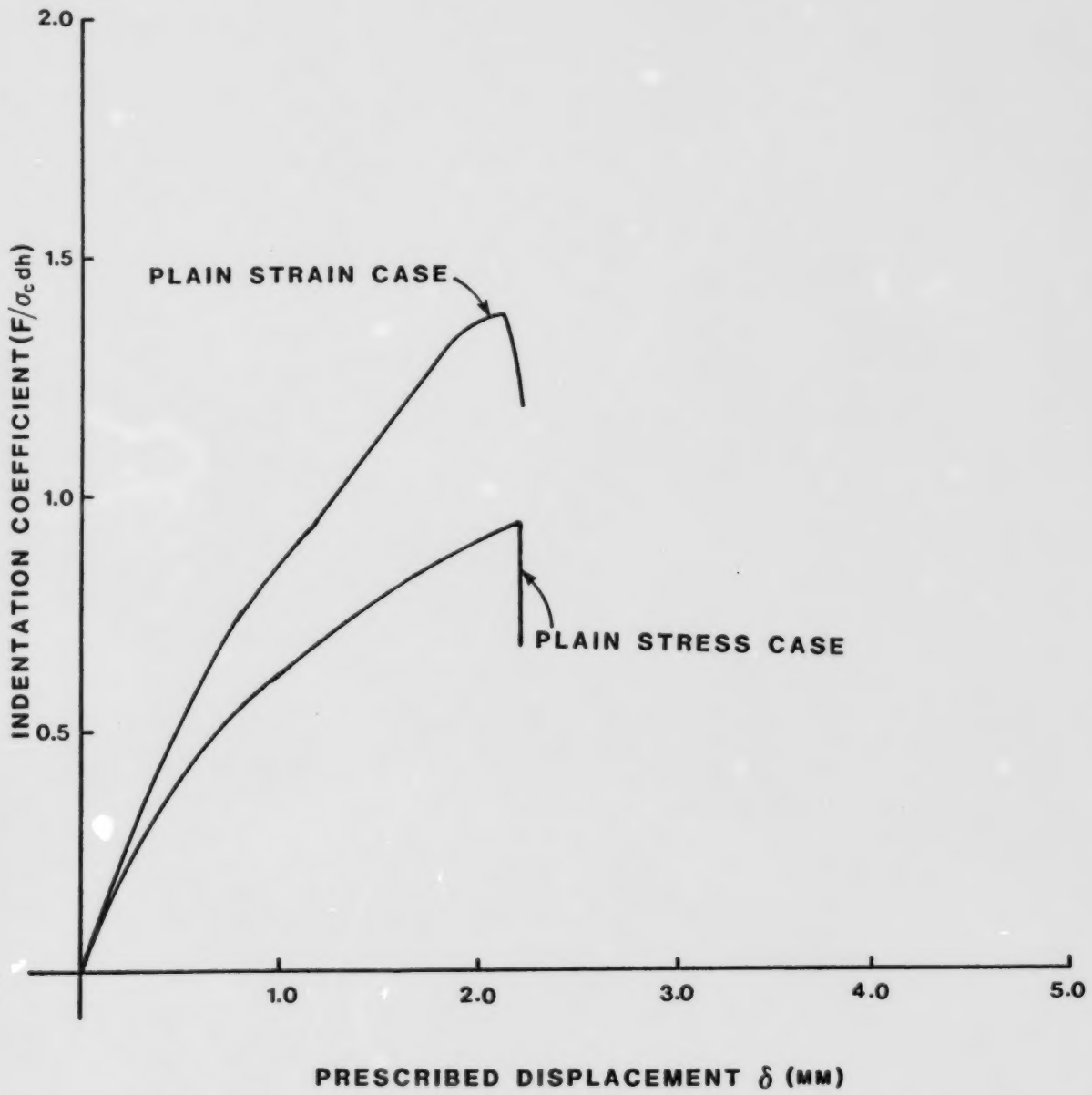

FIGURE 5.20 INDENTATION COEFFICIENT VERSUS PRESCRIBED DISPLACEMENT - CIRCULAR INDENTOR

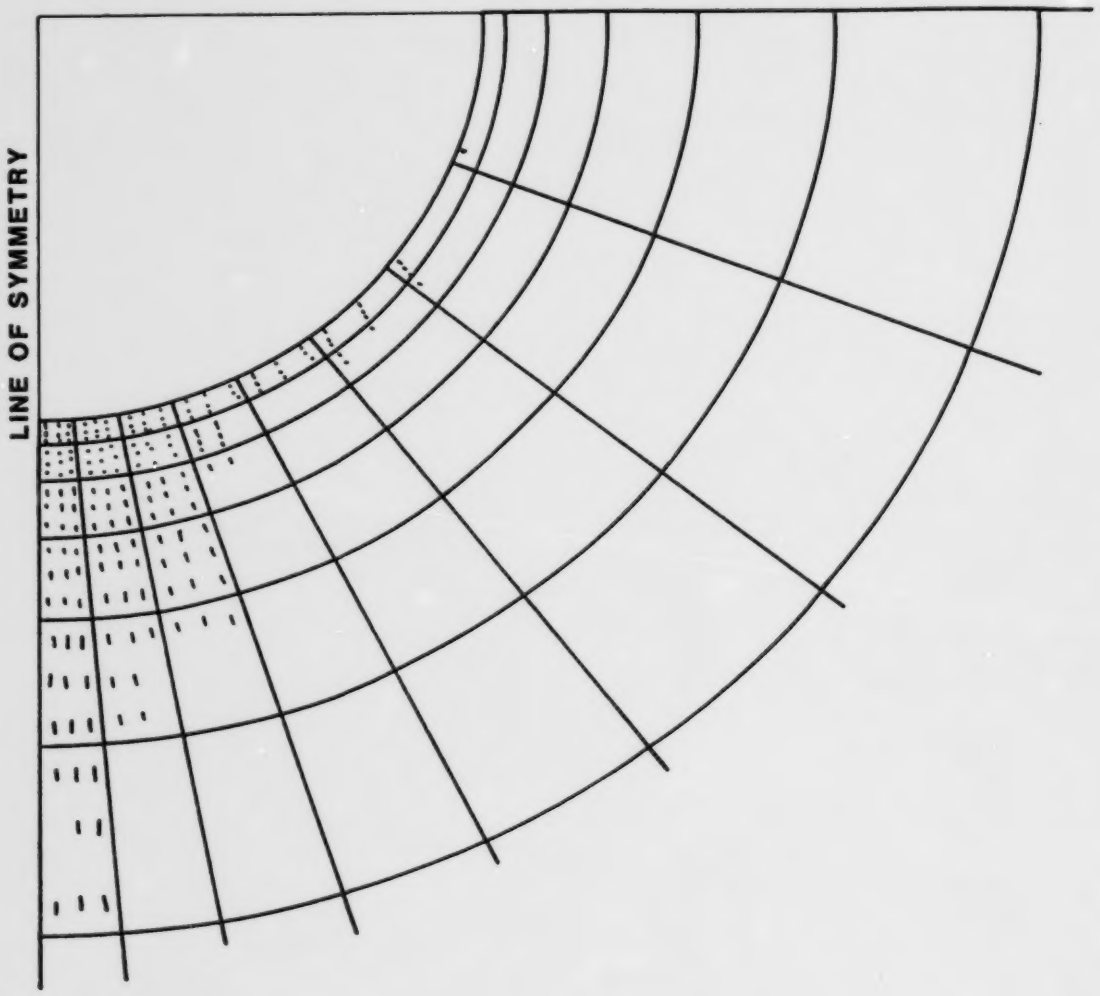

FIGURE 5.21 CRACK PATTERN AT FAILURE - CIRCULAR INDENTOR

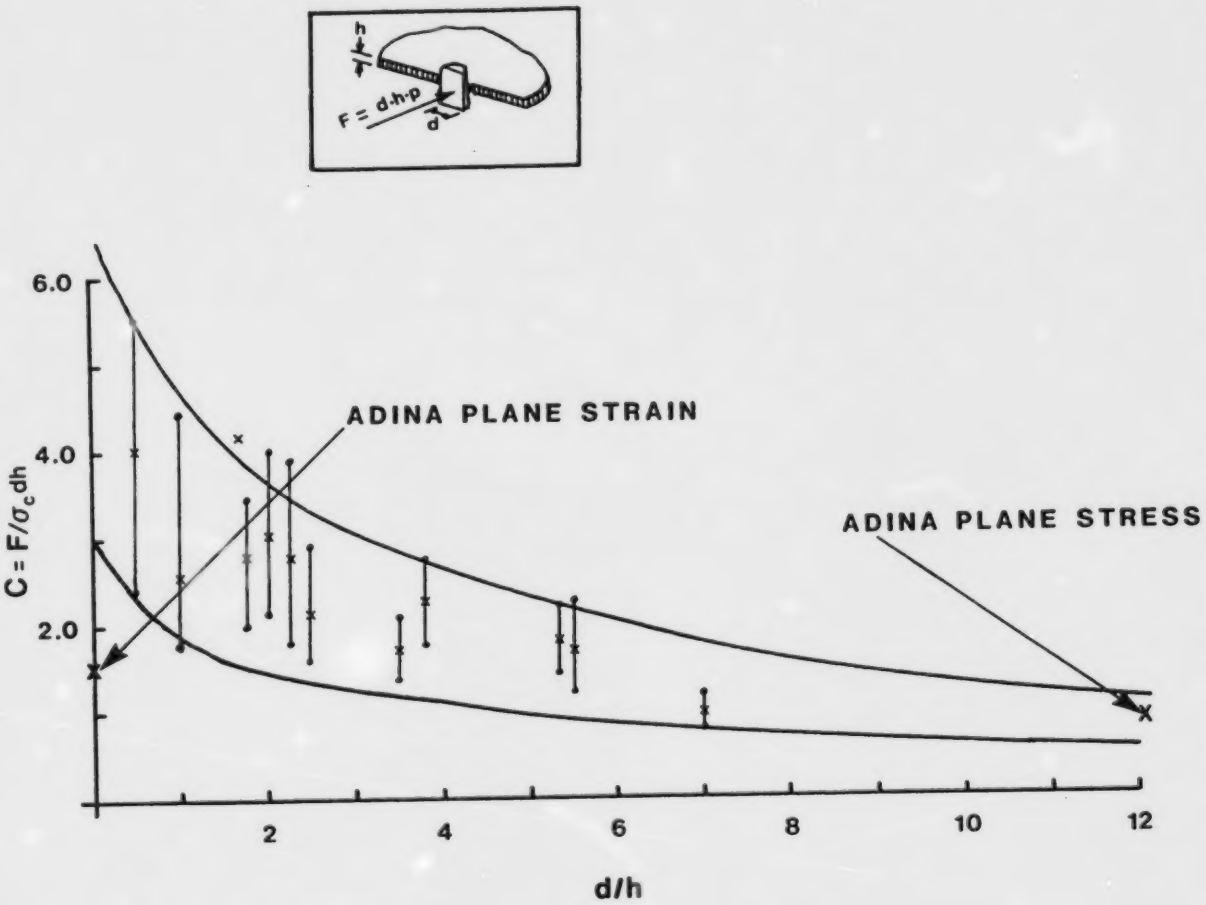

FIGURE 5.22 INDENTATION COEFFICIENT C AS FUNCTION OF d/h FOR CIRCULAR INDENTOR [126]

30 mm/sec. The standard deviation of the ice force variation is indicated with a vertical bar plotted on both sides of this mean normalized pressure indicated by a small cross. Thus the plot produced here represents a zone within which the magnitude of the mean pressure is expected to fall for a given aspect ratio. The curves for lower and upper limits of the zone have been extrapolated beyond the aspect ratio value of 7 and appear to be asymptotic about the coefficient value of about 0.90. It may be observed that the spread of zone (i.e. standard deviation) decreases as the aspect ratio increases.

The ADINA plane stress and plane strain results are superimposed on Figure 5.22. It is observed that good agreement has obtained between the indentation coefficient for the ADINA plane stress analysis and for the experimental results when aspect ratio is high. However, the indentation coefficient for ADINA plane strain underestimates the experimental value for zero aspect ratio by at least a factor of 3. The reason for this is believed to be that the ADINA concrete model does not adequately describe the behaviour of ice after compression crushing. Better agreement is expected if extrusion mechanics are properly accounted for.

Elliptical Indentor:

As shown above, the pressure distribution for a rectangular indentor is characterized by very high edge pressure, while in the case of a circular indentor, the pressure along the contact surface exhibits relatively smooth variation. A circular shape is a special case of elliptical shape where the ratio of major axis to minor axis of the ellipse is unity. However, the effect of this ratio upon the indentation force and also upon the indentation pressure variation needs to be investigated. As far as we are aware, there are no experimental results available for elliptical indentor and one has to resort to analytical methods to estimate the $dentation force in such a case.

In this study, the ADINA analysis has been carried out for an elliptical indentor having the ratio of major axis to minor axis equal to ten. The finite element grid used for the purpose of analysis is shown in Figure 5.4. The relative motion between the indentor and the ice is considered to be in the direction of major axis and the resulting pressure variation and the indentation force fluctuation are plotted in Figures 5.23 and 5.24 respectively. The maximum value of the force is reached when the prescribed displacement is of the order of 0.80 mm; and the corresponding indentation coefficient, C, is about 0.62. This value is considerably lower than the coefficient value obtained for either the circular indentor (C = 0.92) or rectangular indentor (C = 1.58). Figure 5.25 shows the extent of the cracked zone at or near failure. It can be observed that the extension of this zone is mainly along the major axis of the indentor. The compressive crushing of the material, on the other hand, is of a much more local nature and is, in fact, limited only to a single element adjacent to the leading tip of the indentor.

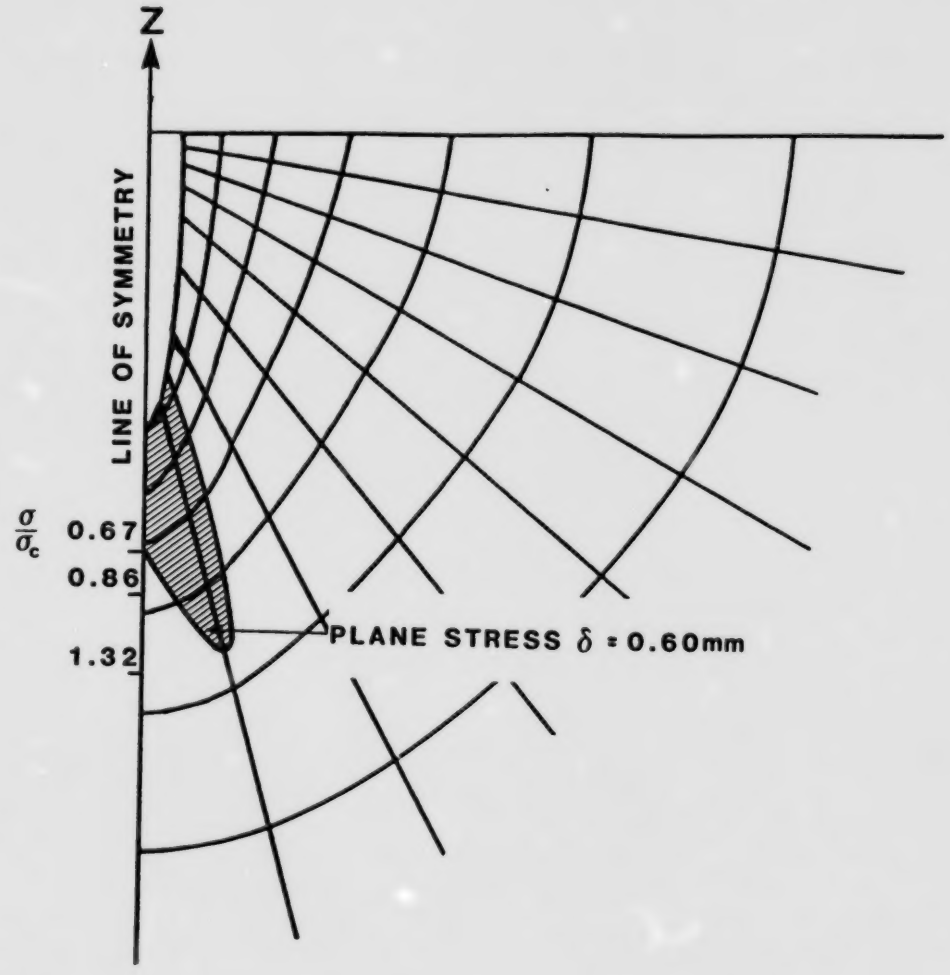

FIGURE 5.23 CONTACT PRESSURE DISTRIBUTION FOR ELLIPTICAL INDENTOR

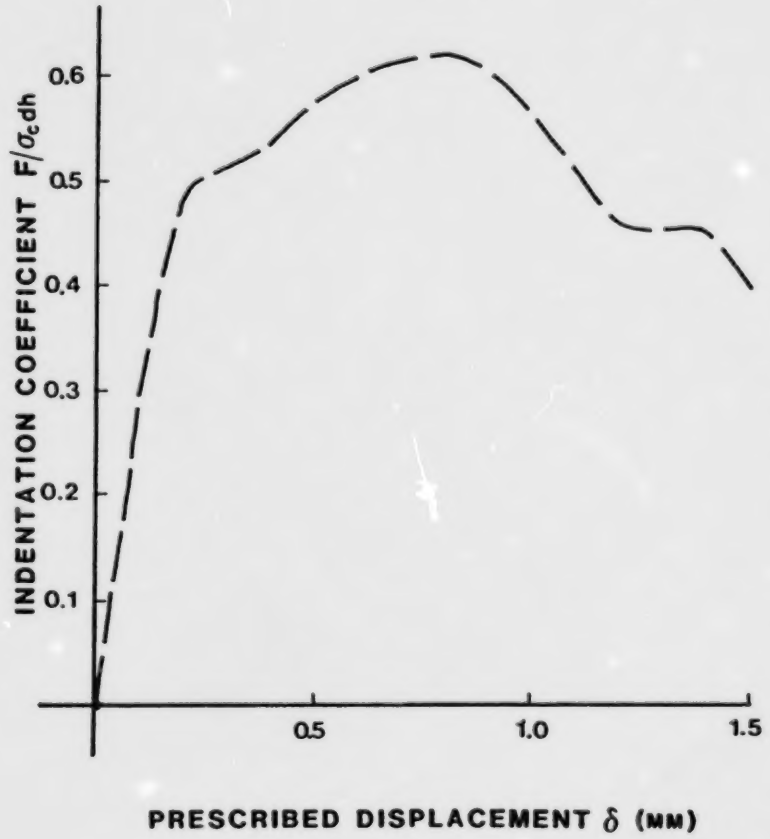

FIGURE 5.24 INDENTATION COEFFICIENT VERSUS PRESCRIBED DISPLACEMENT - ELLIPTICAL INDENTOR

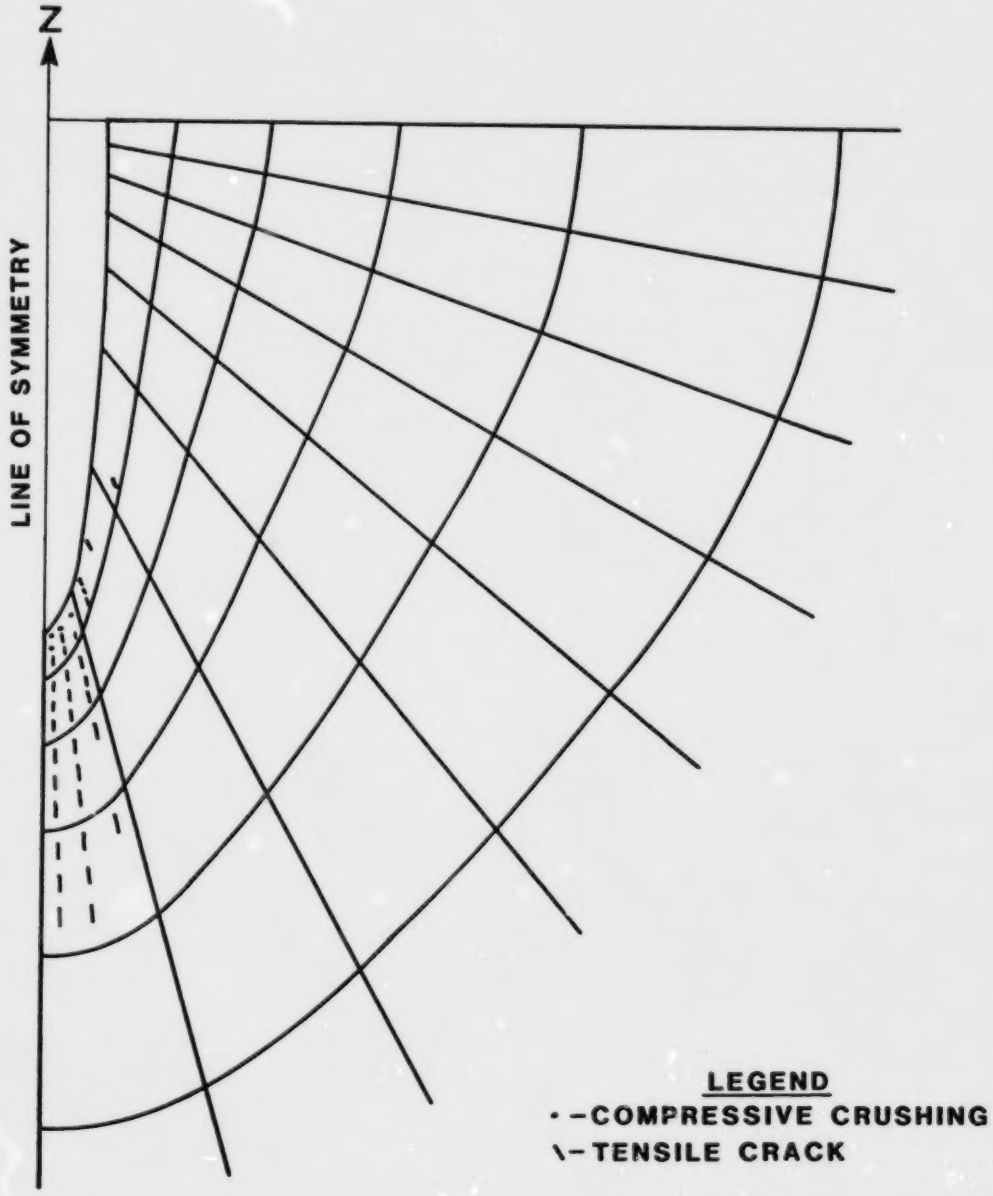

FIGURE 5.25 CRACK PATTERN AT FAILURE - ELLIPTICAL INDENTOR

Wedge Indentor:

The wedge indentation problem investigated involved a right angled wedge orientated symmetrically about line Y=0 and immersed to a depth of 1 m within an ice-sheet. As with other symmetrical indentation problems considered previously, only one half of the wedge indentation problem on either side of the symmetry plane was modelled. The finite element model generated for this problem is shown in Figure 5.5. Along the symmetry line, horizontal displacements are constrained.

A square ice block of side dimension 4 m was modelled. This is believed to be a sufficiently extensive ice block size in order for the applied boundary conditions to have a negligible effect on the stresses in the vicinity of the indentor. Vertical displacement components were constrained along the bottom of the ice block, as were horizontal displacement components along the right hand edge.

Everywhere along the inclined blade-to-ice interface, ice is forced to move in prescribed increments along a direction normal to the interface. But being unconstrained along the direction tangential to the interface, ice can slide (translate) in a manner consistent with a frictionless interface. These conditions were simulated through the introduction of the stiff rod elements orientated normal to the indentor-to-ice interface. A skewed coordinate system is defined at the free end of each rod so that boundary conditions can be applied independently in directions along the rod axis and normal to it. In particular, in the direction corresponding to the rod axis, prescribed displacements of same magnitude are applied to all nodes. In the normal direction, all nodes are constrained.

The boundary conditions at the wedge tip are unique and some comments are made regarding this special point. A dilemma arises from the normal to the indentor-to-ice interface not being single-valued there. The basic question is therefore whether the associated ice node should move normal to the interface or directly downward.

The difficulty with the first option is that the ice node directly below the wedge tip moves off the symmetry line with the slightest application of indentor load. A corresponding ice node (point) associated with ice material on other side of the symmetry line (in the complete ice block, when symmetry conditions are not exploited) would then move off symmetry line as well. In effect, therefore, a crack develops under the wedge tip with the slightest application of load. At first, this approximation may be somewhat inconsistent with reality. However, as cracking progresses throughout a zone of increasing size beneath the indentor (subjected to prescribed displacement type of loading), element stiffnesses would be modified to reflect the presence of microcracking in the ice material. Stiffnesses normal to microcrack orientation are reduced to almost zero (not exactly zero to avoid potential problems in decomposing the structural stiffness matrix). There appears to be no significant difference from assuming that some cracking already exists along the symmetry plane.

Alternately by the second option, the node at the indentor tip is forced to move directly downward. This causes adjacent ice along the indentor-to-ice interface (within first element) to experience large shear strains. As the first element along the indentor-to-ice interface (nearest crack tip) is reduced in size, the portion of the interface experiencing the large strains decreases. This alone suggests that a requirement for the node at the wedge tip moving down is wrong unless the mesh is sufficiently detailed to model the end curvature. In reality no indentor has a perfectly sharp leading edge. If one were to examine it sufficiently closely, some nonzero edge curvature would be observed. Even though the elements are graded in the mesh adopted for this problem and the first element along the indentor-to-ice interface is quite small, the effect on interface pressure distributions are nonetheless expected to be noticeable. The first option is therefore preferred.

The contact force (Z component) versus prescribed vertical (Z component) displacement is shown Figure 5.26. The simulation was not taken to completion. This is partly due to a mistaken belief that maximum contact force would be considerably less than the contact force obtained in this finite element simulation and the load stepping was decreased far too early. The progression of cracking is shown in Figure 5.27. As speculated when selecting boundary conditions to be implemented, cracking can be observed to be confined to the region near the symmetry plane. Seven elements had more than half of their integration points 'cracked'. In effect, the crack zone penetrated to a depth of 1.7 m below the wedge tip. For a prescribed vertical displacement of 3.7 mm where the simulation was terminated, a crushing zone had begun to form at both ends of the indentor-to-ice interface. A total of 9 integration points within elements near the wedge tip had reached material crushing conditions and another 4 experienced a similar fate at the opposite end of the interface.

Crushing near the top surface of the ice block is somewhat unexpected but the reason for it becomes evident from an examination of the contact pressure distribution plots in Figure 5.28. The pressure increases sharply towards both ends of the indentor-to-ice interface, the pressures at the top surface of the ice block being generally smaller than those at the wedge tip. For a vertical displacement of 0.2 mm, the pressure at the wedge tip is approximately twice the pressure at the other end. As the vertical displacement increases, the difference in pressure at the two ends decreases. One interesting observation is that contact pressures do not increase proportionally as applied displacements on the indentor are increased; in fact, deviation from proportionality is largest at the two ends of the indentor-to-ice interface.

5.4.2 Slicing

In the early stages of the analysis of this type of milling, the model shown in Figure 5.7 was used for a flat cutter, while the model shown in Figure 5.8 was used for an inclined cutter. Once a workable procedure for the ADINA analysis was established (see Section 5.3.4), the

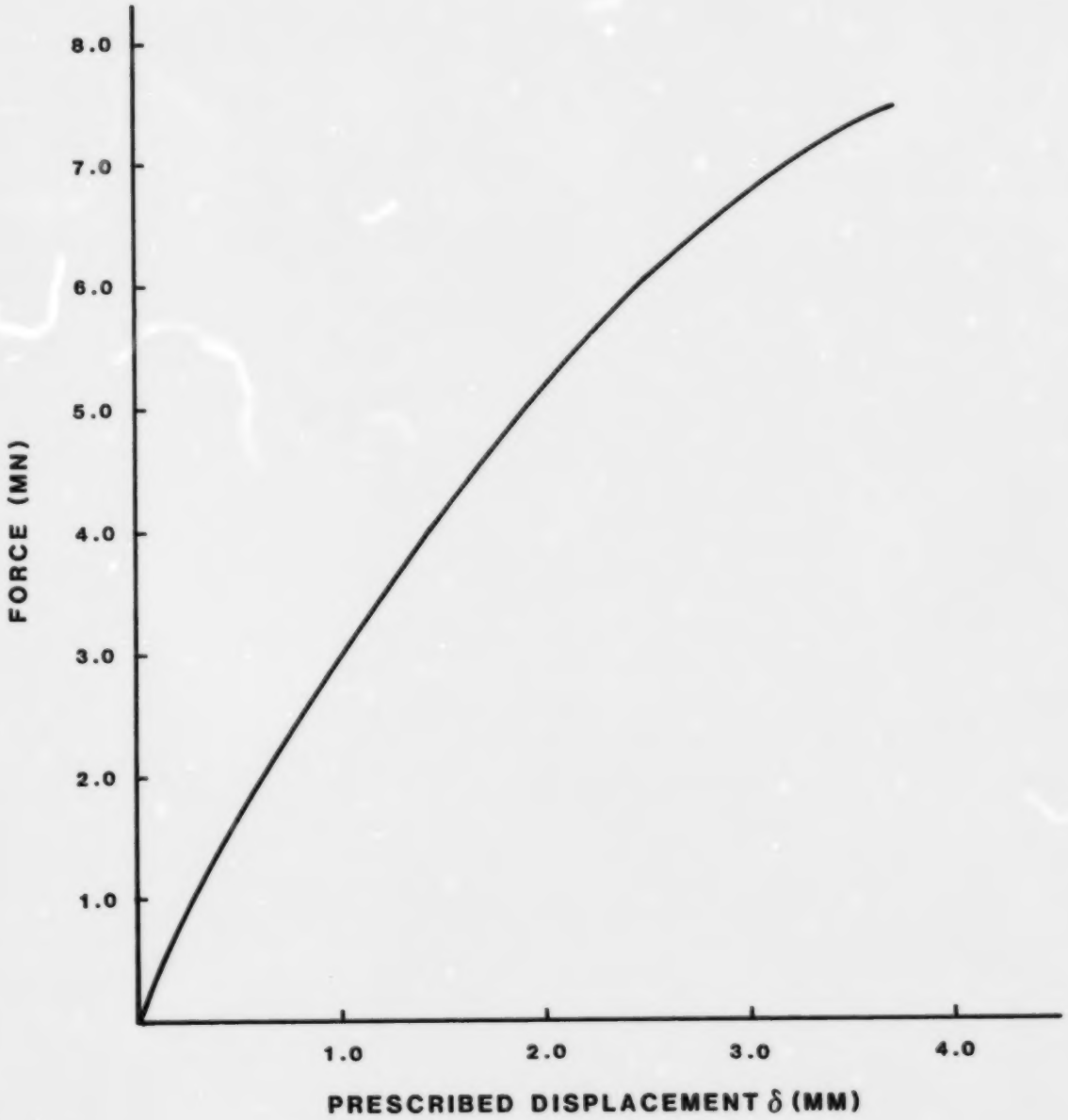

FIGURE 5.26 CONTACT FORCES VERSUS PRESCRIBED DISPLACEMENT FOR WEDGE INDENTOR

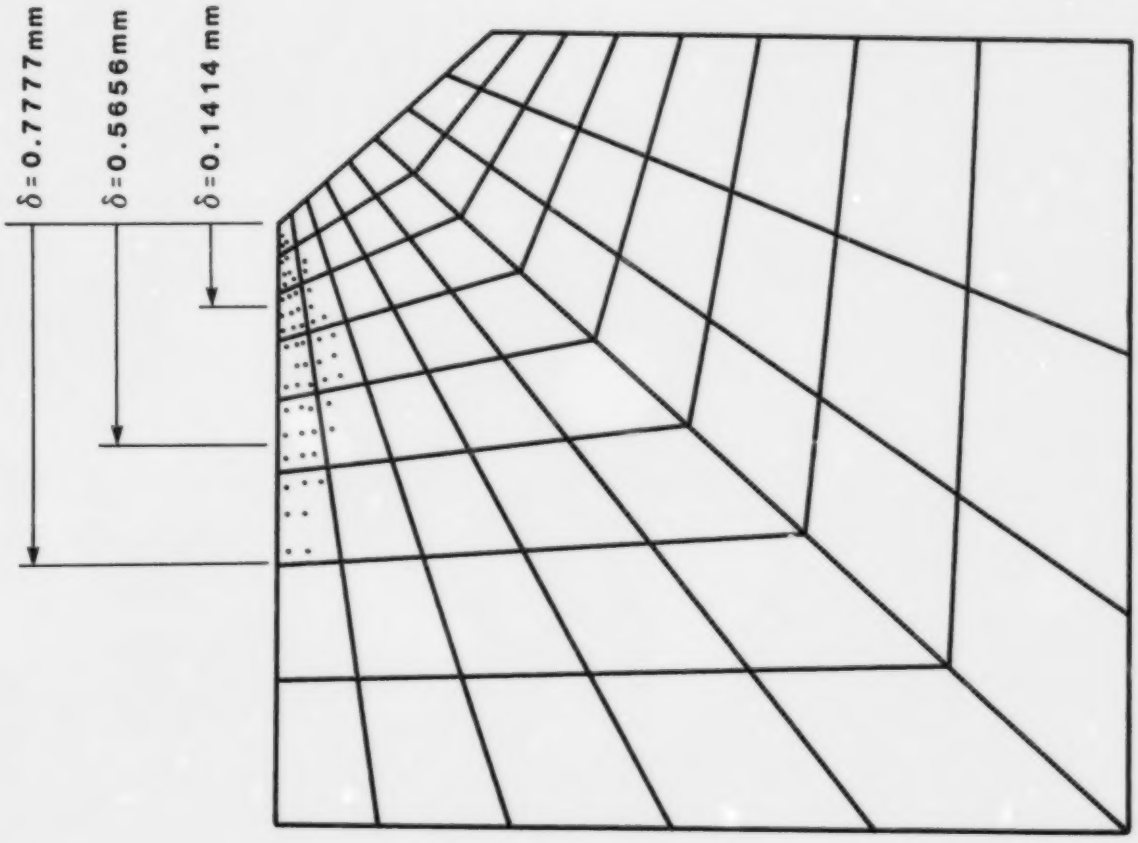

FIGURE 5.27 PROGRESSION OF CRACKING FOR WEDGE INDENTOR

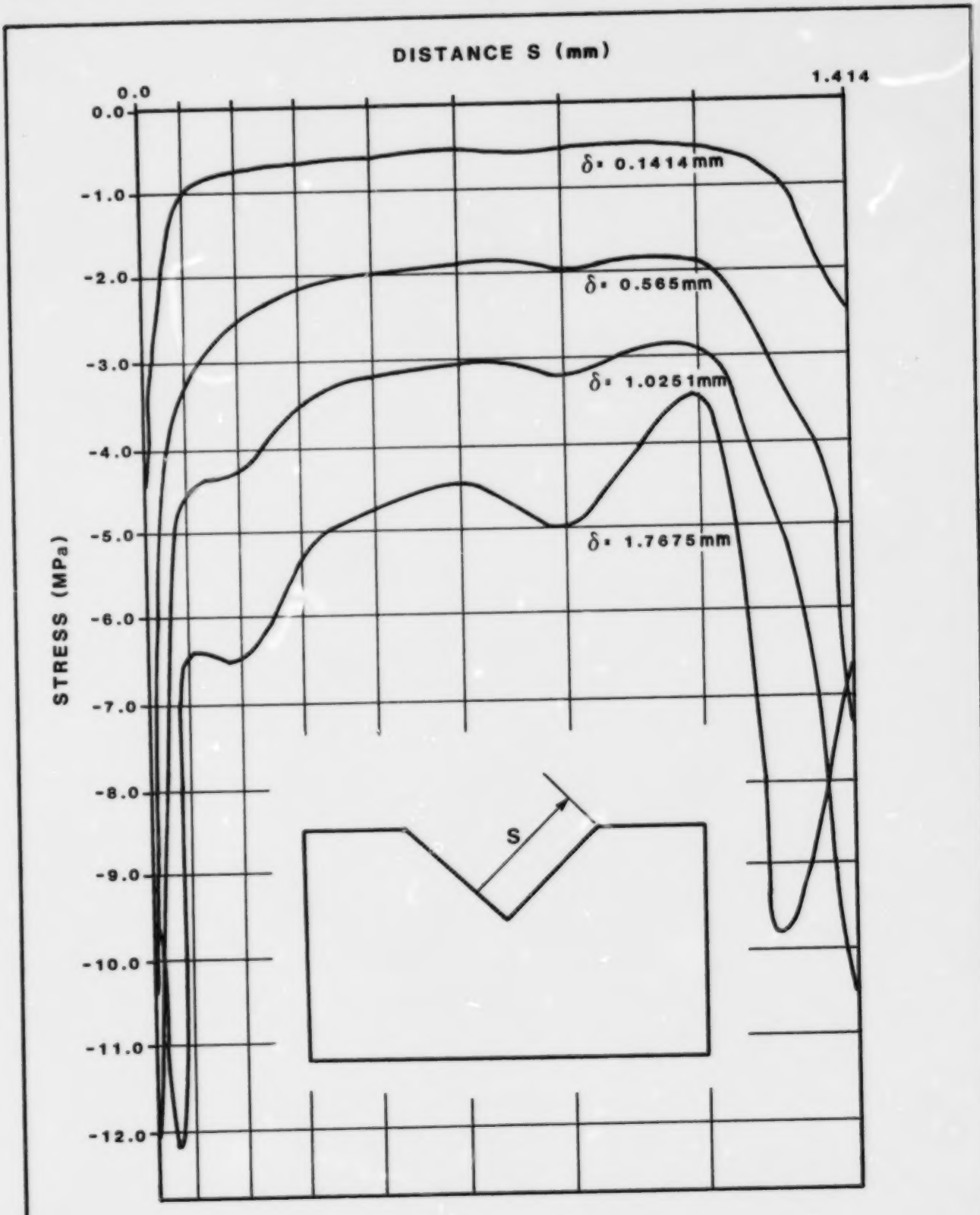

FIGURE 5.28 STRESSES IN ICE-BLOCK AT INDENTOR-ICE INTERFACE

model shown in Figure 5.8 was dropped in favor of the more refined models shown in Figures 5.9 and 5.10.

Everywhere along the cutter-to-ice interface, ice was forced to move in prescribed increments along a direction normal to the interface. But being unconstrained along the direction tangential to the interface, ice can slide (translate) in a manner consistent with a frictionless interface. These conditions were simulated through the introduction of the stiff rod elements oriented normal to the indentor-to-ice interface. A skewed coordinate system is defined at the free end of each rod so that boundary conditions can be applied independently in directions along the rod axes and normal to it. In particular, in the direction corresponding to the rod axes, prescribed displacements of same magnitude are applied to all nodes. The nodes are constrained in the direction perpendicular to the rod axis.

Both plane stress and plane strain material conditions were considered. Various cutting widths, W, and cutting angles, γ (see Figure 5.29), were investigated. For each case, load and interface pressure distribution versus cutter movement (displacement) was determined.

In the case of plane stress conditions, results for nine different milling situations were obtained, i.e. four cutting angles, ($\gamma = 0°$, 45°, 60°, and 75°) for each cutting width, and an additional cutting angle of 30° for W = 750 mm (see Figure 5.29). In the case of plane strain conditions, results for two different milling situations were obtained, i.e. W = 250 mm, $\gamma = 0°$ and W = 250 mm, $\gamma = 75°$.

Results for the case of W = 750 mm and $\gamma = 75°$ are shown in Figures 5.30 and 5.31. Contact pressure as a function of distance along the cutter-to-ice interface for two different positions of the cutter (i.e. displacement normal to interface) is shown in Figure 5.30. As can be seen, contact pressures are concentrated at the cutter tip. A plot of total contact force, F_c, versus cutter movement is shown in Figure 5.31. This force is the summation of axial forces in all rod elements, and is, therefore, normal to the cutter.

Using the results from the eleven different milling situations (i.e. nine plane stress and two plane strain), the contact force versus cutting angle curves shown in Figure 5.32 were constructed. The curves show clearly the rapid increase in milling force with increasing angle of attack ($90° - \gamma$). For small angles of attack (i.e. $\gamma > 75°$), constant values for contact force are used to complete the curves.

The ice block finite element models shown in Figures 5.10 have been used to investigate situations where the slicing mode of failure is predominantly shearing. This involved 'positive' cutting angles only, and is analogous to the shearing form of shadowing shown in Figure 3.5(a). For the crushing form of shadowing, shown in Figure 3.5(b), 'negative' cutting angles have to be considered, and, consequently, the models shown in Figure 5.10 cannot be used. For this type of slicing, the model shown

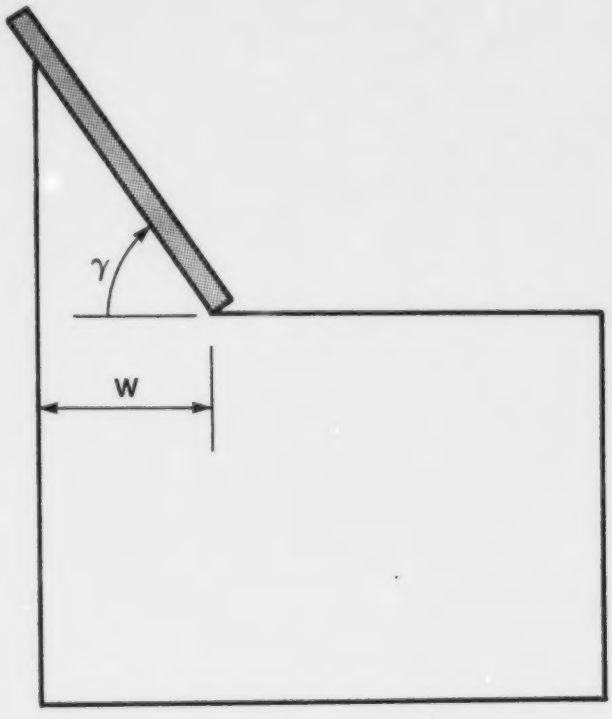

CASE#	W	γ
1	250 mm	0°
2	250 mm	45°
3	250 mm	60°
4	250 mm	75°
5	750 mm	0°
6	750 mm	45°
7	750 mm	60°
8	750 mm	75°
9	750mm	30°

FIGURE 5.29 CASES FOR SLICING ANALYSIS

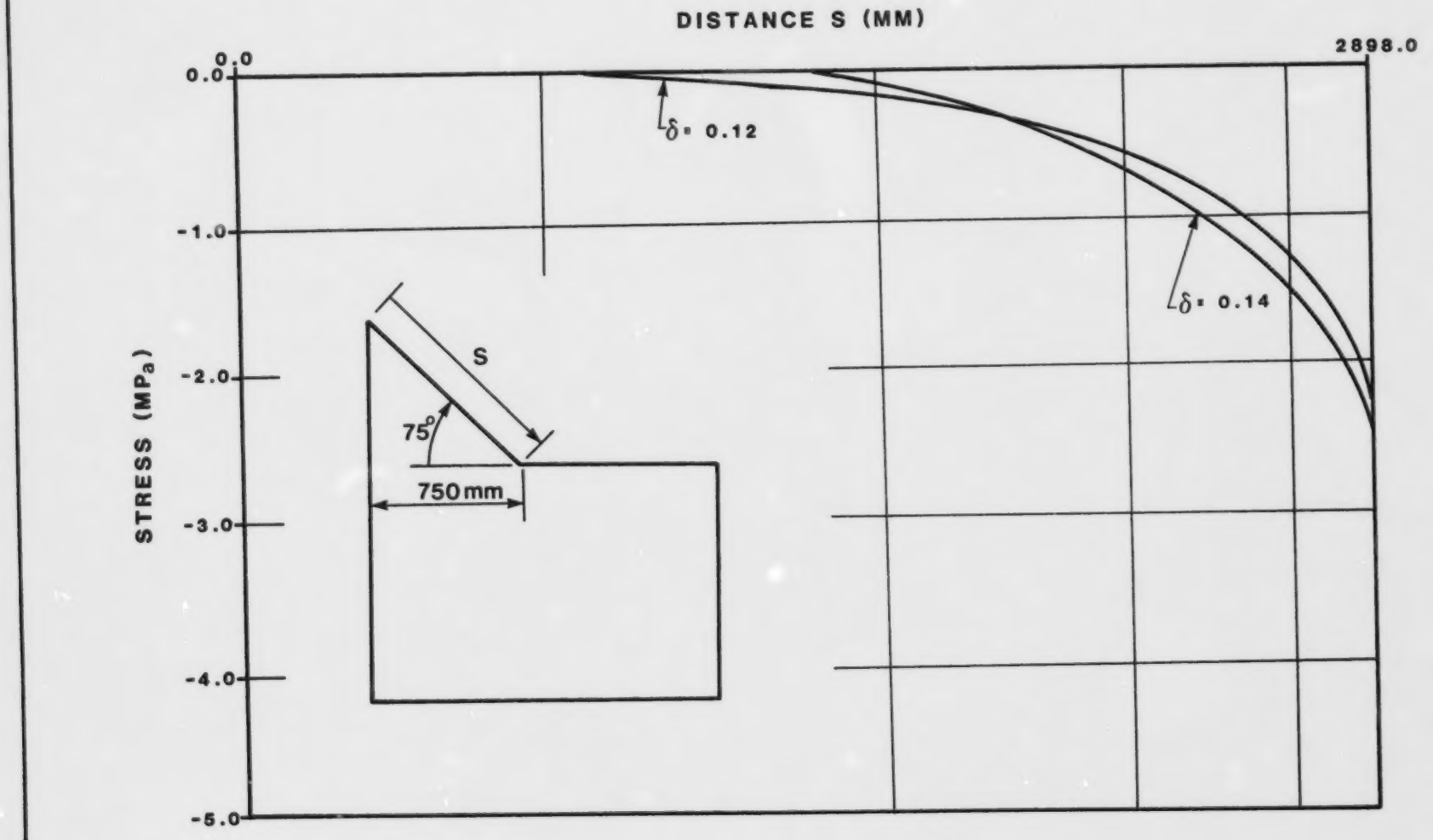

FIGURE 5.30 STRESSES IN ICE-BLOCK AT CUTTER-ICE INTERFACE

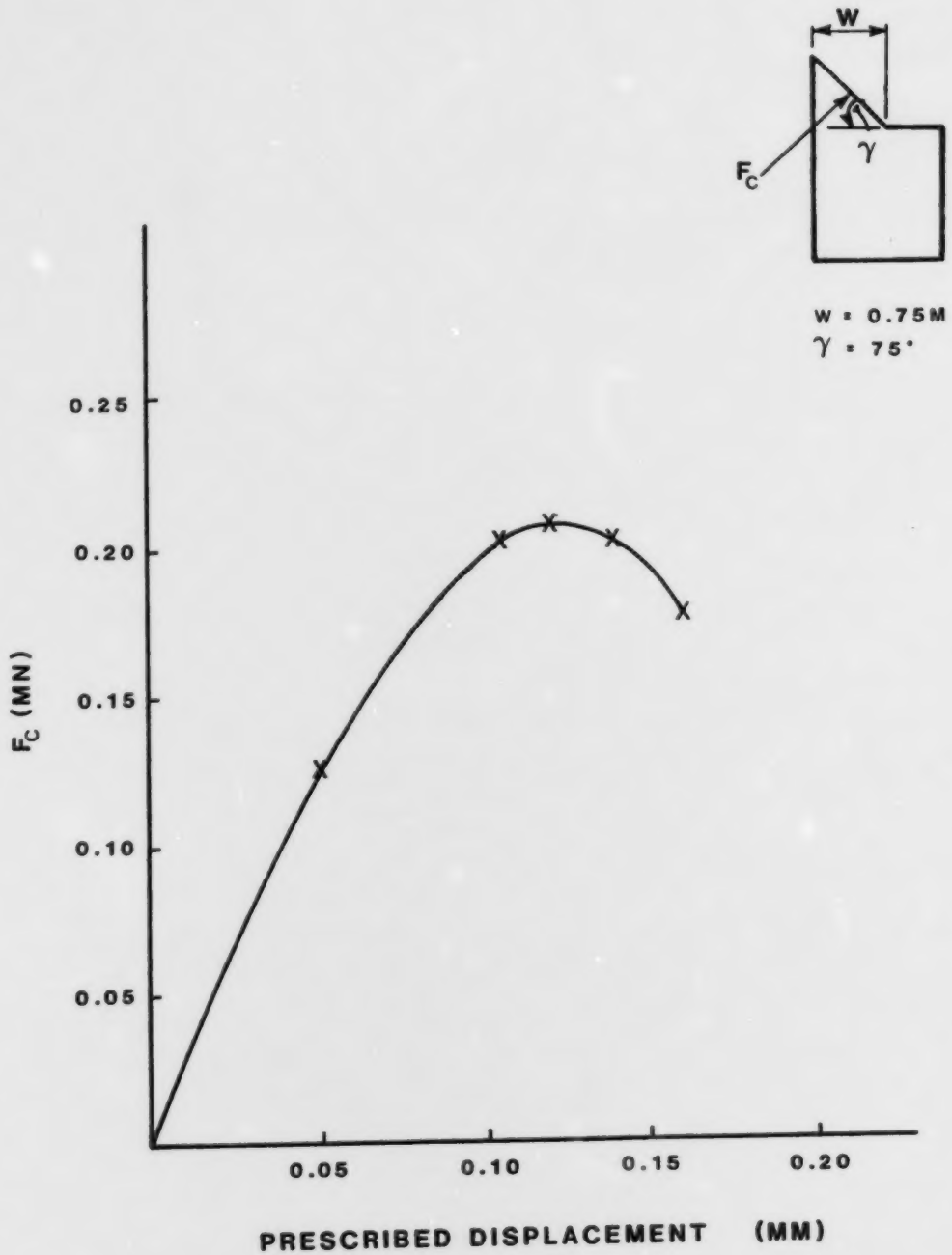

FIGURE 5.31 CONTACT FORCE VERSUS PRESCRIBED DISPLACEMENT FOR CUTTING ANGLE OF 75°

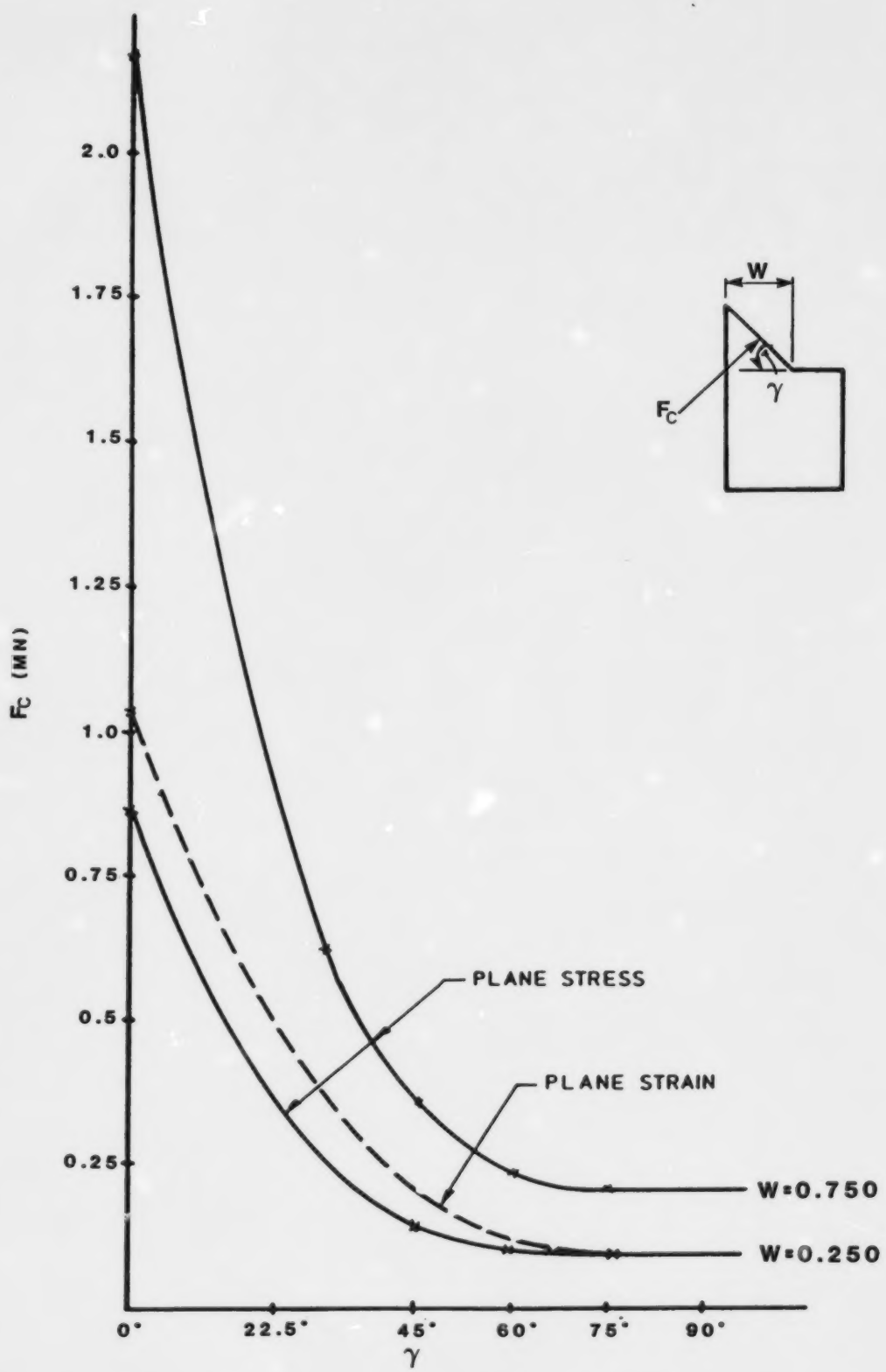

FIGURE 5.32 CONTACT FORCE VERSUS CUTTING ANGLE

in Figure 5.33 was used. This model was generated by the program IDENTM, and is identical to the one used in the wedge indentor analysis, with the exception that the boundary condition dictating symmetry (i.e. zero horizontal displacements along the line of symmetry) were not imposed. Two different cutting angles were investigated, -45° (corresponding to a right angled wedge) and -75°. Results for these two cases are shown in Figures 5.34 and 5.35.

5.4.3 Three-Dimensional Effects

Full three-dimensional computer analysis was not carried out because of cost considerations. An indication of the significance of three-dimensional effects can be gained by comparing the results obtained for the two extreme conditions, plane stress and plane strain. As explained in Section 5.4.1, the plane stress condition refers to the situation where ice thickness is relatively small in comparison to the indentor or cutter length, while the plane strain refers to the situation where ice is thick in relation to indentor width. For the latter, stresses in the third direction (normal to the plane of discretization) are large enough to affect the failure condition.

The manner in which a stress in the third direction can affect milling forces and contact pressure distributions can be seen in Figures 5.15, 5.16, 5.19, 5.20 and 5.32. In general, the effect is increased maximum force and maximum contact pressure, and a change in the shape of the contact pressure distribution curve (see Figures 5.15 and 5.19). Force and pressure can increase by as much as 50%.

5.5 Incorporation of Results into Computer Program PVICE

Here the objective was to use the results obtained from the ice-block analyses to establish curves for P_1, P_2 and F, as defined in Section 3.3, and shown in Figures 3.14 and 3.15. The basic philosophy upon which this was based is shown in Figures 5.36 to 5.38. As can be seen, the P_1 curve (Figure 5.36) is approximated as the pressure distribution corresponding to a curved indentor, while the P_2 curve (Figure 5.37) is approximated as the pressure distribution corresponding to a slicing mode with negative cutting angle. The concentrated force F is approximated as the force F_c associated with a slicing mode with positive cutting angle, as shown in Figure 5.38.

The curves for P_1, P_2 and F, as extracted from the results presented in Section 5.4, are shown in Figures 5.39 and 5.40. These curves have been incorporated into the program PVICE.

The fact that P_1 is based on results obtained from symmetric indentation analysis, and that P_2 and F pertain to a flat structure-ice interface, poses some question on the validity of these curves. The effects of the implied assumptions were not investigated under the present contract. Obviously, the finite element method of modelling the ice block is versatile enough to permit the analysis of unsymmetric indentors

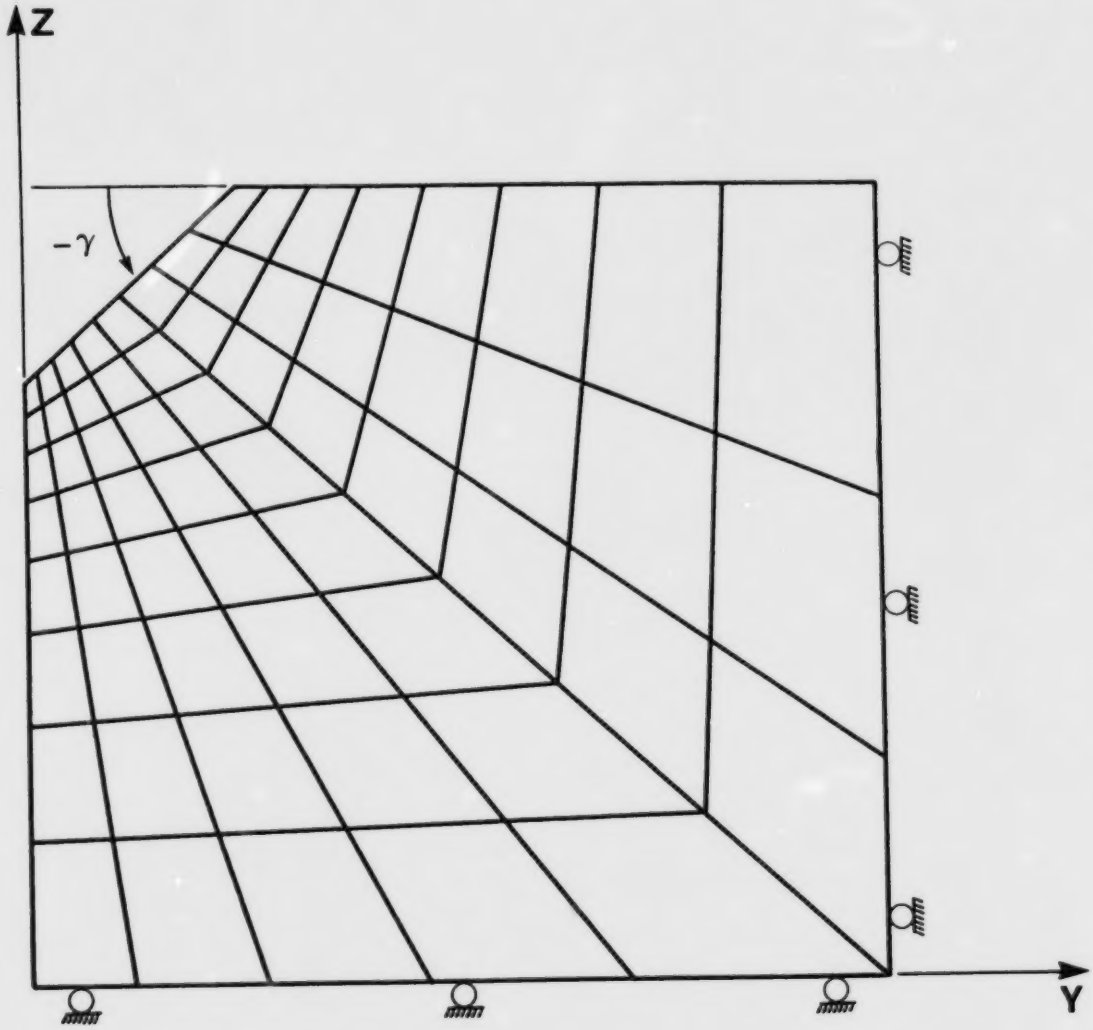

FIGURE 5.33 FINITE ELEMENT MODEL FOR NEGATIVE CUTTING ANGLES

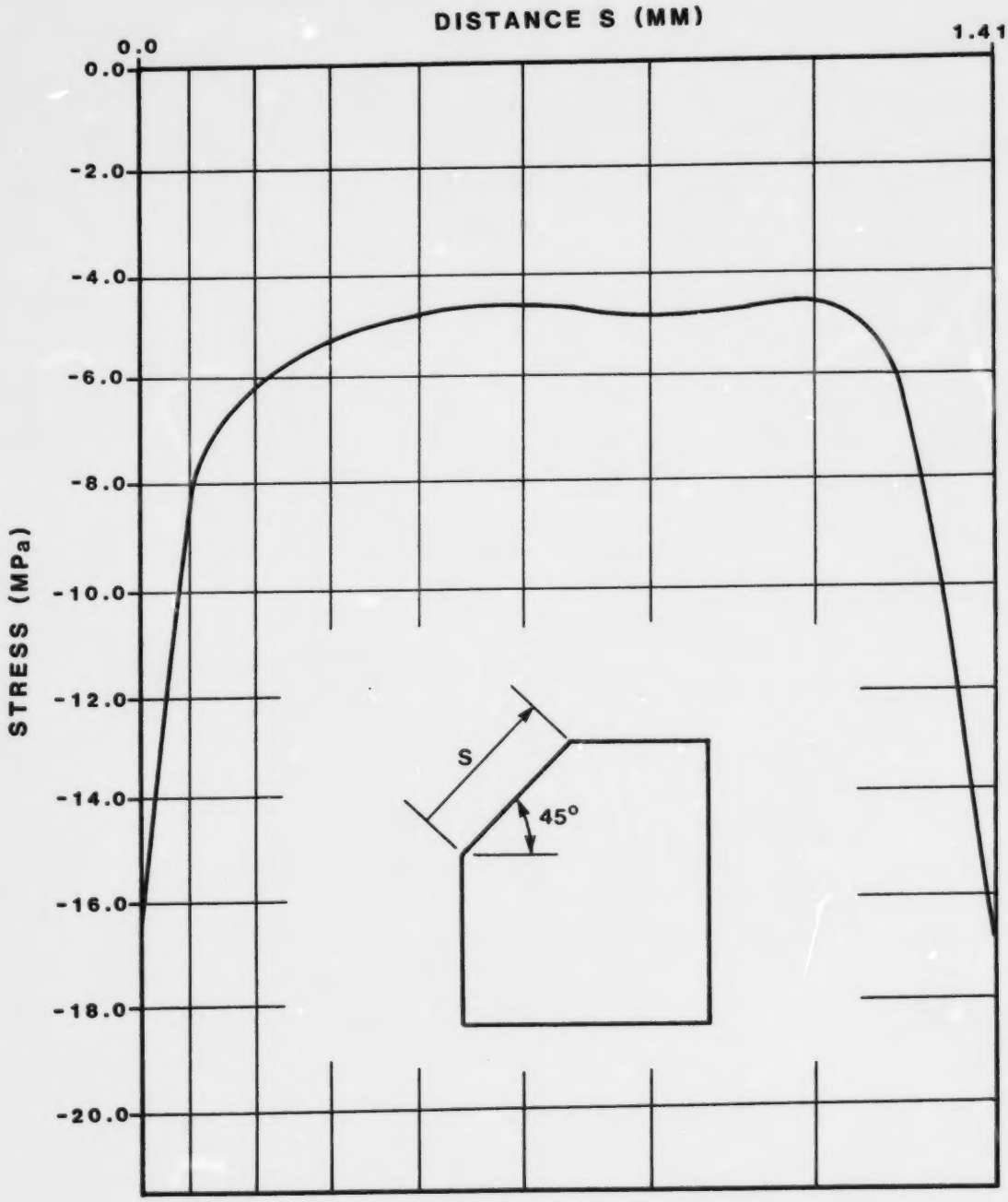

FIGURE 5.34 STRESSES IN ICE-BLOCK AT CUTTER-ICE INTERFACE FOR CUTTING ANGLE OF -45°

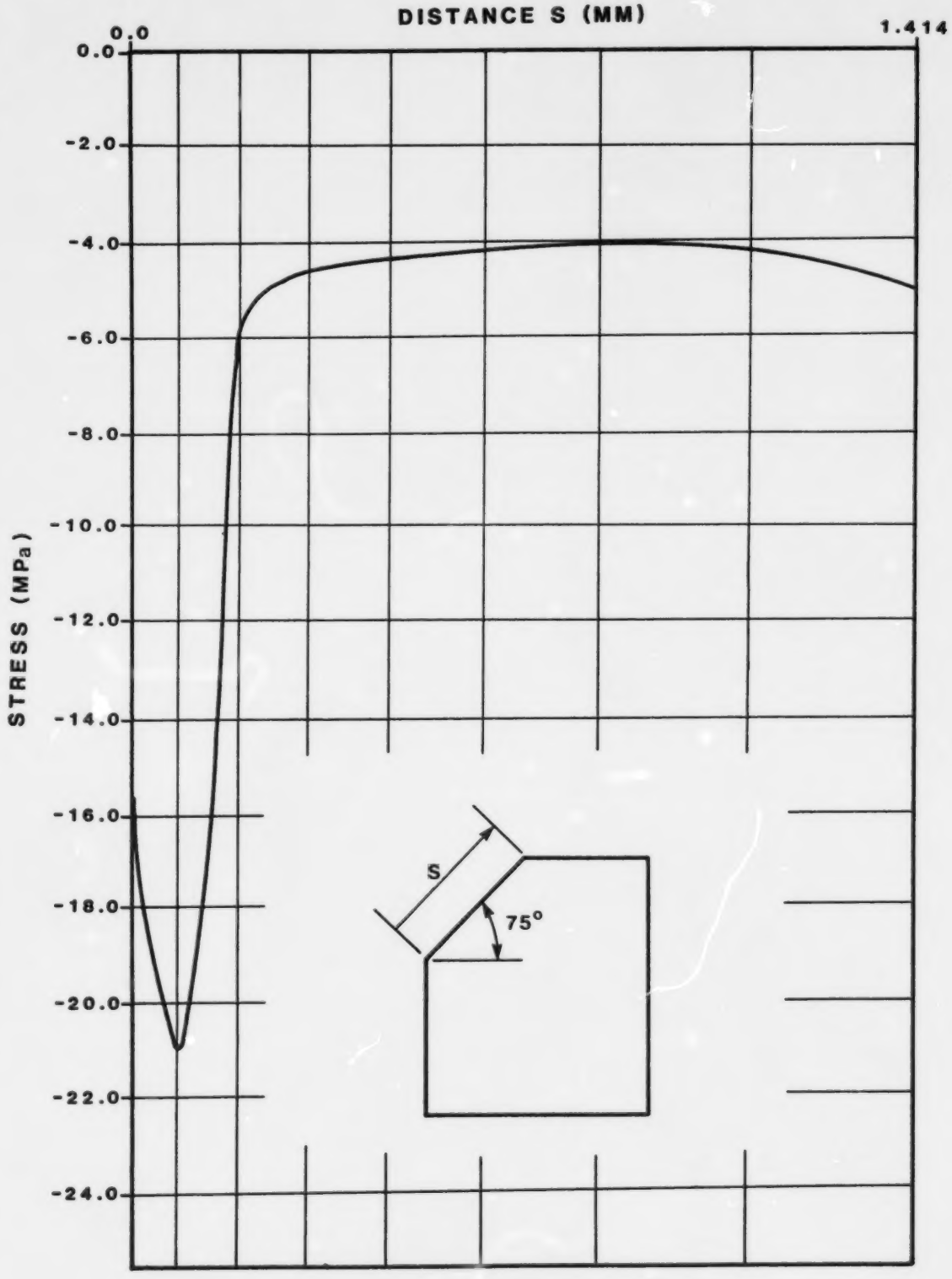

FIGURE 5.35 STRESSES IN ICE-BLOCK AT CUTTER-ICE INTERFACE FOR CUTTING ANGLE OF -75°

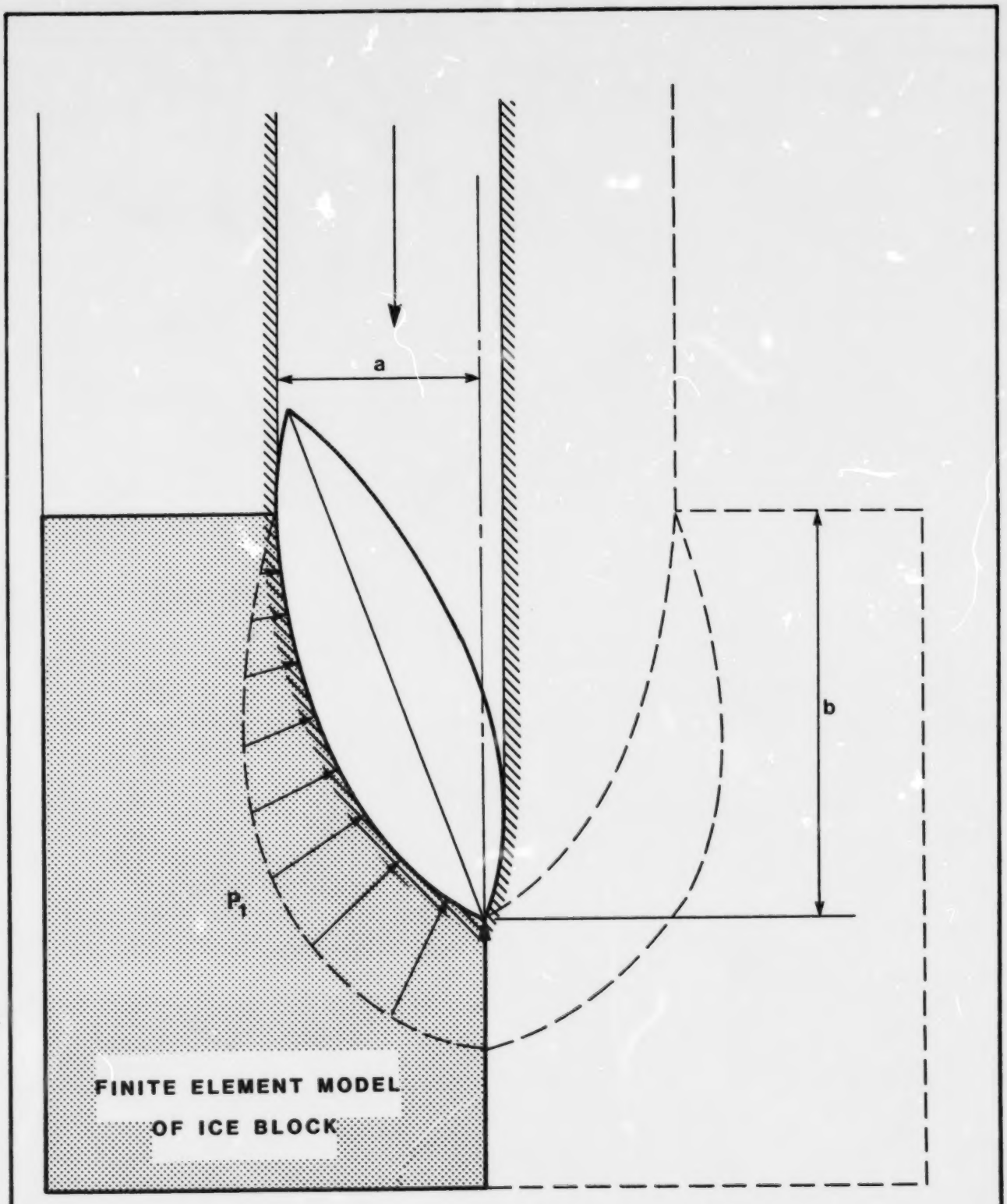

FIGURE 5.36 USE OF CURVED INDENTOR MODEL TO APPROXIMATE P_1

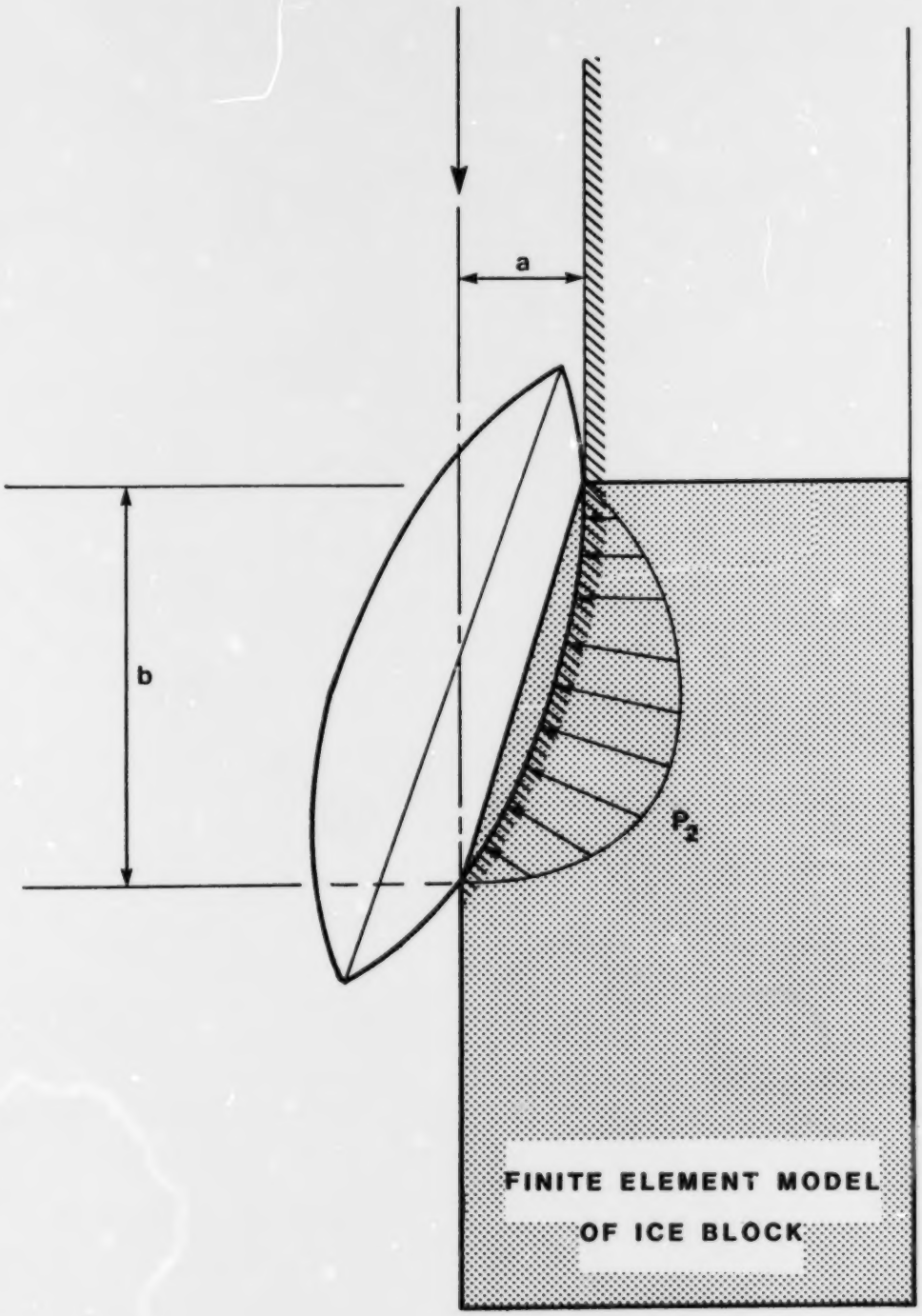

FIGURE 5.37 USE OF SLICING MODEL TO APPROXIMATE P_2

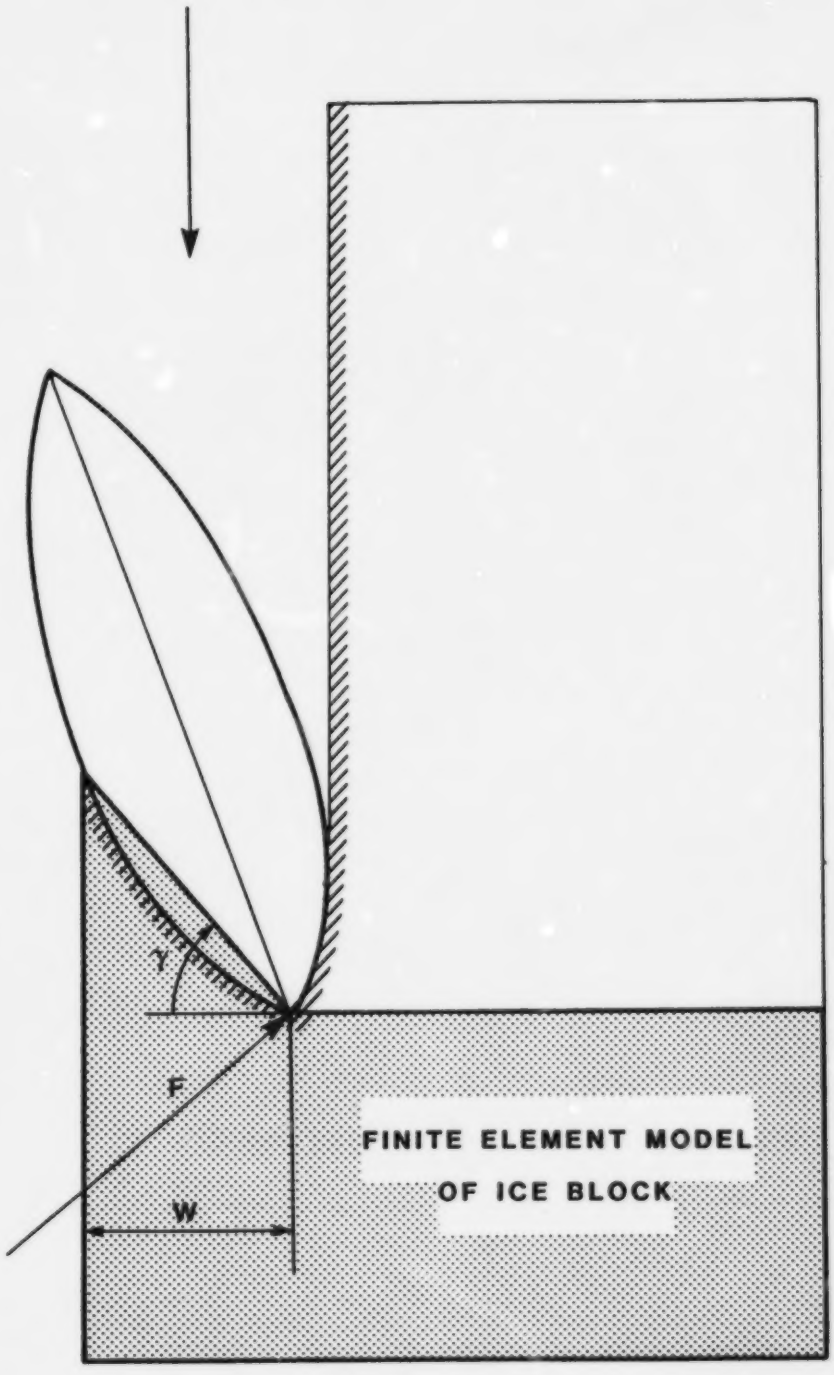

FIGURE 5.38 USE OF SLICING MODEL TO APPROXIMATE F

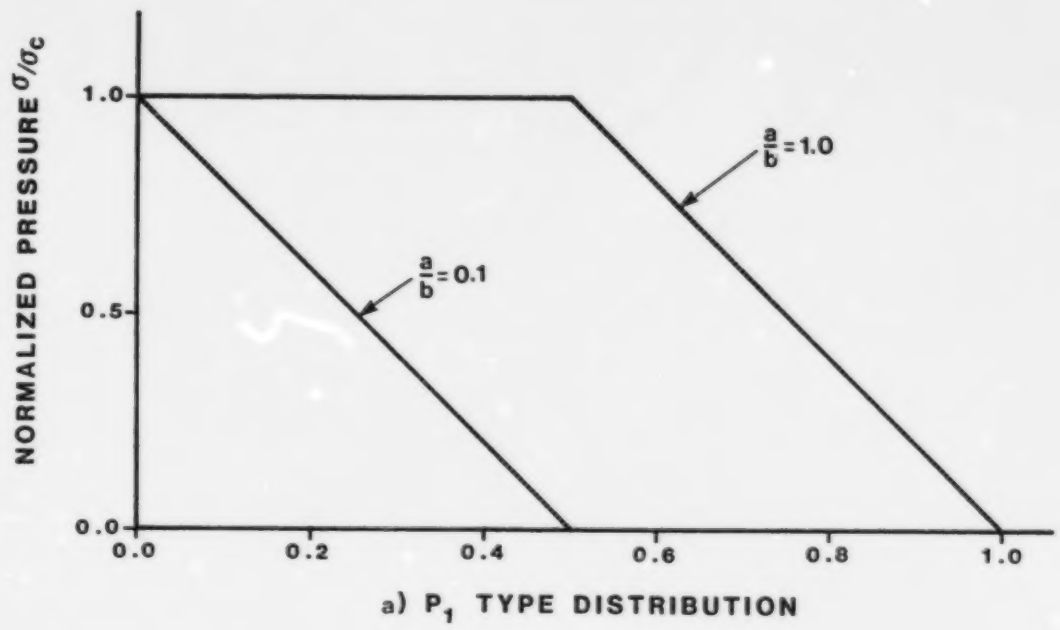

a) P_1 TYPE DISTRIBUTION

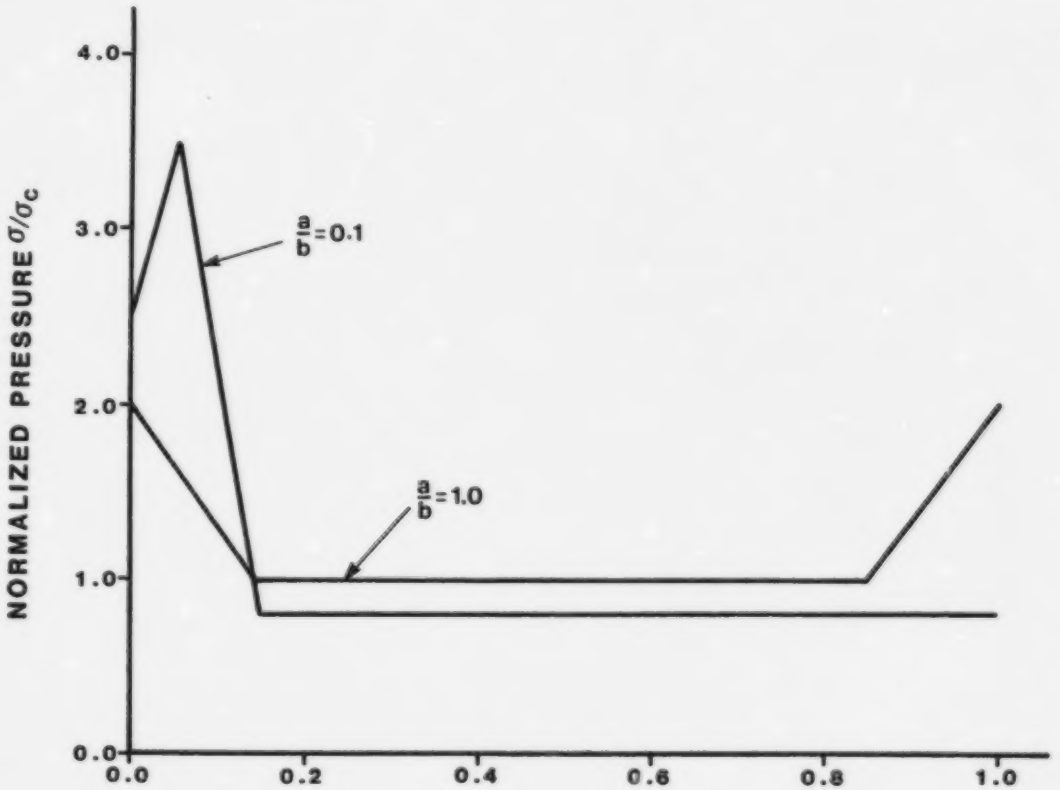

b) P_2 TYPE DISTRIBUTION

FIGURE 5.39 BLADE-ICE INTERACTION PRESSURE DISTRIBUTION CURVES INCORPORATED INTO PVICE

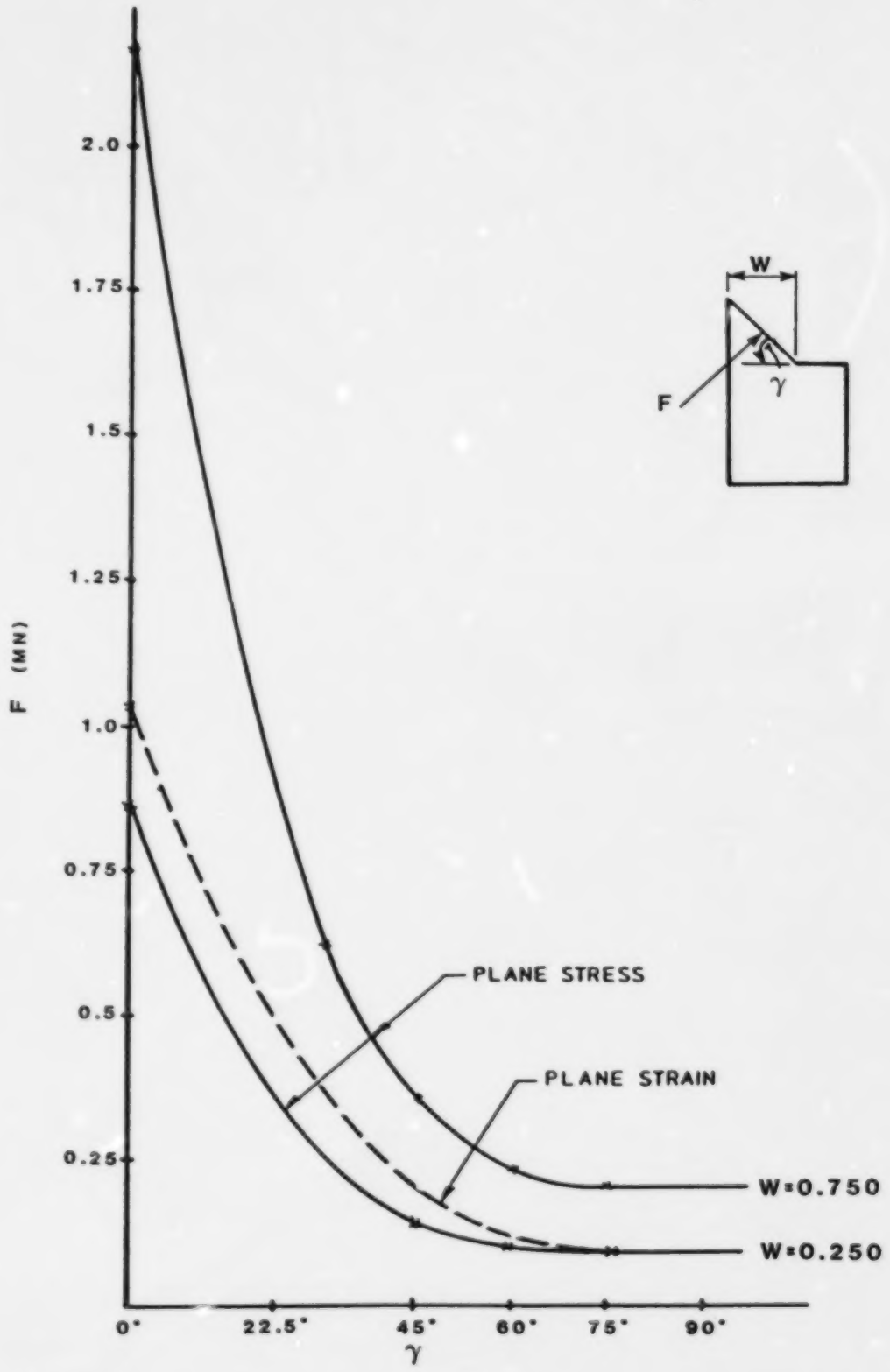

FIGURE 5.40 F CURVES INCORPORATED INTO PVICE

and curved structure-ice interfaces. Consequently, revised curves for P_1, P_2 and F could be established, and incorporated into PVICE. This is discussed further in Section 6.0.

6.0 ANALYSIS OF A TYPICAL ICEBREAKER PROPELLER

6.1 Analysis of Blade Passage Through Ice Using Uniform Pressure Loading on Blade

The stress levels and patterns in a propeller blade were investigated as it passes through the ice using a uniform pressure distribution determined from program PVICE described in Section 3. The CCGS Pierre Radisson/Franklin propeller was selected as the typical icebreaker propeller to be analyzed. The finite element model of the blade and root is shown in Figure 6.1. The geometric data for the model was adopted from the previous work [1]. For the purpose of analysis, the following three loading cases were considered:

Load Case L1 - Cutting depth = 0.17 R
Load Case L2 - Cutting depth = 0.33 R
Load Case L3 - Cutting depth = 0.50 R

where R is maximum b ade radius.

In each case, the analyses were carried out with the PVICE and VAST programs for 10 different equispaced angular positions of the blade, i.e. 10 different values of θ (see Figure 6.2) at regular intervals between the position at which the blade just touches the ice-line and the position at which it leaves the ice-line. Thus each loading condition is designated by the letters L1, L2 or L3 followed by a two digit number (between 01 and 10) indicating the angular position.

All the analyses were carried out for a unit pressure load of 1.0 MPa. The results for loading cases L1, L2 and L3 are summarized in Tables 6.1, 6.2 and 6.3, respectively.

For each loading case maximum stress area can be located by reference to Tables 6.1 and 6.2. These tables indicate the maximum stress value and the node where it occurs. It will be seen that under all loading cases, in general maximum stress occurs at the top of the blade root fillet except in a situation where either the area close to the leading edge or the area close to the trailing edge only is loaded. In these latter cases, maximum stress occurs close to the loaded area.

The stress contours plots for 10 cutting positions of the blade under the loading case L3 are shown in Figures 6.3 to 6.12. It is seen from these plots that loaded areas show the presence of rapid stress gradient when the pressure is on the leading edge (i.e. loading cases L3-01 to L3-03). As the blade gets more embedded in the ice-block (i.e. loading cases L3-04 to L3-07), the variation in stress gradient becomes more gradual over the surface except near the root area. The stress gradient in this area generally remains high with the location of maximum stress remaining more or less in the same position which is just above the blade root fillet. As the loading shifts to the trailing edge (i.e. loading cases L3-08 to L3-10), the area of maximum stress moves slightly

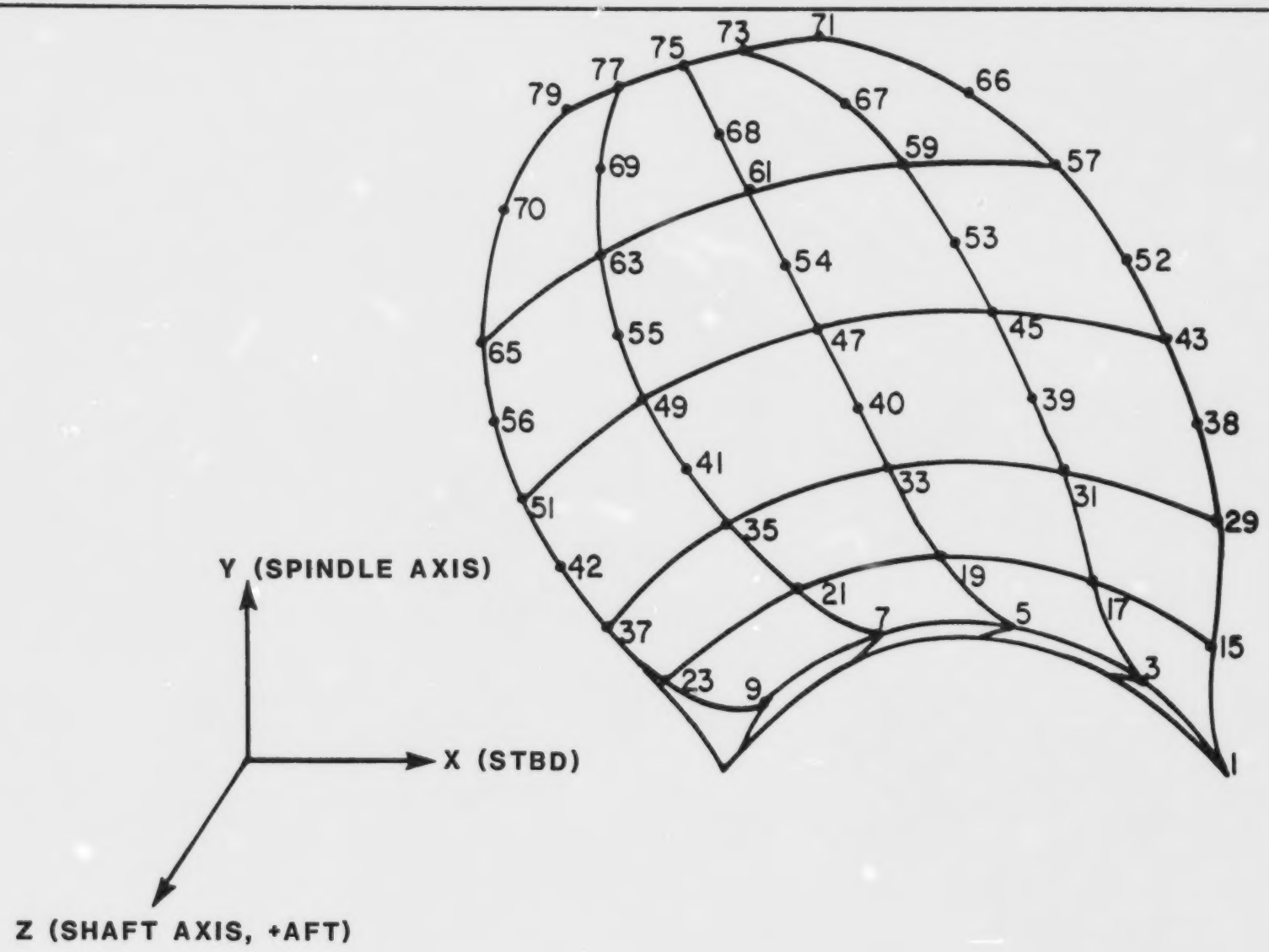

FIGURE 6.1 FINITE ELEMENT MODEL OF CCGS PIERRE RADISSON/FRANKLIN PROPELLER

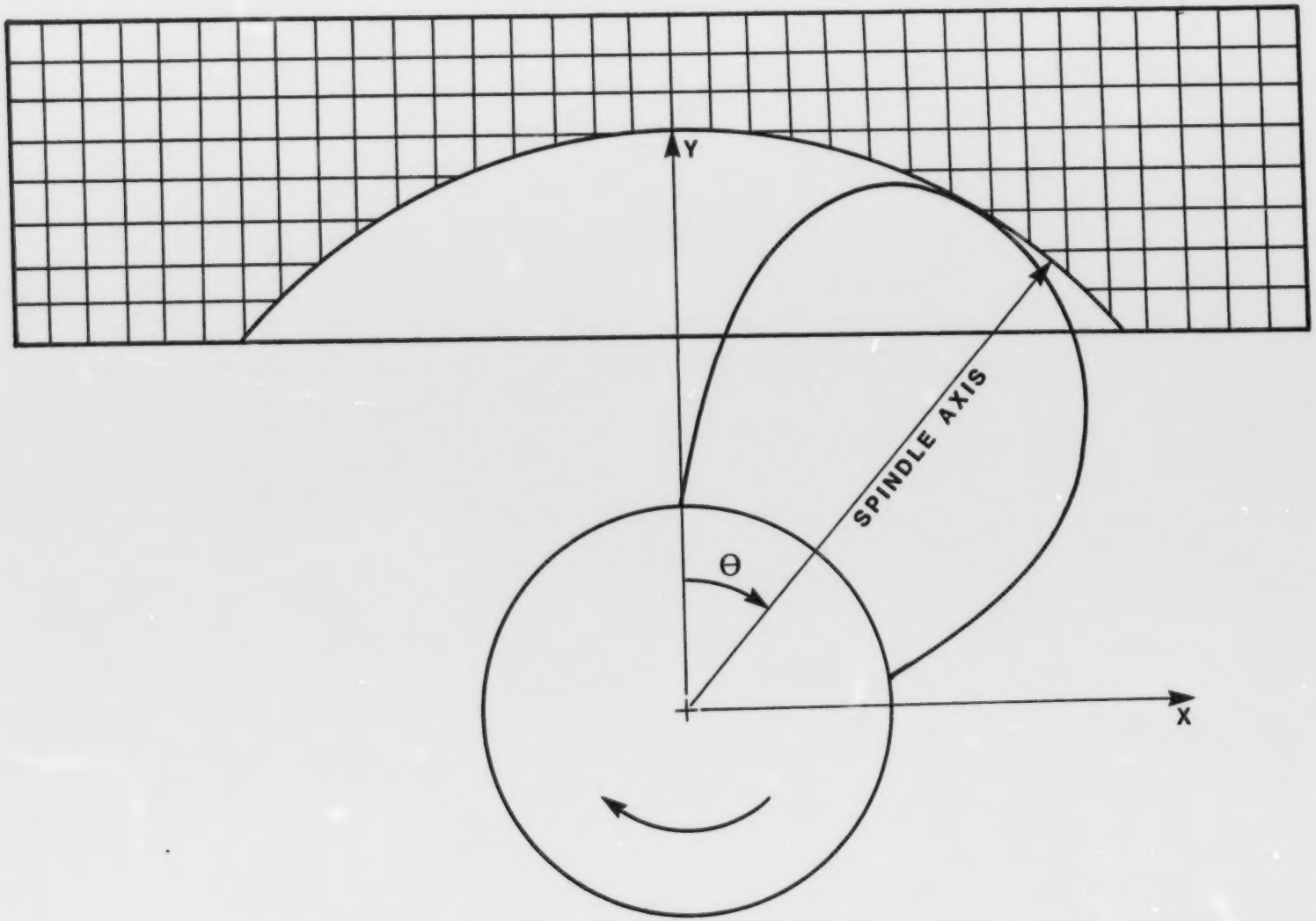

FIGURE 6.2 ANGULAR POSITION Θ OF BLADE IN ICE

TABLE 6.1

SUMMARY OF RESULTS FOR LOADING CASE L1

Loading Case	θ	Uniform Pressure = 1.0 MPa Coefficient of Friction = 0.0					Node Number Where Maximum Stress Occurs
		F_X (MN)	F_Y (MN)	F_Z (MN)	Maximum Deflection (MM)	Maximum Stress (MPa)	
L1-01	-18.25°	-0.014	0.003	-0.046	-0.477	-14.2	59
L1-02	-10.50°	-0.036	0.010	-0.118	-1.142	-28.5	53
L1-03	-2.75°	-0.058	0.021	-0.193	-1.725	-43.9	19
L1-04	5.0	-0.073	0.033	-0.252	-2.139	-55.7	19
L1-05	12.75	-0.078	0.044	-0.282	-2.378	-60.6	19
L1-06	20.50	-0.074	0.052	-0.283	-2.459	-61.6	47
L1-07	28.25	-0.062	0.052	-0.254	-2.335	-57.3	47
L1-08	36.00	-0.045	0.045	-0.200	-1.981	-47.1	47
L1-09	43.75	-0.026	0.030	-0.125	-1.381	-32.1	62
L1-10	51.50	-0.009	0.013	-0.051	-0.637	-19.8	63

TABLE 6.2

SUMMARY OF RESULTS FOR LOADING CASE L2

Loading Case	θ	Uniform Pressure = 1.0 MPa Coefficient of Friction = 0.0					Node Number Where Maximum Stress Occurs
		F_X (MN)	F_Y (MN)	F_Z (MN)	Maximum Deflection (MM)	Maximum Stress (MPa)	
L2-01	-34°	-0.044	-0.016	-0.131	-0.916	-27.5	45
L2-02	-23°	-0.112	0.008	-0.330	-2.219	-65.6	19
L2-03	-12°	-0.175	0.033	-0.522	-3.204	-101.0	19
L2-04	-1°	-0.216	0.070	-0.663	-3.815	-122.0	19
L2-05	10°	-0.227	0.110	-0.735	-4.135	-130.0	19
L2-06	21°	-0.211	0.142	-0.740	-4.177	-127.0	19
L2-07	32°	-0.173	0.156	-0.679	-3.987	-114.0	19
L2-08	43°	-0.121	0.144	-0.553	-3.541	-93.5	33
L2-09	54°	-0.068	0.106	-0.374	-2.715	-66.9	47
L2-10	65°	-0.024	0.051	-0.170	-1.427	-39.3	49

TABLE 6.3

SUMMARY OF RESULTS FOR LOADING CASE L3

Loading Case	θ	Uniform Pressure = 1.0 MPa Coefficient of Friction = 0.0					Node Number Where Maximum Stress Occurs
		F_X (MN)	F_Y (MN)	F_Z (MN)	Maximum Deflection (MM)	Maximum Stress (MPa)	
L3-01	-47°	-0.097	-0.024	-0.263	-1.208	-41.1	19
L3-02	-33°	-0.231	-0.024	-0.619	-2.991	-100.0	19
L3-03	-19°	-0.351	0.018	-0.941	-4.119	-147.0	19
L3-04	-5°	-0.423	0.094	-1.155	-4.701	-170.0	19
L3-05	9°	-0.434	0.185	-1.257	-4.834	-175.0	19
L3-06	23°	-0.387	0.263	-1.251	-4.771	-169.0	19
L3-07	37°	-0.298	0.302	-1.145	-4.573	-153.0	19
L3-08	51°	-0.191	0.284	-0.934	-4.161	-123.0	19
L3-09	65°	-0.093	0.206	-0.624	-3.269	-86.5	33
L3-10	79°	-0.026	0.091	-0.265	-1.581	-49.9	49

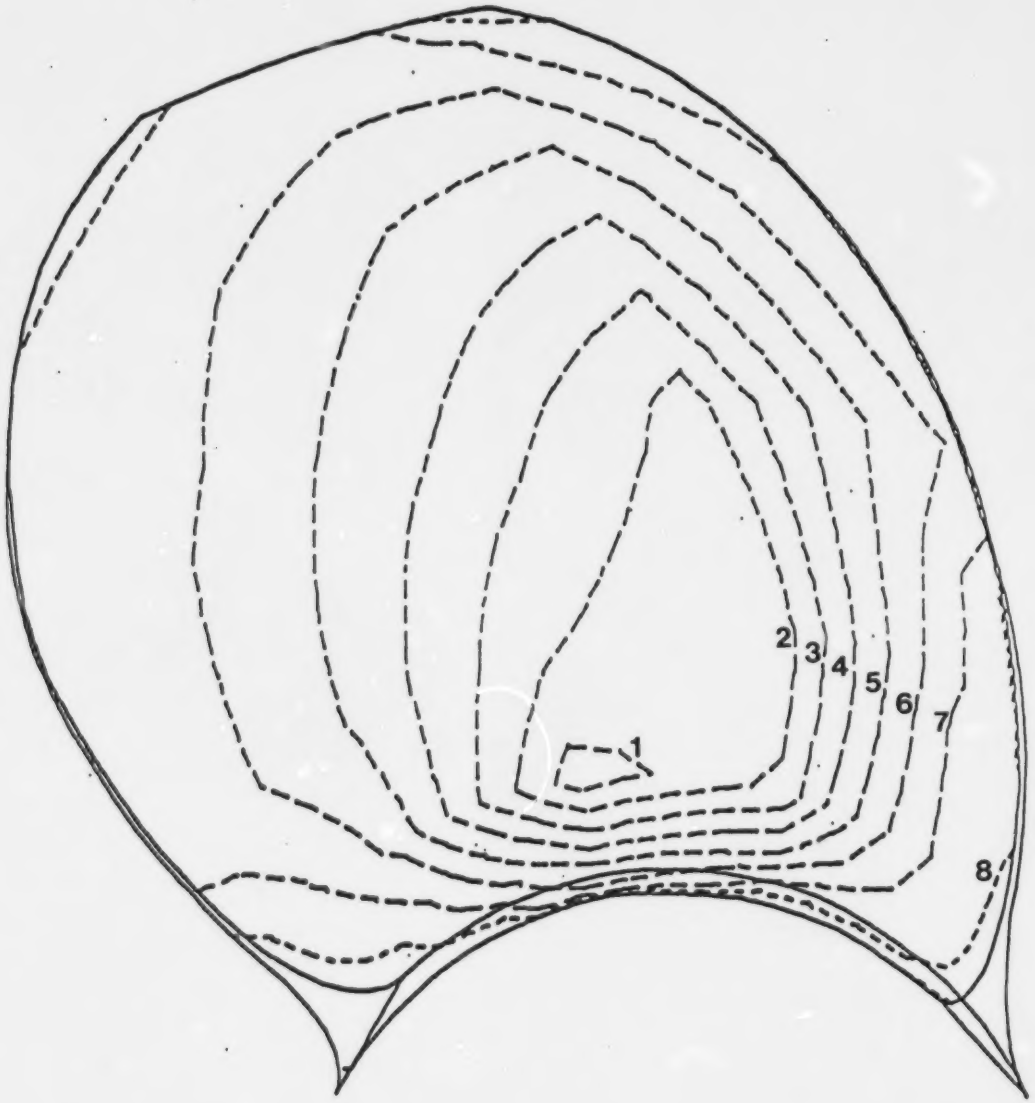

SECOND PRINCIPAL
STRESS CONTOURS
(STATIC ANALYSIS)

STRESS LEVELS

CODE	STRESS
1	-38.5
2	-33.0
3	-27.5
4	-22.0
5	-16.5
6	-11.0
7	-5.5
8	0.0
9	5.5

532.445 MM.

FIGURE 6.3 LOAD CASE L3-01

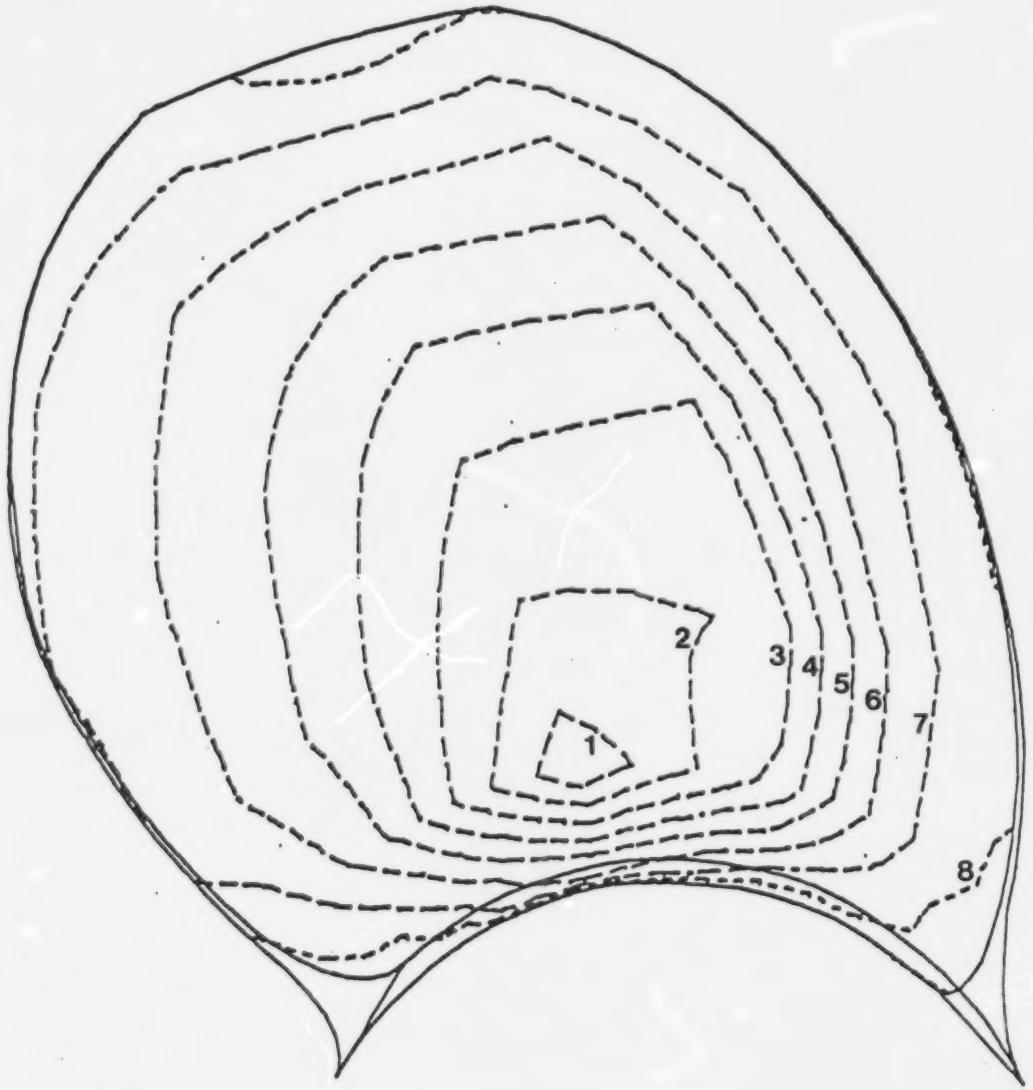

SECOND PRINCIPAL
STRESS CONTOURS
(STATIC ANALYSIS)

STRESS LEVELS

CODE	STRESS
1	-91.
2	-78.
3	-65.
4	-52.
5	-39.
6	-26.
7	-13.
8	0.
9	13.

532.445 MM.

FIGURE 6.4 LOAD CASE L3-02

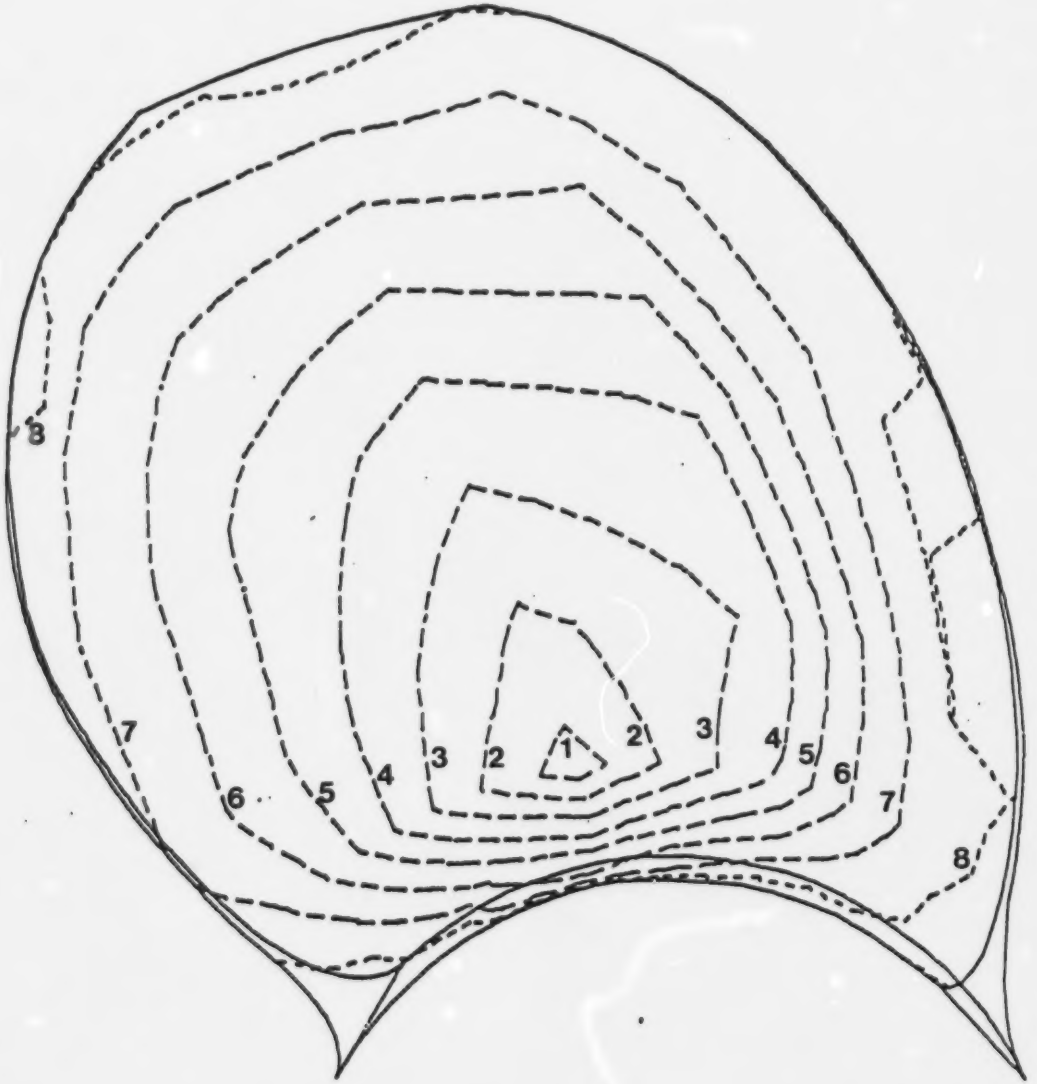

SECOND PRINCIPAL
STRESS CONTOURS
(STATIC ANALYSIS)

STRESS LEVELS

CODE	STRESS
1	-140.
2	-120.
3	-100.
4	-80.
5	-60.
6	-40.
7	-20.
8	0.
9	20.

532.445 MM.

FIGURE 6.5 LOAD CASE L3-03

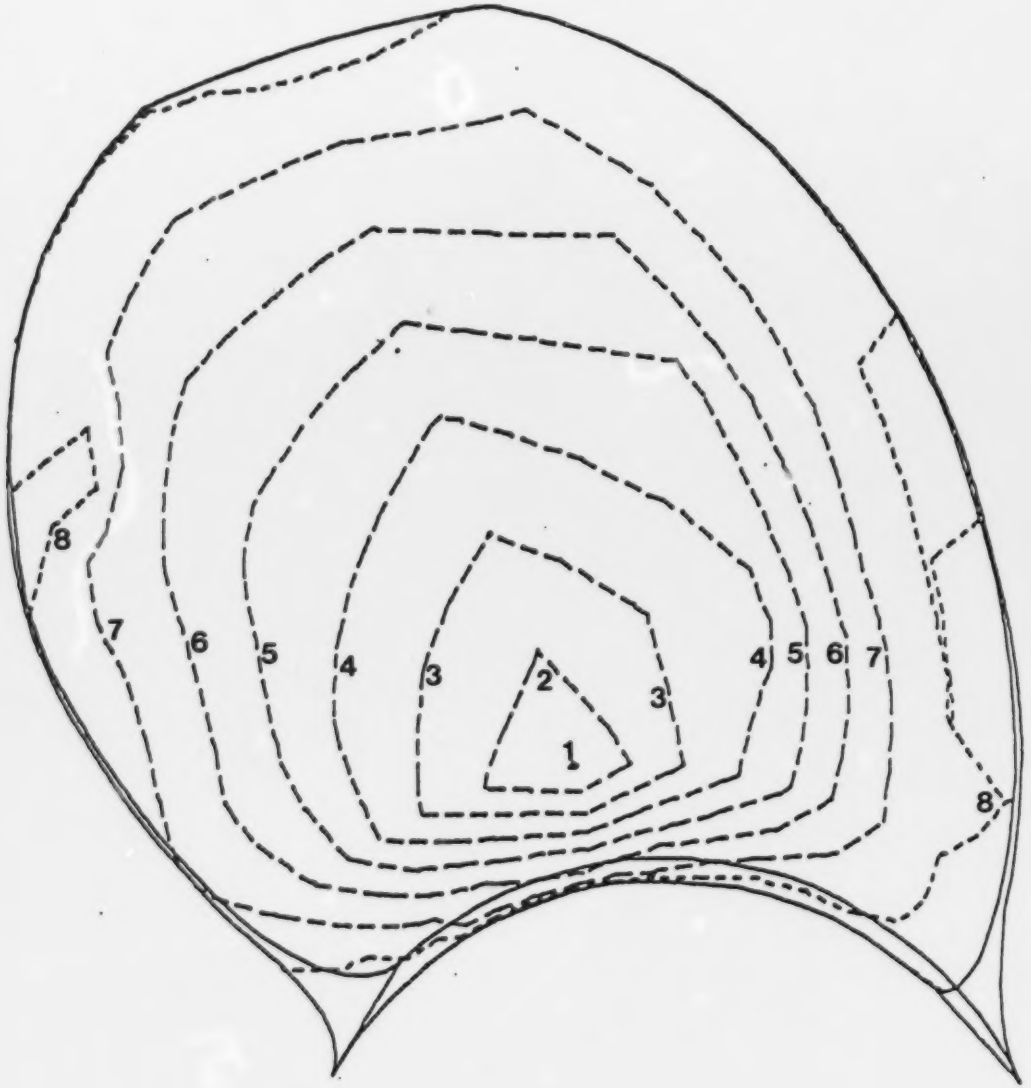

SECOND PRINCIPAL
STRESS CONTOURS
(STATIC ANALYSIS)

STRESS LEVELS

CODE	STRESS
1	-168.
2	-144.
3	-120.
4	-96.
5	-72.
6	-48.
7	-24.
8	0.
9	24.

532.445 MM.

FIGURE 6.6 LOAD CASE L3-04

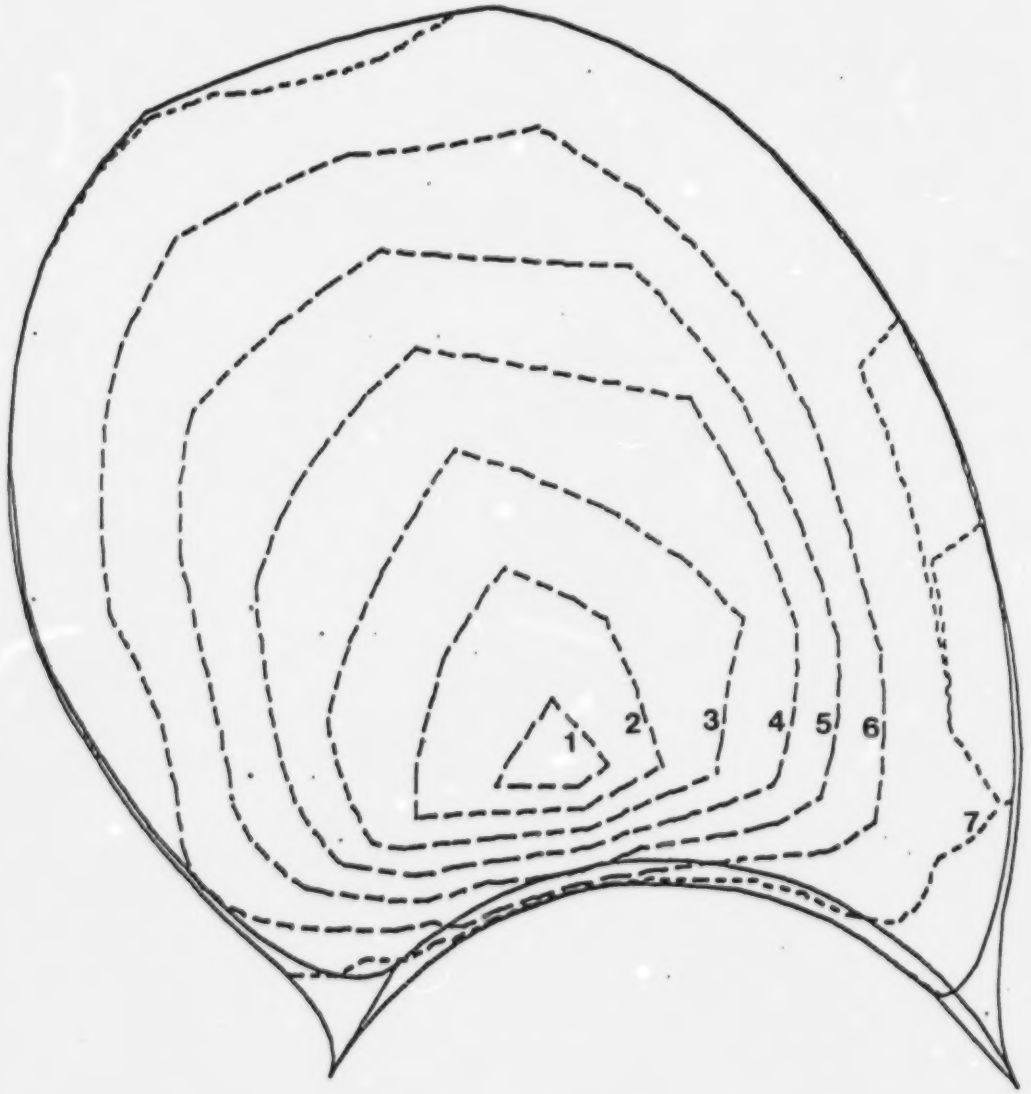

SECOND PRINCIPAL
STRESS CONTOURS
(STATIC ANALYSIS)

STRESS LEVELS

CODE	STRESS
1	-150.
2	-125.
3	-100.
4	-75.
5	-50.
6	-25.
7	0.
8	25.

532.445 MM.

FIGURE 6.7 LOAD CASE L3-05

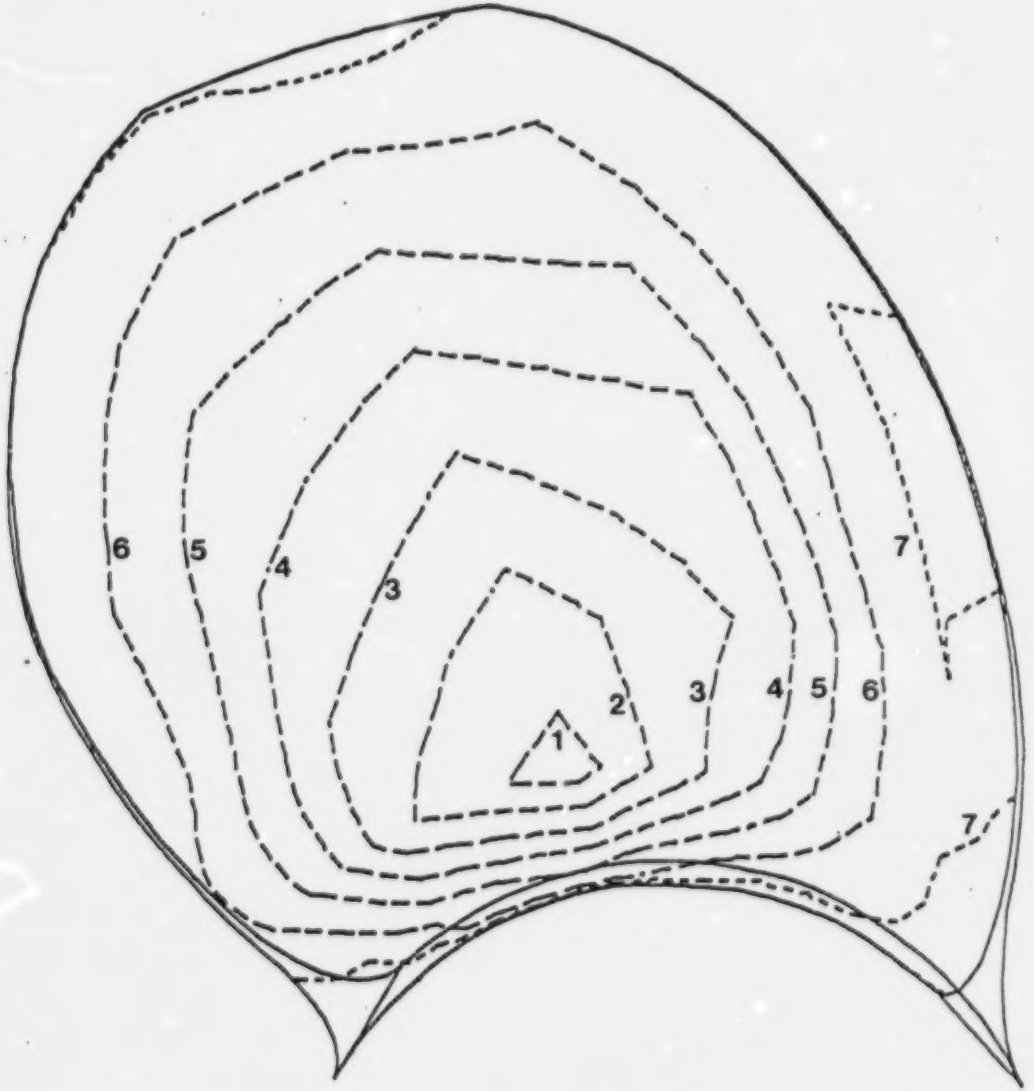

SECOND PRINCIPAL
STRESS CONTOURS
(STATIC ANALYSIS)

STRESS LEVELS

CODE	STRESS
1	-156.
2	-130.
3	-104.
4	-78.
5	-52.
6	-26.
7	0.
8	26.

532.445 MM.

FIGURE 6.8 LOAD CASE L3-06

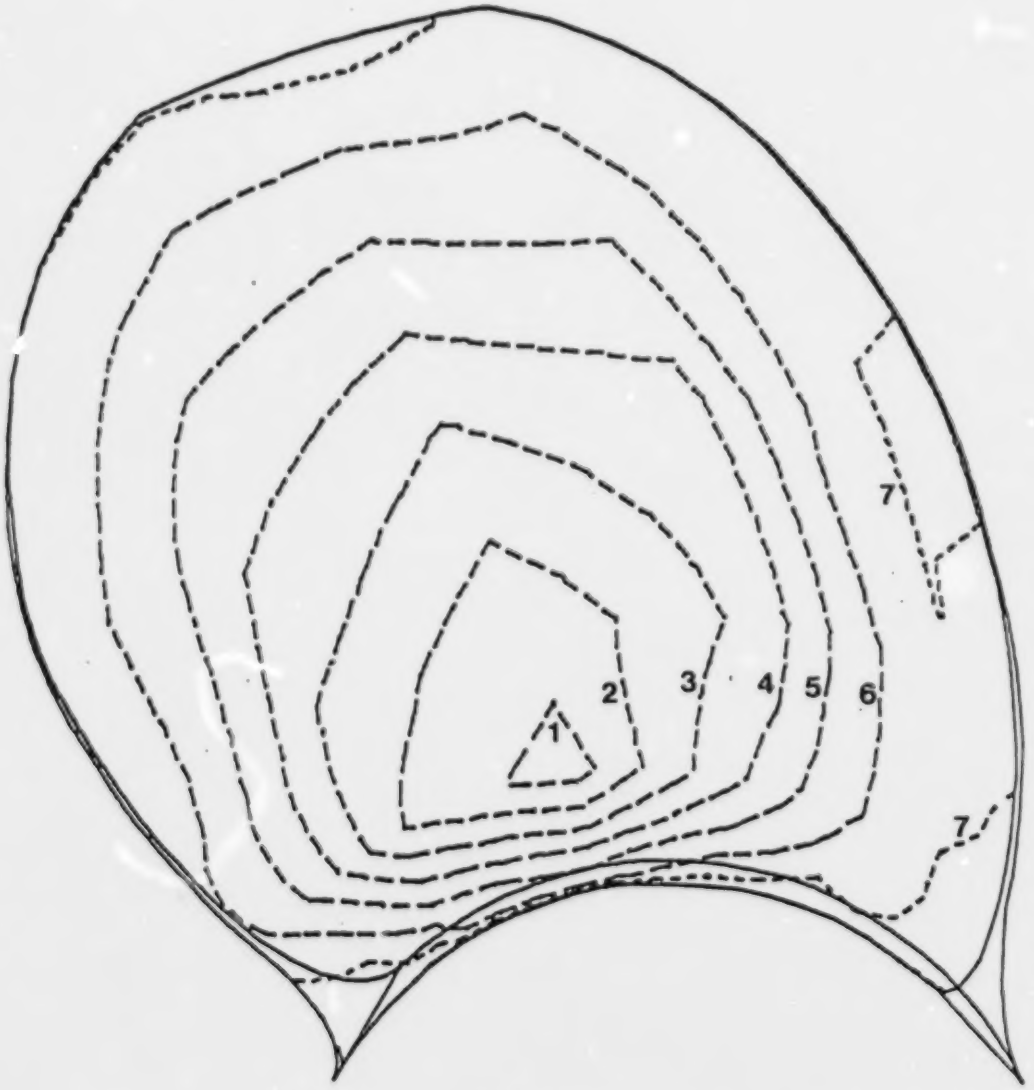

SECOND PRINCIPAL
STRESS CONTOURS
(STATIC ANALYSIS)

STRESS LEVELS

CODE	STRESS
1	-144.
2	-120.
3	-96.
4	-72.
5	-48.
6	-24.
7	0.
8	24.

532.445 MM.

FIGURE 6.9 LOAD CASE L3-07

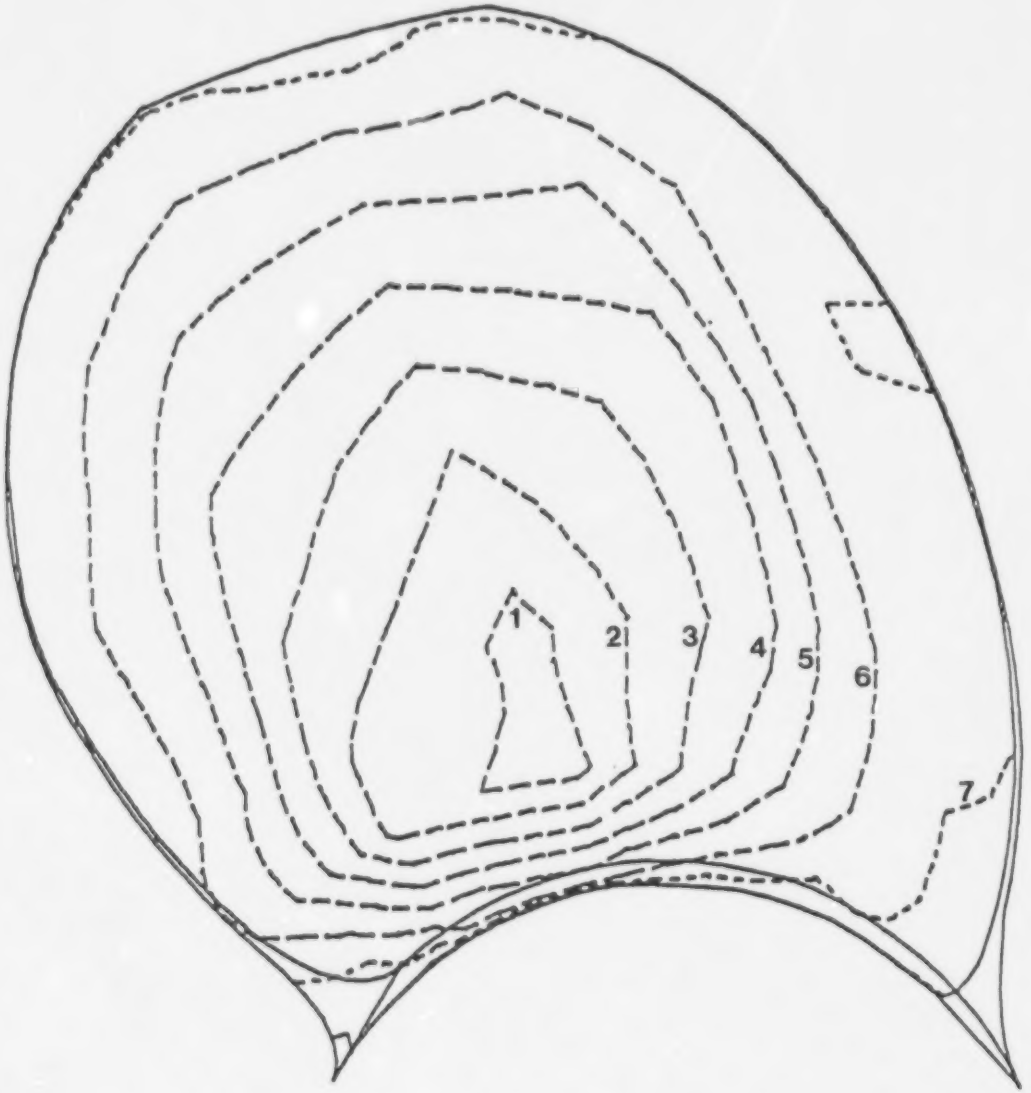

SECOND PRINCIPAL
STRESS CONTOURS
(STATIC ANALYSIS)

STRESS LEVELS

CODE	STRESS
1	-117.0
2	-97.5
3	-78.0
4	-58.5
5	-39.0
6	-19.5
7	0.0
8	19.5

532.445 MM.

FIGURE 6.10 LOAD CASE L3-08

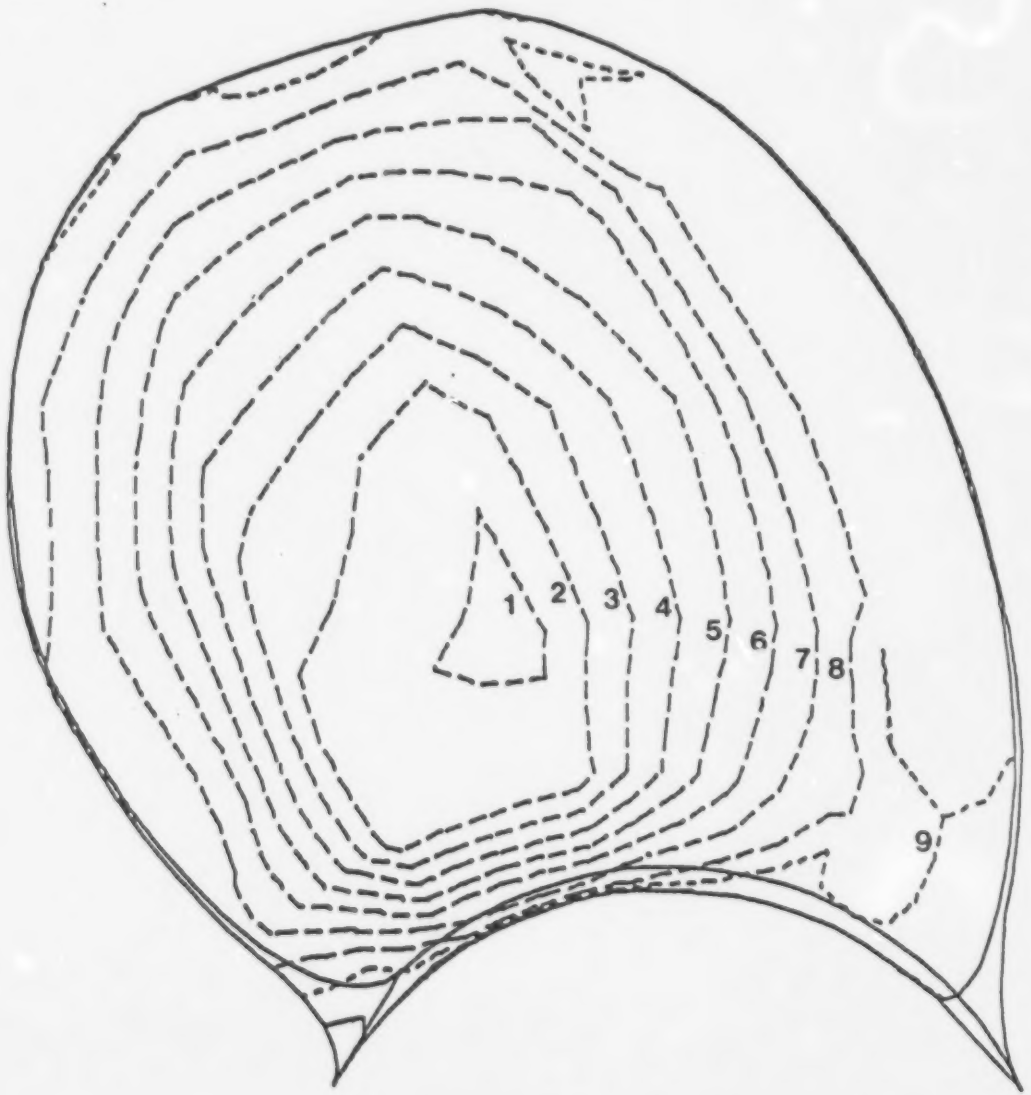

SECOND PRINCIPAL
STRESS CONTOURS
(STATIC ANALYSIS)

STRESS LEVELS

CODE	STRESS
1	-80.
2	-70.
3	-60.
4	-50.
5	-40.
6	-30.
7	-20.
8	-10.
9	0.
10	10.
11	20.

532.445 MM.

FIGURE 6.11 LOAD CASE L3-09

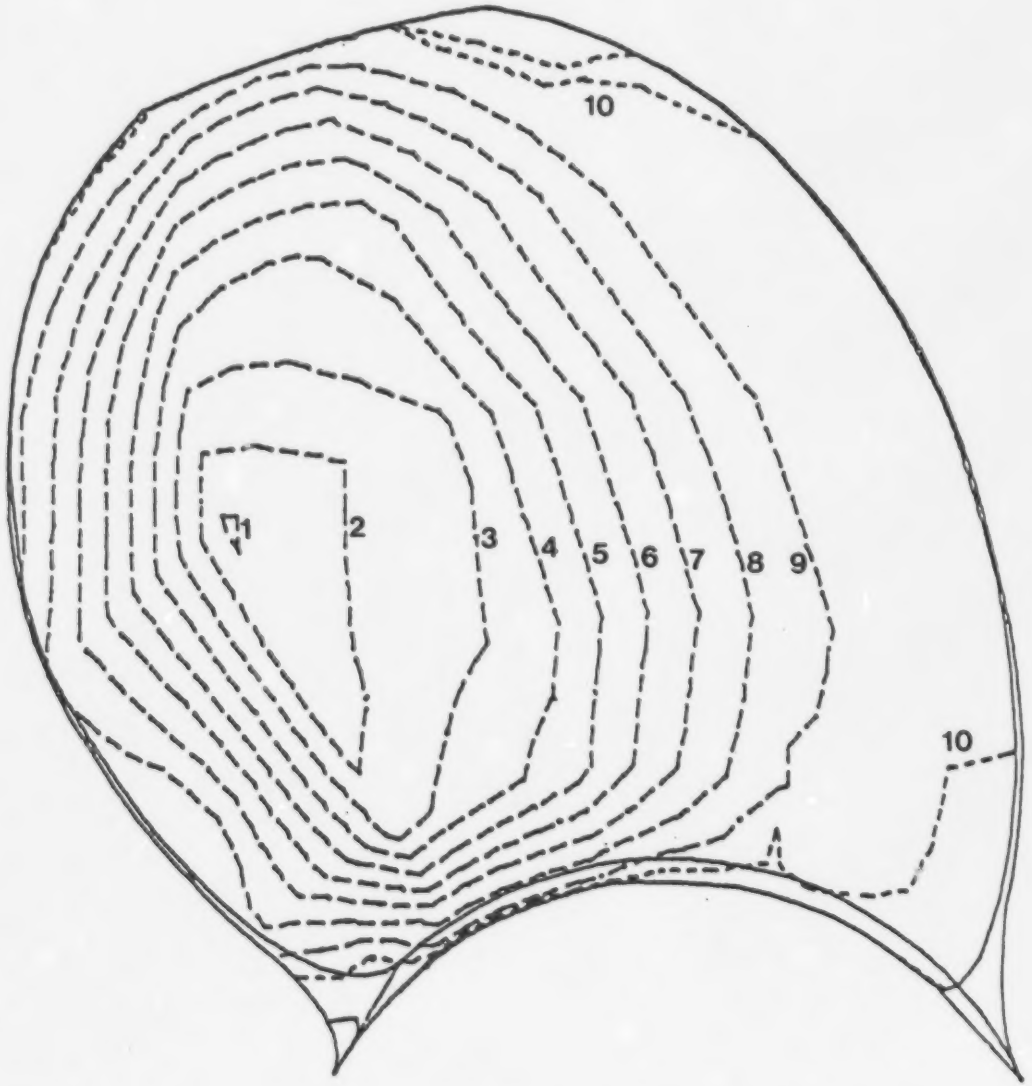

SECOND PRINCIPAL
STRESS CONTOURS
(STATIC ANALYSIS)

STRESS LEVELS

CODE	STRESS
1	-49.5
2	-44.0
3	-38.5
4	-33.0
5	-27.5
6	-22.0
7	-16.5
8	-11.0
9	-5.5
10	0.0
11	5.5
12	11.0

532.445 MM.

FIGURE 6.12 LOAD CASE L3-10

towards the tip and near the trailing edge although the stresses near the blade root area still remain high.

In order to investigate the effects of friction, loading case L3 was repeated for coefficients of friction equal to 0.1 and 0.4. Table 6.4 shows the variation in results due to friction effects. The stress contour plots corresponding to three loading conditions (L3-01, L3-05 and L3-10) where friction effects are included, can be seen in Figures 6.13, 6.14 and 6.15, respectively. It should be noted that a coefficient of friction equal to 0.10 is probably more realistic for the propeller-ice interaction problem, and the other case with the coefficient of friction equal to 0.40 should be considered as rather extreme. It will be seen that even under this case, the effect on stresses and deflections is not very significant.

In order to investigate the effects of dynamic loading on the blade, the loads generated under load case 3 were applied in the form of dynamic load based on the propeller speed of 141 RPM. The dynamic analysis was carried out by modal superposition method and the first 10 natural frequencies were included in evaluating the response. These frequencies are listed in Table 6.5. The maximum response occurs at time t equal to 0.069 sec after the propeller-blade enters the ice-block and this is more or less the same position in which the maximum static response is produced in the blade. The dynamic factor is found to be in the order of 1.20. From the stress contour plot (Figure 6.16) corresponding to the time step at which maximum stress occurs, it will be seen that the location of maximum stress and the nature of stress variation remains similar to the stress contours obtained in the case of corresponding static load case. It should be noted that the hydrodynamic added mass has not been accounted for in this analysis. The presence of the ice block significantly alters fluid flow around the propeller and must be reliably accounted for when studying hydrodynamic added mass effects.

The results presented in this section were carried out for a uniform pressure of 1.0 MPa. In a typical propeller-ice interaction loading definition, the value of pressure would be taken as the crushing strength of the ice. Consequently, the stresses in the blade corresponding to a particular loading condition can be obtained by simply multiplying the stresses obtained under uniform pressure of 1.0 MPa, by the factor equal to the crushing strength of ice.

6.2 Analysis of Blade Passage Through Ice Using Detailed Definition of Propeller-Ice Interaction Forces

The finite element analyses of ice-block in contact with a propeller-blade has shown that the pressure-distribution on the blade is not uniform (see Section 5.0). The effect of this detailed definition of the contact pressure distribution upon the stress levels and pattern upon the Pierre Radisson/Franklin blade were investigated. The dynamic loads were generated using the program PVICE taking uniaxial ice crushing strength equal to 6.0 MPa. As mentioned already, the propeller-ice interaction

TABLE 6.4

SUMMARY OF RESULTS FOR LOADING CASE L4
INCLUDING FRICTION

Loading Case	Coefficient of Friction	Uniform Pressure = 1.0 MPa				
		F_X (MN)	F_Y (MN)	F_Z (MN)	Maximum Deflection (MM)	Maximum Stress (MPa)
L3-01	0.0	-0.097	-0.024	-0.263	-1.170	-41.1
	0.10	-0.117	-0.042	-0.257	-1.194	-41.3
	0.40	-0.177	-0.097	-0.239	-1.159	-42.1
L3-05	0.0	-0.434	0.185	-1.257	-4.834	-175.0
	0.10	-0.554	0.168	-1.215	-4.92	-179.0
	0.40	-0.915	0.115	1.09	-5.18	-193.0
L3-10	0.0	-0.026	0.091	-0.265	-1.581	-49.9
	0.10	-0.046	0.108	-0.255	-1.596	-49.9
	0.40	-0.107	0.157	-0.227	-1.642	-50.0

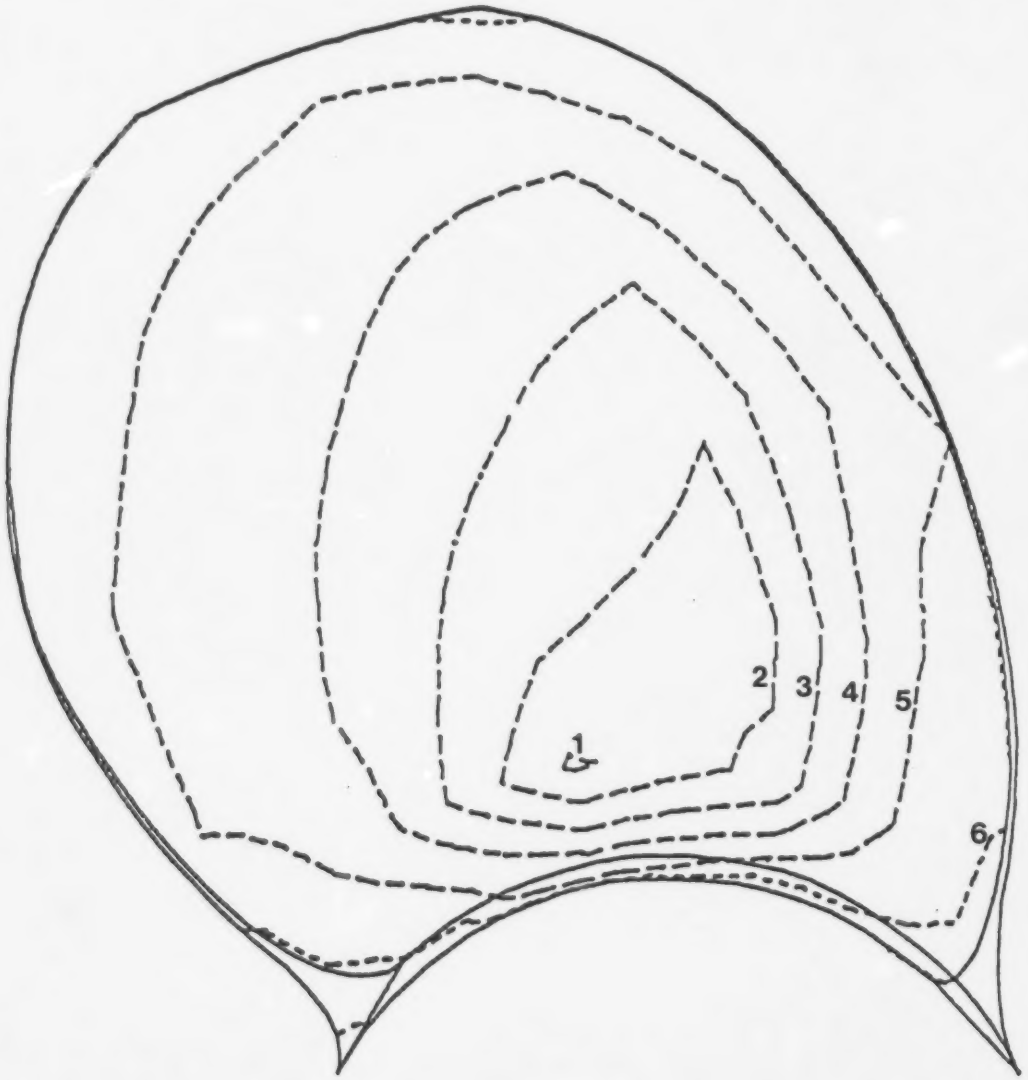

SECOND PRINCIPAL
STRESS CONTOURS
(STATIC ANALYSIS)

STRESS LEVELS

CODE	STRESS
1	-41.25
2	-33.0
3	-24.75
4	-16.5
5	-8.25
6	0.0

532.445 MM.

FIGURE 6.13 LOAD CASE L3-01 WITH COEFFICIENT OF FRICTION = 0.40

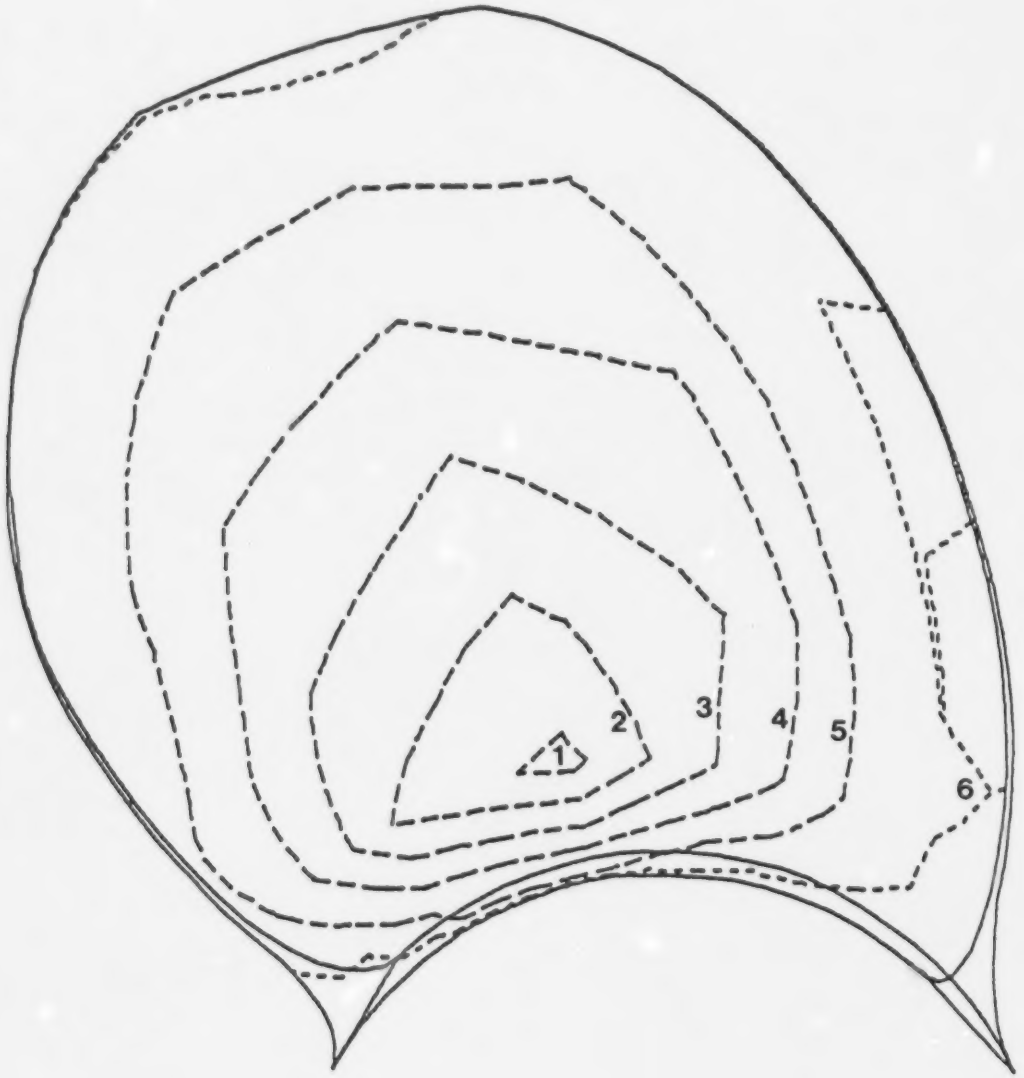

SECOND PRINCIPAL
STRESS CONTOURS
(STATIC ANALYSIS)

STRESS LEVELS

CODE	STRESS
1	-177.5
2	-142.0
3	-106.5
4	-71.0
5	-35.5
6	0.0
7	35.5

532.445 MM.

FIGURE 6.14 LOAD CASE L3-05 WITH COEFFICIENT OF FRICTION = 0.40

SECOND PRINCIPAL
STRESS CONTOURS
(STATIC ANALYSIS)

STRESS LEVELS

CODE	STRESS
1	-49.2
2	-41.0
3	-32.8
4	-24.6
5	-16.4
6	-8.2
7	0.0
8	8.2

532.445 MM.

FIGURE 6.15 LOAD CASE L3-10 WITH COEFFICIENT OF FRICTION = 0.40

TABLE 6.5

NATURAL FREQUENCIES OF BLADES

Mode Number	Frequency (CPS)
1	121.39
2	224.50
3	324.38
4	445.52
5	470.82
6	576.84
7	638.24
8	820.26
9	954.17
10	1,016.27

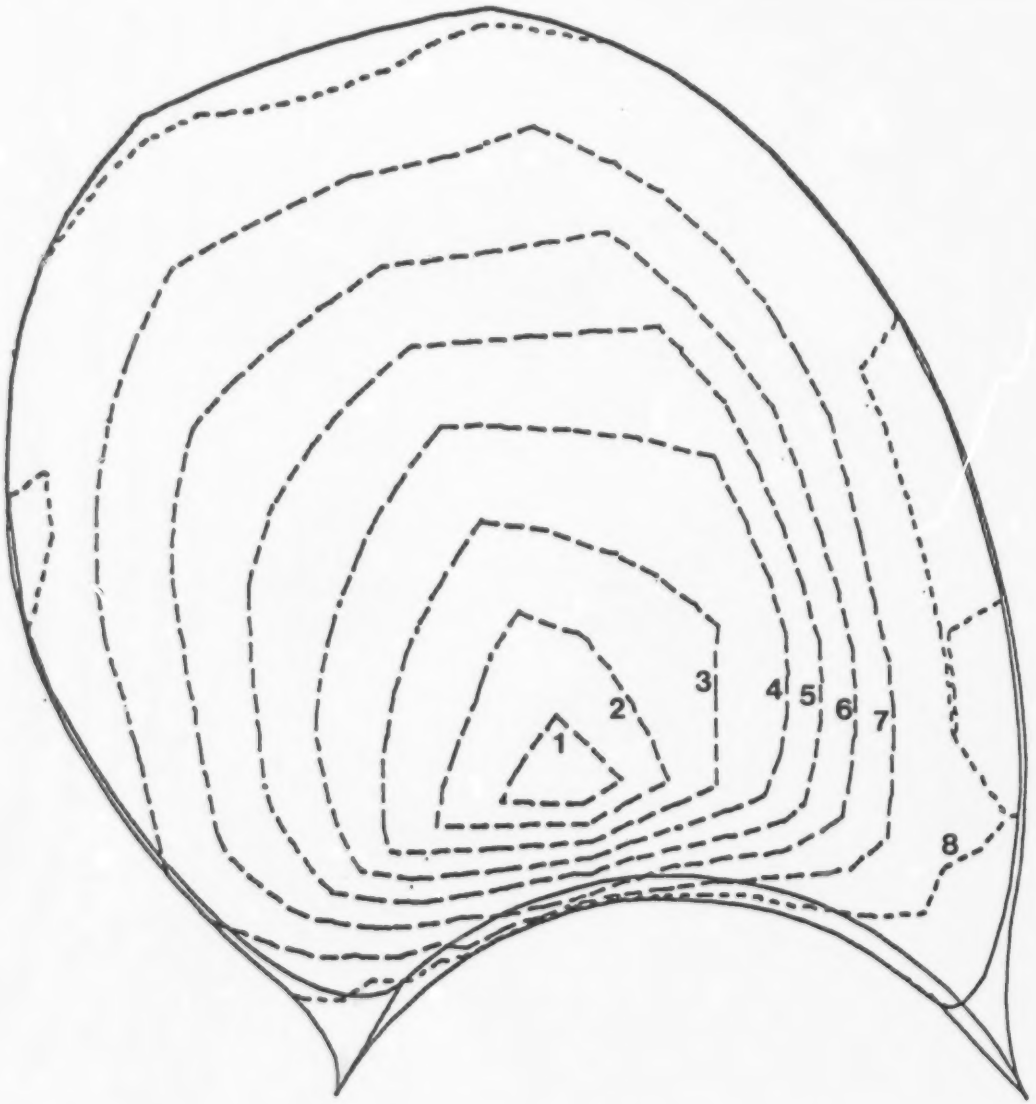

SECOND PRINCIPAL
STRESS CONTOURS
(DYNAMIC ANALYSIS)

TIME STEP 7
0.069 SU

STRESS LEVELS

CODE	STRESS
1	-203.
2	-174.
3	-145.
4	-116.
5	-87.
6	-58.
7	-29.
8	0.
9	29.

532.445 MM.

FIGURE 6.16 DYNAMIC LOAD CASE - L3

phenomenon is a dynamic one and this value of ice-strength is consistent with the ice unconfined uniaxial compressive strength obtained experimentally when sea-ice is subjected to a high strain rate (see Section 4.4). The loads were derived based on the propeller speed of 141 RPM and the cutting radius of 0.5 R which corresponds to the load case L3 (Section 6.1). As before, the dynamic analysis using the revised form of loading was carried out by modal superposition method and the first 10 natural frequencies were included in evaluating the response.

PVICE was executed for ship speeds ranging from 2.5 to 17.5 knots and propeller RPM equal to 141. The effect of ship speed on peak ice induced thrust (herein defined as being positive in the +Z direction, i.e. aft) is shown in Figure 6.17. The change in direction of thrust as the ice load shifts from the face of the blade to the back of the blade is indicated. It is also seen that the ice load on a shadowed blade is negligible in the low ship speed range, which is consistent with the definition of W_2 (Figure 3.9).

The nature of variation of dynamic thrust for a ship speed of 2.5 knots produced by PVICE for the detailed definition of interaction pressure for the nonshadowed blade is shown in Figure 6.18. Also shown is the variation of dynamic thrust based on uniform pressure distribution of 6.0 MPa. As can be seen, the loads based on a uniform pressure distribution are significantly greater than those based on the detailed definition of the interaction pressure. As will be shown in the following section the forces based on the latter are reasonably close to those observed in field tests. Thus the assumption of uniform pressure distribution equal to the unconfined uniaxial compressive strength of ice is likely to lead to unduly high forces, much greater than the forces encountered in the real situation.

A VAST analysis was performed for the blade subjected to the nonshadowing loading case, at a ship speed of 2.5 knots. The resulting displacement variation of the blade surface in the direction of shaft axis (i.e. Z direction) under the interaction pressures is presented in Figures 6.19 and 6.20; and the variation of displacements in the direction normal to the shaft-axis in the horizontal plane (i.e. X-direction) is presented in Figure 6.21. Under the uniform pressure distribution of load case L3 (Section 6.1), the maximum deflection in the Z-direction occurred at node 79, i.e. at the trailing edge of the blade. With the detailed definition of pressure, the maximum Z deflection occurs at node 71 which is located at the leading edge of the blade. This clearly indicates the effect of concentration of interaction forces at the leading edge.

The plots of maximum principal stress (tensile) and minimum principal stress (compressive) for the detailed pressure loading are presented in Figures 6.22 and 6.23, respectively. The latter figure may be compared with Figure 6.16 which shows the minimum principal stress contour plot obtained assuming uniform pressure distribution. It is seen that principal stresses attain the maximum value near the blade root area. If

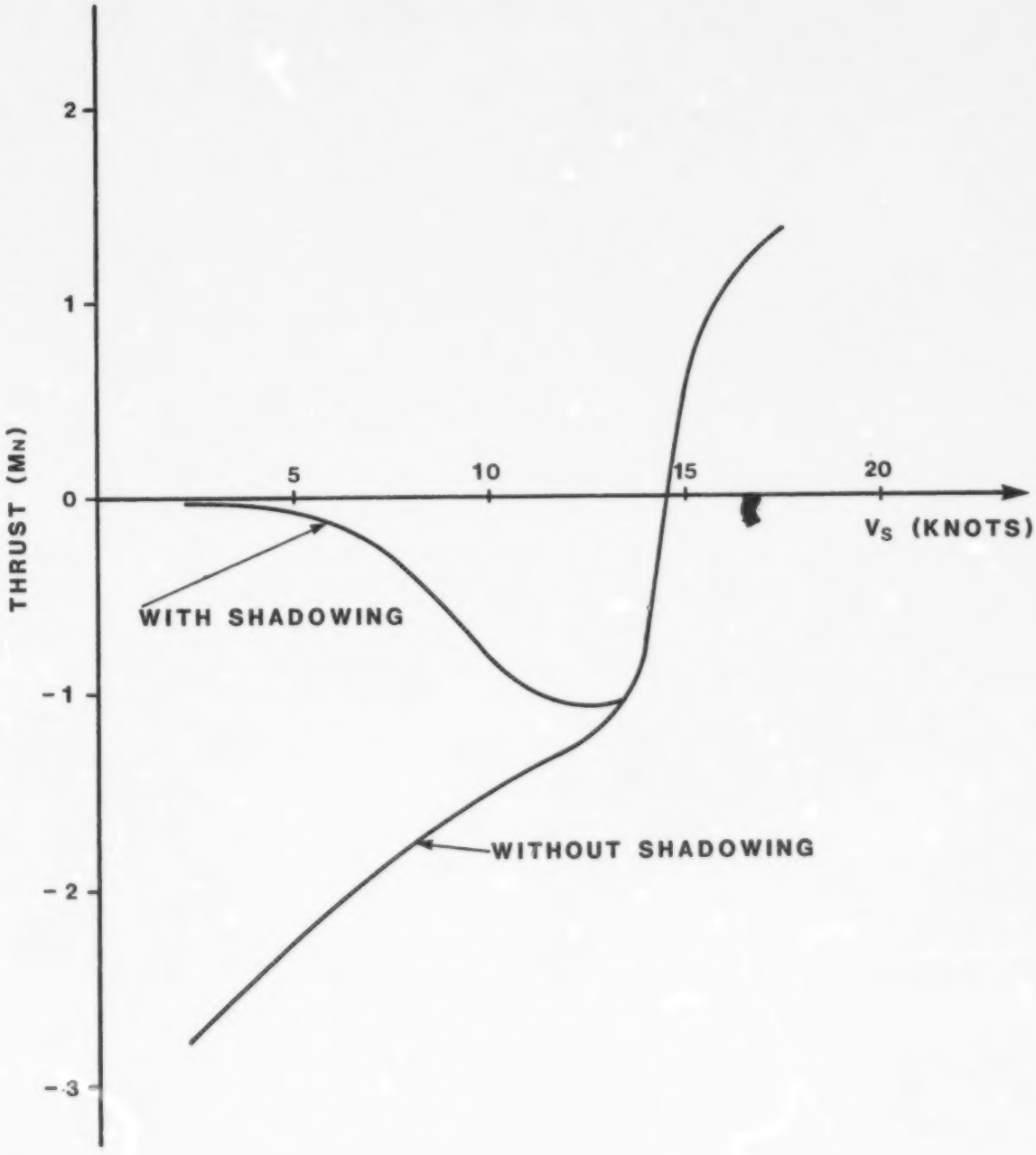

FIGURE 6.17 BLADE THRUST VERSUS SHIP SPEED (CONSTANT 141 RPM)

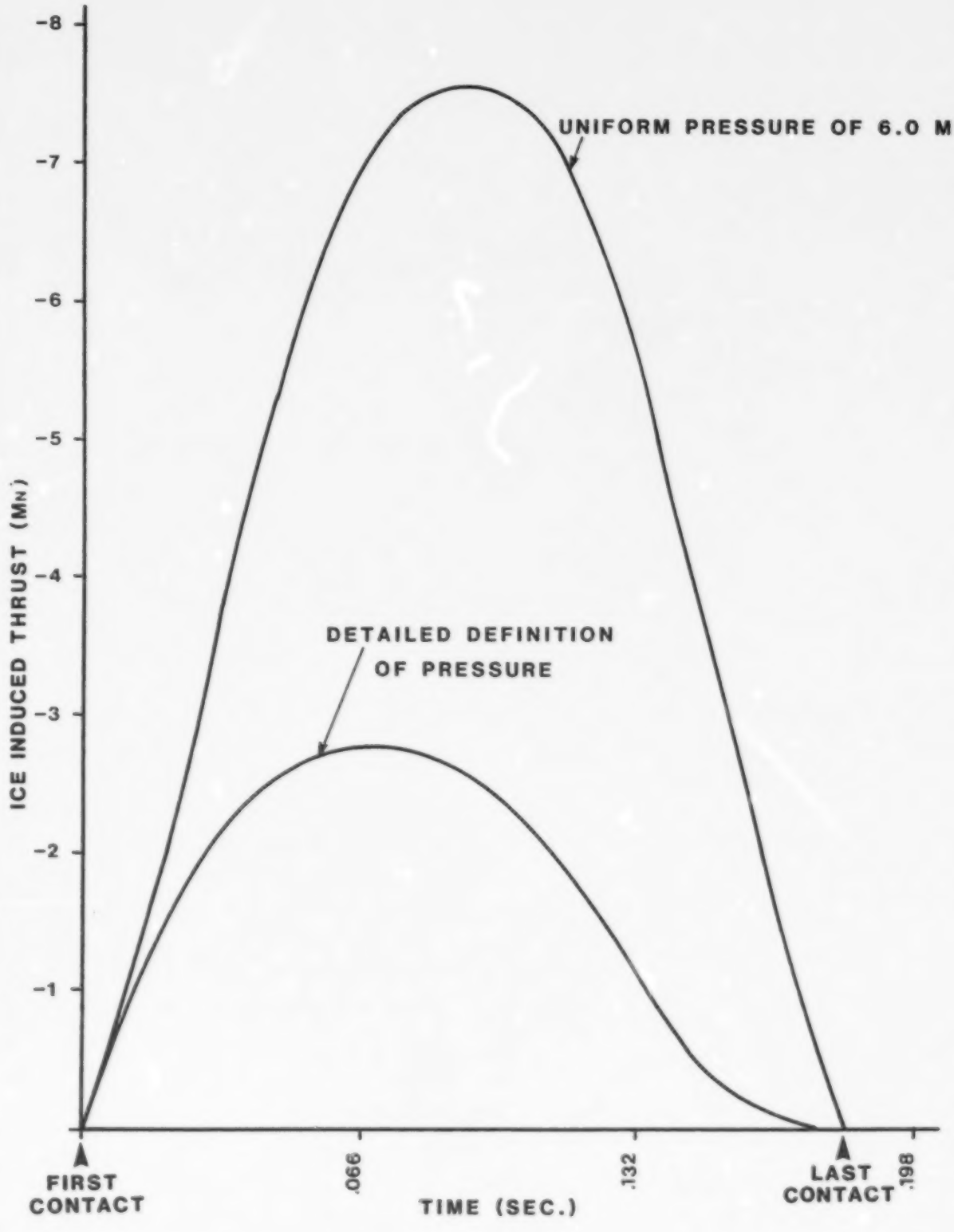

FIGURE 6.18 DYNAMIC ICE THRUST TIME HISTORY (UNSHADOWED BLADE)

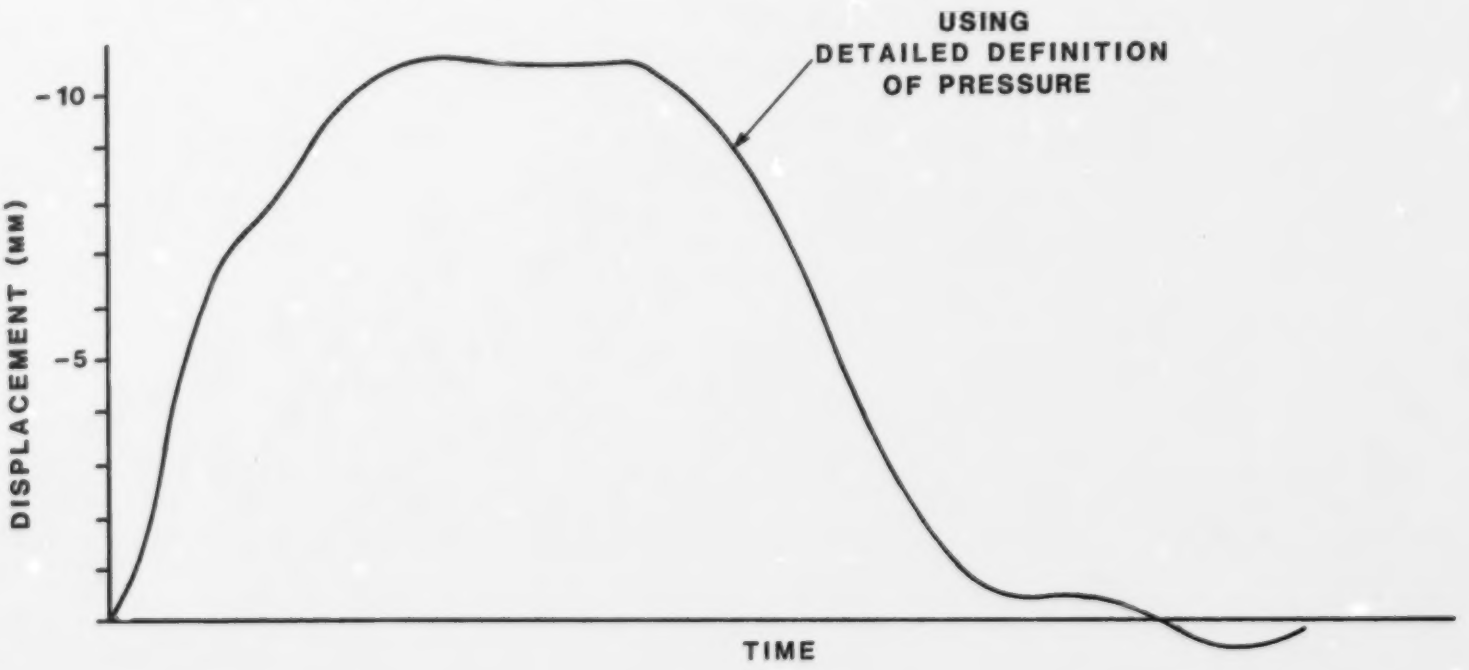

FIGURE 6.19 DYNAMIC DISPLACEMENT (Z-COMPONENT) AT NODE 71 (LEADING EDGE AT BLADE TIP FOR MODEL SHOWN IN FIGURE 6.1)

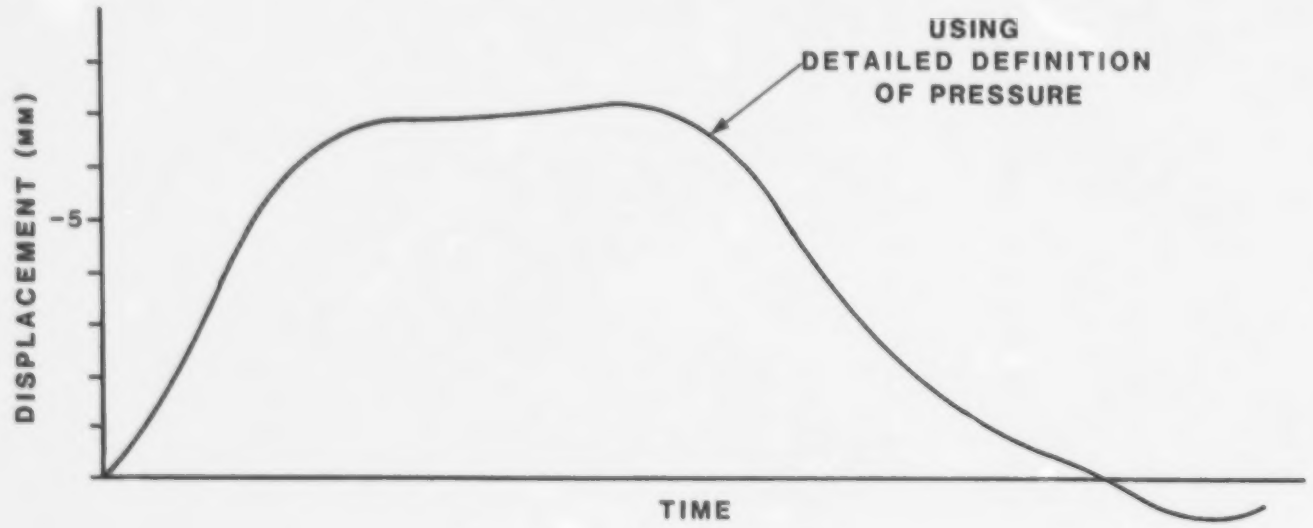

FIGURE 6.20 DYNAMIC DISPLACEMENT (Z-COMPONENT) AT NODE 79
(TRAILING EDGE AT BLADE TIP FOR MODEL SHOWN IN FIGURE 6.1)

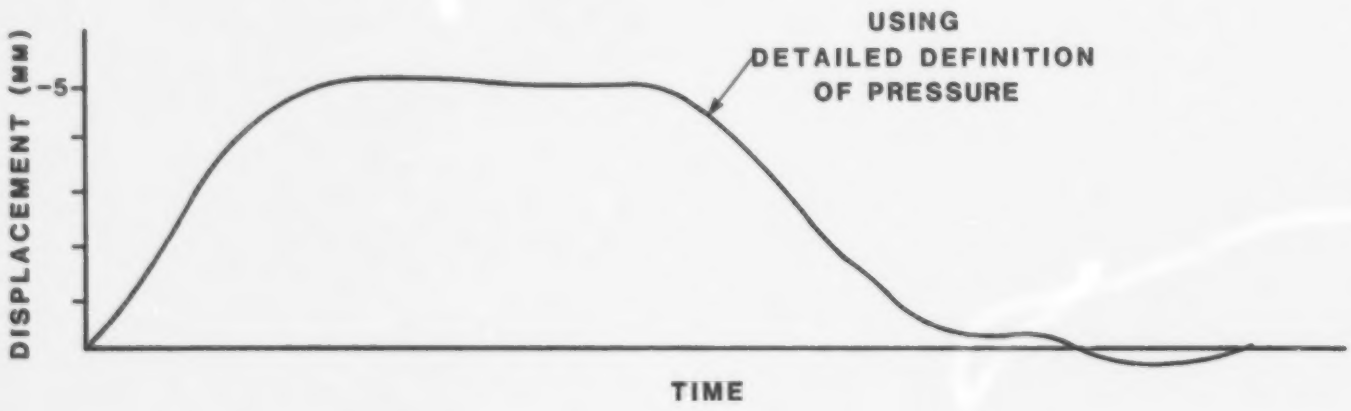

FIGURE 6.21 DYNAMIC DISPLACEMENT (X-COMPONENT) AT NODE 71 (IN MODEL SHOWN IN FIGURE 6.1)

TENSILE PRINCIPAL
STRESS CONTOURS
(DYNAMIC ANALYSIS)

TIME STEP 5
0.0492 SEC

STRESS LEVELS

CODE	STRESS
1	5.000E+01
2	1.000E+02
3	1.500E+02
4	2.000E+02
5	2.500E+02
6	3.000E+02

FIGURE 6.22 DYNAMIC STRESSES - DETAILED DEFINITION OF PRESSURE

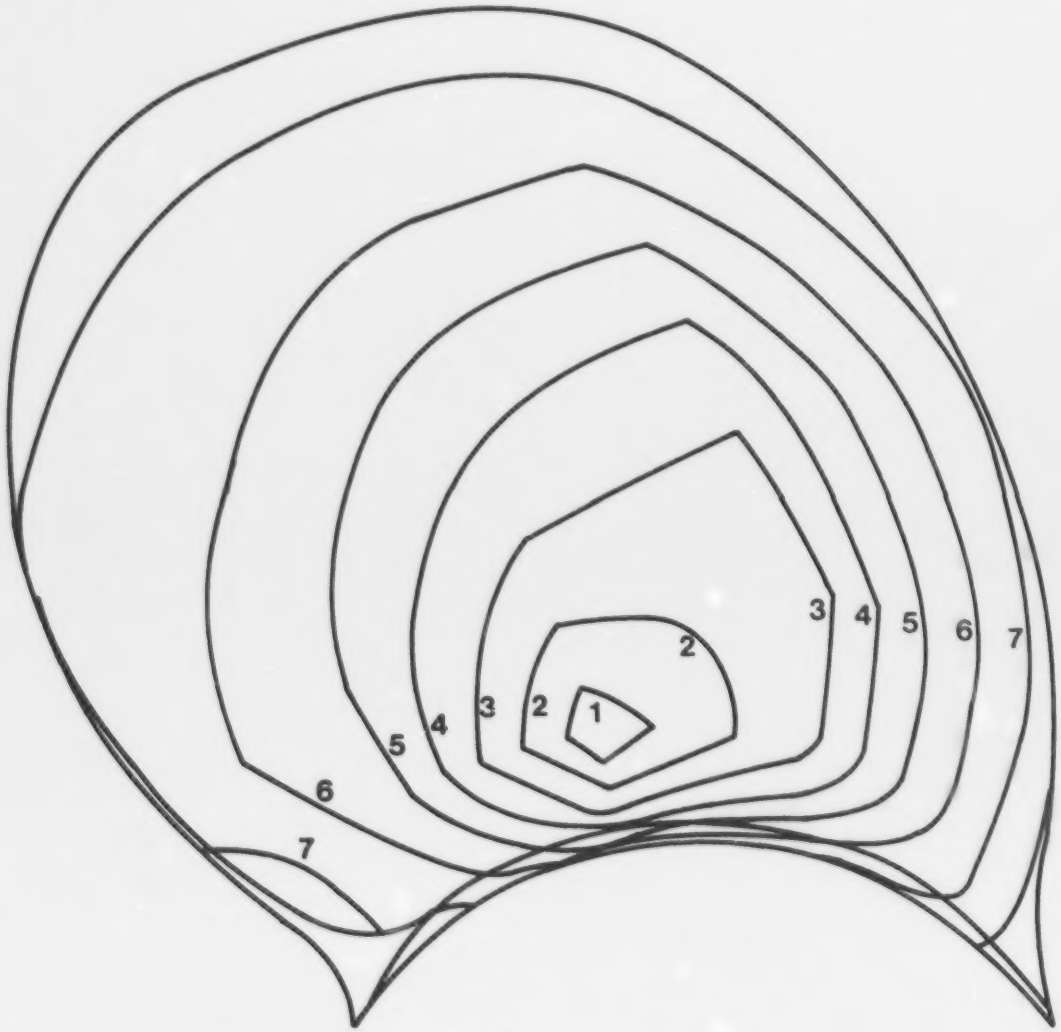

COMPRESSIVE PRINCIPAL
STRESS CONTOURS
(DYNAMIC ANALYSIS)

TIME STEP 5
0.0492 SEC

STRESS LEVELS

CODE	STRESS
1	-3.500E+02
2	-3.000E+02
3	-2.500E+02
4	-2.000E+02
5	-1.500E+02
6	-1.000E+02
7	-5.000E+01

FIGURE 6.23 DYNAMIC STRESSES - DETAILED DEFINITION OF PRESSURE

the stress values obtained under the uniform pressure are multiplied by the factor 6.0, it will be seen that very high stress levels are predicted for the blade. However, the magnitudes of principal stresses estimated using the detailed definition of interaction pressures are close to the yield stress of the material used for the Pierre Radisson propeller blade (350 MPa). The Radisson sister ship, Franklin, sustained broken propeller blades while operating in the Arctic ice in the 1979 season. Metallurgical tests on the failed propeller showed the 0.2% yield stress of 250 MPa, considerably lower than the reported anticipated stress levels [116]. It is worthwhile to mention that the region of high stress concentration indicated by the present analysis coincides with the actual line of failure observed from the photographic records [116].

6.3 Comparison with Measured Results

In order to validate the computer procedure developed under this contract, comparisons were made between predicted thrust and torque with the available experimental data. It must be pointed out that the suitable data is scarce in the open technical literature and whatever that is available is full of uncertainties and unknowns. In some recent papers [116, 127 and 10], the authors have presented the measured data gathered on CCGS Pierre-Radisson/Franklin concerning the forces exerted on the propeller during various ice encounters. However, the data lacks certain information such as the actual depth of cut during various encounters, or ship speed during the incident. Furthermore the crushing strength and the tensile strength of the ice encountered is not known and at best can only be assumed to be based on the ice strength data related to multi-year Arctic ice that is available elsewhere.

Using the Pierre Radisson/Franklin propeller blade configuration with the PVICE (detailed ice pressure) model, the propeller-ice interaction thrust, bending moment, and the torque were obtained for a range of ship speeds for three different propeller RPM, i.e. 90, 130 and 170. In order to ensure that the limiting cases are covered, extreme values of ship speed are used, e.g. very low ship speed is taken equivalent to ship speed being zero; and at the other extreme, very high ship speed is accounted for by adopting ship speed values greater than the normal speed of operation in ice infested water. The uniaxial ice-strength was taken as 6.0 MPa, and a cutting depth of 1 m was used.

The variation of thrust, torque and bending moment against the variation in angle of attack (at 0.7 radius) are presented in Table 6.6 and Figures 6.24 to 6.26 for a blade speed of 130 RPM. Recall that from the instance the blade enters the ice block until it leaves it, the forces exerted on the blade vary in magnitude, with maximum value generally occurring at some intermediate position (see Figure 6.18). The peak values of the dynamic forces are dependent upon the angle of attack, (α). From these plots, it can be seen that although the variation in α during the normal operating conditions is within a narrow limit of about $\pm 20°$, the forces exerted on the blade are a strong function of its value. With near zero angle of attack, the axial load, bending moment

TABLE 6.6

GENERALIZED FORCES ON PROPELLER-BLADE
BLADE RPM = 130

Ship Speed		Angle of Attack (α) at 0.7 Radius		Maximum		
Knots	mm/sec	Rad.	Degrees	Thrust (SFZ) KN	Torque (SMZ) KN-M	Bending Moment (SMX) KN-M
0	0	0.359	21	-3,190	1,650	-4,650
2.5	1,285	0.294	17	-2,790	1,500	-4,120
7.0	3,600	0.177	10	-1,950	1,240	-2,870
9.7	5,000	0.108	6	-1,510	1,090	-2,230
13.6	7,000	0.015	1	474	214	645
16.5	8,500	-0.052	-3	1,440	-237	2,100
19.5	10,000	-0.115	-7	2,000	-459	2,910
24.3	12,500	-0.211	-12	2,650	-780	3,870
29.2	15,000	-0.297	-17	3,040	-993	4,450

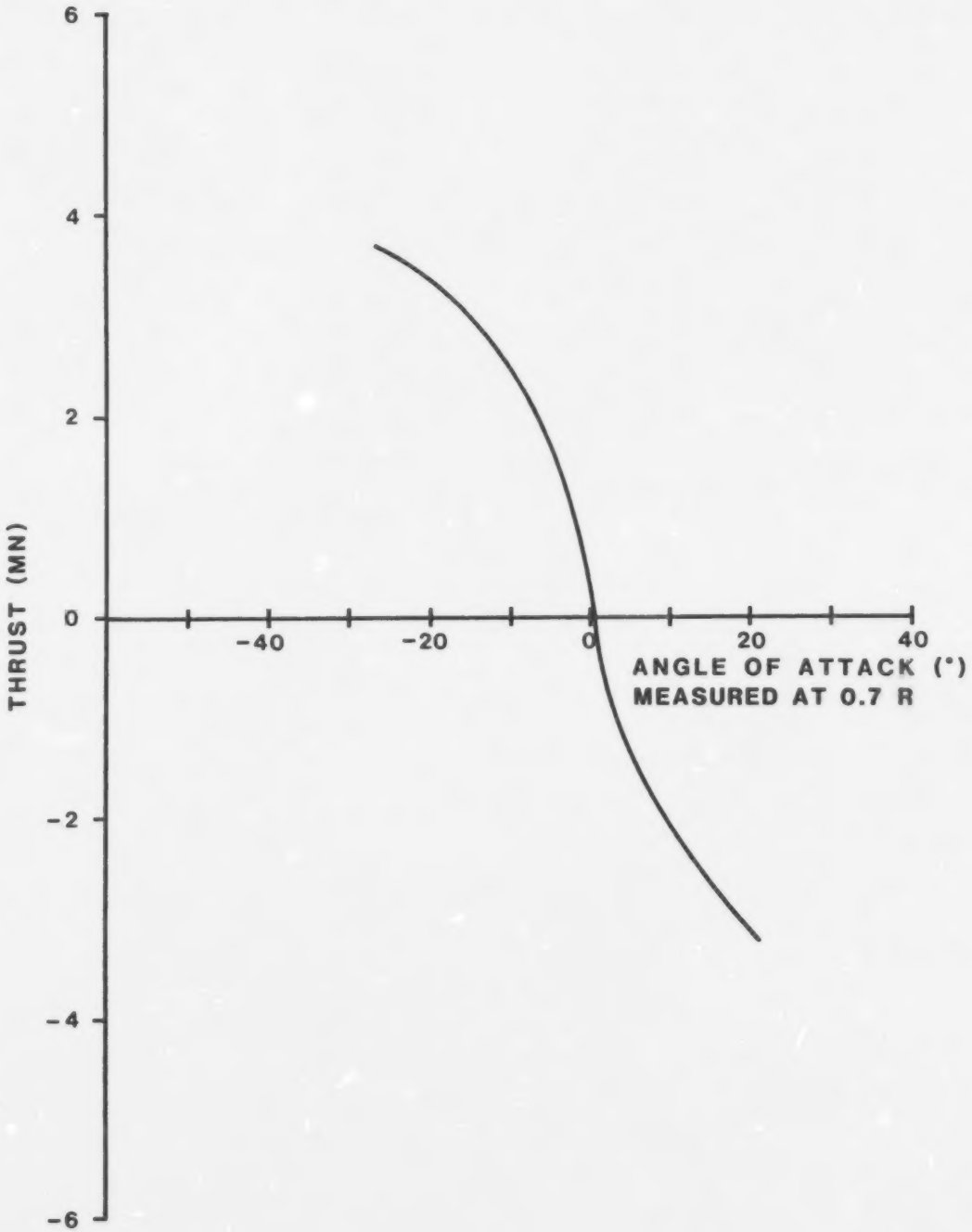

FIGURE 6.24 PEAK THRUST VERSUS ANGLE OF ATTACK - 130 RPM

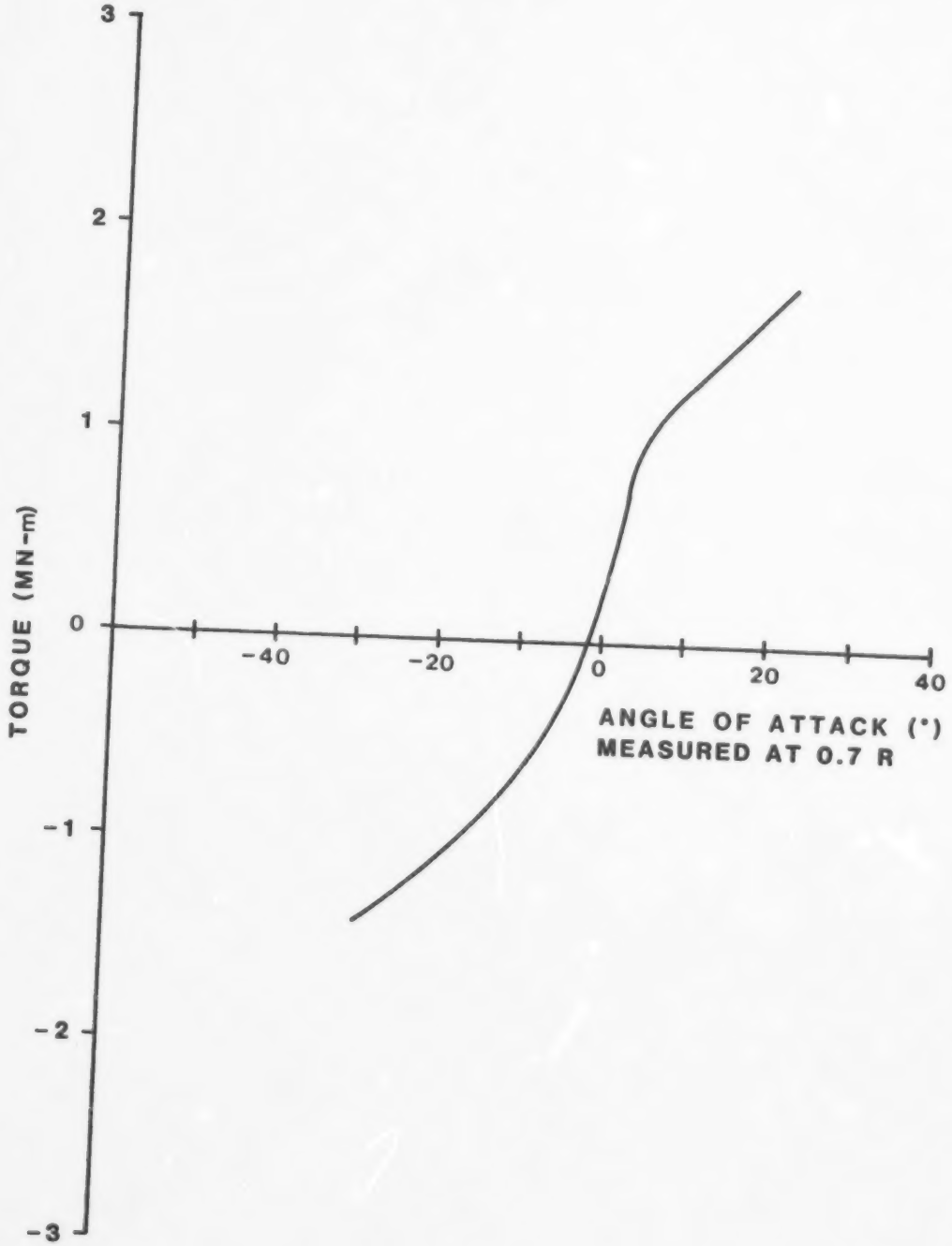

FIGURE 6.25 PEAK TORQUE VERSUS ANGLE OF ATTACK - 130 RPM

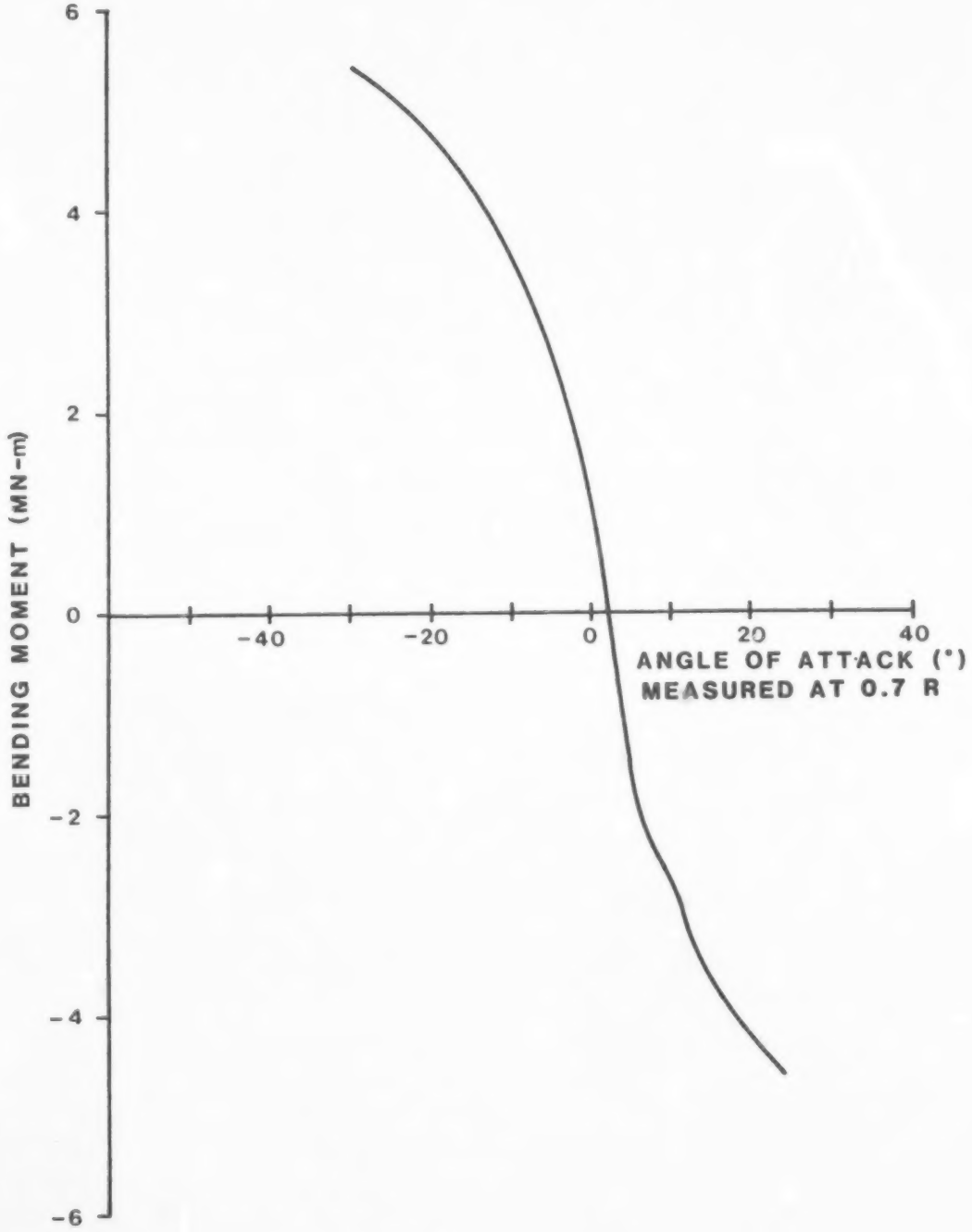

FIGURE 6.26 PEAK BENDING MOMENT VERSUS ANGLE OF ATTACK - 130 RPM

and torque are small. However, a small deviation from zero in the angle of attack tends to produce significantly greater loads on the blade. This predicted relationship between blade forces and angle of attack is well supported by experiment [124, 128 and 129].

Figures 6.27 and 6.28 show a comparison between measured and predicted peak milling loads for CCGS Pierre Radisson. The measured values were obtained from Reference [127], where it is suggested that the cutting depth was in the range of 0.5 to 1.25 meters. Corresponding ship speeds for this data were not established. The predicted values shown are for a cutting depth of 1 m and a ship speed of 7 knots.

The comparison between predicted and measured results shown in Figures 6.27 and 6.28 is encouraging. However, it is obvious that further validation of the computer procedure is necessary. Correlation based on results from more controlled and precise measurements (full scale and/or model) are required in order to properly calibrate the procedure for use in establishing ice class rules.

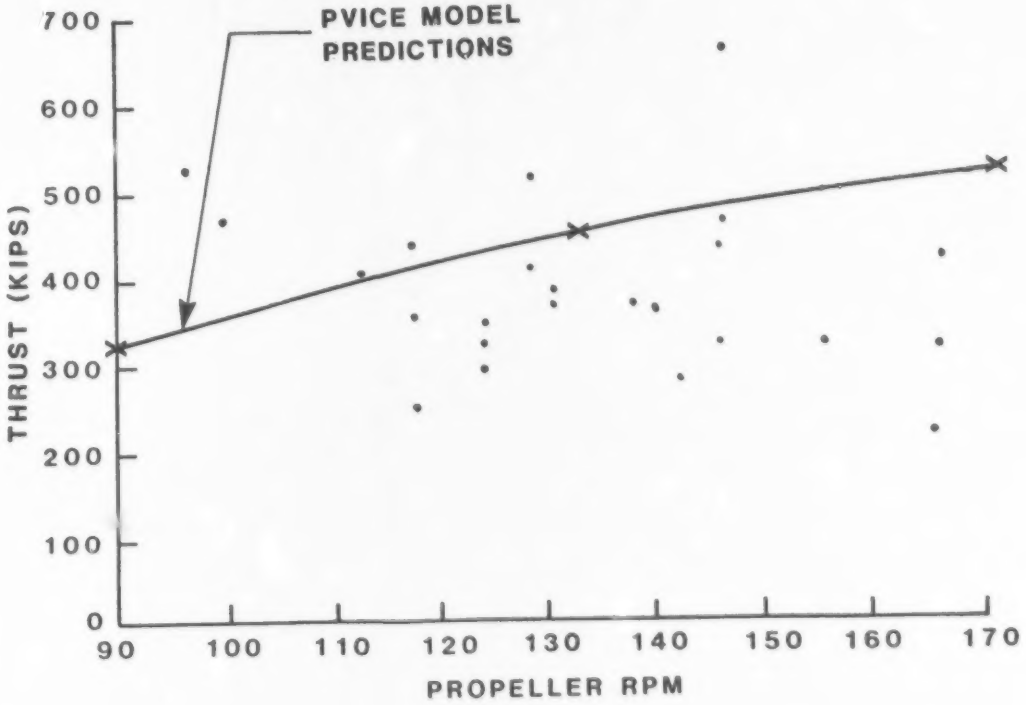

FIGURE 6.27 PREDICTED VERSUS MEASURED THRUST FOR CCGS PIERRE RADISSON PROPELLER

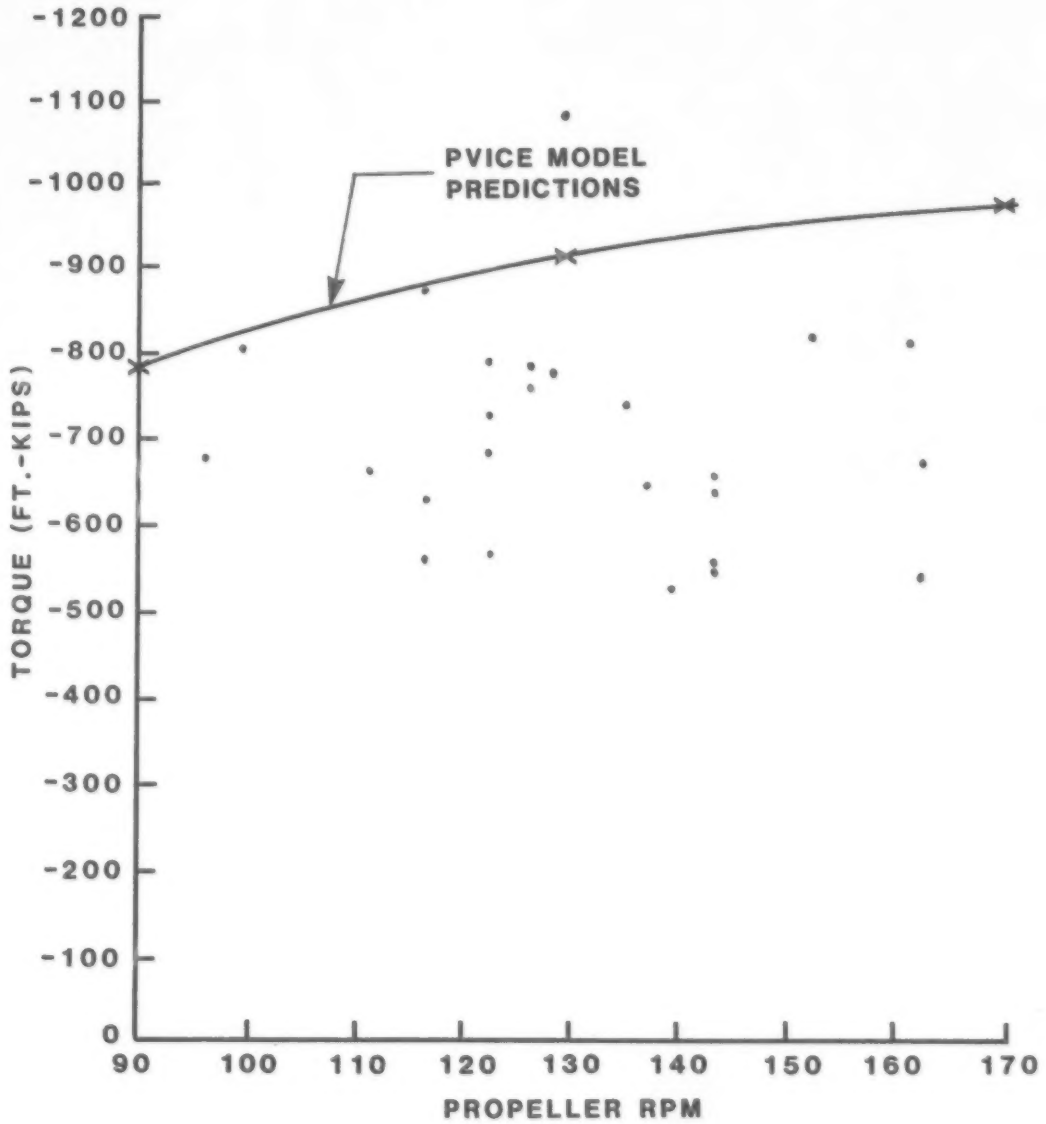

FIGURE 6.28 PREDICTED VERSUS MEASURED TORQUE FOR CCGS PIERRE RADISSON PROPELLER

7.0 CONCLUSIONS AND RECOMMENDATIONS FOR FUTURE WORK

The work presented in this report represents the second phase in a program of study to investigate propeller responses to ice interaction pressures using the finite element method. In this work, the finite element method has been applied to model the ice block as well as the propeller blade with the aim of determining improved estimates of operational ice loads.

The utilization of numerical techniques based on the finite element method for these investigations has helped to develop some interesting insights into the complex physical processes taking place during propeller-ice interactions.

At high rates of loading, representative of the propeller-ice interaction process, ice displays brittle characteristics in the form of microcracking damage and irreversible deterioration of mechanical properties. Strain softening is one manifestation of these physical properties.

A literature search has identified several different alternative brittle material models developed for numerical simulation purposes which reproduce these physical characteristics and one of these, a smeared-crack damage material model available within the ADINA finite element code, was adopted.

Some difficulties were encountered in locating suitable data defining the above-mentioned material characteristics for ice with sufficient detail and reliability.

Validation of the numerical approach being proposed involved the analysis of two-dimensional indentation problems for several different indentor geometries including rectangular, wedge, circular and elliptical shapes under idealized conditions of plane stress and plane strain.
The results of these simulations show that the pressure distribution is not uniform and its form is very much dependent on the indentor shape.

A comparison of computed forces to full scale and laboratory experimental results was performed for the limited cases available. Reasonable agreement has been obtained considering the uncertainties about the degree of agreement between the material model adopted for numerical simulation purposes with the ice employed in experiments.

One of the advantages of the numerical simulations over experimental measurements is the ability of the numerical model to assess sensitivities with respect to material constant inputs. Although force resultants from numerical simulations are primarily dependent on uniaxial (unconfined) compressive strength of ice, they have also been shown to depend on other mechanical properties such as tensile strength, failure surface definition and the stress-strain relationship.

Careful monitoring of solution progress throughout the simulations was required. As the zone of ice microfracturing progressively developed, the prescribed incremental displacement loading had to be continuously adjusted in accordance with the amount of material experiencing stress conditions near the microfracturing failure thresholds.

Numerical results for two-dimensional pseudo-static milling simulations were obtained as well as associated pressure distributions along the contact surface. Plane stress and plane strain conditions were considered. A number of different cutting angles and widths were analyzed. Plots of contact force versus cutting angle which were constructed show clearly a rapid increase in milling force with decreasing cutting angle.

The Martec/TDC propeller ice interaction load determination model, called PVICE, applies two dimensional finite element results to propeller strips at constant radius in order to establish propeller loads associated with the propeller-ice interaction process.

The PVICE model was applied to determine the response of a CCGS Pierre Radisson Franklin propeller blade in its passage through an ice block.

The effect of a detailed (non-uniform) pressure distribution upon dynamic loads, displacements, stress levels and patterns was investigated for the Pierre Radisson/Franklin blade and compared with the uniform pressure loading. The loads based on the detailed definition of the interaction pressure were significantly less than those based on a uniform pressure distribution (equal to uniaxial crushing strength of ice). Blade principal stress levels estimated using the detailed definition of interaction pressures occur near the blade root area.

As a validation of the computer procedure developed for the analysis of the propeller-ice interaction process, comparisons were made between predicted thrust and torque with available data for a range of ship speed and propeller RPM. Variation of thrust, torque and bending moment against variation in angle of attack were investigated. It was shown that peak values of dynamic force are critically dependent on angle of attack. This predicted relationship is well supported by experiments. A comparison was made between measured and predicted peak milling loads (thrust and torque). The results are reasonable considering the assumptions made in modelling the ice properties and propeller loading configuration.

It is evident from the results that a useful modelling framework has been developed to analyze propeller-ice interaction problems. To establish more clearly the confidence that one can place on the results, it is recommended that further work be carried out as follows:

- Determine additional information on ice material properties to better define both the stress-strain curve and the failure surface appropriate for ice loaded at high strain rates;

- Perform indentation tests under more controlled conditions such that the physical constants of ice are better defined;

- Acquire better data on propeller-ice tests to assist in obtaining forces (hence, thrust, torque and bending moments) and stresses for a wide range of parameter variations (eg. ship speed, propeller RPM cutting depth);

- Further development of numerical procedures to establish more accurately the pressure distribution curves and contact forces, specifically

  a. Improved ice block models to handle a wide variety of cutter and indenter shapes;

  b. Perform analyses with various uniaxial ice crushing and tensile strength values (σ_c and σ_t) to determine, for example, the effect of the σ_c/σ_t ratio;

  c. Investigate methods for quantifying extrusion processes;

  d. Establish the sensitivity of the model responses to variations in stress-strain curve;

  e. Consider the effect of the shear reduction factor.

- Further improvement of the ice interaction force definition in program PVICE in order to

  a. Incorporate more realistic pressure and force curves which could reflect more accurately, blade section shape, σ_c/σ_t effect and other parameters;

  b. Include the effect of strain rate (to incorporate the two extremes, i.e., blade rotating at high RPM and shaft stopped resulting in "dragging mode");

  c. Extend to incorporate variable propeller speed (shaft slowed by ice interaction);

  d. Include the capability to handle additional milling configurations of the blade relative to the ice block.

REFERENCES

1. M.E. NORWOOD, C.G. DesROCHERS and J.L. WARNER. Final Report on Propeller/Ice Interaction: A Parametric Study of Propellers Operating in an Ice Environment, Prepared for the Transport Development Centre, Report #TP4021E, Martec Limited (Dec. 1982).

2. M.E. NORWOOD, M.W. CHERNUKA and J.L. WARNER. Final Report on Propeller/Ice Interaction: An Investigation into the Problem of Predicting Propeller/Ice Interaction Forces, Prepared for the Transport Development Centre, Report #TP4022E, Martec Limited (Dec. 1982).

3. V.J. JAGODKIN. Analytical Determination of the Resistance Moment of a Propeller During Its Interaction with Ice, Problemy Arktiki i Antarktiki (Problems of the Arctic and Antarctic), Translated from Russian, Vol. 13, pp. 79-81 (1963).

4. M.A. IGNATJEV. The design of a propeller shaft of adequate strength for ice-going vessels (In Russian), Sudostrojenie (January 1959).

5. M.A. IGNATJEV. Determination of ice load encountered by ship propeller blades, Translated from Russian by the U.S. Dept. of Commerce, Office of Technical Services, Problemy Antiki i Antarktiki, No. 15, pp. 41-51 (1964).

6. M.A. IGNATJEV. Strength calculations for propeller blades of ice-breakers and ice-going vessels (In Russian), Sudostrojenie (January 1964).

7. M.A. IGNATJEV. Screw-propellers for Ships Navigating in Ice (In Russian). Textbook published by Sudostrojenie, Leningrad (1966).

8. M.A. IGNATJEV. Ship propellers for ice navigation vessels; features of design (In Russian). Leningrad: Izd-vo Sudostrojenie (1966).

9. M.A. IGNATJEV. Calculating the strength of screw propeller blades for ships used in ice navigation, Translation, Problemy Arktiki i Antarktiki, Vol. 16, pp. 75-82 (1976).

10. T. KOTRAS, D. HUMPHREYS, A. BAIRD, G. MORRIS and G. MORLEY. Determination of Propeller-Ice Milling Loads, pp. 336-343, Vol. 2, Proceedings of the Fourth International Offshore Mechanics and Arctic Engineering Symposium, American Society of Mechanical Engineers, New York (1985).

11. M.J. TOMIN, A. CORMEAU and J.J. JORDAAN. Development of Analytical Models Related to Experimental Work on Ice-Structure Interaction. Technical Report, Det norske Veritas (Canada) Ltd., Calgary, Alberta, 254 p. (Sept. 1985).

12. M.J. TOMIN, M. CHEUNG, I.J. JORDAAN and A. CORMEAU. Analysis of failure modes and damage processes of freshwater ice in indentation tests. Proceedings of the 5th International Offshore Mechanics and Arctic Engineering (OMAE) Symposium held on 13-18 April 1986 in Tokyo, Japan, Vol. 4, pp. 453-460 (1986).

13. M.E. NORWOOD, M.W. CHERNUKA and D.F. FANNING. Propeller Vibration and Stress Analysis by Finite Element Methods (PVAST): User's Manual. Martec Technical Report (December 1986).

14. O.C. ZIENKIEWICZ. The Finite Element Method, Third Edition, McGraw-Hill Book Company (UK) Limited (1977).

15. Vibration and Strength Analysis Program (VAST): User's Manual - Version #04, Martec Limited, Halifax (Dec. 1986).

16. F.U. HAUSLER. Multiaxial compressive strength tests on saline ice with brush-type loading platens. Proceedings of the IAHR International Symposium on Ice held at Quebec, Canada on 27-31 July 1981, pp. 526-539 (1981).

17. M.E. MERCHANT. Basic mechanics of the metal cutting process, Journal of Applied Mechanics, Trans. ASME, Vol. 11, No. 3, pp. A168-A175 (Sept. 1944).

18. M.E. MERCHANT. Mechanics of the metal cutting process: orthogonal cutting and a type-2 chip, Journal of Applied Mechanics, Vol. 16, No. 5, pp. 267-275 (1945).

19. E.H. LEE and B.W. SHAFFER. The theory of plasticity applied to a problem of machining, Journal of Applied Mechanics, Trans. ASME, Vol. 73, pp. 405-413 (Dec. 1951).

20. E. USUI and T. SHIRAKASHI. Mechanics of machining - from "descriptive" to "predictive" theory. In: "On the Art of Cutting Metals - 75 Years Later", Proceedings of the Winter Annual Meeting of the American Society of Mechanical Engineers in Phoenix, Arizona on 14-19 November 1982, Published by ASME, pp. 13-35 (1982).

21. K. IWATA, K. OSAKADA, Y. TERASAKA. Process modelling of orthogonal cutting by the rigid-plastic finite element method, Journal of Engineering Materials and Technology, Transactions of the ASME, Vol. 106, pp. 132-138 (April 1984).

22. M.E. NORWOOD. Analysis of Shell Structures by Curved Finite Elements, Canplan Oceanology Limited, Technical Report, Halifax (July 1974).

23. P. HOBBS. Ice Physics, Oxford, Clarendon Press, 837 p. (1974).

24. R. FREDERKING. Plane-strain compressive strength of columnar-grained and granular-snow ice. Journal of Glaciology, Vol. 18, No. 80, pp. 505-516 (1977).

25. B. MICHEL and N. TOUSSAINT. Mechanisms and theory of indentation of ice plates. Journal of Glaciology, Vol. 19, No. 81, pp. 285-301 (1977).

26. W.F. WEEKS and A. ASSUR. Fracture of Lake and Sea Ice, CRREL Research Report 269269, 77 p. (1969).

27. K. RISKA. On the Role of Failure Criterion of Ice in Determining Ice Loads, VTT (Technical Research Center of Finland), Ship Laboratory Report 7, 36 p. (March 1980).

28. B. MICHEL. The strength of polycrystalline ice. Canadian Journal of Civil Engineering, Vol. 5, No. 3, pp. 285-300 (Sept. 1978).

29. B. MICHEL. Advances in ice mechanics. POAC81, Proceedings of the Sixth International Conference on Port and Ocean Engineering Under Arctic Conditions held on 27-31 July, 1981, at Quebec City, Canada, pp. 189-204 (1981).

30. G.W. TIMCO and R. FREDERKING. Uniaxial compressive strength and deformation of Beaufort Sea ice, POAC83, Proceedings of the Seventh International Conference on Port and Ocean Engineering under Arctic Conditions held at Helsinki, Finland on 5-9 April, 1983. Vol. 1, pp. 89-98 (1983).

31. S.J. JONES. The confined compressive strength of polycrystalline ice, Journal of Glaceology, Vol. 28, No. 98, pp. 171-177 (1982).

32. N.K. SINHA. Uniaxial compressive strength of first-year and multi-year sea ice. Presented at the 6th Can. Hydrotech. Conf., Canadian Society of Civil Engineering, 2-3 June 1983. Also published in Canadian Journal of Civil Engineering, Vol. 11, No. 1, pp. 82-91 (1984).

33. Y.C. FUNG. Foundations of Solid Mechanics. Prentice-Hall Inc., Englewood Cliffs, New Jersey (1965).

34. O.C. ZIENKIEWICZ. The Finite Element Method. McGraw-Hill Book Company (UK) Limited, London (1977).

35. B. VENKATRAMAN and S.A. PATEL. Structural Mechanics with Introductions to Elasticity and Plasticity. McGraw-Hill Book Company, New York (1970).

36. K.-J. BATHE. Finite Element Procedures in Engineering Analysis. Prentice Hall Inc., Englewood Cliffs, New Jersey (1982).

37. A.A. GRIFFITH. Theory of Rupture. Proceedings of the First International Congress on Applied Mechanics, pp. 55-63, Delft (1924).

38. C. FAIRHURST. On the validity of the 'Brazilian' test for brittle materials, Int. J. Rock. Mech. Min. Sci., Vol. 1, pp. 535-546 (1964).

39. B. LADANYI. Expansion of cavities in brittle media. Int. J. Rock Mech. Min. Sci., Vol. 4, pp. 301-328 (1967).

40. F.A. McCLINTOCK and J.B. WALSH. Friction on Griffith cracks in rock under pressure. Proceedings of the International Congress on Applied Mechanics, Berkeley, pp. 1015-1021 (1962).

41. M. MELLOR. Mechanical properties of polycrystalline ice. In "Physics and Mechanics of Ice", Proceedings of IUTAM Symposium held at the Technical University of Denmark on 6-10 August 1979. Edited by P. TRYDE, Springer-Verlag, Berlin, pp. 217-245. (1979).

42. R. FREDERKING and L. GOLD. Experimental study of edge loading of ice plates, Can. Geotech. Journal. Vol. 12, No. 4 (1975).

43. N.V. FOKEYEV. Determination of the compressive strength of artificial ice specimens of different salinities under conditions of combined stress. Proceedings of the Arctic Research Institute, Vol. 331, 1976, pp. 189-202. (Original in Russian, English translation, Ottawa, 1980).

44. S.J. JONES. Triaxial testing of polycrystalline ice. Proceedings of Third International Conference on Permafrost held in Edmonton, Alberta on July 10-13, 1978, pp. 671-675 (1978).

45. T. RALSTON. An analysis of ice sheet indentation, IAHR Symposium on Ice Problems, Lulea, Sweden (1978).

46. T.D. RALSTON. Plastic limit analysis of ice splitting failure, POAC 81, Proceedings of the Sixth International Conference on Port and Ocean Engineering under Arctic Conditions held at Québec, Canada on 27-31 July 1981, Les Presses de l'Université Laval, pp. 205-215 (1981).

47. A.C.T. CHEN. Transverse pressure effects on an embedded ice pressure sensor. POAC 81, Proceedings of the Sixth International Conference on Port and Ocean Engineering under Arctic conditions held at Quebec, Canada on 27-31 July 1981, Les Presses de l'Université Laval, pp. 375-383 (1981).

48. N.K. SINHA and R. FREDERKING. Effect of test system stiffness on strength of ice. POAC79, Proceedings of the 5th International Conference on Port and Ocean Engineering under Arctic Conditions, held August 13-17, 1979 at Trondheim, Norway, pp. 708-777 (1979).

49. N.K. SINHA. Comparative study of ice strength data. Proceedings of IAHR International Symposium on Ice held July 27-31, 1981 at Quebec, Canada, pp. 581-592 (1981).

50. N.K. SINHA. Rate sensitivity of compressive strength of columnar-grained ice, Presented at Spring Meeting, Society of Experimental Stress Analysis held on 20-25 May 1979 at San Francisco, California. Published in "Experimental Mechanics", Vol. 21, No. 6, pp. 209-218 (June 1981).

51. J.R. RICE. On the stability of dilatant hardening for saturated rock masses. Journal of Geophysical Research, Vol. 80, No. 11, pp. 1531-1536 (April 1975).

52. J.W. RUDNICKI and J.R. RICE. Conditions for the localization of deformation in pressure-sensitive dilatant materials. J. Mech. Phys. Solids, Vol. 23, pp. 371-394 (1975).

53. J.R. RICE. The initiation and growth of shear bands, In: "Plasticity and Soil Mechanics" (Edited by A.C. PALMER), pp. 263-274, Cambridge University Engng. Dept., Cambridge, England (1973).

54. J.R. RICE. The localization of plastic deformation. Preprints, 14th Congress, International Union of Theoretical and Applied Mechanics, held in Delft, Netherlands (Edited by W. KOITER), pp. 207-220, North-Holland, Amsterdam (September 1976).

55. Z.P. BAZANT. Instability, ductility and size effect in strain-softening concrete. Journal of the Structural Division, Proc. ASCE, Vol. 102, pp. 331-334 (1976).

56. G.C. NAYAK and O.C. ZIENKIEWICZ. Elasto-plastic stress analysis. A generalization for various constitutive relations including strain softening. Int. J. Numer. Methods in Engng., Vol. 5, pp. 113-135 (1975).

57. K.Y. LO and C.F. LEE. Stress analysis and slope stability in strain softening materials. Geotechnique, Vol. 23, pp. 1-11 (1973).

58. J.H. PREVOST and K. HOEG. Soil mechanics and plasticity analysis of strain softening. Geotechnique, Vol. 25, pp. 279-297 (1975).

59. ST. PIETRUSZCZAK and Z. MROZ. Numerical analysis of elastic-plastic compression of pillars accounting for material hardening and softening. Int. J. Rock Mech. Min. Sci. and Geomech. Abstr., Vol. 17, pp. 199-207 (1980).

60. ST. PIETRUSZCZAK and Z. MROZ. Finite element analysis of deformation of strain-softening materials. Int. J. Numer. Methods in Engng., Vol. 17, pp. 327-334 (1981).

61. G. MAIER and T. HUECKEL. Nonassociated and coupled flow rules of elastoplasticity for rock-like materials. Int. J. Rock Mech. Min. Sci. and Geomech. Abstr., Vol. 16, pp. 77-92 (1979).

62. A. DRAGON and Z. MROZ. A continuum model for plastic brittle behaviour of rock and concrete. Internat. J. Engng. Sci., Vol. 17, pp. 121-137 (1979).

63. N.G. GEROGIANNOPOULOS and E.T. BROWN. The critical state concept applied to rock. Int. J. Rock Mech. Min. Sci. and Geomech. Abstr., Vol. 15, pp. 1-10 (1978).

64. K.J. CHANG and T.W. YANG. A constitutive model for the mechanical properties of rock. Int. J. Rock Mech. Min. Sci. and Geomech. Abstr., Vol. 19, pp. 123-133 (1982).

65. J.W. DOUGILL. Some remarks on path independence in the small in plasticity, Quarterly of Applied Mathematics, pp. 233-243 (Oct. 1975).

66. J.W. DOUGILL and M.A.M. RIDA. Further consideration of progressively fracturing solids, J. Engrg. Mech. Div., ASCE, Vol. 106 (EM5) pp. 1021-1038 (1980).

67. J.W. DOUGILL. On stable progressively fracturing solids. Zeitschrift fuer Angewandte Mathematik und Physik, Vol. 27, Fasc. 4, pp. 423-437 (1976).

68. J.W. DOUGILL. On stable progressive fracturing solids. J. Appl. Math. and Phys. (ZAMP) Vol. 27, pp. 423-437 (1976).

69. Z.P. BAZANT and S.S. KIM. Plastic-fracturing theory for concrete. J. Engng. Mech. Div., Proc ASCE, Vol. 105, No. EM3, pp. 407-428 (June 1979).

70. B. LADANYI. Expansion of cavities in brittle media, International Journal of Rock Mechanics and Mining Science, Vol. 4, pp. 301-328 (1967).

71. K.E. LOLAND. Continuous damage model for load response estimation of concrete. Cement and Concrete Research, Vol. 10, pp. 395-402 (1980).

72. J. MAZARS. Mechanical damage and fracture of concrete structures, In: "Advances in Fracture Research," 5th International Conference on Fracture, Ed. by D. FRANCOIS, Cannes, March-April 1981, pp. 1499-1506 (1981).

73. D.E. GRADY and M.E. KIPP. Continuum modelling of explosive fracture in oil shale. International Journal of Rock Mechanics Mining Science and Geomechanics Abstracts, Vol. 17, pp. 147-157 (1980).

74. A. DRAGON and Z. MROZ. A continuum model for plastic-brittle behaviour of rock and concrete. International Journal of Engineering Science, Vol. 17, pp. 121-137 (1979).

75. L. DAVISON and A.L. STEVENS. Thermomechanical constitution of spalling elastic bodies. Journal of Applied Physics, Vol. 44, pp. 668-674 (1973).

76. D. KRAJCINOVIC and U. FONSEKA. The continuous damage theory of brittle materials. Journal of Applied Mechanics, Vol. 48, No. 4, pp. 809-824 (December 1981).

77. W. SUARIS and S.P. SHAH. Rate sensitive damage theory for brittle solids. Journal of Engineering Mechanics, ASCE, Vol. 110, No. 6, pp. 985-997 (June 1984).

78. Z.P. BAZANT. Work inequalities for plastic fracturing materials. Int. J. Solids Structures, Vol. 16, pp. 873-901 (1980).

79. L. RESENDE and J.B. MARTIN. A progressive 'continuum' model for granular materials, Computer Methods in Applied Mechanics and Engineering, Vol. 42, pp. 1-18 (1984).

80. K.C. VALANIS. A theory of viscoplasticity without a yield surface, Parts I and II, Theory and Applications, Archives of Mechanics, Vol. 23, pp. 517-551 (1971).

81. Z.P. BAZANT and P.D. BHAT. Endochronic theory of inelasticity and failure of concrete, Journal of Engineering Mechanics Division, ASCE, Vol. 102, No. EM4, pp. 701-722 (1976).

82. Z.P. BAZANT, A.M. ANSAL and R.J. KRIZEK. Endochronic models for soils, soil mechanics - transient and cyclic loads, Ed. by G.N. PANDE and O.C. ZIENKIEWICZ, John Wiley and Sons Ltd., pp. 419-438 (1982).

83. S.I. SORENSEN, A. ARNESAN and P.G. BERGAN. Nonlinear finite element analysis of reinforced concrete using endochronic theory, Proceedings of International Conference on Finite Elements in Nonlinear Solids and Structural Mechanics, Geilo, Norway, pp. 167-180 (1977).

84. H.C. WU and J.C. SHEU. Endochronic modelling for shear hysteresis of sand, Journal of Geotechnical Engineering Division, ASCE, Vol. 199, No. 12, pp. 1539-1550 (1983).

85. H.C. WU and T.P. WANG. Endochronic description of sand response to static loading, Journal of Engineering Mechanics Division, ASCE, Vol. 109, No. 4, pp. 970-999 (1983).

86. R.S. RIVLIN. Some comments on the endochronic theory of plasticity, Int. J. Solids and Structures, Vol. 17, pp. 231-248 (1981).

87. I.S. SANDLER. On the uniqueness and stability of endochronic theories of material behaviour, Journal of Applied Mechanics, ASME, Vol. 45, pp. 263-266 (June 1978).

88. K.C. VALANIS. On the substance of Rivlin's remarks on the endochronic theory, Int. J. Solids and Structures, Vol. 17, pp. 249-265 (1981).

89. Z.P. BAZANT and R.J. KRIZEK. Endochronic constitutive law for liquefaction of sand. Journal of Engineering Mechanics Division, Proc. ASCE, Vol. 102, pp. 225-238 (1976).

90. G. WEMPNER and J. ABERSON. A formulation of inelasticity from thermal and mechanical concepts. Int. J. Solids Structures, Vol. 12, pp. 705-721 (1976).

91. Z.P. BAZANT and P. BHAT. Prediction of hysteresis of reinforced concrete beams. Journal of Structural Mechanics Division, Proc. ASCE, Vol. 103, pp. 153-167 (1977).

92. Z.P. BAZANT and C.L. SHIEH. Endochronic model for nonlinear triaxial behaviour of concrete. Nuclear Engineering Design (1977).

93. V. CUELLAR, Z.P. BAZANT, R.J. KRIZEK and M.L. SILVER. Densification and hysteresis of sand under cyclic shear. J. Geotechnical Engng. Div., Proc. ASCE, Vol. 103 (GT5), pp. 399-416 (1977).

94. A. ANSAL, Z.P. BAZANT and R.J. KRIZEK. Constitutive relation for isotropically consolidated clays. Report 77-12/643-1, Department of Civil Engineering, Northwestern University, Evanston, Illinois (December 1977).

95. Z.P. BAZANT, A. ANSAL and R.J. KRIZEK. Viscoplasticity of anisotropically consolidated clays. Report 77-12/643-2, Department of Civil Engineering, Northwestern University, Evanston, Illinois (December 1977).

96. Z.P. BAZANT. Endochronic and classical theories of plasticity in finite element analysis, pp. 151-165 In: "Finite Elements in Nonlinear Mechanics," Proceedings of the International Conference on Finite Elements in Nonlinear Solid and Structural Mechanics, held at Geilo, Norway, in August 1977, Tapir Press, Trondheim (1977).

97. Z.P. BAZANT. Endochronic inelasticity and incremental plasticity. Int. J. Solids Structures, Vol. 14, pp. 691-714 (1978).

98. H.C. WU and T.P. WANG. Endochronic description of sand response to static loading. Journal of Engineering Mechanics, Vol. 109, No. 4, pp. 970-989 (August 1983).

99. Z.P. BAZANT, R.J. KRIZEK and C.-L. SHIEH. Hysteretic endochronic theory for sand. Journal of Engineering Mechanics, Vol. 109, No. 4, pp. 1073-1095 (August 1983).

100. K.R. GOPAL, D.V. REDDY and M. AROCKIASAMY. Endochronic constitutive modelling of ice behaviour. Proceedings of the Speciality Conference on Computer Methods in Offshore Engineering held in Halifax, on 23-25 May, 1984, ASCE, pp. 459-474 (1984).

101. M. SUIDAN and W.C. SCHNOBRICH. Finite element analysis of reinforced concrete. Journal of the Structural Division, ASCE, Vol. 99, No. ST10, Proc. Paper 10081, pp. 2109-2122 (Oct. 1973).

102. Z.P. BAZANT and L. CEDOLIN. Blunt crack band propagation in finite element analysis. Journal of the Engineering Mechanics Division, ASCE, Vol. 105, No. EM2, pp. 297-315 (April 1979).

103. M. MODEER. A Fracture Mechanics Approach to Failure Analysis of Concrete Materials. Division of Building Materials, University of Lund, Lund, Sweden. Report TVBM-1001 (1979).

104. D.A. SHOCKEY, L. SEAMAN, D.R. CURRAN, P.S. DeCARLI, M. AUSTIN and J.P. WILHELM. A Computational Model for Fragmentation of Armor Under Ballistic Impact, Stanford Research Institute Report, Project PYU-2151 (Dec. 1973).

105. D.A. SHOCKEY, D.R. CURRAN, M. AUSTIN and L. SEAMAN. Development of a Capability for Predicting Cratering and Fragmentation Behaviour in Rock, Stanford Research Institute Report DNA-3730F (May 1975).

106. L. SEAMAN, D.R. CURRAN and D. SHOCKEY. Computational models for ductile and brittle fracture, Journal of Applied Physics, Vol. 47, No. 11, pp. 4814-4826 (Nov. 1976).

107. F.P. STECHER and W.L. FOURNEY. Prediction of crack motion from detonation in brittle materials, Int. J. Rock Mech. Min. Sci. & Geomech. Abst., Vol. 18, pp. 23-33 (1981).

108. K.-J. BATHE and S. RAMASWAMY. On three-dimensional nonlinear analysis of concrete structures. Nuclear Engineering and Design, Vol. 52, pp. 385-409 (1979).

109. A Finite Element Program for Automatic Dynamic Incremental Nonlinear Analysis (ADINA), ADINA Engineering Inc., Massachusetts, USA (September 1981).

110. N.K. SINHA. Field test 1 of compressive strength first-year sea ice, Presented at the Second Symposium on Applied Glaciology held in New Hampshire, USA, August 23-27, 1982, hosted by U.S. Army Cold Regions Research and Engineering Lab and co-sponsored by American Geophysical Union and American Meteorological Society. Also published in Annals of Glaciology, Vol. 4, pp. 253-259 (1983).

111. N.K. SINHA. Rate sensitivity of compressive strength of columnar-grained ice. Presented at Spring Meeting, Society of Experimental Stress Analysis held on 20-25 May 1979 at San Fransico, California. Published in "Experimental Mechanics", Vol. 21, No. 6, pp. 209-218 (June 1981).

112. E.M. SCHULSON and J.H. CURRIER. The tensile strength of polycrystalline ice. Presented at the Second Symposium on Applied Glaciology held in New Hampshire, USA, August 23-27, 1982, hosted by U.S. Army Cold Regions Research and Engineering Lab and co-sponsored by American Geophysical Union and American Meteorological Society. Abstract published in Annals of Glaciology, Vol. 4, pp. 305 (1983). Also published in "Acta Metallurgica, Vol. 30, No. 8, pp. 1511-1514 (1982).

113. D.E. NEVEL and F.D. HAYNES. Interpretation of the Tensile Strength of Ice Under Triaxial Stresses, Cold Regions Research and Engineering Report 76-5, New Hampshire, USA (1976).

114. G.F.N. COX and J.A. RICHTER-MERGE. Tensile strength of multi-year pressure ridge sea ice samples, pp. 186-193, Vol. 2, Proceedings of the Fourth International Offshore Mechanics and Arctic Engineering Symposium in Dallas, Texas on 17-21 February 1985, ASME. (1985).

115. W.W. DENNER. The relationship of stress and strain in sea-ice, Proceedings of the Worshop on Sea Ice Field Measurement, St. John's, Newfoundland, April 29-May 1, 1980, co-sponsored by National Research Council, pp. 7-32 (1980).

116. P. NOBLE and V. BULAT. Ice Rules for Propellers and Propeller Shafting, Report submitted to Transport Canada Research and Development Centre, Montreal, Quebec, submitted by ARCTEC Canada Ltd., Calgary, Alberta (March 1980).

117. A. TRAETTEBERG, L.W. GOLD and R. FREDERKING. The strain rate and temperature dependence of Young's modulus of ice, Proceedings of Third International Symposium on Ice Problems, Hanover, N.H., USA, August 18-21, 1975, sponsored by International Association of Hydraulic Research Committee on Ice Problems, pp. 479-486 (1975).

118. R.M.W. FREDERKING, N.K. SINHA and L.W. GOLD. Mechanical properties of sea ice, Proceedings of Eighth Canadian Congress of Applied Mechanics, June 7-12, 1981, University of Moncton, N.B., pp. 125-128 (1981).

119. S.J. CALABRESE, R. BUXTON and G. MARSH. Frictional characteristics of materials sliding against ice, ASCE Preprint No. 79-AM-3B-2, Presented at the 34th Annual Meeting on April 30-May 3, 1979 in St. Louis, Missouri (1979).

120. R.Y. EDWARDS, Jr. Modelling the interaction between ice and ships, Physics and Mechanics of Ice, Symposium held at Copenhagen, August 6-10, 1979, Technical University of Denmark, Ed. Per Tryde, sponsored by International Union of Theoretical and Applied Mechanics, pp. 60-81.

121. VAST/ADINA Interface Program (ADIDAT): Final Report, Martec Limited, Halifax, N.S. (July 1983).

122. B. MICHEL. Ice Mechanics, Les Presses de l'Universite Laval, Quebec (1978).

123. H. EL-TAHAN, A.S.J. SWAMIDAS, M. AROCKIASSAMY and D.V. REDDY. Strength of iceberg and artificial snow-ice under high strain rates and impact loads, Proceedings of the Third International Offshore Mechanics and Arctic Engineering Symposium, Vol. III, ASME, pp. 158-165 (1984).

124. R.Y. EDWARDS. Methods for Predicting Forces Encountered by Propellers During Interactions with Ice. ARCTEC Canada Limited, Rep 75C-1, 1976. Presented at 3rd Lips Propeller Symposium, Drunen - The Netherland (1976). See also International Shipbuilding Progress Vol. 23, pp. 406-419 (Dec. 1976).

125. B. MICHEL and D. BLANCHET. Indentation of an S2 floating ice sheet in the brittle range. Presented at the Second Symposium on Applied Glaciology held in New Hampshire, USA on 23-27 August 1982. Also in Annals of Glaciology, Vol. 4, pp. 180-187 (1983).

126. D.S. SODHI and C.E. MORRIS. Ice Forces on Rigid, Vertical, Cylindrical Structures, CRREL Report 84-33. USA Cold Regions Research and Engineering Laboratory, Hanover, NH (1984).

127. P.G. NOBLE and V. BULAT. A study of ice class rules for propellers, Paper 4 presented at Propellers '81 Symposium held on May 26-27, 1981 at Virginia Beach, Virginia. Published by SNAME (The Society of Naval Architects and Marine Engineering), pp. 49-65 (1981).

128. H. OKAMOTO, K. NOZAWA, H. KAWAKAMI and F. YAMAMOTO. Dynamic ice loads and stress analysis on the propeller of the Arctic ship; model test in ice. POAC81, Proceedings of the Sixth International Conference on Port and Ocean Engineering under Arctic Conditions held on 27-31 July 1981 at Quebec City, Canada, pp. 253-262 (1981).

129. T. SASAJIMA, V. BULAT and I. GLEN. An experimental investigation of two candidate propeller designs for ice capable vessels. POAC81, Proceedings of the Sixth International Conference on Port and Engineering under Arctic Conditions held at Quebec City, Canada on 27-31 July 1981, pp. 263-275 (1981).

APPENDIX A

EVALUATIONS OF ANALYSIS PROGRAMS

APPENDIX A

EVALUATIONS OF ANALYSIS PROGRAM

Program NONSAP

This nonlinear analysis program has been in use over the past decade mainly as a research tool at various educational and research institutions. The source listing of this program can be purchased at relatively low cost and provides the capability to incorporate user defined special purpose subroutines.

The program offers a very limited choice of element types. Nonetheless this is not a serious drawback for the present problem since the types of elements being contemplated for the analyses are available. In its present form, the program is incapable of applying loads in the form of prescribed displacements. The latter is desirable to model the milling action of the propeller. However, this difficulty can be overcome by using very stiff spring elements at nodes corresponding to the interface and prescribing forces at these nodes to produce the desired amount of displacement.

The stress-strain curve can be specified in an arbitrary manner to closely model the experimental data on the mechanical behaviour of ice. However, this may require the knowledge of bulk modulus and shear modulus for ice. This information cannot be readily obtained from the literature search and thus NONSAP is not a practical choice for modelling the ice behaviour at this stage.

Program ADINA

This program includes a number of element types, and displacements can be prescribed within a static nonlinear analysis or a dynamic nonlinear analysis. User supplied subroutines for material models and loads can be added.

The availability of the Drucker-Prager and concrete material criteria is noteworthy. The latter, which is a damage material model, is particularly suitable for brittle materials like concrete and rock. Since ice under milling action tends to behave as a brittle material, the use of this model has particular advantages. However, the model is formulated on the basis of certain parameters, not all of which can be estimated for ice with a degree of reliability. This can be overcome, to some extent, by suitably adjusting these parameters to reflect the ice properties and the anticipated failure envelope for ice as closely as possible.

Program MARC

This program has a comprehensive library for elements, materials and structural procedures. The displacements can be prescribed as a static load or dynamic load.

The material property can be defined in the form of a piecewise linear approximation in a general way. However, this model is restricted to only one yield criterion (von Mises) which is not particularly applicable to ice.

Linear elastic-plastic relationships can be used with a number of yield criteria. These criteria are formulated on the basis of Mohr-Coloumb yield condition and any one of these can be considered as a suitable criterion for a first approximation to model the failure behaviour of the ice. A special yield criterion, which takes into account 'cracking' of the material and originally developed for concrete under biaxial stress condition is specially relevant to the propeller-ice problem. This criterion is restricted to two-dimensional (planar) elements only and so obviously not suitable for a three-dimensional analysis.

The user defined subroutines can be employed mainly to ease data preparation task. However, insertion of a totally new subroutine for material modelling may not be a straightforward task and would require a considerable effort.

Program ANSYS

ANSYS is a general purpose finite element program suitable for linear and non-linear analysis. For material property description, the stress-strain curve may be defined in an arbitrary manner with a capability for handling the 'loading' and 'unloading' part of the material property curve separately. The curve is given in the form of stress against total strain. This formulation is not particularly suitable for ice since it involves knowledge of ice-properties such as bulk modulus and shear modulus. The variation of these material constants against the total strain is not readily available from the literature and therefore presents a difficulty in using this program.

Only one yield surface (von Mises) is available and this is a severe restriction for the present analysis. The program does not provide the capability to include user applied subroutines which represents a serious drawback.

Program ABAQUS

The program can be used for a linear as well as non-linear analysis and has a good selection of element types. The program is particularly suitable for soil modelling to evaluate non-linear response. In the elastic-plastic material types, a limited number of yield criterion are available which are not applicable to ice. The facility to incorporate user defined special subroutines does not seem to be available.

Linear elastic-plastic material properties can be used with von Mises yield function with isotropic yield or a variation of it in the form of anisotropic yield, the latter referred as Hill's yield condition. For dynamic problems, strain-rate sensitivity of the plastic

behaviour is important and the program provides for this with a constitutive model wherein the strain-rate dependence is included.

Program PISCES

This is a two-dimensional explicit finite-difference computer program which can be used to study the response and interaction of fluids and solids to static and dynamic loads. The organization of the program is such that it is more suited for dynamic analysis and treats static analysis as a special case of dynamic loading.

The program has a unique feature in that the user can analyse the program in an Eulerian coordinate system or Langragian coordinate system The latter system, in which the grid-points move with the material, is commonly used in finite-element or finite-difference programs. The former system in which the coordinates are fixed in space and material moves through the grid is used in regions where distortions are great or where fluid or gas dynamics are being studied. Therefore Eulerian coordinate system is particularly useful to deal with non-linearities arising from large deformations.

During propeller-ice interaction large deformations are likely and the choice of adopting either system is advantageous.

Linear elastic-plastic relationships with von Mises yield criterion or Mohr-Coulomb type criterion are available. Alternatively, material property can be defined by a piecewise linear approximation. The program also offers the capability of inserting an user defined subroutine to determine yield conditions.

APPENDIX B

BIBLIOGRAPHY

APPENDIX B1

BIBLIOGRAPHY ON BRITTLE FRACTURE (GENERAL REFERENCES)

1. J.A. ABERSON, J.M ANDERSON and W.W. KING. Finite element analysis of dynamic fracture. In "Advances in Engineering Science", Vol. 1, pp. 215-225. NASA CP-2001 (1976).

2. J.H. ARGYRIS, G. FAUST, J. SZIMMAT, E.P. WARNKE and K.J. WILLAM. Recent developments in the finite element analysis of prestressed concrete reactor vessels. Nuclear Engineering and Design, Vol. 28, pp. 42-75 (1974).

3. T.W. BARBEE Jr., L. SEAMAN, R. CREWDSON, and D. CURRAN. Dynamic fracture criteria for ductile and brittle metals, J. Mater. JMLSA, Vol. 7, pp. 393-401 (1972)

4. K.-J. BATHE and S. RAMASWAMY. On three-dimensional nonlinear analysis of concrete structures. Nuclear Engineering and Design, Vol. 52, pp. 385-409 (1979).

5. Z.P. BAZANT. Instability, ductility and size effect in strain softening concrete. Journal of the Structural Division, Proc. ASCE, Vol. 102, pp. 331-344 (1976).

6. Z.P. BAZANT. Endochronic inelasticity and incremental plasticity. Int. J. Solids and Structures, Vol. 14, pp. 691-714 (1978).

7. Z.P. BAZANT. Work inequalities for plastic fracturing materials. Int. J. Solids Structures, Vol. 16, pp. 873-901 (1980).

8. Z.P. BAZANT. Crack band model for fracture of geomaterials. Proceedings of the 4th International Conference on Numerical Methods in Geomechanics held in June 1982 at Edmonton, Alberta. Ed. by Z. EISENSTEIN, Vol. 3 (1982).

9. Z.P. BAZANT and L. CEDOLIN. Fracture mechanics of reinforced concrete. Journal of the Engineering Mechanics Division, Proc. ASCE, Vol. 106, No. EM6, pp. 1287-1306 (Dec. 1980).

10. Z.P. BAZANT and L. CEDOLIN. Finite element modelling of crack band propagation. Journal of Structural Engineering, Proc. ASCE, Vol. 109, No. ST2, pp. 69-82 (Jan. 1983).

11. Z.P. BAZANT. Imbricate continuum and its variational derivation. Journal of Engineering Mechanics, ASCE, Vol. 110, No. 12, Proc. Paper 19334 (Dec. 1984).

12. Z.P. BAZANT, A.M. ANSAL and R.J. KRIZEK. Endochronic models for soils, soil mechanics - transient and cyclic loads, Ed. by G.N. PANDE and O.C. ZIENKIEWICZ, John Wiley and Sons Ltd., pp. 419-438 (1982).

13. Z.P. BAZANT, T.B. BELYTSCHKO and T.-P. CHANG. Continuum theory for strain-softening. Journal of Engineering Mechanics, ASCE, Vol. 110, No. 12, Proc. Paper 19333 (Dec. 1984).

14. Z.P. BAZANT and P.D. BHAT. Endochronic theory of inelasticity and failure of concrete, Journal of Engineering Mechanics Division, ASCE, Vol. 102, No. EM4, pp. 701-722 (1976).

15. Z.P. BAZANT and L. CEDOLIN. Blunt crack band propagation in finite element analysis. Journal of the Engineering Mechanics Division, Proc. ASCE, Vol. 105, No. EM2, pp. 297-315 (April 1979).

16. Z.P. BAZANT and T.-P. CHANG. Instability of nonlocal continuum and strain averaging. J. Eng. Mech., ASCE, Vol. 110, No. 10, Proc. Paper 19198 (Oct. 1984).

17. Z.P. BAZANT and P.G. GAMBAROVA. Crack shear in concrete: crack band microplane model. Journal of Structural Engineering, ASCE, Vol. 110, No. 9, Proc. Paper 19145 (Sept. 1984).

18. Z.P. BAZANT and S.S. KIM. Plastic-fracturing theory for concrete. Journal of the Engineering Mechanics Division, Proc. ASCE, Vol. 105, No. EM3, pp. 407-428 (June 1979).

19. Z.P. BAZANT and B.H. OH. Strain-rate effect in rapid triaxial loading of concrete. Journal of the Engineering Mechanics Division, ASCE, Vol. 108, No. EM5, Proc. Paper 17376, pp. 764-782 (Oct. 1982).

20. C.P. BAZANT and B.H. OH. Crack band theory for fracture of concrete. Matériaux et Constructions, Vol. 16, No. 93, pp. 155-177 (1983).

21. Z.P. BAZANT and B.H. OH. Rock fracture via strain-softening finite elements, ASCE, Vol. 110, EM7, Proc. Paper 18979, pp. 1015-1035 (July 1984).

22. Z.P. BAZANT and T. TSUBAKI. Total strain theory and path dependence of concrete. Journal of the Engineering Mechanics Division, Proc. ASCE, Vol. 106, No. EM6, pp. 1151-1173 (1980).

23. Z.P. BAZANT and T. TSUBAKI. Ship dilatancy model for cracked reinforced concrete. Journal of the Structural Division, Proc. ASCE, Vol. 106, No. ST9, pp. 1947-1966 (Sept. 1980).

24. W.L. BEASON. A Failure Prediction Model for Window Glass, Institute for Diaster Research, Texas Technical University, Lubbock, Texas, 212p (1980).

25. R. BENJUMEA. A note on the penetration of a rigid wedge into a nonisotropic brittle material. Int. J. Rock Mech. and Mining Sci., Vol. 6, p. 343-352 (1969).

26. BROBERG K.B. The propagation of a brittle crack. Ark.Fys. Vol. 18, pp. 159-192 (1960).

28. L. CEDOLIN and Z.P. BAZANT. Effect of finite element choice in blunt crack band analysis. Computer Methods in Applied Mechanics and Engineering, Vol. 24, No. 3, pp. 305-316 (Dec. 1980).

29. K.J. CHANG and T.W. YANG. A constitutive model for the mechanical properties of rock. Int. J. Rock Mech. Min. Sci. and Geomech. Abstr., Vol. 19, pp. 123-133 (1982).

30. J.B. CHEATHAM. An analytical study of rock penetration by a single bit tooth. Proc. 8th Drilling and Blasting Symp., Minnesota, pp. 1A-24A. Pergamon, NY (1958).

31. J.B. CHEATHAM. Indentation analysis for rock having a parabolic yield envelope. Int. J. Rock Mech. and Mining Sci., Vol. 1, pp 431-440 (1964).

32. A.C.T. CHEN and W.F. CHEN. Constitutive relations for concrete. Journal of Engineering Mechanics Division, Proc. ASCE, Vol. 101, No. EM4, pp. 465-481 (1975).

33. A.C.T. CHEN and W.F. CHEN. Constitutive equations and punch indentation of concrete. Journal of Engineering Mechanics Division, Proc. ASCE, Vol. 101, No. EM6, Proc. Paper 11809, pp. 889-906 (Dec. 1975)

34. W.F. CHEN. Nonlinear analysis of pressure-resistant concrete cylinder structures, pp. 19.1-19.31. Proceedings of the Conference on "Engineering Application of the Finite Element Method", held 9-11 May 1979 in Norway, A.S. Computas, Hovik, Norway (1979).

35. W.F. CHEN and H. SUZUKI. Constitutive models for concrete. Computers and Structures, Vol. 12, pp. 23-32 (1980).

36. W.-F. CHEN and E.C. TING. Fracture in Concrete. Proceedings of a session by the ASCE Committee on Properties of Materials, American Society of Civil Engineers, New York, 109p (1980).

37. W.F. CHEN and E.C. TING. Constitutive models for concrete structures. Journal of the Engineering Mechanics Division, Proc. ASCE, Vol. 106, No. EM2, pp. 1-19 (1980).

38. G.P. CHEREPANOV. Mechanics of brittle fracture. Translation of Mekhanika Khrupkogo Razrusheniia, McGraw-Hill International Book Co., 939p (1979).

39. A. CHUDNOVSKY and M. KACHANOV. Interaction of a crack with a field of microcracks, Lett. Appl. Engng. Sci., Vol. 21, No. 8, pp. 1009-1018 (1983).

40. N.G.W. COOK, M. HOOD and F. TSAI. Observations of crack growth in hard rock loaded by an indentor, Int. J. Rock. Mech. Min. & Geomech. Abstr., Vol. 21, No. 2, pp. 97-107 (1984).

41. L. DAVISON and A.L. STEVENS. Thermomechanical constitution of spalling elastic bodies. Journal of Applied Physics, Vol. 44, pp. 668-674 (1973).

42. J.W. DOUGILL. On stable progressively fracturing solids. Zeitschrift fuer Angewandte Mathematik und Physik, Vol. 27, Fasc. 4, pp. 423-437 (1976).

43. J.W. DOUGILL and M.A.M. RIDA. Further consideration of progressively fracturing solids, J. Engrg. Mech. Div., ASCE, Vol. 106 (EM5) pp. 1021-1038 (1980).

44. A. DRAGON and Z. MROZ. A continuum model for plastic brittle behaviour of rock and concrete. Internat. J. Engng. Sci., Vol. 17, pp. 121-137 (1979).

45. A. DRAGON and Z. MROZ. A continuum model for plastic-brittle behaviour of rock and concrete. International Journal of Engineering Science, Vol. 17, pp. 121-137 (1979).

46. P.K. DUTTA. A theory of percussive drill bit penetration. Int. J. Rock Mech. Min. Sci., Vol. 9, pp. 543-567 (1972).

47. V.M. ENTOV and V.I. YAGUST. Experimental investigation of laws governing quasi-static development of macrocracks in concrete. Mechanics of Solids (translation from Russian) Vol. 10, No. 4, pp. 87-95 (1975).

48. J.M. ETHERIDGE. Determination of the stress intensity factor K from isochromatic fringe loops. Ph.D. Thesis, Department of Mechanical Engineering, University of Maryland (1976).

49. R.H. EVANS and M.S. MARATHE. Microcracking and stress-strain curves for concrete in tension. Matériaux et Constructions, Vol. 1, No. 1, pp. 61-64 (1968).

50. I. EVANS and C.D. POMEROY. The strength, fracture and workability of coal. Published by the authors (obtainable from National Coal Board, Mining Research and Development Establishment, Stanhope Bretby, Burton-on-Trent, England), 277p. (1973).

51. C. FAIRHURST. On the validity of the "Brazilian" test for brittle materials, Int. J. Rock Mech. Mining Sci., Vol. 1, pp. 535-546 (1964)

52. I. FINNIE and S. VAIDYANATHAN. Initiation and propagation of Hertzian ring cracks. Proc. Conf. Fracture Mechanics of Ceramics (Edited by R.C. Bradt, D.P. H. Hasselman & F.F. Lange). Vol. 1, pp. 231-244. Plenum Press, NY (1974).

53. F.C. FRANK and B.R. LAWN. On the theory of Hertizian fracture. Proc. R. Soc., Vol 1299, pp. 291-306 (1967).

54. L.B. FREUND. Crack propagation in an elastic solid subjected to general loading - I. Constant rate of extension. J. Mech. Phys. Solids, Vol. 20, pp. 129-140 (1972)

55. M. FRIEDMAN, J. HANDIN, and G. ALANI. Fracture-surface energy of rocks. Int. J. Rock Mech. Min Sci., Vol. 9, pp. 757-766 (1972).

56. S.W. FRIEMAN and E.R. FULLER. Fracture Mechanics for Ceramics, Rocks and Concrete: A Symposium. ASTM Special Technical Publication No. ASTM-STP-745, American Society for Testing and Materials, Philadelphia, Pa. (1981).

57. J.S. GEDLING, N.S. MISTRY and A.K. WELCH. Evaluation of material models for reinforced concrete structures. Computers and Structures, Vol. 24, No. 2, pp. 225-232 (1986).

58. C. GEORGIADIS. Probability of failure models in finite element analysis of brittle materials. Computers and Structures, Vol. 18, No. 3, pp. 537-549 (1984).

59. N.G. GEROGIANNOPOULOS and E.T. BROWN. The critical state concept applied to rock. Int. J. Rock Mech. Min. Sci. and Geomech. Abstr., Vol. 15, pp. 1-10 (1978).

60. K.H. GERSTLE et al. Behaviour of concrete under multi-axial stress states. Journal of Engineering Mechanics Divisions, Proc. ASCE, Vol. 106, No. EM6, pp. 1383-1403 (1980).

61. K.R. GOPAL, D.V. REDDY and M. AROCKIASAMY. Endochronic constitutive modelling of ice behaviour. Proceedings of the Speciality Conference on Computer Methods in Offshore Engineering held in Halifax, on 23-25 May 1984, ASCE, pp. 459-474 (1984).

62. D.E. GRADY and M.E. KIPP. Continuum modelling of explosive fracture in oil shale. International Journal of Rock Mechanics Mining Science and Geomechanics Abstracts, Vol. 17, pp. 147-157 (1980).

63. A.A. GRIFFITH. The phenomena of rupture and flow in solids. Philosophical Transactions of the Royal Society of London, Ser. A., Vol. 221, No. 588, pp. 163-198 (1920)

64. A.A. GRIFFITH. Theory of Rupture. Proceedings of the First International Congress on Applied Mechanics, pp. 55-63, Delft (1924).

65. G.T. HAHN, P.C. GEHLEN, R.G. HOALGLAND, M.F. KANNINEN, C. POPELAR and A.R. ROSENFIELD. Critical experiments, measurements and analyses to establish a crack arrest methodology for nuclear pressure vessel steels. Battele Columbus Labs, Report No. BMI-1934, Cat. UC-78d (May 1975).

67. R.G. HOAGLAND, G.T. HAHN and A.R. ROSENFIELD. Influence of microstructure on fracture propagation in rocks. Semiannual Research Report, Batelle Columbus Laboratories, ARPA Contract No. H0210006 (1971).

68. W.A. HUSTRULID and C. FAIRHURST. A theoretical and experimental study of the percussive drilling of rock. Part I: Theory of percussive drilling. Int. J. Rock Mech. and Mining Sci., Vol. 8, pp. 311-333 (1971).

69. A.R. INGRAFFEA. Nodal grafting for crack propagation studies, Short Communication, Int. J. Numer. Meth. in Engng., Vol. 11, pp. 1185-1197 (1977).

70. A.R. INGRAFFEA, F.E. HEUZE, H.-Y KO and K. GERSTLE. Analysis of discrete fracture propagation in rock loaded in compresson. Proc. 18th Symp. Rock Mechanics, Keystone, Co, (June 1977).

71. G.R. IRWIN and J.W. DALLY. A photoelastic study of the dynamic fracture behavior of homalite 100. Nuclear Regulatory Commission NUREG-75/107 (September 1975).

72. G.R. IRWIN, J.W. DALLY, T. KOBAYASHI, W.L. FOURNEY and J.M. ETHERIDGE. A photoelastic characterization of dynamic fracture. Nuclear Regulatory Commission NUREG-0072, NRC5 (December 1976).

73. S.H. IYER. Size effects in ice and their influence on the structural design of offshore structures. POAC83, Proceedings of the Seventh International Conference on Port and Ocean Engineering under Arctic Conditions held at Helsinki, Finland on 5-9 April 1983, Vol. 3, pp. 414-432 (1983).

74. J. JAEGER and N. COOK. Fundamentals of Rock Mechanics. London, Methuen and Co. Ltd., 513 p (1969).

75. J. JANSON and J. HULT. Fracture mechanics and damage mechanics - a combined approach. Journal de Mécanique Appliquée, Vol. 1, No. 1, pp. 69-84 (1977).

76. A. JAYATILAKA. Fracture of Engineering Brittle Materials. Applied Science Publication Ltd., London, 378 p. (1979)

77. W. JOHNSON. Impact Strength of Materials. London, Edward Arnold, 357 p (1972).

78. J.W. KASPAR, N. BICANIC and S. STURE. Constitutive and computational aspects of strain-softening and localization in solids. ASME-WAM Symposium on Constitutive Equations: Micro, Macro and Computational Aspects, New Orleans, 10-14 December, 1984.

79. P. KENNY and J.D. CAMPBELL. Fracture toughness: an examination of the concept in predicting the failure of materials. Progress in Materials Science, Vol. 13, No. 3, pp. 137-181 (1967).

80. J.F. KNOTT. Fundamentals of fracture mechanics. London, Butterworth (1973).

81. A.S. KOBAYASHI, A.F. EMERGY and S. MALL. Dynamic-finite-element and dynamic-photoelastic analysis of two fracturing homolite 100 plates. Expl. Mech., Vol. 16 (1976).

82. K.N. KORZHAVIN. Action of Ice on Engineering Structures. Publishing House of Siberian Branch of USSR Academy of Sciences (1962) (English translation by CRREL, 1971).

83. M.D. KOTSOVOS. Concrete: a brittle fracturing material. Matériaux et Constructions, Vol. 17, No. 98, pp. 107-115 (1984).

84. D. KRAJCINOVIC and U. FONSEKA. The continuous damage theory of brittle materials. Journal of Applied Mechanics, Vol. 48, No. 4, pp. 809-824 (December 1981).

85. B. LADANYI. Expansion of cavities in brittle media, International Journal of Rock Mechanics and Mining Science, Vol. 4, pp. 301-328 (1967).

86. F.B. LANGITAN and B.R. LAWN. Effect of a reactive environment on the Hertzian strength of brittle solids. J. Appl. Phys., Vol. 41, pp. 3357-3365 (1970).

87. B.R. LAWN, A.G. EVANS and D.B. MARSHALL. Elastic/plastic damage in ceramics: the median/radial crack system. American Ceramics Society Bulletin, Vol. 63 (9-60) pp. 574-581 (1980).

88. B.R. LAWN and E.R. FULLER. Equilibrium penny-like cracks in indentation fracture. J. Mat. Sci., Vol. 10, pp. 2016-2024 (1970).

89. B.R. LAWN, T. JENSEN and A. ARORA. Brittleness as an indentation size effect. J. Mat. Sci., Vol. 11, pp. 573-575 (1976).

90. B.R. LAWN and M.V. SWAIN. Microfracture beneath point indentations in brittle solids. J. Mat. Sci., Vol. 10, pp. 113-122 (1975).

91. B.R. LAWN, M.V. SWAIN and K. PHILLIPS. On the mode of chipping fracture in brittle solids. J. Mat. Sci., Vol. 10, pp. 1236-1239 (1975).

92. B.R. LAWN and T.R. WILSHAW. Indentation fracture: principles and applications. J. Mat. Sci., Vol. 10, pp. 1049-1081 (1975).

93. B.R. LAWN and T.R. WILSHAW. Fracture of Brittle Solids. Cambridge, University Press (1975).

94. P.-A. LINDQUIST and H.H. LAI. Behaviour of the crushed zone in rock indentation. Rock Mech. Rock Engng., Vol. 16, pp. 199-207 (1983).

95. K.Y. LO and C.F. LEE. Stress analysis and slope stability in strain softening materials. Geotechnique, Vol. 23, pp. 1-11 (1973).

96. K.E. LOLAND. Continuous damage model for load response estimation of concrete. Cement and Concrete Research, Vol. 10, pp. 395-402 (1980).

97. M. LORRAIN. On the application of the damage theory to fracture mechanics of concrete. A State-of-the-Art Report, Civil Engineering Department, I.N.S.A., 31077 Toulouse, Cedex, France.

98. B. LUNDBERG. Penetration of rock by conical indenters. Int. J. Rock Mech. Min. Sci and Geomech. Abstr., Vol. 11, pp. 209-214 (1974).

99. G. MAIER and T. HUECKEL. Nonassociated and coupled flow rules of elastoplasticity for rock-like materials. Int. J. Rock Mech. Min. Sci. and Geomech. Abstr., Vol. 16, pp. 77-92 (1979).

100. J. MAZARS. Mechanical damage and fracture of concrete structures, In: "Advances in Fracture Research," 5th International Conference on Fracture, Ed. by D. FRANCOIS, Cannes, 29 March - 3 April 1981, Vol. 4, pp. 1499-1506 (1981).

101. F.A. McCLINTOCK and J.B. WALSH. Friction on Griffith cracks in rock under pressure. Proceedings of the International Congress on Applied Mechanics, Berkeley, pp. 1015-1021 (1962).

102. M. MELLOR. Mechanics of Cutting and Boring; Part 5: Dynamics and Energetics of Indentation Tools, CRREL Report CR80-21, 82 p (Sept. 1980).

103. M.A. MEYERS and C.T. AIMONE. Progress in Materials Science, Vol. 28, pp. 1-96 (1983).

104. A.G. MIKOSZA and B.R. LAWN. Section-and-etch study of Hertzian fracture mechanics. J. Appl. Phys., Vol. 42, pp. 5540-5545 (1971m.

105. M.H. MILLER and D.L. SIKARSKIE. On the penetration of rock by three dimensional indentors. Int. J. Rock Mech. and Mining Sci., Vol. 5, pp. 375-398 (1968).

106. M. MODEER. A Fracture Mechanics Approach to Failure Analysis of Concrete Materials. Division of Building Materials, University of Lund, Lund, Sweden. Report TVBM-1001 (1979).

107. D.W. MURRAY, L. CHITNUYANONDH, K.Y. RIJUB-AGHA and C. WONG. Concrete plasticity theory for biaxial stress analysis. ASCE, Vol. 105, EM6, Proc. Paper 15046, pp. 989-1006 (Dec. 1979).

108. G.C. NAYAK and O.C. ZIENKIEWICZ. Elasto-plastic stress analysis. A generalization for various constitutive relations including strain softening. Int. J. Numer. Methods in Engng., Vol. 5, pp. 113-135 (1975).

109. F. OUCHTELONY. Self-similar Solution in Plane Elastodynamics. Part II: Some Examples of Symmetrically Extending Plane Cracks. Swedish Detonic Research Foundation, Stockholm, Sweden, Report No. DS 1976: 12, (1976).

110. R.A. PALMER. Fracture Mechanics and Failure Predictions for Glass, Glass-Ceramic, and Ceramic Systems. Ph.D. thesis, University of Florida, 155 p. (1981).

111. J. PAONE and S. TANDANAND. Inelastic deformation of rock under a hemispherical drill bit. Trans. Am. Inst. Min. Engrs., Vol. 235, pp. 113-123 (1966).

112. P.C. PARIS and G.C. SIH. Stress analysis of cracks. American Society for Testing and Materials, Publication No. 381, pp. 30-82, June 21-26 (1964).

113. W.G. PARISEAU and C. FAIRHURST. The force-penetration characteristics for wedge penetration into rock. Int. J. Rock Mech. and Mining Sci., Vol. 4, pp. 165-180 (1967).

114. B. PAUL and D.L. SIKARSKIE. A preliminary model for wedge penetration in brittle materials. Trans. Am. Inst. Min. Engrs., Vol. 232, pp. 372-383 (1965).

115. B. PAUL. Macroscopic criteria for plastic flow and brittle fracture. Chapter 4 in "Fracture: An Advanced Treatise, Vol. II, Mathematical Fundmentals", Ed. by H. LIEBOWITZ, Academic Press, New York pp. 313-496 (1968).

116. P.-E. PETERSON. Crack Growth and Development of Fracture Zones in Plane Concrete and Similar Materials. Report TVBM-1006. Division of Building Materials, Lund Institute of Technology, 174 p. (1981).

117. D.V. PHILLIPS and O.C. ZIENKIEWICZ. Finite element non-linear analysis of concrete structures. Proceedings of the Institute of Civil Engineers, Part 2, Vol. 61, pp. 59-88 (1976).

118. ST. PIETRUSZCZAK and Z. MROZ. Numerical analysis of elastic-plastic compression of pillars accounting for material hardening and softening. Int. J. Rock Mech. Min. Sci. and Geomech. Abstr., Vol. 17, pp. 199-207 (1980).

119. ST. PIETRUSZCZAK and Z. MROZ. Finite element analysis of deformation of strain-softening materials. Int. J. Numer. Methods in Engng., Vol. 17, pp. 327-334 (1981).

120. J.H. PREVOST and K. HOEG. Soil mechanics and plasticity analysis of strain softening. Geotechnique, Vol. 25, pp. 279-297 (1975).

121. K.E. PUTTICK, L.E. MILLER and E. GILLHAM. Stress fields around indentation in polymethylmethacrylate, to be published (Referenced in 1976).

122. K. RAVI-CHANDAR and W.G. KNAUSS. An experimental investigation into dynamic fracture: I Crack initiation and arrest. International Journal of Fracture, Vol. 25, pp. 247-262 (1984).

123. K. RAVI-CHANDAR and W.G. KNAUSS. An experimental investigation into dynamic fracture: II Micro structural aspects. International Journal of Fracture, Vol. 26, pp. 65-80 (1984).

124. K. RAVI-CHANDAR and W.G. KNAUSS. An experimental investigation into dynamic fracture: III. On steady-state crack propagation and crack branching. Int. J. Fracture, Vol. 26, pp. 141-154 (1984).

125. L. RESENDE and J.B. MARTIN. Constitutive Modelling and Finite Element Analysis in Rock Mechanics. University of Cape Town, Appl. Mech. Res. Unit, Tech. Report No. 57 (1985).

126. L. RESENDE and J.B. MARTIN. A progressive 'continuum' model for granular materials, Computer Methods in Applied Mechanics and Engineering, Vol. 42, pp. 1-18 (1984).

127. L. RESENDE and J.B. MARTIN. Damage Constitutive Model for Geotechnical Applications. University of Cape Town, Nonlinear Structural Mech. Res. Unit, Tech. Report No. 44 (Nov. 1983).

128. J.R. RICE. Mathematical analysis in the mechanics of fracture. Chapter 3 in "Fracture: An Advanced Treatise, Vol. II, Mathematical Fundamentals", Ed. by H. LIEBOWITZ, Academic Press, New York, pp. (1968).

129. J.R. RICE. On the stability of dilatant hardening for saturated rock masses. Journal of Geophysical Research, Vol. 80, No. 11, pp. 1531-1536 (April 1975).

130. R.S. RIVLIN. Some comments on the endochronic theory of plasticity, Int. J. Solids and Structures, Vol. 17, pp. 231-248 (1981).

131. H.P. ROSSMANITH and G.R. IRWIN. The determination of stress intensity factors from dynamic isochromatic fringe patterns - Parts I-V. University of Maryland (June 1978).

132. J.W. RUDNICKI and J.R. RICE. Conditions for the localization of deformation in pressure-sensitive dilatant materials. J. Mech. Phys. Solids, Vol. 23, pp. 371-394 (1975).

133. R.S. SANDHU and S.W. HUANG. Application of Griffith's theory to analysis of progressive fracture. International Journal of Fracture, Vol. 11, pp. 107-121 (1975).

134. I.S. SANDLER. On the uniqueness and stability of endochronic theories of material behaviour, Journal of Applied Mechanics, ASME, Vol. 45, pp. 263-266 (June 1978).

135. L. SEAMAN, D.R. CURRAN and D. SHOCKEY. Computational models for ductile and brittle fracture, Journal of Applied Physics, Vol. 47, No. 11, pp. 4814-4826 (Nov. 1976).

136. D.A. SHOCKEY, L. SEAMAN, D.R. CURRAN, P.S. DeCARLI, M. AUSTIN and J.P. WILHELM. A Computational Model for Fragmentation of Armor Under Ballistic Impact, Stanford Research Institute Report, Project PYU-2151 (Dec. 1973).

137. D.A. SHOCKEY, D.R. CURRAN, M. AUSTIN and L. SEAMAN. Development of a Capability for Predicting Cratering and Fragmentation Behaviour in Rock, Stanford Research Institute Report DNA-3730F (May 1975).

138. G.C. SIH. (Editor). Dynamic Crack Propagation, Noordhoff International Publishing, The Netherlands (1973).

139. N. SMITH. High explosive cratering in frozen and unfrozen soils in Alaska, CRREL Report CR 80-09 (Feb. 1980).

140. S.I. SORENSEN, A. ARNESAN and P.G. BERGAN. Nonlinear finite element analysis of reinforced concrete using endochronic theory, Proceedings of International Conference on Finite Elements in Nonlinear Solids and Structural Mechanics, Geilo, Norway, pp. 167-180 (1977).

141. D.C. SPOONER and J.W. DOUGILL. A quantitative assessment of damage sustained in concrete during compressive loading. Magazine of Concrete Research, Vol. 27, No. 92, pp. 151-160 (1975).

142. F.P. STECHER. A numerical method for simulating controlled blasting techniques. Ph.D. Dissertation, Univ. of Maryland (1978).

143. F.P. STECHER and W.L. FOURNEY. Prediction of crack motion from detonation in brittle materials, Int. J. Rock. Mech. Min. Sci. & Geomech. Abstr., Vol. 18. pp. 23-33 (1981).

144. W. SUARIS and S.P. SHAH. Rate sensitive damage theory for brittle solids. Journal of Engineering Mechanics, ASCE, Vol. 110, No. 6, pp. 985-997 (June 1984).

145. M. SUIDAN and W.C. SCHNOBRICH. Finite element analysis of reinforced concrete. Journal of the Structural Division, ASCE, Vol. 99, No. ST10, Proc. Paper 10081, pp. 2109-2122 (Oct. 1973).

146. H. SUZUKI and W.-F. CHEN. Elastic-plastic-fracture analysis of concrete structures. Computers and Structures, Vol. 16, No. 6, pp. 697-705 (1983).

147. M.V. SWAIN and B.R. LAWN. Indentation fracture in brittle rock and glasses. International Journal of Rock Mechanics and Mining Science, Vol. 13, No. 4, pp. 311-319 (1976).

149. H. TADA, P. PARRIS and G.R. IRWIN. The Stress Analysis of Cracks Handbook. Del Research Corp. (1973).

150. Y. TANIGAWA and Y. KOSAKA. Mechanisms of fracture and failure of concrete as a composite material. In "Memoirs of the Faculty of Engineering", Vol. 27, No. 2, pp. 208-263, Nagoya University (1975).

151. K.C. VALANIS. A theory of viscoplasticity without a yield surface, Parts I and II, Theory and Applications, Archives of Mechanics, Vol. 23, pp. 517-551 (1971).

152. K.C. VALANIS. On the substance of Rivlin's remarks on the endochronic theory, Int. J. Solids and Structures, Vol. 17, pp. 249-265 (1981).

153. J.J-G. WANG. Influence of Microstructure, Stress-State and Environment on Superplastic Flow and Fracture in Glass-Ceramics. Ph.D. Thesis, Cornell University, 199 p. (1984).

154. J.K. WANG and T.F. LEHNHOFF. Bit penetration into rock - a finite element study. Int. J. Rock. Mech. Sci. & Geomech. Abstr., Vol. 13, pp. 11-16 (1976).

155. S.M. WIEDERHORN. Fracture surface energy of glass. J. Am. Ceram. Soc., Vol. 52, pp. 99-105 (1969).

156. F.H. WITTMANN. Fracture Mechanics of Concrete. Vol. 7 in "Developments in Civil Engineering", Elsevier, Amsterdam and New York, 680 p. (1983).

157. H.C. WU and J.C. SHEU. Endochronic modelling for shear hysteresis of sand, Journal of Geotechnical Engineering Division, ASCE, Vol. 199, No. 12, pp. 1539-1550 (1983).

158. H.C. WU and T.P. WANG. Endochronic description of sand response to static loading, Journal of Engineering Mechanics Division, ASCE, Vol. 109, No. 4, pp. 970-999 (1983).

159. O.C. ZIENKIEWICZ, D.R.J. OWEN, D.V. PHILLIPS and G.C. NAYAK. Finite element methods in the analysis of reactor vessels. Paper M5/1 presented at the First International Conference in Structural Mechanics in Reactor Technology held on 20-24 September 1971 at Berlin. Also published in Nuclear Engineering and Design, Vol. 20, pp. 507-541 (1972).

160. ASCE. State-of-the-Art Report on Finite Element Analysis of Reinforced Concrete. Prepared by a Task Committee chaired by A. NILSON. American Society of Civil Engineers, New York (1982).

161. _____(Ed.). Mechanical Behaviour of Materials, Vol. 4: Concrete and Cement Paste, Glass and Ceramics, Proceedings of the International Conference on the Mechanical Behaviour of Materials held in Kyoto, Japan on 15-20 August 1971, Society of Materials Science, Kyoto, Japan (1972).

APPENDIX B2

BIBLIOGRAPHY ON PROPELLER-ICE INTERACTION/MILLING

1. K. AIRAKSINEN and M. MARTILLA. On propulsion of icebreakers, International Ship Building Progress, Vol. 23, June, 1976.

2. S.-O. ANDERSSON. CPP in ice. Proceedings of Offshore Gottenburg '83, International conference on offshore and marine technology held at Gothenburg, Sweden between 1-4 March 1983. Session A4: Technology for the Arctic; Arctic Shipping and Navigation, 18 p. (1983).

3. G. ANTONIDES, A. HAGEN and D. LANGROCK. Full scale icebreaking stresses on propellers of the Polar Star. Paper No. 6 presented at the Propeller '81 Symposium, Virginia Beach, Virginia on 26-27 May 1981. Published by SNAME (The Society of Naval Architects and Marine Engineers) pp. 93-110 (1981).

4. A.C. CHURCHER, G. HUBBARD and A. KOLOMOJCEV. Design of the Icebreaking Supply Ship Robert LeMeur. Marine Technology. Vol. 21, No. 2, pp. 134-146 (April 1984).

5. R.Y. EDWARDS. Methods for Predicting Forces Encountered by Propellers During Interactions with Ice. ARCTEC Canada Limited, Rep 75C-1, 1976. Presented at 3rd Lips Propeller Symposium, Drunen - The Netherland (1976). See also International Shipbuilding Progress Vol. 23, pp. 406-419 (Dec. 1976).

6. M.H. EDGECOMBE, P.A. SPENCER and I.M. BAYLY. The M.V. Robert LeMeur Ice-Propeller Interaction Project: Instrumentation. POAC85, Proceedings of the Port and Ocean Engineering Under Arctic Conditions Symposium, Paper H3, Vol. 2, pp. 778-786 (1985).

7. E. ENKVIST and B.M. JOHANSSON. On icebreaker screw design, European Shipbuilding, No. 1, pp. 2-14 (1968).

8. I.U. FILICHEV, Breakage of ship propellers during ice navigation, Morskoi flot, April 1968, No. 4, pp. 21-22, (In Russian).

9. D.G. GABEL, M.G. PARSONS and M.J. KALDJIAN. Finite Element Structural Analysis for Displacements Occurring in the Hub of a Polar Class Icebreaker Controllable Pitch Propeller Operating in Ice. The University of Michigan, The Department of Naval Architecture and Marine Engineering, Report No. 217, September, 1979.

10. S.V. IAKONOVSKII and A.N. SMIRNOV. Effect of geometric and kinematic parameters of a propeller on the magnitude of exterior forces acting on the icebreaker propeller colliding with ice, Leningrad: Tsentral'nyi nauchno-issle dovatel'ski institut morskogo flota. Trudy, Vol. 93, pp. 38-55 (1968) (In Russian).

11. M.A. IGNATJEV. The design of a propeller shaft of adequate strength for ice-going vessels (In Russian). Sudostrojenie, January 1959.

12. M.A. IGNATJEV. Determination of ice load encountered by ship propeller blades, Translated from Russian by the U.S. Dept. of Commerce, Office of Technical Services, Problemy Antiki i Antarktiki, No. 15, pp. 41-51 (1964).

13. M.A. IGNATJEV. Strength calculations for propeller blades of ice-breakers and ice-going vessels (In Russian). Sudostrojenie, January 1964.

14. M.A. IGNATJEV. Screw-propellers for Ships Navigating in Ice (In Russian). Textbook published by Sudostrojenie, Leningrad (1966).

15. M.A. IGNATJEV. Ship propellers for ice navigation vessels; features of design. Leningrad: Izd-vo Sudostrojenie (1966) (In Russian).

16. M.A. IGNATJEV. Calculating the strength of screw propeller blades for ships used in ice navigation, Translation, Problemy Arktiki i Antarktiki, Vol. 16, pp. 75-82 (1976).

17. V.J. JAGODKIN. Analytical Determination of the Resistance Moment of a Propeller During Its Interaction with Ice, Problemy Arktiki I Antarktiki (Problems of the Arctic and Antarctic) Translated from Russian. Vol. 13, pp. 79-81 (1963).

18. M. JUSSILA. Ice loads on the propulsion system of an ice breaking tug, POAC83, Proceedings of the Seventh International Conference on Port and Ocean Engineering under Arctic Conditions held at Helsinki, Finland on 5-9 April 1983. Vol. 3, pp. 575-590 (1983).

19. M. JUSSILA. Ice loads of propulsion machinery, pp. 201-212, Proceedings of Technical Research of Finland (VTT) Symposium 52 on Ship Strength and Winter Navigation, held in Espoo, Finland on 10-11 Jan. 1984, 231 pp. (1984).

20. A.B. KHAJKIN. Dynamics of icebreaker's propeller power unit during interaction of the propeller with ice (Translation) Sudostroenie, Vol. 29, pp. 31-34 (Sept. 1963).

21. A. KHAJKIN. Work of the propeller power plant of an icebreaker during breaking of ice by propeller blades. Morskoj flot Vol. 26, pp. 26-27 (August 1966).

22. A. KHAJKIN and V. JAGODKIN. Calculation of statistical characteristics of propeller electric facilities of icebreaking ships, (Translation) Sudostroenie, Vol. 32, pp. 57-60 (Jan. 1966).

23. R.L. KOCH. Electrical transmission systems for Arctic tankers, Marine Technology, July 1971.

24. T. KOTRAS, D. HUMPHREYS, A. BAIRD, G. MORRIS and G. MORLEY. Determination of Propeller-Ice Milling Loads, pp. 336-343, Vol. 2, Proceedings of the Fourth International Offshore Mechanics and Arctic Engineering Symposium, American Society of Mechanical Engineers, New York (1985).

25. R.E. KRAMEK and R.W. GULICK. Polar class ice-breakers: contribution to technology, STAR Symposium (IceTech'81), SNAME (1981).

26. I.U. KUCHIEV. Damage to ship propellers by ice. Morskoi flot, No. 9, p. 18 (Sept. 1968) (In Russian).

27. D.G. LANGROCK, W. WUERHER and L. VASSILOPOULOS. The performance of the controllable pitch propellers on the U.S. Coast Guard Polar Class Icebreakers, STAR Symposium (IceTech'81), SNAME (1981).

28. V. LASKOW, P.A. SPENCER and I.M. BAYLY. The MV Robert LeMeur Ice/Propeller Interaction: Full-Scale Data. Presented at the 20 November 1985 Meeting of the Arctic Section of the Society of Naval Architects and Marine Engineers. Also published in Marine Technology, Vol. 23, No. 4, pp. 301-319 (Oct. 1986).

29. J.W. LEWIS, F.W SCOVILLE and E.J. LECOURT. Icebreaker Propulsion System Simulation - Phase I, U.S. Coast Guard. Office of Engineering, September 1967.

30. J.W. LEWIS. Some aspects of the design of diesel electric icebreaker propulsion systems. Naval Engineers Journal, April 1979.

31. V.E. MALISHEVSKIJ. Special working features of propeller's power equipment of icebreakers during impact or wedging of blades in ice, (Translation) Sudostroenie, Vol. 27, pp. 30-31 (May 1961).

32. T.M. MAZUR. Cutting of Ice and Its Specific Resistance, Low Temperature Laboratory, Division of Mechanical Engineering, National Research Council, Report LTR-LT-53, October 1974.

33. M. MELLOR. Mechanics of Cutting and Boring; Part 4: Dynamics and Energetics of Parallel Motion Tools, CRREL Report CR77-07, 85 p. (Apr. 1977).

34. M. MELLOR. Mechanics of Cutting and Boring; Part 5: Dynamics and Energetics of Indentation Tools, CRREL Report CR80-21, 82 p. (Sept. 1980).

35. P. NOBLE and V. BULAT. Ice Rules for Propellers and Propeller Shafting, Arctec Canada Limited, Transport Canada Report TP 2556 (1980).

36 P.G NOBLE and V. BULAT. A study of ice class rules of propellers, Paper No. 4 presented at Propellers '81 Symposium at Virginia Beach, Virginia on 26-27 May 1981. Published by SNAME (The Society of Naval Architects and Marine Engineers) pp. 49-65 (1981).

37. M.E. NORWOOD, C.G. DesROCHERS and J.L. WARNER. Final Report on Propeller/Ice Interaction: A Parametric Study of Propellers Operating in an Ice Environment, Prepared for the Transport Development Center, Report # TP4021E, Martec Limited, Dec. 1982, 130 p.

38. M.E. NORWOOD, M.W. CHERNUKA and J.L. WARNER. Final Report on Propeller Ice Interaction: An Investigation into the Problem of Predicting Propeller/Ice Interaction Forces, Prepared for the Transportation Development Center, Report # TP4022E, Martec Ltd., Dec. 1982, 29 p.

39. H. OKAMOTO, K. NOZAWA, H. KAWAKAMI and F. YAMAMOTO. Dynamic ice loads and stress analysis on the propeller of the Arctic ship; model test in ice. POAC81, Proceedings of the Sixth International Conference on Port and Ocean Engineering under Arctic Conditions held on 27-31 July 1981 at Quebec City, Canada, pp. 253-262 (1981).

40. H. OKAMOTO, K. NOZAWA, H. KAWAKAMI, T. YOSHIKAWA, F. YAMAMOTO and K. IIZUKA. Experimental Study on Propeller Ice Interaction for Ice-Breaking Merchant Ship. Translated from Japanese by Transport Canada, April 1984.

41. S.C. POWELL. Performance and blade torque of a series of controllable pitch propellers, Dept. of Naval Architecture, Massachusetts Institute of Technology, AD283972, June 1962.

42. T. SASAJIMA, V. BULAT and I. GLEN. An experimental investigation of two candidate propeller designs for ice capable vessels. POAC81, Proceedings of the Sixth International Conference on Port and Engineering under Arctic Conditions held at Quebec City, Canada on 27-31 July 1981, pp. 263-275 (1981).

43. T. SASAJIMA and E. MUSTAMAKI. Ice-milling load encounters by a controllable pitch propeller, pp. 297-307, Vol. II, Proceedings ofIAHR (International Association for Hydraulic Research) 7th International Symposium on Ice held in Hamburg on 27-31 August 1984 (1984).

44. P.A. SPENCER and S. CORNETT. The Robert LeMeur Nozzle Propeller Ice Force Measurements Project - 1983. Final Report No. TP5685E. Submitted to the Transportation Development Center, Transport Canada (1984).

45. Y. UEDA and S. TAKEZAWA. An investigation on action of ice-breaker Fuji in the Antarctic Sea, Report of Ship Research Institute of Japan, Vol. 14, No. 3, 1977.

46. A.A. VOZHAKOV and B.N. RASSKAZOV. Interaction between ship's propeller and ice. Leningrad: Tsentral'nyi nauchnoissledovatel'-skii institut morskogo flota. Trudy. Vol. 87,pp. 34-36 (1967) (In Russian).

47. J. WIND. The dimensioning of high power propeller system for Arctic icebreakers and icebreaking vessels, Proceedings of the 5th LIPS Propeller Symposium, Druen, the Netherlands (1983).

48. S.V. YAKONOVSKIY and A.N. SMIRNOV. Effect of geometric and kinematic parameters of a screw propeller on the value of external forces acting on an icebreaker during collision with ice. Tsentral'nyy n.i.i. Rechnogo Flota, Trudy Vol. 93, pp. 38-55 (1968) (In Russian).

49. Life Expectancy Analysis of USCG Icebreaker Propeller Blade. Allis Chalmers Corp., October 1976.

50. Results of Trails in Ice and Open Water of CCGS PIERRE RADISSON, Arctec Canada Limited, June 1977.

51. Ice Trials to Evaluate Low Friction Coating on CCGS LOUIS ST. LAURENT, Arctec Canada Limited, November 1979.

APPENDIX B3

BIBLIOGRAPHY ON METAL MILLING/MACHINING

1. J.T. BLACK. Flow stress model in metal cutting. Journal of Engineering for Industry, Trans. ASME, Vol. 101, Nov. 1979, pp. 403-415.

2. H. CHANRASEKARAN and R. NAGARAJAN. On certain aspects of transient stresses in cutting tools. Journal of Engineering for Industry, Trans. ASME, Vol. 102, May 1980, pp. 133 - .

3. H. GLAESER and H. WEISER. Machining process as quasi elastic-plastic process analyzed by finite element method. Wiss. Z. Tech. Hochsch Karl Marx Stadt., Vol. 20, No. 1, 1978, pp. 131-142.

4. K. IWATA, K. OSAKADA, Y. TERASAKA. Process modelling of orthogonal cutting by the rigid-plastic finite element method, Journal of Engineering Materials and Technology, Transactions of the ASME, Vol. 106, pp. 132-138 (April 1984).

5. J.A. KIRK, D.K. ANAND and C. McKINDRA. Matrix representation and prediction of three-dimensional cutting forces. Journal of Engineering for Industry, Trans. ASME, Nov. 1977, pp. 828-834.

6. R. KOMANDURI and R.H. BROWN. On the mechanics of chip segmentation in machining. Journal of Engineering for Industry, Trans. ASME, Vol. 103, Feb. 1981, pp. 33-51.

7. E.H. LEE and B.W. SHAFFER. The theory of plasticity applied to a problem of machining, Journal of Applied Mechanics, Trans. ASME, Vol. 73, pp. 405-413 (Dec. 1951).

8. M. MELLOR. Mechanics of Cutting and Boring; Part 4: Dynamics and Energetics of Parallel Motion Tools, CRREL Report CR77-07, 85 p. (Apr. 1977).

9. M. MELLOR. Mechanics of Cutting and Boring; Part 5: Dynamics and Energetics of Indentation Tools, CRREL Report CR80-21, 82 p. (Sept. 1980).

10. M.E. MERCHANT. Basic mechanics of the metal cutting process, Journal of Applied Mechanics, Trans. ASME, Vol. 11 (3), Sept. 1944, pp. A168-A175.

11. W.A. MORCOS. A slip line field solution of the free oblique continuous cutting problem in conditions of light friction at chip-tool interface. Journal of Engineering for Industry, Trans. ASME, Vol. 102, Nov. 1980, pp. 310-314.

12. S.M. PANDIT and S. REVACH. A data dependent system approach to dynamics of surface generation in turning. Journal of Engineering for Industry, Trans. ASME, Vol. 103, Nov. 1981, pp. 437-445.

13. S. RAMALINGAM, E.D. DOYLE and D.M TURLEY. On chip curl in orthogonal machining. Journal of Engineering for Industry, Trans. ASME, Vol. 102, August 1980, pp. 177-183.

14. T. SHIRAKASHI and E. USUI. Simulation analysis of orthogonal metal cutting mechanism. Proceedings on the International Conference on Production Engineering held in Tokyo, Japan on 26-29 August 1974, Part 1, pp. 535-540. Published by the Japanese Society of Precision Engineering, Tokyo (1974).

15. E. USUI, A. HIROTA and M. MASUKO. Analytical prediction of three dimensional cutting process; Part 1 - Basic cutting model and energy approach. Paper No. 77-WA/PROD-9 presented at the ASME Winter Annual Meeting held in Atlanta, Ga. between 27 November and 2 December 1977. Also Journal of Engineering for Industry, Trans. ASME, Vol. 100, May 1978, pp. 222-228.

16. E. USUI and H. HIROTA. Analytical prediction of three dimensional cutting process; Part 2 - Chip formation and cutting force with conventional single point tool. Journal of Engineering for Industry, Trans. ASME, Vol. 100, May 1978, pp. 229 - .

17. E. USUI, T. SHIRAKASHI and T. KITAGAWA. Analytical prediction of three dimensional cutting process; Part 3 - Cutting temperature and crater wear of carbide tool. Paper No. 77-WA/PROD -11 presented at the Winter Annual Meeting held in Atlanta, Ga., between 27 November and 2 December 1977 by the ASME (Production Engineering Division), 8 p. (1977).

18. E. USUI and T. SHIRAKASHI. Mechanics of machining - from "descriptive" to "predictive" theory. In "On the Art of Cutting Metals - 75 Years Later", Proceedings of the Winter Annual Meeting of the American Society of Mechanical Engineers in Phoenix, Arizona on 14-19 November 1982, Published by ASME (1982), pp. 13-35.

APPENDIX B4

BIBLIOGRAPHY ON ICE MECHANICS/MECHANICAL PROPERTIES OF ICE/TESTING METHODS

1. B.D. ALKIRE and O.B. ANDERSLAND. The effect of confining pressure on the mechanical properties of sand-ice materials. Journal of Glaciology, Vol. 12, No. 66, pp. 469-481 (1973).

2. A. ASSUR. Sea ice engineering. POAC75, Proceedings of the Third International Conference on Port and Ocean Engineering Under Arctic Conditions held at Fairbanks on 11-15 August 1975. Published by University of Alaska, Vol. 1, pp. 231-234 (1976).

3. P. BARNES, D. TABOR and J.C.F. WALKER. The friction and creep of polycrystalline ice. Proceedings of the Royal Society of London, Ser. A., Vol. 324, No. 1557, pp. 127-155 (1971).

4. F.G. BERCHA and ASSOCIATES. Engineering Properties of Ice in the Beaufort Sea. APOA Report #130-3, Prepared for Dome Petroleum. September 1976.

5. F.G. BERCHA and J.V. DANYS. Friction in ice structure interactions. NRC Ice Problems Workshop, Calgary, Canada (1977).

6. F.G. BERCHA. On the scale effect in ice mechanics. Sixth Canadian Congress of Applied Mechanics, Vancouver, Canada (1977).

7. L. BERGDAHL. A theory on the elasticity of sea ice, POAC83. Proceedings of the Seventh International Conference on Port and Ocean Engineering under Arctic Conditions held at Helsinki, Finland on 5-9 April 1983, Vol. 1, pp. 52-68 (1983).

8. B. BLANCHET and H. HAMZA. Plane-strain compressive strength of first year Beaufort Sea ice, POAC83, Proceedings of the Seventh International Conference on Port and Ocean Engineering under Arctic Conditions held at Helsinki, Finland on 5-9 April 1983, Vol. 3, pp. 84-96 (1983).

9. D. BLANCHET. Variations of the local failure pressure with depth through first-year and multi-year ice. Proceedings of the 5th International Offshore Mechanics and Arctic Engineering (OMAE) Symposium held on 13-18 April 1986 in Tokyo, Japan, Vol. 4, pp. 310-319 (1986).

10. F.P. BOWDEN and T.P. HUGHES. The mechanism of sliding on ice and snow. Proc. R. Soc., London A, Vol. 172, pp. 280-297 (1939).

11. F.P. BOWDEN. Friction on snow and ice, Proc. R. Soc., London A, Vol. 217, pp. 462-478 (1953).

12. S.J. CALABRESE, R. BUXTON and G. MARSH. Frictional characteristics of materials sliding against ice. Presented at the 34th Annual Meeting of ASCE in St. Louis, Missouri between 30 April and 3 May 1979. Reprint No. 79-AM-3B-2.

13. E. CHAMBERLAIN, C. GROVES and R. PERHAM. The mechanical behaviour of frozen earth materials under high pressure triaxial test conditions, Geotechnique (London), Vol. 22, No. 3, pp. 469-483 (1972).

14. M. CHANG, C. SHAO, T. YIN and S. DONG. A preliminary research for mechanical properties of sea ice in Bohai, pp. 79-81, POAC83, Proceedings of Port and Ocean Engineering under Arctic Conditions Conference, Helsinki, Finland, Vol. 1 (1983).

15. A.C.T. CHEN and J. LEE. Large-scale ice strength tests at slow strain rates. Proceedings of the 5th International Offshore Mechanics and Arctic Engineering (OMAE) Symposium held on 13-18 April 1986 in Tokyo, Japan, Vol. 4, pp. 374-378 (1986).

16. D.M. COLE. The influence of grain size on the ductility of ice. Proceedings of the Third International Offshore Mechanics and Arctic Engineering Symposium - Vol. III, Ed. by V.J. LUNARDINI, ASME (1983).

17. D.M. COLE. Grain size and the compressive strength of ice, pp. 220-226, Vol. 2, Proceedings of the Fourth International Offshore Mechanics and Arctic Engineering Symposium held in Dallas, Texas on 17-21 February 1985, ASME (1985).

18. D.M. COLE. The Effect of Grain Size on the Internal Fracturing of Polycrystalline Ice. Master of Science Thesis, Thayer School of Engineering, Dartmouth College (June 1984).

19. G. COMFORT and B. MENON. Arctec Canada Ltd., Report FR-450C, Prepared for the Ship Safety Branch of the Canadian Coast Guard, 279 p (April 1981).

20. M.D. COON, R.J. EVANS and D.H. GIBSON. Failure criterion for sea ice and loads resulting from crushing, pp. 1-16, Vol. III, Proceedings of IAHR (International Association for Hydraulic Research) 7th International Symposium on Ice held in Hamburg on 27-31 August 1984 (1984).

21. A. CORMEAU, I.J. JORDAAN, M. NESSIM and M. TOMIN. Ice-structure interaction: A fundamental energy-based approach, pp. 161-174, Vol. III, Proceedings of IAHR (International Association for Hydraulic Research) 7th International Symposium on Ice held in Hamburg on 27-31 August 1984 (1984).

22. G.F.N. COX, J.A. RICHTER-MENGE, W.F. WEEKS, M. MELLOR and H.W. BOSWORTH. Mechanical Properties of Multi-Year Sea Ice, Phase I: Test Results, U.S. Army Cold Regions Research and Engineering Laboratory, CRREL Report 84-9, 105 p. (1984).

23. G.F.N. COX and J.A. RICHTER-MENGE. Tensile strength of multi-year pressure ridge sea ice samples, pp. 186-193, Vol. 2, Proceedings of the Fourth International Offshore Mechanics and Arctic Engineering Symposium held in Dallas, Texas on 17-21 February 1985, ASME (1985).

24. G.F.N. COX, J.A. RICHTER-MENGE, W.F. WEEKS, M. MELLOR, H.W. BOSWORTH, G. DURELL and N. PERON. The Mechanical Properties of Multi-Year Sea Ice, Phase II: Test Results. U.S. Army Cold Regions Research and Engineering Laboratory, CRREL Report in press.

25. G.F.N. COX and W.F. WEEKS. Equations for determining the gas and brine volumes in sea ice samples. Journal of Glaciology, Vol. 29, No. 2, pp. 306-316 (1983).

26. C.F.N. COX and J.A. RICHTER-MENGE. Confined compressive strength of multi-year pressure ridge sea ice samples. Proceedings of the 5th International Offshore Mechanics and Arctic Engineering (OMAE) Symposium held on 13-18 April 1986 in Tokyo, Japan, Vol. 4, pp. 365-373 (1986).

27. K.R. CROASDALE. Crushing strength of arctic ice. In "The Coast and Shelf of the Beaufort Sea". Ed. by J.C. REED and J.E. SLATER, Arctic Institute of North America, Arlington, Va., pp. 377-399 (1974).

28. J.H. CURRIER. The Brittle to Ductile Transition in Polycrystalline Ice Under Tension. M.S. Thesis, Thayer School of Engineering, Dartmouth College, Hanover, NH (1981).

29. J.H. CURRIER and E.M. SCHULSON. The tensile strength of ice as a function of grain size, Acta Metallurgica, Vol. 30, pp. 1511-1514 (1982).

30. J.H. CURRIER, E.M. SCHULSON and W.F. St. LAWRENCE. A Study on the Tensile Strength of Ice as a Function of Grain Size. CRREL Report 83-14, U.S. Army Cold Regions Research and Engineering Laboratory, Hanover, NH (1983).

31. W.W. DENNER. The relationship of stress and strain in sea ice. Proceedings of Workshop on Sea Ice Field Measurement held at St. John's, Newfoundland on 29 April-1 May, 1980, co-sponsored by NRC, pp. 7-32 (1980).

32. P. DUVAL. An elastic behaviour of polycrystalline ice. Journal of Glaciology, 21 (85), pp. 621-628 (1978).

33. H. EL-TAHAN, A.S.J. SWAMIDAS, M. AROCKIASSAMY and D.V. REDDY. Strength of iceberg and artificial snow ice under high strain rates and impact loads, Proceedings of the Third International Offshore Mechanics and Arctic Engineering Symposium, Vol. III, ASME, pp. 158-165 (1984).

34. E. ENKVIST. On ice resistance encountered by ships in the continuous mode of ice breaking. The Swedish Academy of Engineering Sciences in Finland, Report No. 24, 1972.

35. V.P. EPIFANOV. On the mechanical properties of ice. Mech. Solids, Vol. 17, No. 1, pp. 172-177 (1982).

36. V.P. EPIFANOV AND M.A. FAUSTOV. Mech. Solids, Vol. 17, No. 6, pp. 156-162 (1982).

37. D.C.B. EVANS, J.F. NYE and K.J. CHEESEMAN. The kinetic friction of ice. Proc. R. Soc., London A, Vol. 347, pp. 493-512 (1976).

38. A.G. EVANS, A.C. PALMER, D.J. GOODMAN, M.F. ASHBY, J.W. HUTCHINSON, A.R.S. PONTER and G.J. WILLIAMS. Indentation spalling of edge-loaded ice sheets, pp. 113-121, Vol. I, Proceedings of IAHR (International Association for Hydraulic Research) 7th International Symposium on Ice held in Hamburg on 27-31 August 1984 (1984).

39. N.V. FOKEYEV. Determination of the compressive strength of artificial ice specimens of different salinities under conditions of combined stress. Proceedings of the Arctic Research Institute, Vol. 331, 1976, pp. 189-202 (Original in Russian, English Translation, Ottawa, 1980).

40. K.A. FORLAND. Laboratory investigation of the kinetic friction coefficient of ice, pp. 19-28, Proceedings of IAHR (International Association for Hydraulic Research) 7th International Symposium on Ice held in Hamburg on 27-31 August 1984 (1984).

41. R. FREDERKING. Plane-strain compressive strength of columnar-grained and granular-snow ice. Journal of Glaciology, Vol. 18, No. 80, pp. 505-516 (1977).

42. R. FREDERKING and F.U. HAUSLER. The flexural behaviour of ice from in situ cantilever beam tests, pp. 197-215, Proceedings of the International Association for Hydraulic Research Symposium on Ice Problems, Lulea, Sweden (1978).

43. R.M.W. FREDERKING, N.K. SINHA and L.W. GOLD. Mechanical Properties of Sea Ice, Proceedings of the Eighth Canadian Congress of Applied Mechanics (CANCAM81) held in Moncton, N.B. on 7-12 June 1981, pp. 125-128 (1981).

44. R.M.W. FREDERKING and G.W. TIMCO. NRC Ice Property Measurements During the Canmar Kigoriak Trials in the Beaufort Sea Winter 1979-80, NRC-DBR Paper No. 947, National Research Council Canada, Ottawa, Ont. NRCE-18722, 63 p.(1980).

45. R.M.W. FREDERKING and G.M. TIMCO. Mid-winter mechanical properties of ice in the southern Beaufort Sea. POAC81, Proceedings of the Sixth International Conference on Port and Ocean Engineering under Arctic Conditions held on 27-31 July 1981 at Quebec, Canada, pp. 225-234 (1981).

46. R. FREDERKING and G.W. TIMCO. Uniaxial compressive strength and deformation of Beaufort Sea ice, POAC83, Proceedings of the Seventh International Conference on Port and Ocean Engineering under Arctic Conditions held at Helsinki, Finland on 5-9 April 1983, Vol. 1, pp. 89-98 (1983).

47. R.M.W. FREDERKING and G.W. TIMCO. Compressive behaviour of Beaufort Sea ice under vertical and horizontal loading, Proc. of 3rd Int. Symp. on Offshore Mechanics and Arctic Technology, Vol. III, pp. 145-149, New Orleans, U.S.A. (1984).

48. J.W. GLEN. The Mechanics of Ice. Cold Regions Science and Engineering Monograph II. C2b, U.S. Army, Cold Regions Research and Engineering Laboratory, Hanover, N.H. (1975).

49. I.F. GLEN and G. COMFORT. Ice impact pressure and load: investigation by laboratory experiments and ship trials, POAC83, Proceedings of the Seventh International Conference on Port and Ocean Engineering Under Arctic Conditions held at Helsinki, Finland on 5-9 April 1983, Vol. 1, pp. 516-533 (1983).

50. C.F. GOETZE. A Study of Brittle Fracture as Applied to Ice. CRREL Technical Note (1965).

51. L.W. GOLD. Crack formation in ice plates by thermal shocks. Canadian J. Physics 41 1712-1738 (1963).

52. L.W. GOLD. Some observations on the dependence of strain on stress for ice. Can. J. Phys., Vol. 36, No. 10, pp. 1265-1275 (1958).

53. L.W. GOLD. The Failure Process in Columnar - Grained Ice. Ph.D. Thesis. McGill University (1970).

54. L.W. GOLD. Process of failure in ice. Canadian Geotechnical Journal, Vol. 7, pp. 405-413 (1970).

55. L.W. GOLD and A.S. KRAUSZ. Investigation of the mechanical properties of St. Lawrence River ice, Can. Geotech. J., 8(2) pp. 163-169 (1971).

56. L.W. GOLD. The failure process in columnar - grained ice. Technical paper 369, Division of Building Research, National Research Council of Canada, Ottawa, Ont. NRCC12637 (1972).

57. L.W. GOLD. The process of failure of columnar - grained ice, Phil, Mag., 26 (2) pp. 311-328 (1972).

58. L.W. GOLD and A. TRAETTEBERT. Young's modulus of ice and ice engineering problems. Proc. 2nd Symposium on Applications of Solid Mechanics held on 17-18 June 1974 at Hamilton, Canada. Ed. by D.S. WEAVER, Facility of Engineering, McMaster pp. 1-16 (1975).

59. L.W. GOLD. Engineering properties of fresh-water ice, Journal of Glaciology, 19(81) pp. 197-212 (1977).

60. L.W. GOLD and N.K. SINHA. The rheological behaviour of ice at small strains, In "Physics and Mechanics of Ice", Proceedings of IUTAM Symposium held at the Technical University of Denmark in Copenhagen on 6-10 August 1979. Edited by P. TRYDE, Springer-Verlag, Berlin, pp. 117-128 (1979).

61. D.J. GOODMAN. Creep and fracture of ice, and surface strain measurements on glaciers and sea ice. Ph.D. thesis, University of Cambridge (1977).

62. D.J. GOODMAN. Critical stress intensity factor (K_{Ic}) measurements at high loading rates for polycrystalline ice. In "Physics and Mechanics of Ice", Proceedings of IUTAM Symposium held at the Technical University of Denmark on August 6-10, 1979. Edited by P. TRYDE, Springer-Verlag, Berlin, pp. 129-146 (1979).

63. D.J. GOODMAN and D. TABOR. Fracture toughness of ice; a preliminary account of some new experiments. Journal of Glaciology, Vol. 21, pp. 651-660 (1978).

64. K.R. GOPAL, D.V. REDDY and M. AROCKIASAMY. Endochronic constitutive modelling of ice behaviour. Proceedings of the Speciality Conference on Computer Methods in Offshore Engineering held in Halifax, N.S. on 23-25 May 1984, ASCE, pp. 459-474 (1984).

65. R.R. GOUGHNOUR and O.B. ANDERSLAND. Mechanical properties of a sand-ice system. Journal of the Soil Mechanics and Foundations Division, American Society of Civil Engineers, Vol. 94, No. SM4, pp. 923-950 (1968).

66. H. HAMZA. Creep, Failure and Failure of Ice. Ph.D. Dissertation, Faculty of Engineering and Applied Science, Memorial University of Newfoundland, St. John's, Nfld., Canada (1981).

67. H. HAMZA. The critical strain energy and failure and crack propagation criterion of ice, pp. 1-17, Vol. I, Proceedings of IAHR (International Association for Hydraulic Research) 7th International Symposium on Ice held in Hamburg on 27-31 August 1984 (1984).

68. H. HAMZA. A numerical algorithm to predict the visco-elastic response of ice under different loading conditions, pp. 177-183, Vol. 2, Proceedings of the Fourth International Offshore Mechanics and Arctic Engineering Symposium, held in Dallas, Texas on 17-21 February 1985, ASME (1985).

69. H. HAMZA and D.B. MUGGERIDGE. Plain strain fracture toughness (K_{Ic}) of fresh water ice. POAC79, Proceedings of the 5th International Conference on Port and Ocean Engineering under Arctic Conditions, held on 13-17 August 1979 at Trondheim, Norway. pp. 708-777 (1979).

70. H. HAMZA and D.B. MUGGERIDGE. Non-linear fracture toughness of freshwater ice, POAC83, Proceedings of the Seventh International Conference on Port and Ocean Engineering Under Arctic Conditions held at Helsinki, Finland on 5-9 April 1983, Vol. 3, pp. 153-162 (1983).

71. F.U. HAUSLER. Multiaxial compressive strength tests on saline ice with brush-type loading platens. Proceedings of the IAHR International Symposium on Ice held at Quebec, Canada on 27-31 July 1981, pp. 526-539.

72. F.U. HAUSLER. Comparison between different failure criteria for saline ice. Presented at Second Symposium on Applied Glaciology held in New Hampshire, U.S.A. on 23-27 August 1982. Also in Annals of Glaciology, Vol. 4, pp. 105-109 (1983).

73. I. HAWKES and M. MELLOR. Uniaxial testing in rock mechanics laboratories, Engineering Geology, Vol. 4, No. 3, pp. 177-285 (1970).

74. I. HAWKES and M. MELLOR. Deformation and fracture of ice under uniaxial stress, Journal of Glaciology, Vol. 11, No. 61, pp. 103-131 (1972).

75. F.D. HAYNES. Effect of temperature and strain rate on the strength of polycrystalline ice, National Research Council of Canada, Committee on Geotechnical Research, Technical Memorandum, No. 121, pp. 107-111 (Oct. 1977) (CRREL Miscellaneous publication MP1127).

76. F.D. HAYNES. Effect of temperature on the strength of snow ice. U.S. Army Cold Regions Research and Engineering Laboratory, CRREL Report 78-27, 18 p. (1978).

77. F.D. HAYNES and M. MELLOR. Measuring the uniaxial compressive strength of ice, Journal of Glaciology, Vol. 19, No. 81, pp. 213-223 (1977).

78. J.-H. HELLMANN. Basic investigations on mesh-ice, pp. 37-55, Vol. III, Proceedings of IAHR (International Association for Hydraulic Research) 7th International Symposium on Ice held in Hamburg on 27-31 August 1984 (1984).

79. P.V. HOBBS. Ice Physics, Clarendon Press, Oxford (1974).

80. R. LeB. HOOKE, M. MELLOR et al. Mechanical Properties of Polycrystalline Ice: An Assessment of Current Knowledge and Priorities for Research. Report prepared for the International Commission on Snow and Ice with support from the U.S. National Science Foundation. Published in Cold Regions Science and Technology, 3, pp. 263-275 (1980).

81. K. IGAGAKI. Implications of surface energy in ice adhesion, J. Adhes., Vol. 16, No. 1, pp. 41-48 (July 1983).

82. K. ITAGAKI and L. SABOURIN. Fracture behaviour of ice in Charpy impact testing, CRREL Report CR80-13, 13 p. (June 1980).

83. S.H. IYER. Size effects in ice and their influence on the structural design of offshore structures, POAC83, Proceedings of the Seventh International Conference on Port and Ocean Engineering Under Arctic Conditions held at Helsinki, Finland on 5-9 April 1983, Vol. 3, pp. 414-432 (1983).

84. S.J. JONES. Triaxial testing of polycrystalline ice. Proceedings of Third International Conference on Permafrost held in Edmonton, Alberta on July 10-13, 1978, pp. 671-675.

85. S.J. JONES. The confined compressive strength of polycrystalline ice. Journal of Glaciology, Vol. 28, No. 98, pp. 171-177 (1982).

86. S.J. JONES and H.A.M. CHEW. Effect of sample and grain size on the compressive strength of ice. Annals of Glaciology, pp. 129-132 (1983).

87. I. JORDAAN, S. LANTOS and M.A. NESSIM. A probablistic approach to the estimation of environmental driving forces acting upon Arctic structures. Presented at ARCTIC85, San Francisco (1985).

88. I. JORDAAN and M.A. MAES. Probability, exchangeability and extremes. Civil Eng. Systems, Vol. 1, No. 5, pp. 234-241 (Sept. 1984).

89. C.W. KAPLAR. Some strength properties of frozen soils and effect of loading rate. U.S. Cold Regions Research and Engineering Laboratory. Special Report 159.

90. D.G. KARR. Applications of continuous damage models in ice mechanics, pp. 73-77. Proceedings of the 4th International Conference on Applied Numerical Modelling held at National Cheng Kung University in Tainan, Taiwan, Republic of China (1984).

91. D.G. KARR. A damage mechanics model for uniaxial deformation of ice, pp. 227-233, Vol. 2, Proceedings of the Fourth International Offshore Mechanics and Arctic Engineering Symposium held in Dallas, Texas on 17-21 February 1985, ASME (1985).

92. D.G. KARR. Constitutive equations of ice as a damaging material. Proceedings of the ASCE Speciality Conference: ARCTIC85 - Civil Engineering in the Arctic Offshore, San Francisco, CA (March 1985).

93. D.G. KARR and S.C. DAS. Ice strength in brittle and ductile modes, Journal of Structural Engineering, ASCE, Vol. 109, No. 2, pp. 2802-2811, (Dec. 1983).

94. S. KAWAKAMI, H. MIZUTANI, Y. TAKAGI, M. KUMAZAWA and M. KATO. Impact experiments on ice, J. Geophys. Res., Vol. 88, B7, pp. 5806-5814 (July 1983).

95. Y. KAYO, T. KAWASAKI, T. MINAMI, S. TOZAWA, A. TANAKA and R. ABDELNOUR. Field study on mechanical strength of sea ice at east coast of Hokkaido, POAC83, Proceedings of the Seventh International Conference on Port and Ocean Engineering Under Arctic Conditions held at Helsinki, Finland on 5-9 April 1983, Vol. 1, pp. 109-118 (1983).

96. D.Ye. KHEYSIN and V.A. LIKHOMANOV. An experimental determination of the specific enerby of mechanical crushing in ice by impact. Problemy Arktiki i Antarktiki, Vol. 41, pp. 55-61 (English translation) (1973).

97. D.Y. KHEYSIN, V.A. LIKHOMANOV and V.A. KURDYUMOV. Determination of Specific Breakup Energy and Contact Pressures Produced by the Impact of a Solid Against Ice, pp. 210-218, Symposium on Physical Method of Studying Snow and Ice, Leningrad, Oct. 1973 (CRREL Translation TL 539).

98. N. KHARAPATY and E. WESSELS. A new testing technique of ice strength in compression and bending, pp. 83-90, Vol. I, Proceedings of IAHR (International Association for Hydraulic Research) 7th International Symposium on Ice held in Hamburg on 27-31 August 1984 (1984).

99. J.J. KOLLE. Fracture toughness of ice; crystallographic anisotropy. POAC81, Proceedings of the Sixth International Conference on Port and Ocean Engineering under Arctic Conditions held on July 27-31, 1981 at Quebec, Canada. pp. 366-374 (1981).

100. A. KOVACS and J. KALAFUT. Brazil Tensile Strength Tests on Sea Ice: A Data Report, CRREL Special Report SR 77-24, 39 p. (Aug. 1977).

101. P.R. KRY. Stress Distribution During Continuous Crushing of Ice. APOA Report #148-1, May, 1979.

102. L. LAINEY and R. TINAWI. The mechanical properties of sea ice - a compilation of available data. Can. J. Civ. Eng., Vol. 11, No. 4, pp. 884-923 (1984).

103. M.A. LANGE and T.J. AHRENS. Dynamic tensile strength of ice and ice-silicate mixtures.

104. M.P. LANGLEBEN and E. POUNDER. Elastic parameters of sea ice, In "Ice and Snow Properties, Process and Application", Ed. by W.D. KINGERY, MIT Press, Cambridge, MA (1963).

105. R.W. LEE and E.M. SCHULSON. The strength and ductility of ice under tension. Proceedings of the 5th International Offshore Mechanics and Arctic Engineering (OMAE) Symposium held on 13-18 April 1986 in Tokyo, Japan, Vol. 4, pp. 298-302 (1986).

106. H.W. LIU and K.J. MILLER. Fracture toughness of fresh-water ice. Journal of Glaciology, Vol. 22, pp. 135-143 (1979).

107. M.A. MAES, I.J. JORDAAN, A. CORMEAU and J. BALDWIN. Probablistic theories for the failure of sea ice, pp. 37-54, Proceedings of the First International Conference on Ice Technology held in Cambridge, Mass., U.S.A. on 10-12 June 1986, Springer Verlag, Berlin (1986).

108. M.A. MAES, et al. Risk assessment of ice loading for fixed structures, Vol. 3, Proc. OMAE Ice Symposium, New Orleans (1986).

109. E. MAKINEN, A. LAHTI and M. RIMPPI. Influence of friction on ice resistance; search for low friction surfaces. Paper presented at "Ice Tech 75" in Montreal between 9-11 April, 1975.

110. S. MANTOVANI and S. VALERI. Mechanical behaviour at ice-metal interfaces. Philosophical Magazine 37 pt.A, pp. 17-26 (Jan. 1978).

111. K.R. MASER. An analysis of the small-scale strength testing of ice. Massachusetts Institute of Technology, Sea Grant Project Office, Cambridge, MA, Report No. MITSG 72-6 (1972).

112. M. MATSUDA and G. WAKAHAMA. Crystallographic Structure of polycrystalline ice. Journal of Glaciology, Vol. 21, No. 85, pp. 607-619 (1978).

113. T.M. MAZUR. Cutting of Ice and its Specific Resistance, Low Temperature Laboratory, Division of Mechanical Engineering, National Research Council, Report LTR-63, October 1974.

114. M. MELLOR. Mechanical properties of polycrystalline ice. In "Physics and Mechanics of Ice", Proceedings of IUTAM symposium held at the Technical University of Denmark on 6-10 August 1979. Edited by P. TRYDE, Springer-Verlag, Berlin, pp. 217-245. (1979).

115. M. MELLOR. Mechanical behaviour of sea ice, CRREL Report 83-1, NTIS No. ADA 131-852, 105 p. (June 1983).

116. M. MELLOR and D.M. COLE. Deformation and failure of ice under constant stress or constant strain-rate, Cold Regions Science and Technology, Vol. 5, No. 3, pp. 201-219 (March 1982).

117. M. MELLOR and D.M. COLE. Stress/strain/time relations for ice under uniaxial compression, Cold Regions Science and Technology, Vol. 6, No. 3, pp. 207-230 (Feb. 1983).

118. M. MELLOR, G.F.N. COX and H.W. BOSWORTH. Mechanical properties of multi-year sea ice: testing techniques, U.S.A. Cold Regions Research and Engineering Laboratory, CRREL Report 84-8 (1984).

119. B. MICHEL. The strength of polycrystalline ice. Can. J. Civil Eng., Vol. 5, pp. 285-300 (1978).

120. B. MICHEL. Ice Mechanics, Les Presses de l'Universite Laval, Quebec, 1978.

121. B. MICHEL. Advances in ice mechanics. POAC81, Proceedings of the Sixth International Conference on Port and Ocean Engineering under Arctic Conditions held on July 27-31, 1981 at Quebec, Canada, pp. 189-204 (1981).

122. B. MICHEL and R.O. RAMSEIER. Classification of river and lake ice. Canadian Geotechnical Journal, Vol. 8, pp. 36-45 (1971).

123. B. MICHEL and N. TOUSSAINT. Mechanisms and theory of indentation of ice plates. Journal of Glaciology, Vol. 19, No. 81, pp. 285-301 (1977).

124. K.J. MILLER. The application of fracture mechanics to ice problems. In "Physics and Mechanics of Ice", Proceedings of IUTAM Symposium held at the Technical University of Denmark on August 6-10, 1979. Edited by P. TRYDE, Springer-Verlag, Berlin, pp. 265-277 (1979).

125. L.W. MORLAND. Constitutive laws for ice. Cold Regions Science and Technology, Vol. 1, pp. 101-108 (1979).

126. L.W. MORLAND. Correlation of shear behaviour of ice with biaxial stress response, POAC83, Proceedings of the Seventh International Conference on Port and Ocean Engineering Under Arctic Conditions held at Helsinki, Finland on 5-9 April 1983, Vol. 3, pp. 183-192 (1983).

127. J.R. MURAT and L.M. LAINEY. Some experimental observations on the Poisson's ratio of sea ice. Cold Regions Science and Technology, Vol. 6, No. 2, pp. 105-113 (Nov. 1982).

128. J.P. NADREAU. Lois de comportement et de fluage de la glace granulaire simulée de crêtes de pression. Phd Thesis, Laval University, Québec City, Québec (1985).

129. J.P. NADREAU and B. MICHEL. Ice properties in relation to ice forces. Second state-of-the-art report. IAHR working group on ice forces, Vol. 4, pp. 63-115, Proceedings of IAHR (International Association for Hydraulic Research) 7th International Symposium on Ice held in Hamburg on 27-31 August 1984 (1984).

130. J.P. NADREAU AND B. MICHEL. Yield envelope for confined ice, pp. 25-36, Proceedings of the First International Conference on Ice Technology held in Cambridge, Mass., U.S.A. on 10-12 June 1986, Springer Verlag, Berlin (1986).

131. J.P. NADREAU and B. MICHEL. Yield and failure envelope for ice under multiaxial compressive stresses. Submitted to Cold Regions Science and Technology, Elsevier Science Publishers, Amsterdam (1986).

132. M. NAKAWO. Measurements on air porosity of sea ice. Annals of Glaciology, Vol. 4, pp. 204-208 (1983).

133. M. NAKAWO and N.K. SINHA. A note on brine layer spacing of first-year sea ice. Atmosphere-Ocean, Vol. 22, No. 2, pp. 193-206 (1984).

134. A.M. NAWWAR, J.P. NADREAU and Y.S. WANG. Triaxial compressive strength of saline ice, POAC83, Proceedings of the Seventh International Conference on Port and Ocean Engineering Under Arctic Conditions held at Helsinki, Finland on 5-9 April 1983, Vol. 3, pp. 193-202 (1983).

135. D.E. NEVEL and F.D. HAYNES. Interpretation of the Tensile Strength of Ice Under Triaxial Stresses, CRREL Report CR76-05, 9 p. (April 1976).

136. D.E. NEVEL and F.D. HAYNES. Interpretation of the tensile strength of ice under triaxial stress, POAC75, Proceedings of the Third International Conference on Port and Ocean Engineering Under Arctic Conditions held at Fairbanks on 11-15 August 1975. Published by University of Alaska, Vol. 1, pp. 375-387 (1976).

137. W.A. NIXON and E.M. SCHULSON. The fractor toughness of ice over a range of grain sizes. Proceedings of the 5th International Offshore Mechanics and Arctic Engineering (OMAE) Symposium held on 13-18 April 1986 in Tokyo, Japan, Vol. 4, pp. 349-353 (1986).

138. W.A. NIXON and E.M. SCHULSON. Fracture toughness of freshwater ice as a function of loading rate, pp. 287-296, Proceedings of the First International Conference on Ice Technology held in Cambridge, Mass., U.S.A. on 10-12 June 1986, Springer Verlag, Berlin (1986).

139. P.K. OKSANEN. Friction and adhesion of ice, Proceedings of the IAHR International Symposium on Ice held in Quebec City in July, 1981, pp. 453-462.

140. P. OKSANEN and J. KEINONEN. Mechanisms of friction of ice, Wear, Vol. 78, No. 3, pp. 315-324 (June, 1982).

141. H.R. PEYTON. Sea ice strength. Geophysical Institute, University of Alaska, Report No. UAGR-182 (1966).

142. V.R. PARAMESWARAN. Deformation behaviour and strength of frozen sand. Canadian Geotechnical Journal, Vol. 17, No. 1, pp. 74-88 (1980).

143. V.R. PARAMESWARAN. Fracture criterion for ice using a dislocation model, Journal of Glaciology, Vol. 28, No. 98, pp. 161-169 (1982).

144. V.R. PARAMESWARAN and S.J. JONES. Triaxial testing of frozen sand. Journal of Glaciology, Vol. 27, No. 95, pp. 147-155 (1981).

145. E.J. PARRY and D. TABOR. Effect of hydrostatic pressure on the mechanical properties of polymers: A brief review of published data. Journal of Materials Science, Vol. 8, No. 10, pp. 1510-1516 (1973).

146. B.L. PARSONS, J.B. SNELLEN and B. HILL. Physical modelling and the fracture toughness of sea ice. Proceedings of the 5th International Offshore Mechanics and Arctic Engineering (OMAE) Symposium held on 13-18 April 1986 in Tokyo, Japan, Vol. 4, pp. 358-364 (1986).

147. R.O. RAMSEIER. Growth and Mechanical Properties of River and Lake Ice, Ph.D. Thesis, Laval University, Quebec City, Canada (1976).

148. K.M. REINICKE and T.D. RALSTON. Plastic limit analysis with an anisotropic, parabolic yield function, In. J. Rock Mech. Sci. and Geomech. Abstr. Vol. 14 pp. 147-154 (1977).

149. J.A. RICHTER-MENGE et al. Triaxial testing of first year sea ice. U.S. Army Cold Regions Research and Engineering Laboratory, Hanover, NH, Internal Research Report 877 (1985).

150. K. RISKA. On the Role of Failure Criterion of Ice on Determining Ice Loads, VTT (Technical Research Center of Finland), Ships Laboratory Report 7, 36 p. (March 1980).

151. A. IA. RYVLIN. Experimental study of the friction of ice. In "Ice Navigation Qualities of Ships". CRREL Report No. TL-417, pp. 217-234 (Translation).

152. H. SAEKI, T. NOMURA and A. OZAKI. Experimental study on the testing methods of strength and mechanical properties for sea ice, Proceedings of the Fifth IAHR Symposium on Ice Problems held 7-9 August 1978 in Lulea, Sweden, pp. 135-149 (1978).

153. E.M. SCHULSON. An analysis of the brittle to ductile transition in polycrystalline ice under tension. Cold Regions Science and Technology, Vol. 1, pp. 87-91 (1979).

154. E.M. SCHULSON and N.P. CANNON. The effect of grain size on the compressive strength of ice, pp. 29-38, Vol. I, Proceedings of IAHR (International Association for Hydraulic Research) 7th International Symposium on Ice held in Hamburg on 27-31 August 1984 (1984).

155. E.M. SCHULSON and J.H. CURRIER. The tensile strength of polycrystalline ice. Acta Metallurgica, Vol. 30, No. 8, pp. 1511-1514 (1982). Also abstract presented at the Second Symposium on Applied Glaciology held in Hanover, New Hampshire, U.S.A. on 23-27 August 1982. Abstract published in Annals of Glaciology, Vol. 4, pp. 305 (1983).

156. E.M. SCHULSON, P.N. LIM and R.E. LEE. A brittle to ductile transition in ice under tension. Philosophical Magazine, Vol. 49, pp. 353-363 (1984).

157. J. SCHWARZ. Sea-ice investigations in the Weddell Sea during the German Antarctic Expedition. Presented at the Second Symposium on Applied Glaciology held in Hanover, New Hampshire, USA on 23-27 August 1982. Also in Annals of Glaciology, Vol. 4, pp. 246-252 (1983).

158. J. SCHWARTZ and W.F. WEEKS. Engineering properties of sea ice, Journal of Glaciology, Vol. 19, No. 81, pp. 499-530 (1977).

159. J. SCHWARTZ, R. FREDERKING et. al. Standardized testing methods for measuring mechanical properties of ice, Cold Regions Science and Technology, Vol. 4, No. 3, pp. 245-254 (July 1981).

160. M. SERIKOV. Mechanical Properties of Antarctic Sea Ice. Soviet Antarctic Expedition Information Bulletin (English Translation), No. 3, pp. 181-185 (1961).

161. W. SHEN. Fracture toughness of Bohai Bay sea ice. Proceedings of the 5th International Offshore Mechanics and Arctic Engineering (OMAE) Symposi$ held on 13-18 April 1986 in Tokyo, Japan, Vol. 4, pp. 354-357 (1986).

162. S. SHYAM SUNDER. An integrated constitutive theory for the mechanical behaviour of sea ice and micromechanical interpretation, pp. 87-102. Proceedings of the First International Conference on Ice Technology held in Cambridge, Mass., USA on 10-12 June 1986, Springer Verlag, Berlin (1986).

163. S. SHYAM SUNDER. Ice load prediction during indentation, pp. 297-309. Proceedings of the First International Conference on Ice Technology held in Cambridge, Mass., USA on 10-12 June 1986, Springer Verlag, Berlin (1986).

164. N.K. SINHA. Dislocations in ice as revealed by etching, Phil. Mag., 36(6), pp. 1385-1404 (1977).

165. N.K. SINHA. Rheology of columnar-grained ice, Experimental Mechanics, 18(12), pp. 464-470 (1978).

166. N.K. SINHA. Short-term rheology of polycrystalline ice, Journal of Glaciology, 21(85), pp. 457-473 (1978).

167. N.K. SINHA. Grain size influence on effective modulus of ice. Proceedings of Workshop on the Bearing Capacity of Ice Covers held in Winnipeg, Canada on 16-17 October 1978. National Research Council of Canada; Associate Committee on Geotechnical Research, TM No. 123, pp. 65-79 (1979).

168. N.K. SINHA. Grain-boundary sliding in polycrystalline materials, Philosophical Magazine A, 40(6), pp. 825-842 (1979).

169. N.K. SINHA and R. FREDERKING. Effect of test system stiffness on strength of ice. POAC79, Proceedings of the 5th International Conference on Port and Ocean Engineering under Arctic Conditions, held August 13-17, 1979 at Trondheim, Norway. pp. 708-777 (1979).

170. N.K. SINHA. Comparative study of ice strength data. Proceedings of IAHR International Symposium on Ice held 27-31 July 1981 at Quebec, Canada, pp. 581-592 (1981).

171. N.K. SINHA. Constant stress rate deformation modulus of ice. POAC81, Proceedings of the Sixth International Conference on Port and Ocean Engineering under Arctic Conditions held on 27-31 July 1981 at Quebec City, Canada, pp. 216-224 (1981).

172. N.K. SINHA. Deformation behaviour of ice-like materials in engineering applications. Presented at the International Symposium on the Mechanical Behaviour of Structured Media, Carleton University, Ottawa, Ontario, 18-21 May 1981.

173. N.K. SINHA. Rate sensitivity of compressive strength of columnar--grained ice, Presented at Spring Meeting, Society of Experimental Stress Analysis held on 20-25 May 1979 at San Francisco, California. Published in "Experimental Mechanics", Vol. 21, No. 6, pp. 209-218 (June 1981).

174. N.K. SINHA. Constant strain- and stress-rate compressive strength of columnar-grained ice, J. Mater. Sci., Vol. 17, No. 3, pp. 785-802 (March 1982).

175. N.K. SINHA. Field test 1 of compressive strength of first year sea ice. Presented at the Second Symposium on Applied Glaciology held in Hanover, New Hampshire, USA on 23-27 August 1982. Also in Annals of Glaciology, Vol. 4, pp. 253-259 (1983).

176. N.K. SINHA. Field tests on rate sensitivity of vertical strength and deformation of first-year columnar-grained sea ice. POAC83. Proceedings of the Seventh International Conference on Port and Ocean Engineering under Arctic Conditions held at Helsinki, Finland on 5-9 April 1983. Vol. 1, pp. 231-242 (1983).

177. N.K. SINHA. Uniaxial compressive strength of first-year and multi-year sea ice. Presented at the 6th Can. Hydrotech. Conf., Canadian Society of Civil Engineering, 2-3 June 1983. Also published in Canadian Journal of Civil Engineering, Vol. 11, No. 1, pp. 82-91 (1984).

178. N.K. SINHA. Confined strength and deformation of second-year columnar-grained sea ice in Mould Bay, pp. 209-219, Vol. 2. Proceedings of the Fourth International Offshore Mechanics and Arctic Engineering Symposium held in Dallas, Texas on 17-21 February 1985, ASME (1985).

179. N.K. SINHA. Intercrystalline cracking grain-boundary sliding and delayed elasticity at high temperatures. Journal of Materials Science, Vol. 19, pp. 359-376 (?).

180. N.K. SINHA. Does the strength of ice depend on grain size at high temperatures? Scripta Metallurgica, Vol. 17, pp. 1269-1273 (?).

181. N.K. SINHA. The borehole jack: is it a useful arctic tool? Proceedings of the 5th International Offshore Mechanics and Arctic Engineering (OMAE) Symposium held on 13-18 April 1986 in Tokyo, Japan, Vol. 4, pp. 328-335 (1986).

182. L.L. SMITH and J.B. CHEATHAM. Plasticity of ice and sand-ice systems. Transactions of the American Society of Mechanical Engineers, Journal of Engineering for Industry, Vol. 97, Ser. B, No. 2, pp. 479-484 (1975).

183. W.F. St.LAWRENCE and D.M. COLE. Acoustic emissions from polycrystalline ice. Cold Regions Science and Technology, Vol. 5, pp. 183-199 (1982).

184. T. TABATA. Studies of the mechanical properties of sea ice X. The flexural strength of small sea ice beams, Vol. 1, pp. 481-497. Physics of Snow and Ice, International Conference on Low Temperature Science, Sapporo, Japan (1966).

185. T. TABATA, K. FUJINO and M. AOTA. Studies of the mechanical properties of sea ice XI. The flexural strength of sea ice in situ, Vol. 1, pp. 539-550. Physics of Snow and Ice, International Conference on Low Temperature Science, Sappora, Japan (1966).

186. T. TABATA and K. TUSIMA. Friction measurements of sea ice on some plastics and coatings, POAC81, Proceedings of the Sixth International Conference on Port and Ocean Engineering under Arctic Conditions held on 27-31 July 1981 at Quebec City, Canada, pp. 526-535 (1981).

187. T.P. TAYLOR. An experimental investigation of the crushing strength of ice, POAC81, Proceedings of the Sixth International Conference on Port and Ocean Engineering under Arctic Conditions held on 27-31 July 1981 at Quebec City, Canada, pp. 332-345 (1981).

188. G.W. TIMCO and R.M.W. FREDERKING. Compressive strength of multi-year ridge ice. Proceedings of Workshop on Sea Ice Ridges held in Calgary on 22-24 October 1980.

189. G.W. TIMCO and R.M.W. FREDERKING. Comparative strengths of fresh water ice, Cold Regions Science and Technology, Vol. 6, No. 1, pp. 21-27 (August 1982).

190. G.W. TIMCO and R.M.W. FREDERKING. Flexural strength and fracture toughness of sea ice. Cold Regions Science and Technology, Vol. 8, pp. 35-41 (1982).

191. G.W. TIMCO. Uniaxial and plain-strain compressive strength of model ice. Presented at the Second Symposium on Applied Glaciology held in Hanover, New Hampshire, USA on 23-27 August 1982. Also in Annals of Glaciology, Vol. 4, pp. 289-293 (1983).

192. G.W. TIMCO and R. FREDERKING. Confined compressive strength of sea ice, POAC83. Proceedings of the Seventh International Conference on Port and Ocean Engineering under Arctic Conditions held at Helsinki, Finland on 5-9 April 1983. Vol. 1, pp. 243-253 (1983).

193. G.W. TIMCO and R.M.W. FREDERKING. An investigation of the failure envelope of granular/discontinuous-columnar sea ice. Cold Regions Science and Technology, Vol. 9, pp. 17-27 (1984).

194. G.M. TIMCO and R. FREDERKING. A procedure to account for machine stiffness in uni-axial compression tests, pp. 39-47, Vol. 1. Proceedings of IAHR (International Association for Hydraulic Research) 7th International Symposium on Ice held in Hamburg on 27-31 August 1984 (1984).

195. G.W. TIMCO and R.M.W. FREDERKING. Confined compressive tests: outlining the failure envelope of columnar sea ice. Cold Regions Science and Technology, Vol. 12, No. 1, pp. 13-28 (1986).

196. G.W. TIMCO and R.M.W. FREDERKING. The effects of anistropy and microcracks on the fracture toughness (K_{IC}) of freshwater ice. Proceedings of the 5th International Offshore Mechanics and Arctic Engineering (OMAE) Symposium held on 13-18 April 1986 in Tokyo, Japan, Vol. 4, pp. 341-348 (1986).

197. S.-K. TING and S.S. SUNDER. Sea ice indentation accounting for strain-rate variation, pp. 931-941. Proceedings of the ASCE Specialty Conference: ARCTIC85 - Civil Engineering in the Arctic Offshore, San Francisco, CA, (March 1985).

198. A. TRAETTEBERG, L.W. GOLD and R. FREDERKING. The strain rate and temperature dependence of Young's modulus of ice. Proceedings of the 3rd International Symposium on Ice Problems, Hanover, N.H., U.S.A., pp. 479-486 (1975).

199. B.E. TROY Jr., J.P. HOLLINGER, R.O. RAMSEIER, K.W. ASMUS, M.F. HARTMAN and C.C. LUTHER. Microwave emission from High Arctic sea ice during freeze-ups. To be published in Journal of Geophysical Research.

200. K. TUSIMA. Anistropy of the kinetic friction on a single crystal of ice. Journal of Glaciology, Vol. 21, No. 85, pp. 661-668 (1978).

200. K. TUSIMA. Anistropy of the kinetic friction on a single crystal of ice. Journal of Glaciology, Vol. 21, No. 85, pp. 661-668 (1978).

201. K. TUSIMA and T. TABATA. Friction measurements of sea ice on flat shells of metals, plastics and coatings. POAC75 the Proceedings of the 5th International Conference on Port and Ocean Engineering under Arctic Conditions held at Trondheim, Norway on 13-18 August 1979, pp. 741-755. The University, Trondheim, Norway (1979).

202. N. URABE, T. IWASAKI and A. YOSHITAKE, Fracture toughness of sea ice. Cold Regions Science and Technology, 3, pp. 29-37 (1980).

203. N.URABE and A. YOSHITAKE. Fracture toughness of sea ice - in situ measurement and its application. POAC81, Proceedings of the Sixth International Conference on Port and Ocean Engineering under Arctic Conditions held on 27-31 July 1981 at Quebec, Canada. pp. 356-365 (1981).

204. N. URABE and A. YOSHITAKE. Strain rate dependent fracture toughness (K_{IC}) of pure ice and sea ice. Proc. IAHR Symposium on Ice held in Quebec City, Canada. Vol. II, pp. 551-562 (1981).

205. N. URABE, A. YOSHITAKE, T. IWASAKI and M. KAWAHARA. Parameters on fracture strength of sea ice, Journal of Energy Resources Technology, Transactions of ASME, Vol. 105, No. 1, pp. 12-16 (March 1983).

206. N. URABE. Mechanical properties of antarctic sea ice. Proceedings of the 5th International Offshore Mechanics and Arctic Engineering (OMAE) Symposium held on 13-18 April 1986 in Tokyo, Japan, Vol. 4, pp. 303-309 (1986).

207. D. VINOGRADOV and V. BAKALCHUK. Rheological model for ice dynamics, pp. 137-146. Proceedings of the First International Conference on Ice Technology held in Cambridge, Mass., USA on 10-12 June 1986, Springer Verlag, Berlin (1986).

208. V. VIVATRAT and V.L. CHEN. Strain-softening model for simulating local ice contact behaviour. POAC85. Proceedings of the 8th International Conference on Port and Ocean Engineering under Arctic Conditions held at Narssarssuaq, Greenland on 7-14 September 1985, Vol. 2, pp. 689-698 (1985).

209. Y.S. WANG. Uniaxial compressive testing of Arctic sea ice, POAC81, Proceedings of the Sixth International Conference on Port and Ocean Engineering under Arctic Conditions held on 27-31 July 1981 at Quebec, Canada, pp. 346-355 (1981).

210. Y.S. WANG. A rate-dependent stress-strain relationship for sea ice. Journal of Energy Resources Technology, Transactions of the ASME, Vol. 105, pp. 2-5 (March 1983).

211. Y.S. WANG and J.P. POPLIN. Laboratory compression tests of sea ice at slow strain rates from a field test program. Proceedings of the 5th International Offshore Mechanics and Arctic Engineering (OMAE) Symposium held on 13-18 April 1986 in Tokyo, Japan, Vol. 4, pp. 379-384 (1986).

212. W.F. WEEKS. Growth, Structure and Properties of Sea Ice, CRREL Monograph 82-1, 138 p. (November 1982).

213. W.F. WEEKS and D.L. ANDERSON. An experimental study of strength of young sea ice. Transactions, American Geophysical Union, Vol. 39, No. 4, pp. 641-647 (1958).

214. W. WEEKS and A. ASSUR. The Mechanical Properties of Ice, U.S. Army CRREL (Cold Regions Research and Engineering Laboratory), Hanover, N.H., Monograph II-C3 (1967).

215. W.F. WEEKS and A. ASSUR. Fracture of Lake and Sea Ice, CRREL Research Report 269269 (1969).

216. H.C. WU, K.J. CHANG and J. SCHWARTZ. Fracture in the compression of columnar-grained ice. Engineering Fracture Mechanics, Vol. 8, No. 2, pp. 365-372 (1976).

217. Y.K. ZARETSKY, B.D. CHUMICHEV and V.I. SOZOMATIN. Ice behaviour under load, Engng. Geol., Vol. 13, pp. 299-309 (1979).

218. APOA Report #52-3. Ice Crushing Tests 1973.

219. APOA Report #64-1. Static Ice Loading Tests.

220. APOA Report #66-1. Ice Crushing Tests 1974.

221. APOA Report #81-10. Ice Properties Data.

222. APOA Report #106-1. Continuous Crushing of Ice.

223. APOA Report #130-3. Engineering Properties of Ice in the Beaufort Sea. Report prepared by F.G. BERCHA and Associates for Dome Petroleum, September 1976.

224. APOA Report #148-1. Stress Distribution During Continuous Crushing of Ice. Prepared by P.R. KRY for Esso Resources Canada Ltd., May 1979.

225. Standardization of Testing Methods for Ice Properties. Proposed by the Working Group of the IAHR Section on Ice Problems, J. of Hydraulic Research, Vol. 18, No. 2, pp. 153-165 (1980).

APPENDIX B5

BIBLOGRAPHY ON ICE INDENTATION AND PENETRATION

1. V.P. AFANAS'YEV, I.V. DOLGOPOLOV and Z.I. SHVAYSHTEN. Ice pressure on separate supporting structures in the sea. Draft Translation 346, NTIS No. AD741873. U.S.A. Cold Regions Research and Engineering Laboratory, Hanover, NH (1971).

2. M.F. ASHBY, A.C. PALMER, M. THOULESS, D.J. GOODMAN, M. HOWARD, S.D. HALLAM, S.A.F. MURRELL, N. JONES, T.J.O. SANDERSON and A.R.S. PONTER. Nonsimultaneous failure and ice loads on Arctic structures.Paper OTC-5127. Proceedings of the 18th Annual Offshore Technology Conference held in Houston, Texas on 5-8 May 1986, Vol. 1, pp. 399404 (1986).

3. S. BELTAOS. A strain energy criterion for failure of floating ice sheets, Can.J. Civil. Eng., Vol. 5, pp. 352-361 (1978).

4. F.J. BRUEN, R.C. BYRD, V. VIVATRAT and B.J. WATT. Selection of local design ice pressure for arctic systems, Paper OTC-4334. Proceedings of Fourteenth Annual Offshore Technology Conference held on 3-6 May 1982 at Houston, Texas. Vol. 3, pp. 417-435 (1982).

5. F.J. BRUEN and V. VIVATRAT. Ice force prediction based on strain-rate field, Vol. 3, pp. 275-281. Proceedings of the 3rd International Symposium on Offshore Mechanics and Arctic Engineering, New Orleans, LA (1984).

6. F.J. BRUEN and V. VIVATRAT. Ice force prediction based on strain-rate field. Journal of Energy Resources Technology, Transactions of the ASME, Vol. 106, pp. 509-514 (Dec. 1984).

7. T. CARSTENS (Editor). Working Group on Ice Forces on Structures: A State-of-the-Art Report. Prepared by International Association for Hydraulic Research Section on Ice Problems. CRREL Special Report 80-26, NTIS No. AD-A089-674, Cold Regions Research and Engineering Laboratory, Hanover, NH (June 1980).

8. F.S. CHEHAYEB, S.-K. TING, S.S. SUNDER and J.J. CONNER. Sea ice indentation in the creeping mode, OTC-5056. Proceedings of the 17th Offshore Technology Conference held on 6-9 May 1985 in Houston, Tx, Vol. 4, pp. 329-341 (1985).

9. M.D. COON, R.J. EVANS and D.H. GIBSON. Failure criteria for sea ice and loads resulting from crushing, pp. 1-16, Vol. III. Proceedings of IAHR (International Association for Hydraulic Research) 7th International Symposium on Ice held in Hamburg on 27-31 August 1984 (1984).

10. A. CORMEAU, I.J. JORDAAN, M. NESSIM and M. TOMIN. Ice-structure interaction: A fundamental energy-based approach, pp. 161-174, Vol. III. Proceedings of IAHR (International Association for Hydraulic Research) 7th International Symposium on Ice, Hamburg (August 1984).

11. K.R. CROASDALE. Ice forces on marine structures. Proceedings of the Third IAHR (International Association for Hydraulic Research) Symposium on Ice Problems held on 18-21 August 1975 in Hanover, New Hampshire, pp. 315-337 (1975).

12. K.R. CROASDALE, U.R. MORGENSTERN and J.B. NUTTALL. Indentation tests to investigate ice pressures on vertical piers. Journal of Glaciology, Vol. 19, No. 81, pp. 301-312 (1977).

13. K.R. CROASDALE. Ice forces on fixed rigid structures. CRRL Special Report 80-26, U.S. Army Cold Regions Research and Engineering Laboratory, Hanover, NH (1980).

14. K.R. CROASDALE and R.W. MARCELLUS. Ice forces on large marine structures. Proceedings of the IAHR (International Association for Hydraulic Research) International Symposium on Ice held on 27-31 July 1981 at Quebec, Canada, Vol. 1, pp. 755-766 (1981).

15. K.R. CROASDALE. The limiting driving force approach to ice loads. Paper OTC 4716. Proceedings of the 16th Annual Offshore Technology Conference held on 7-9 May, 1984 at Houston, Texas. Vol. 2, pp. 57-64 (1984).

16. P. CROTEAU. Dynamic Interactions between Floating Ice and Offshore Structures. Report No. UCB/EERC-83/06, College of Engineering, University of California, Berkeley, California, 351 pp. (NTIS-P684-119486).

17. E. ERANTI, F.D. HAYES, M. MAATTANEN and T.T. SOONG. Dynamic ice-structure interaction analysis for narrow vertical structures. POAC 81, Proceedings of the the Sixth International Conference on Port and Ocean Engineering under Arctic Conditions held at Quebec City on 27-31 July 1981, pp. 472-479 (1981).

18. A.G. EVANS, A.C. PALMER, D.J. GOODMAN, M.F. ASHBY, J.W. HUTCHINSON, A.R.S. PONTER and G.J. WILLIAMS. Indentation spalling of edge-loaded ice sheets, pp. 113-121, Vol. 1. Proceedings of the Seventh IAHR (International Association for Hydraulic Research) Symposium on Ice held on 27-31 August 1984 in Hamburg (1984).

19. R. FREDERKING and L.W. GOLD. Ice forces on an isolated circular pile. POAC71, Proceedings of the 1st International Conference on Port and Ocean Engineering under Arctic Conditions held in Trondheim, Norway, Vol. 1, pp. 73-92 (1971).

20. R. FREDERKING and L. GOLD. Experimental study of edge loading of ice plates, Can. Geotech. Journal, Vol. 12, No.4, pp. 456-463 (1975).

21. R. FREDERKING et. al. Model investigation of ice forces on cylindrical structures. Proceedings of Intermaritec '82 held in Hamburg, Germany, pp. 341-349 (1982).

22. J. GANGULY. Finite Element Modelling of Sea Ice Indentation in the Creeping Mode. Master of Science Thesis in Civil Engineering, Massachusetts Institute of Technology, Cambridge, MA. (Jan. 1986).

23. E.M. GERSHUNOV. Scale effects and compressive strength of large volumes of ice. Paper OTC-5129. Proceedings of the 18th Annual Offshore Technology Conference held on 5-8 May 1986 at Houston, Texas, Vol. 1, pp. 405-412 (1986).

24. J. GRUNZWEIG, I.M. LONGMAN and N.J. PETCH. Calculations and measurements on wedge indentation, Journal of the Mechanics and Physics of Solids, Vol. 2, pp. 81-86 (1954).

25. K. HIRAYAMA, J. SCHWARZ and H.C. WU. Ice forces on vertical piles indentation and penetration. Proceedings of Third IAHR (International Association for Hydraulic Research)Symposium on Ice Problems, Hanover, USA, pp. 429-445 (1975).

26. S.H. IYER. Size effects in ice and their influence on the structural design of offshore structures. POAC83. Proceedings of the 7th International Conference on Port and Ocean Engineering under Arctic Conditions held on 5-9 April 1983 in Helsinki, Finland. Vol. 3, pp. 414-432 (1983).

27. D.G. KARR and S.C. DAS. Limit analysis of ice sheet indentation. J. of Energy Resources Technology, American Society of Mechanical Engineers, Vol. 105, pp. 352-355 (1983).

28. D.G. KARR. Three-dimensional analysis of ice sheet indentation: lower bound solutions. Proceedings of the 5th International Offshore Mechanics and Arctic Engineering (OMAE) Symposium held on 13-18 April 1986 in Tokyo, Japan, Vol. 4, pp. 472-478 (1986).

29. K. KATO, D.S. SODHI and D. HAYNES. Some effects of friction on ice forces against vertical structures. Proceedings of the 5th International Offshore Mechanics and Arctic Engineering (OMAE) Symposium held on 13-18 April 1986 in Tokyo, Japan, Vol. 4, pp. 528-533 (1985).

30. A.D. KERR. On the Determination of Horizontal Forces on a Floating Ice Plate Exerts on a Structure. CRREL Report 78-15 (1978).

31. K.N. KORZHAVIN. Action of Ice on Engineering Structures. Publishing House of Siberian Branch of USSR Academy of Sciences (1962) (CRREL Draft Translation No. 260, U.S. Army Cold Regions Research and Engineering Laboratory, Hanover, NH, 1971).

32. J.R. KREIDER and V. VIVATRAT. Ice force prediction using a limited driving force approach. Journal of Energy Resources Technology, Trans. of ASME, Vol. 105, pp.17-25 (March 1983).

33. P.R. KRY. Implications of structure width for design ice forces. In "Physics and Mechanics of Ice", Proceedings of IUTAM Symposium held at the Technical University of Denmark, Copenhagen on 6-10 August 1979. Edited by P. TRYDE, Springer - Verlag, Berlin, pp. 179-193 (1979).

34. P.R. KRY. High aspect ratio crushing tests. APOA Project 93, Imperial Oil, Calgary, Alberta, 72 p. (1979).

35. P.R. KRY. Ice forces on wide structures. Canadian Geotechnical Journal, Vol. 17, No. 1, pp. 97-113 (Feb. 1980).

36. P.R. KRY. Scale effects in continuous crushing in ice. Proceedings of the IAHR International Symposium of Ice held in Quebec City in July 1981, pp. 565-580 (1981).

37. B.C. LEE and B.M. KWAK. A computational method for elasto-plastic contact problems, Computers and Structures, Vol. 18, No. 5, pp. 757765 (1984).

38. B.R. LAWN and M.V. SWAIN. Microfracture beneath point indentation in brittle solids, Journal of Material Science, Vol. 10, pp. 113-122 (1975).

39. B. LAWN and R. WILSHAW. Indentation fracture, principles and applications. Journal of Material Science, Vol. 10, pp. 1049-1081 (1975).

40. M. MAATTANEN. Ice forces on fixed, flexible structures. In a state-of-the-art report by the Working Group on Ice Forces in Structures, IAHR. CRREL Special Report 80-26, NTIS No. ADA 089674, USA Cold Regions Research and Engineering Laboratory, Hanover, NH (1980).

41. M. MAATTANEN. Ice structure dynamic interaction-ice forces versus velocity, ice-induced damping. Proceedings of the 5th IAHR (International Association of Hydraulic Research) Symposium on Ice Problems held on 27-31 July 1981 at Laval University, Quebec, Canada, pp. 783-796 (1981).

42. M. MAATTANEN. Dynamic Ice-Structure Interaction during Continuous Crushing. CRREL Report 83-5, USA Cold Regions and Engineering Laboratory, Hanover, NH (1983).

43. M.A. MAES, I.J. JORDAAN, A. CORMEAU and J. BALDWIN, pp. 37-54. Proceedings of the First International Conference on Ice Technology held in Cambridge, Mass., USA on 10-12 June 1986, Springer-Verlag, Berlin (1986).

44. F. MATLOCK, W.P. DAWLING and J.J. PANAK. Analytical model for ice-structure interaction. Journal of Engineering Mechanics Division. Proceedings of Engineering Mechanics, ASCE, pp. 1083-1092 (August 1971).

45. M. MELLOR. Mechanics of Cutting and Boring; Part 5: Dynamics and Energetics of Indentation Tools, CRREL Report CR80-21, 82 p. (September 1980).

46. B. MICHEL and N. TOUSSAINT. Mechanisms and theory of indentation of ice plates. Journal of Glaciology, Vol. 19 No. 81, pp. 285-300 (1977).

47. B. MICHEL. Indentation by a vertical face structure. In "Ice Mechanics" published by Les Presses de l'Universite Laval. Sec. 4.2.2, pp. 281-305 (1978).

48. B. MICHEL and D. BLANCHET. Indentation of an S_2 floating ice sheet in the brittle range. Presented at the Second Symposium on Applied Glaciology held in New Hampshire, USA on 23-27 August 1982. Also in Annals of Glaciology, Vol. 4, pp. 180-188 (1983).

49. B. MICHEL and L. JOLICOEUR. Experimental study of indentation of columnar grained ice sheets in the transition zone. Proceedings of the 5th International Offshore Mechanics and Arctic Engineering (OMAE) Symposium held on 13-18 April 1986 in Tokyo, Japan, Vol. 4, pp. 479-485 (1986).

50. H. NAKAJIMA, N. KOMA and M. INOUE. The ice force on a cylindrical pile, POAC 81, Proceedings of the Sixth International Conference on Port and Ocean Engineering under Arctic Conditions held on 27-31 July 1981 at Quebec City, Canada, Vol. 1, pp. 517-525 (1981).

51. T. NAWATA, T. KAWASAKI, S. YANO and S. ISHIKAWA. Model tests of jacket structure in ice tank. Proceedings of the 5th International Offshore Mechanics and Arctic Engineering (OMAE) Symposium held on 13-18 April 1986 in Tokyo, Japan, Vol. 4, pp. 436-443 (1986).

52. C.R. NEILL. Dynamic ice forces on piers and piles; an assessment of design quidelines in the light of recent research. Can. J. Civil Eng., Vol. 3, pp. 305-341 (1976).

53. D.E. NEVEL, R.E. PERHAM and G.B. HOGUE. Ice Forces on Vertical Piles, CRREL CR 77-10, 9 p. (April 1977).

54. A.C. PALMER, D.J. GOODMAN, M.F. ASHBY, A.G. EVANS, J.W. HUTCHINSON and A.R.S. PONTER. Fracture and its role in determining ice forces on offshore structures. Presented at the Second Symposium on Applied Glaciology held in New Hampshire, USA on 23-27 August 1982. Also in Annals of Glaciology, Vol. 4, pp. 216-221 (1983).

55. H.R. PEYTON. Sea ice forces. National Research Council of Canada, Technical Memorandum 92, Ottawa (1968).

56. A.R.S. PONTER, A.C. PALMER, D.J. GOODMAN, A.G. EVANS and J.W. HUTCHINSON. The force exerted by a moving ice sheet on offshore structure: Part 1, the creep mode. Cold Regions Science and Technology, Vol. 8, pp.109-118 (1983).

57. B.D. PRATTE and G.W. TIMCO. A new model basin for the testing of ice-structure interactions. POAC81. Proceedings of the Sixth Inernational Conference on Port and Ocean Engineering Under Arctic Conditions held on 27-31 July 1981 at Quebec City, Canada, Vol. 2, pp. 857-866 (1981).

58. T.D. RALSTON. An analysis of ice sheet indentation. Proceedings of IAHR Symposium on Ice Problems, Lulea, Sweden, pp. 13-31 (1978).

59. T.D. RALSTON. Plastic limit analysis of ice splitting failure. POAC81, Proceedings of the Sixth International Conference on Port and Ocean Engineering under Arctic Conditions held at Quebec, Canada on 27-31 July 1981, Les Presses de l'Universite Laval, pp. 205-215 (1981).

60. K.M. REINICKE and R. REMER. A procedure for the determination of ice forces illustrated for polycrystalline ice. Proceedings of IAHR Symposium on Ice Problems, Lulea, pp. 217-238 (1978).

61. K.M. REINICKE. Analytical approach for the determination of ice forces using plasticity theory, In "Physics and Mechanics of Ice". Proceedings of IUTAM Symposium held at the Technical University of Denmark in Copenhagen on 6-10 August 1979. Edited by P. TRYDE, Springer-Verlag, Berlin. pp. 325-341 (1979).

62. M. ROJANSKY. Large scale versus small scale ice force predictions. Proceedings of the 5th International Offshore Mechanics and Arctic Engineering (OMAE) Symposium held on 13-18 April 1986 in Tokyo, Japan, Vol. 4, pp. 467-471 (1986).

63. H. SAEKI and A. OZAKI. Ice forces on piles. In "Physics and Mechanics of Ice". Proceedings of IUTAM Symposium held at the Technical University of Denmark in Copenhagen on 6-10 August 1979. Edited by P. TRYDE, Springer-Verlag, Berlin. pp. 342-350 (1979).

64. H. SAEKI, T. ONO, T. TAKEUCHI, E.L. SUENAGA and M. SAKAI. Total ice forces on the clusters of cylindrical piles. Proceedings of the 5th International Offshore Mechanics and Arctic Engineering (OMAE) Symposium held on 13-18 April 1986 in Tokyo, Japan, Vol. 4, pp. 461-466 (1986).

65. T.J.O. SANDERSON. Theoretical and measured ice forces on wide structures. Proceedings of the 7th IAHR (International Association for Hydraulic Research) Symposium on Ice held on August 1984, Vol. 4, pp. 151-207 (1984).

66. J. SCHWARTZ. The pressure of floating ice-fields on piles. Proceedings of IAHR (International Association for Hydraulic Research) Symposium on Ice and its Action on Hydraulic Structures, Iceland, Paper 6.3 (1970).

67. S.S. SUNDER, J. GANGULLY and S.-K. TING.. Anisotropic sea ice indentation in the creeping mode. Proceedings of the 5th International Offshore Mechanics and Arctic Engineering (OMAE) Symposium held on 13-18 April 1986 in Tokyo, Japan, Vol. 4, pp. 486-496 (1986).

68. S.S. SUNDER. Ice load prediction during identation, pp. 297-309. Proceedings of the First International Conference on Ice Technology held in Cambridge, Mass., USA on 10-12 June 1986, Springer-Verlag, Berlin (1986).

69. L.L. SMITH and J.B. CHEATHAM. Plasticity of ice and sand-ice systems. Journal of Engineering for Industry, ASME, Vol. 97, Series B, No. 2, pp. 479-484 (1975).

70. D.S. SODHI and H.E. HAMZA. Buckling analysis of a semi-infinite ice sheet. Proceedings of the 4th International Conference on Port and Ocean Engineering under Arctic Conditions, Vol. 1, pp. 593-604 (1977).

71. G.W. TIMCO. Indentation and penetration of edge-loaded freshwater ice sheets in the brittle range. Proceedings of the 5th International Offshore Mechanics and Arctic Engineering (OMAE) Symposium held on 13-18 April 1986 in Tokyo, Japan, Vol. 4, pp. 444-452 (1986).

72. S.-K. TING and S.S. SUNDER. Sea ice indentation accounting for strain-rate variation. Proceedings of the ASCE Specialty Conference: ARCTIC '85 - Civil Engineering in the Arctic Offshore held in March 1985 in San Francisco, CA, pp. 931-941 (1985).

73. S.-K. TING. Constitutive Modelling of Sea Ice with Applications to Indentation Problems, Doctor of Science Thesis in Structural Engineering, Massachusetts Institute of Technology, Cambridge, MA (Oct. 1985).

74. M.J. TOMIN, A. CORMEAU and J.J. JORDAAN. Development of Analytical Models Related to Experimental Work on Ice-Structure Interaction. Technical Report, Det norske Veritas (Canada) Ltd., Calgary, Alberta, 254 p. (Sept. 1985).

75. M.J. TOMIN, M. CHEUNG, I.J. JORDAAN and A. CORMEAU. Analysis of failure modes and damage processes of freshwater ice in indentation tests. Proceedings of the 5th International Offshore Mechanics and Arctic Engineering (OMAE) Symposium held on 13-18 April 1986 in Tokyo, Japan, Vol. 4, pp. 453-460 (1986).

76. V. VIVATRAT. Strains and strain rates in sea ice indentation. Paper OTC-4311, Proceedings of the Fourteenth Annual Offshore Technology Conference held on 3-6 May 1982 at Houston, Texas. Vol. 3, pp. 113-140 (1982).

77. V. VIVATRAT, V. CHEN and F.J. BRUEN. Ice load prediction for Arctic nearshore zone. Cold Region Science and Technology, Vol. 10, pp. 75-87 (1984).

78. Y.S. WANG. Buckling analysis of a semi-infinite ice sheet moving against cylindrical structures. Proceedings of IAHR (International Association for Hydraulic Research) Symposium on Ice Problems held in Lulea, Sweden, Part I, pp. 117-134 (1978).

79. T. WIERZBICKI. Spalling and buckling of ice sheets. Civil Engineering in the Arctic Offshore. Proceedings of the Conference Arctic'85, San Francisco, 25-27 March 1985.

80. L.J. ZABILANSKY, D.E. NEVEL, and F.D. HAYNES. Ice forces on model structures. Canadian Journal of Civil Engineering, Vol. 2, pp. 400-417 (1975).

Library and Information Centre / Centre de Documentation
RECEIVED / REÇU LE
NOV 25 1989
Transport Canada / Transports Canada